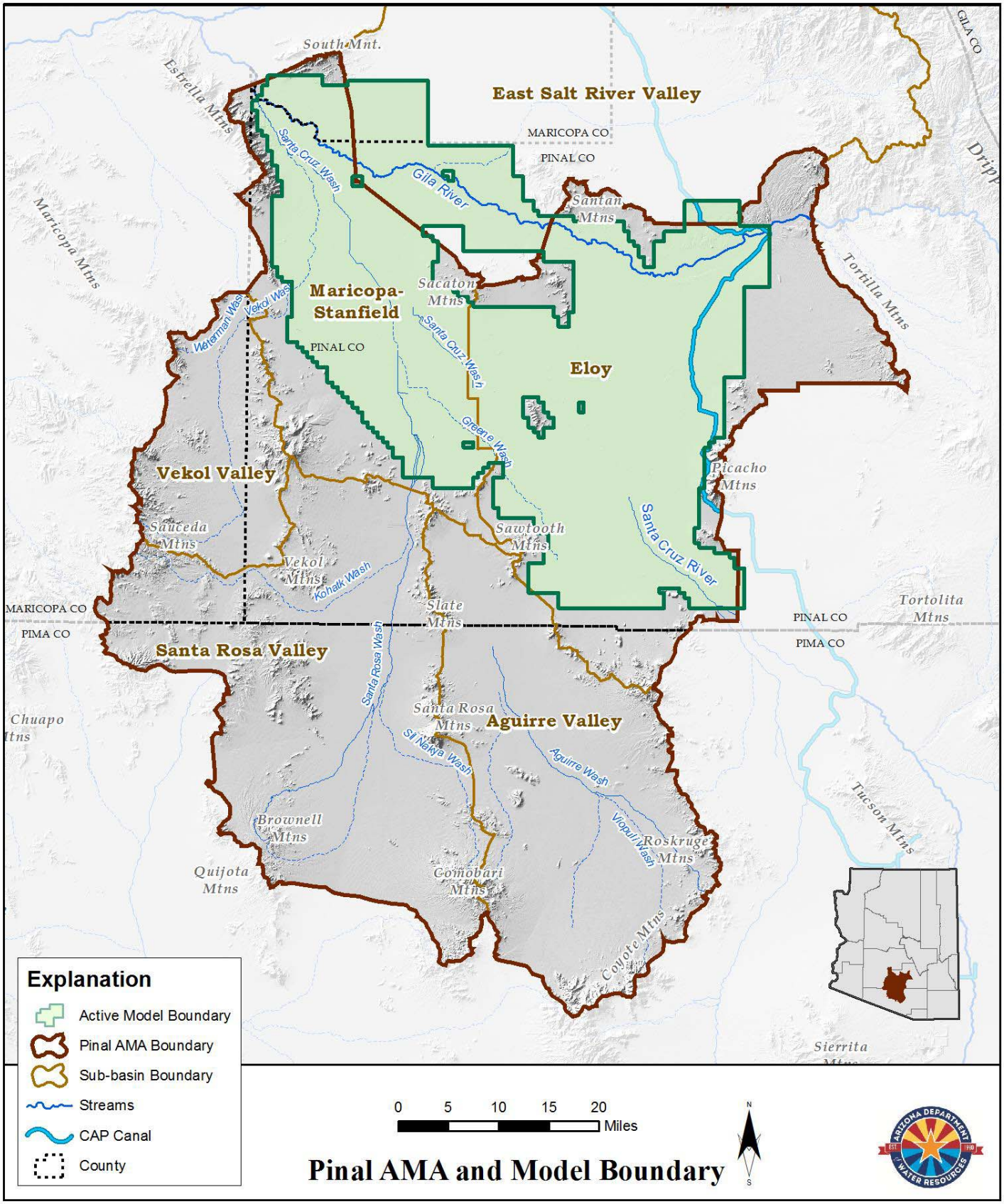

Figure 1 Pinal AMA and Model Boundary

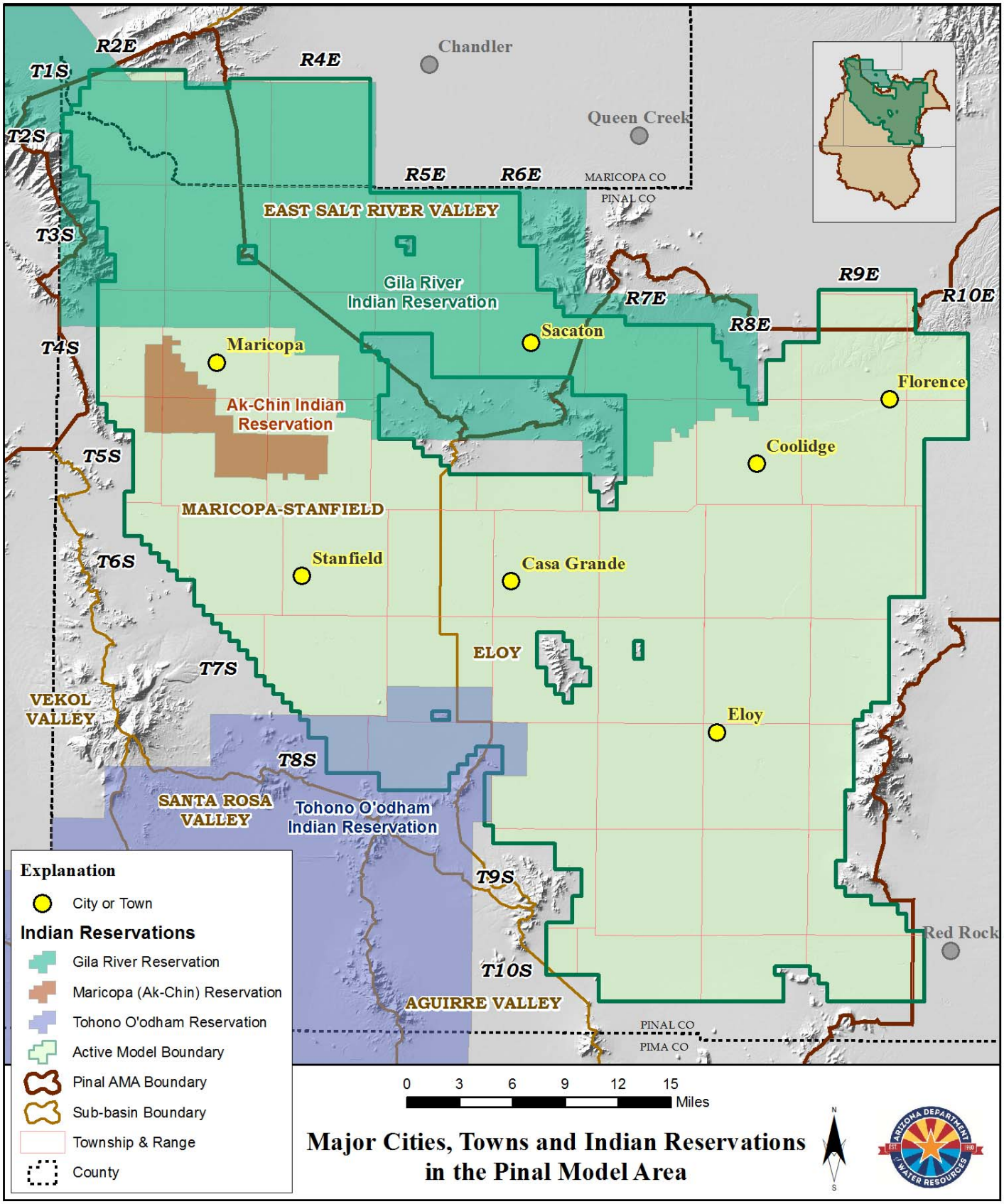

Figure 2 Major Cities, Towns and Indian Reservations in the Pinal Model Area

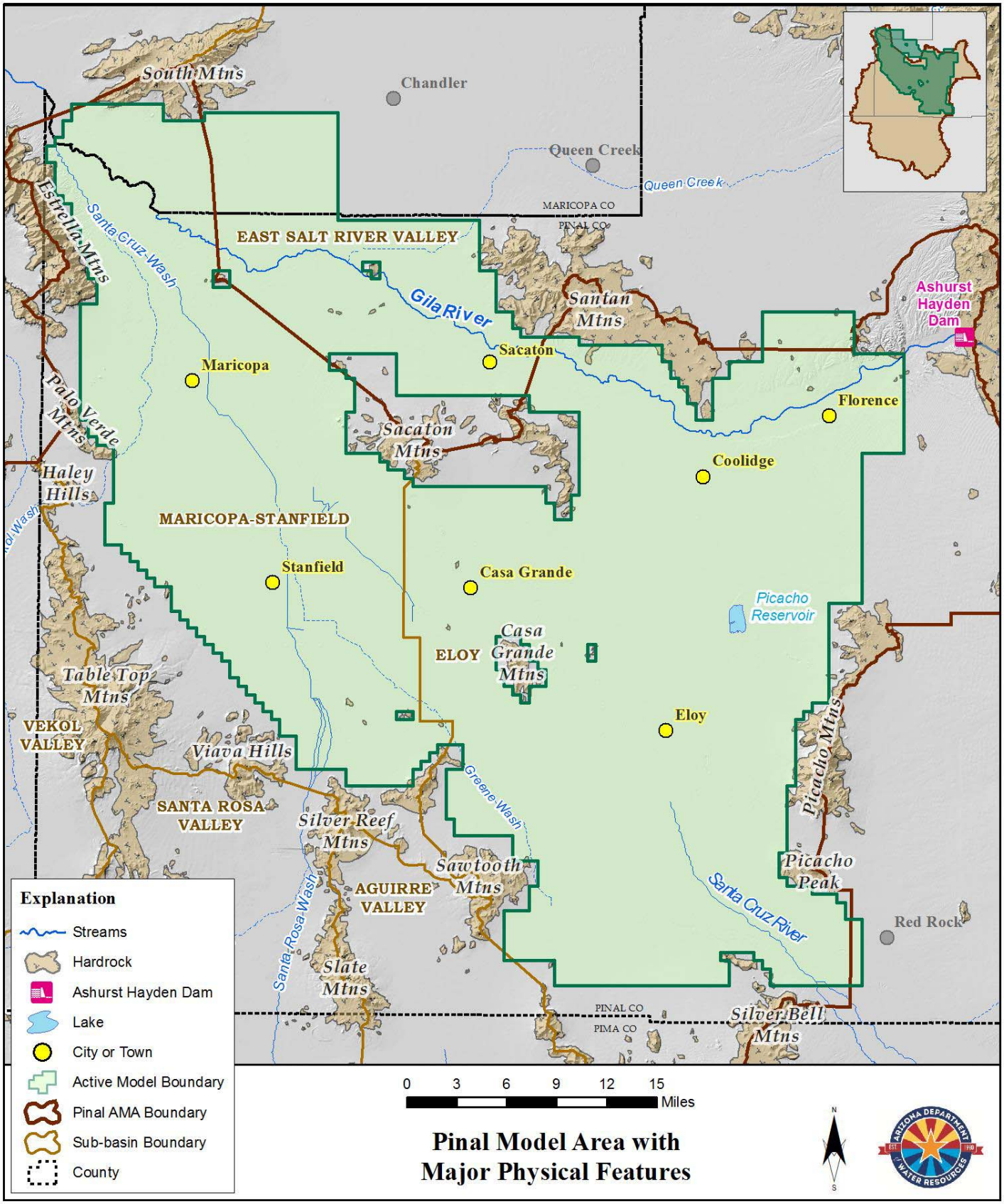

Figure 3 Pinal Model Area

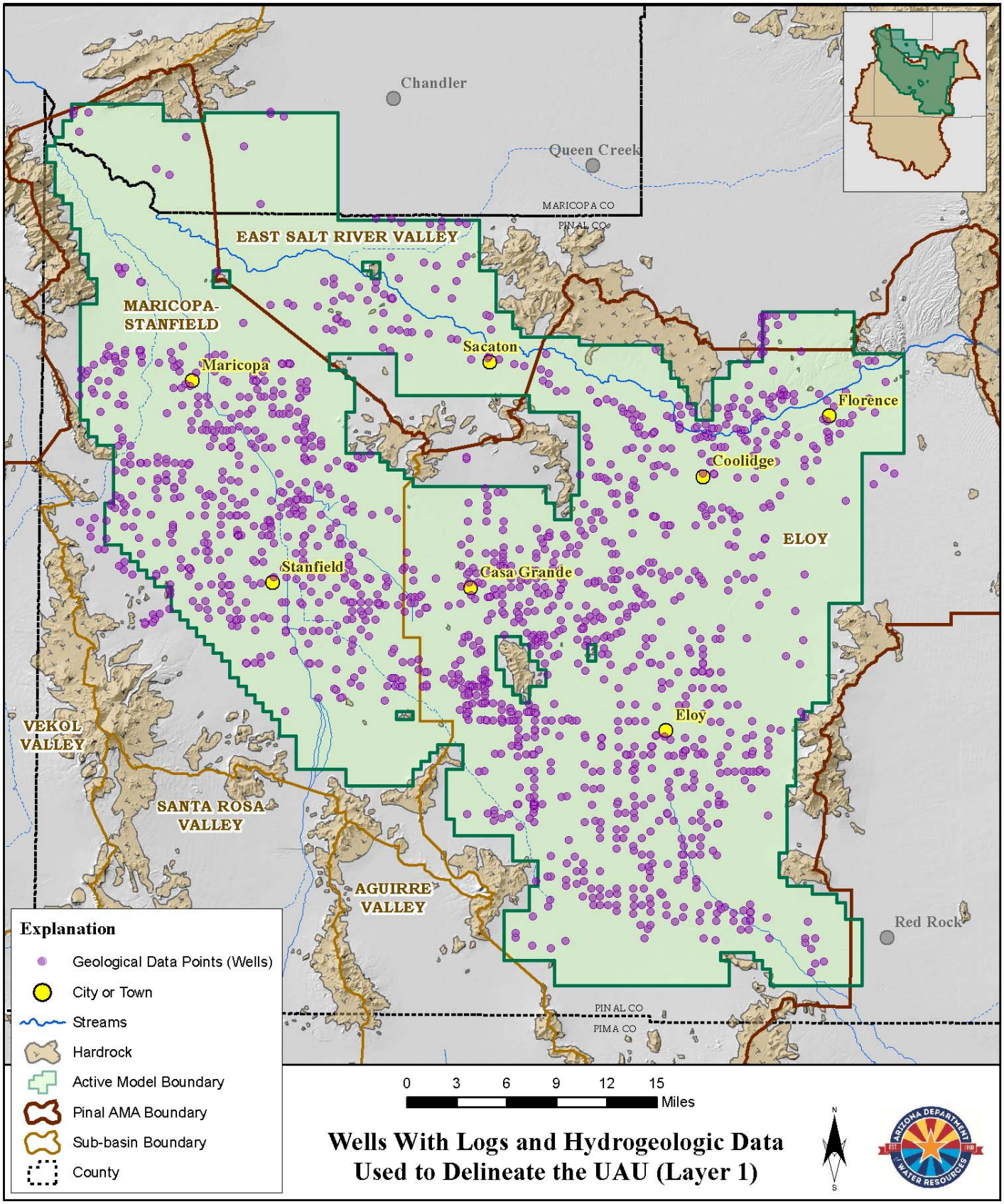

Figure 4 Wells With Logs and Hydrogeologic Data Used to Delineate the UAU (Layer 1)

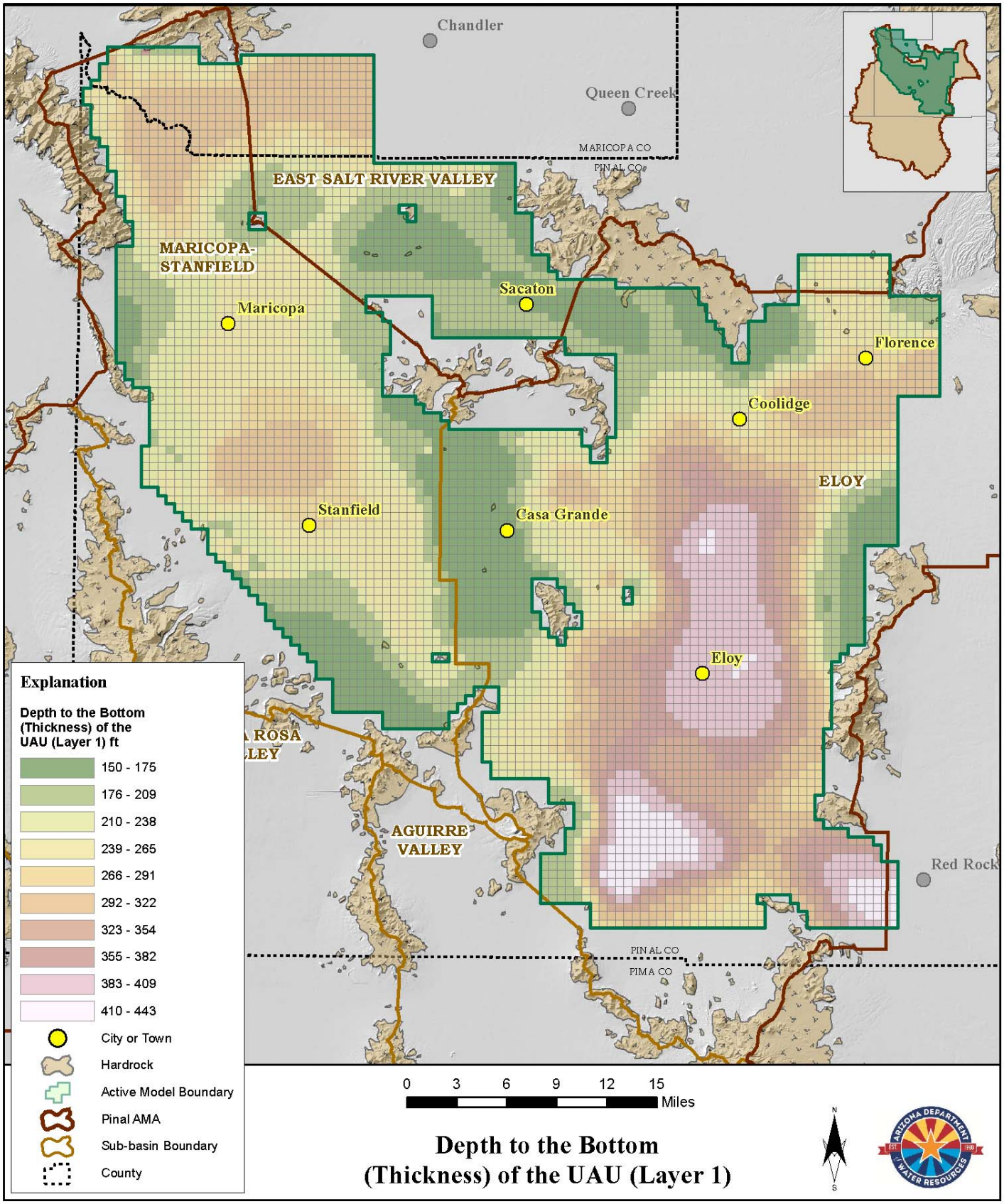

Figure 5 Depth to the Bottom (Thickness) of the UAU (Layer 1)

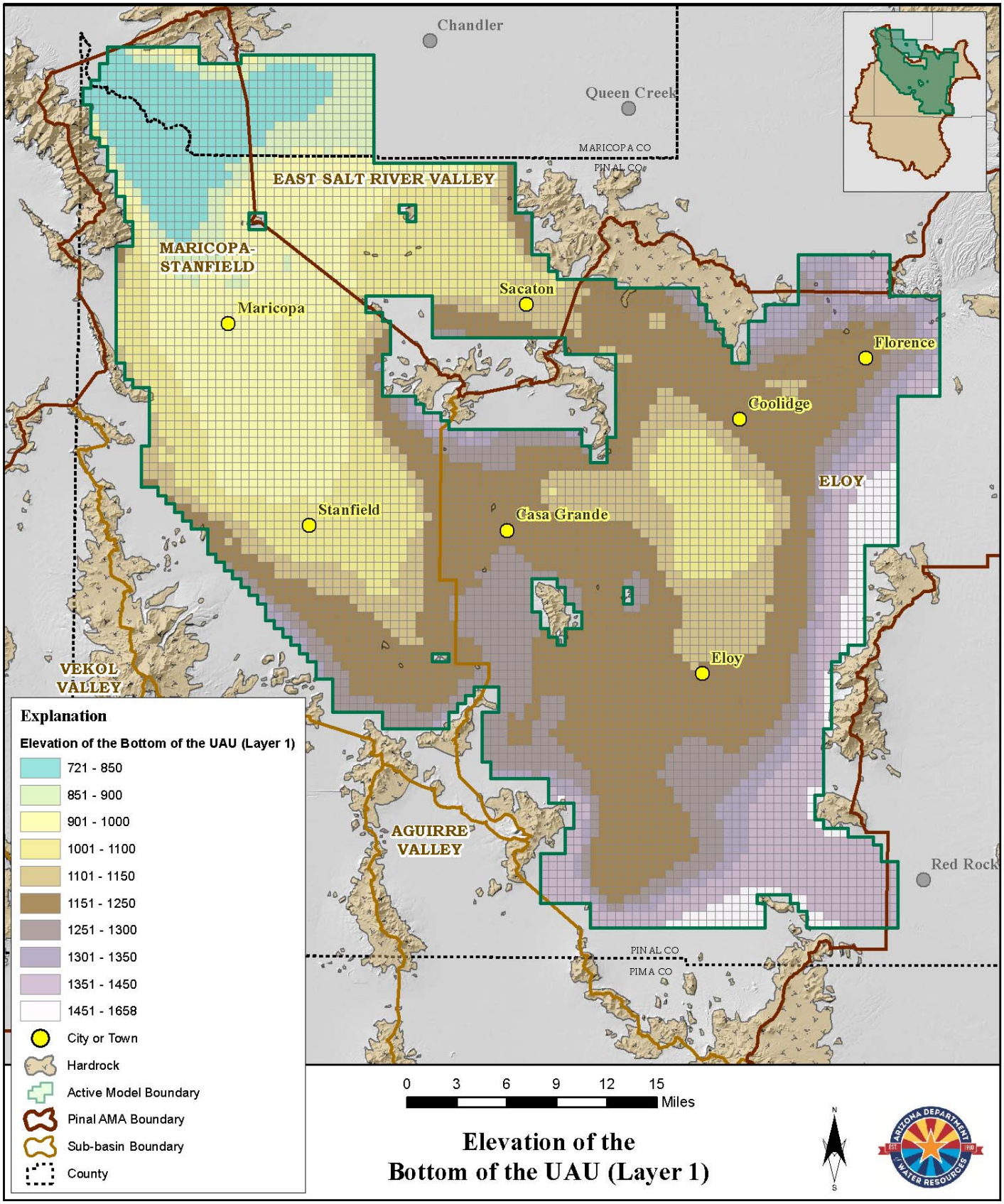

Figure 6 Elevation of the Bottom of the UAU (Layer 1)

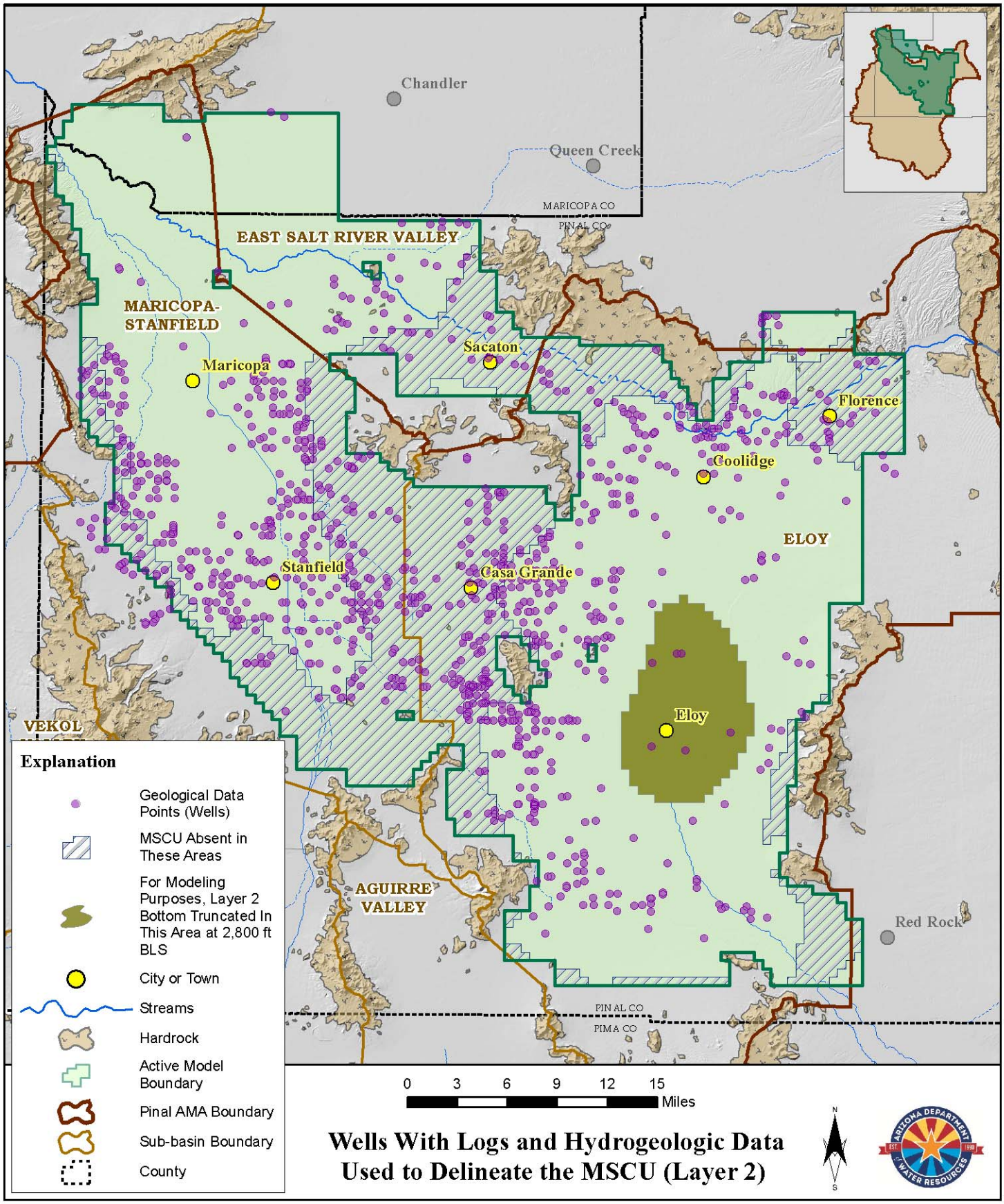

Figure 7 Wells With Logs and Hydrogeologic Data Used to Delineate the MSCU (Layer 2)

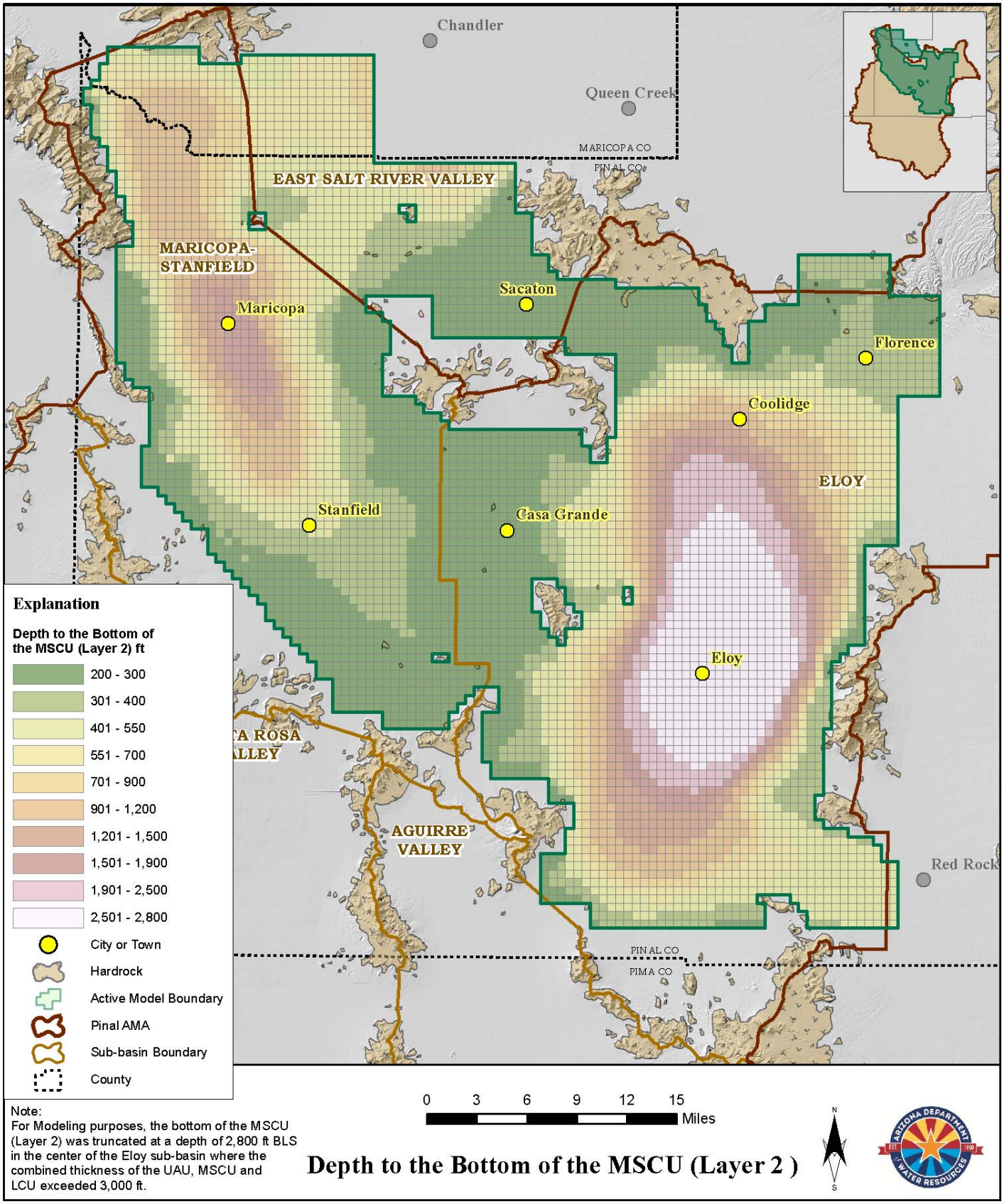

Figure 8 Depth to the Bottom of the MSCU (Layer 2)

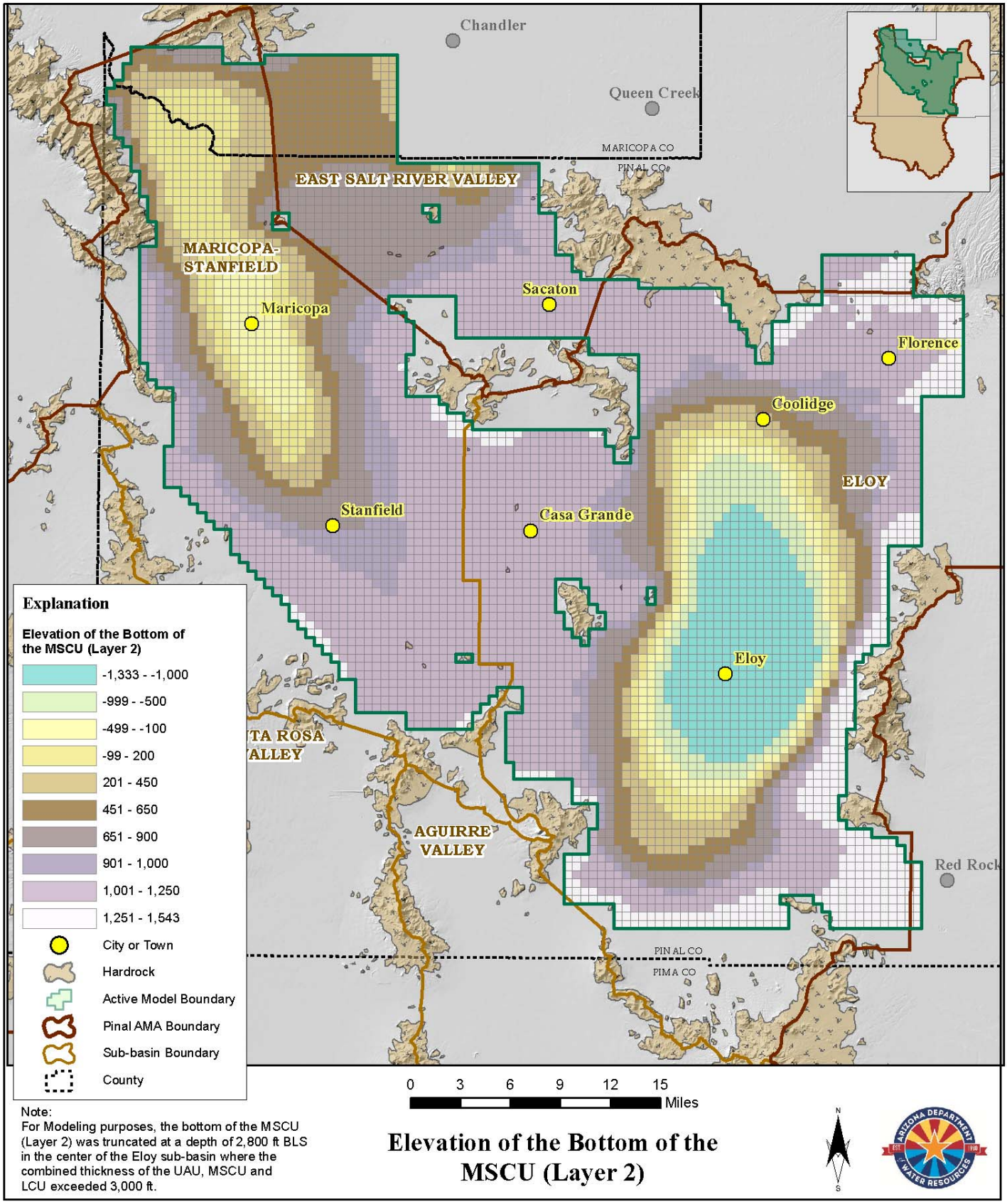

Figure 9 Elevation of the Bottom of the MSCU (Layer 2)

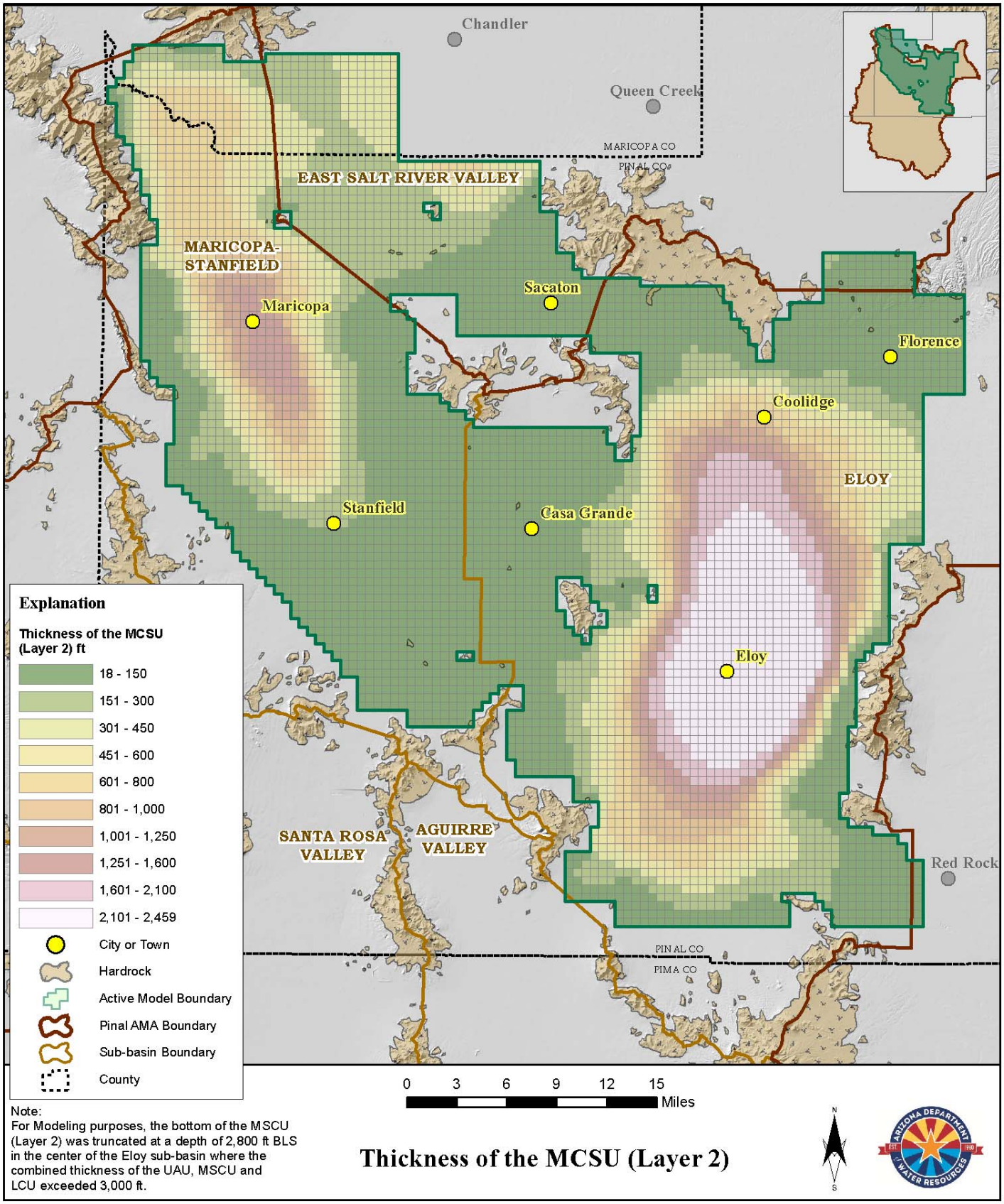

Figure 10 Thickness of the MSCU (Layer 2)

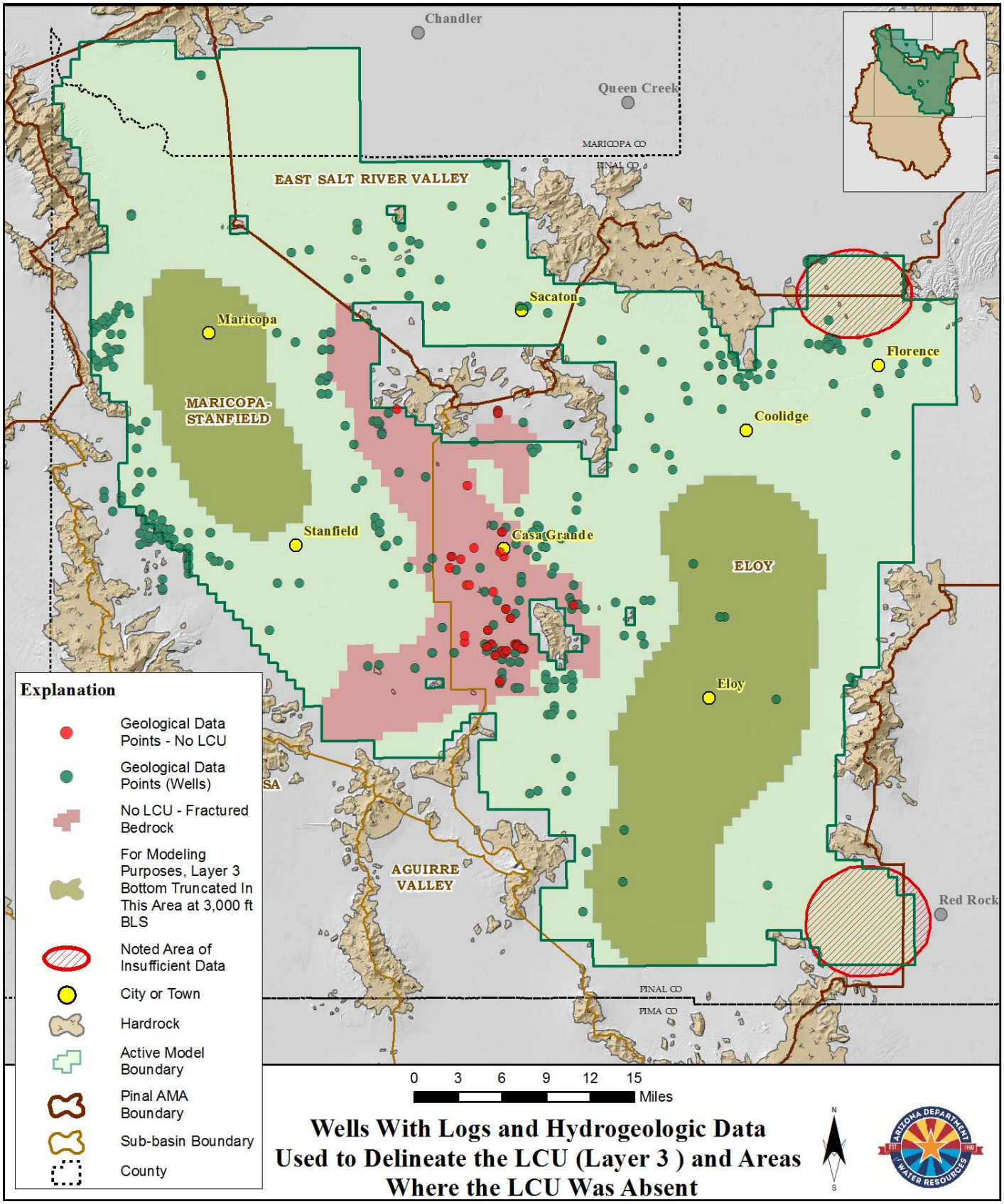

Figure 11 Wells With Logs and Hydrogeologic Data Used to Delineate the LCU (Layer 3) and Areas Where the LCU Was Absent.

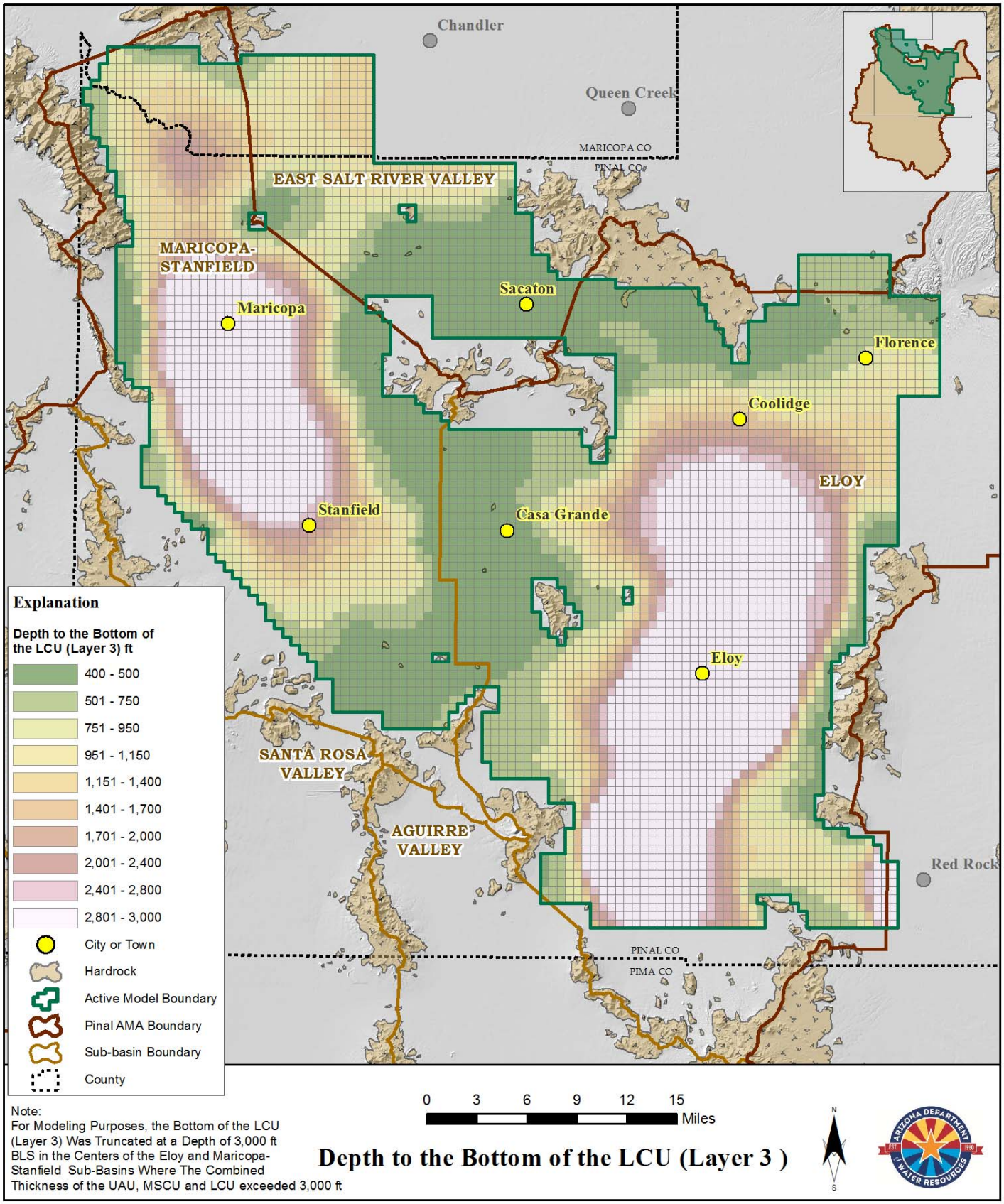

Note:
For Modeling Purposes, the Bottom of the LCU (Layer 3) Was Truncated at a Depth of 3,000 ft BLS in the Centers of the Eloy and Maricopa-Stanfield Sub-Basins Where The Combined Thickness of the UAU, MSCU and LCU exceeded 3,000 ft

Figure 12 Depth to the Bottom of the LCU (Layer 3)

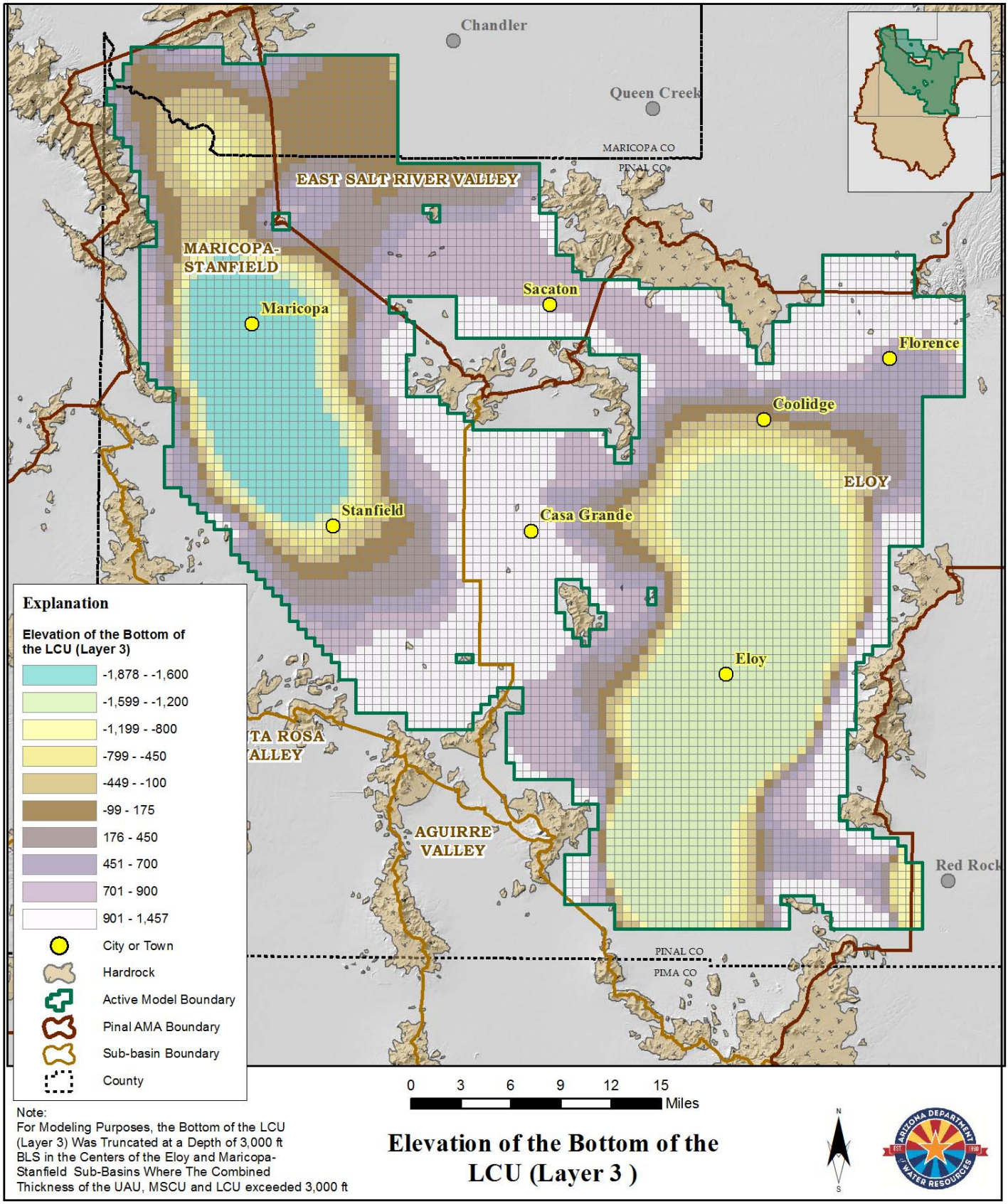

Figure 13 Elevation of the Bottom of the LCU (Layer 3)

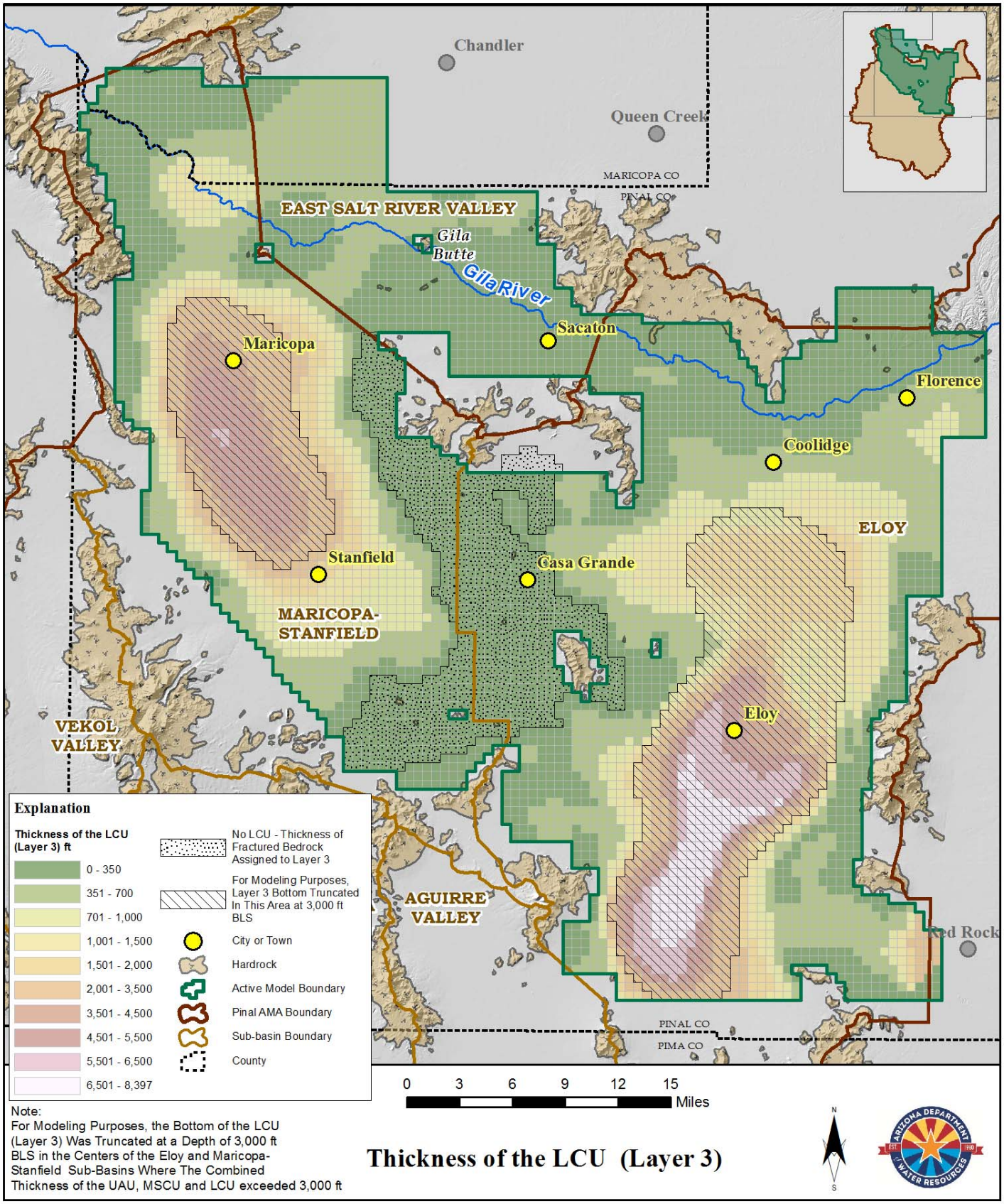

Figure 14 Thickness of the LCU (Layer 3)

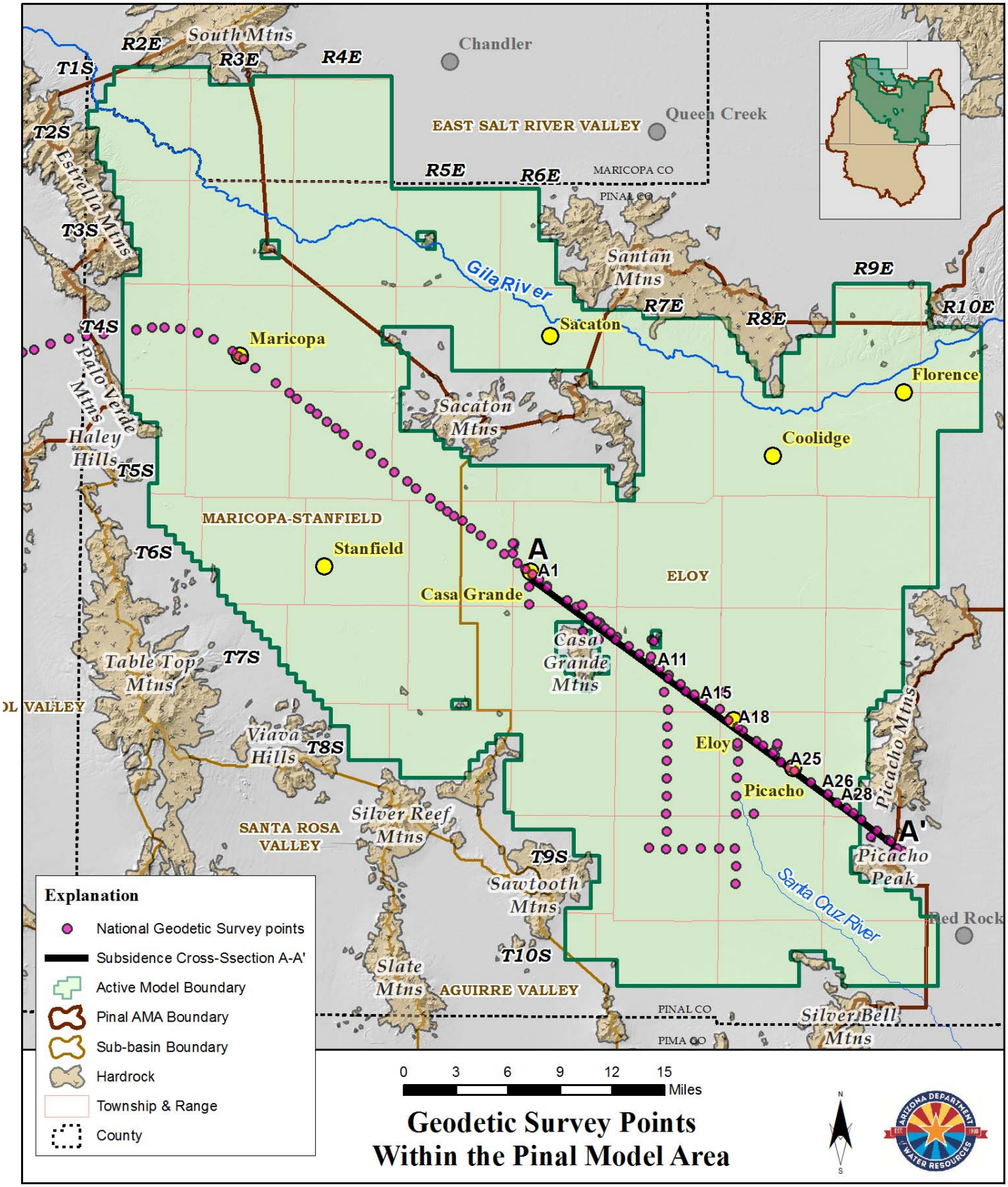

Figure 15 Geodetic Survey Points Within the Pinal Model Area

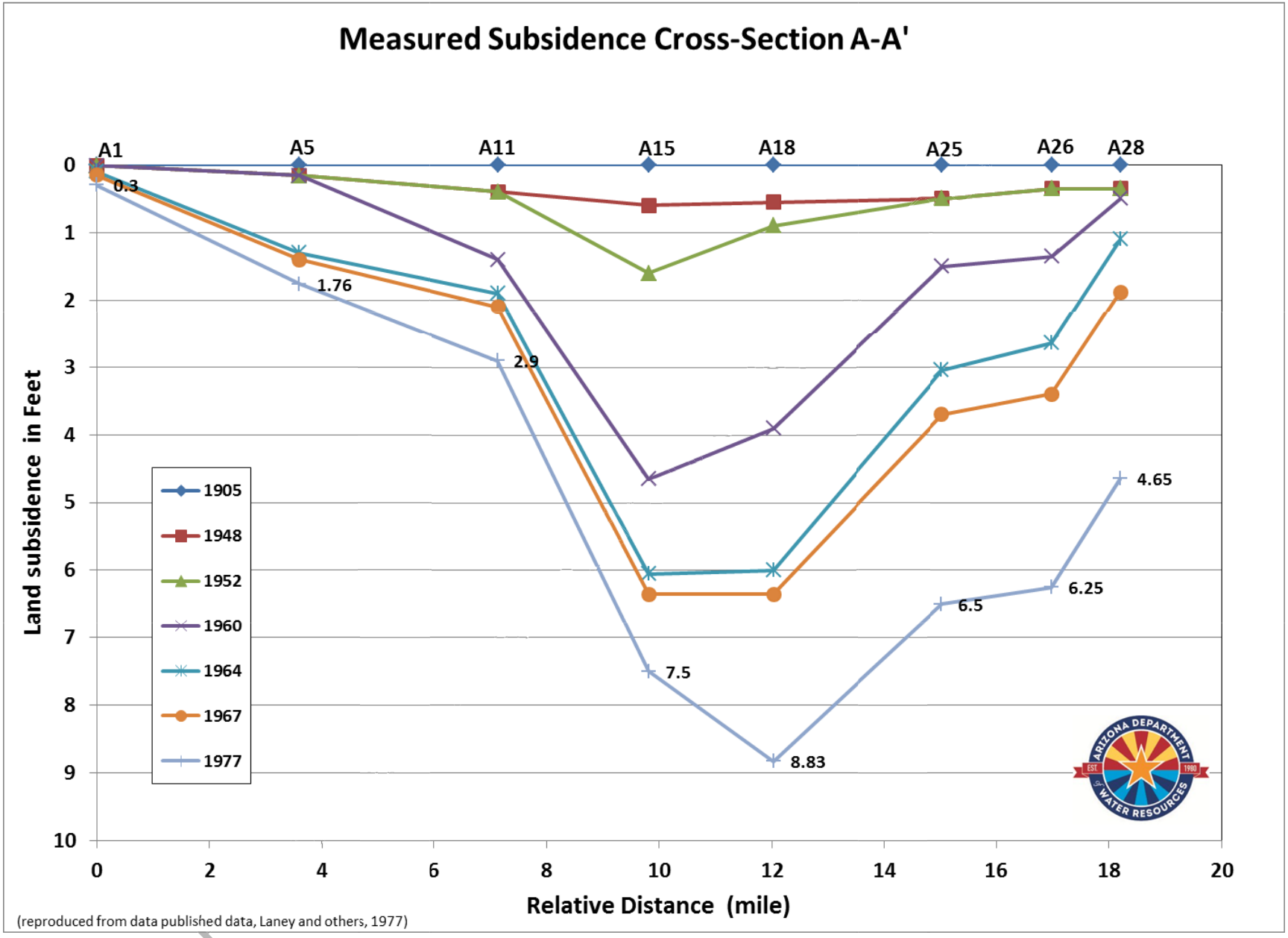

Figure 16 Measured Subsidence Cross-Section A-A'

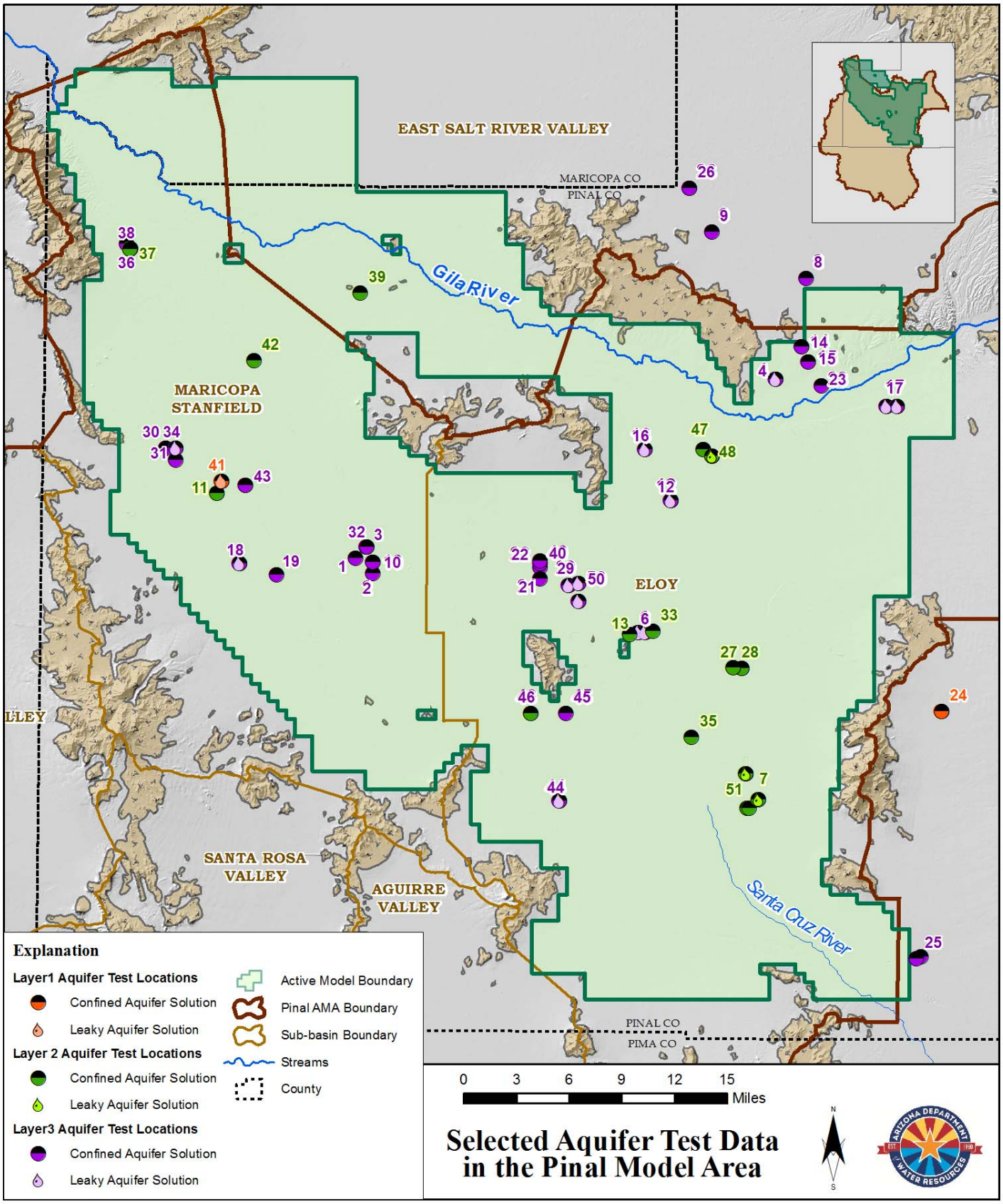

Figure 17 Selected Aquifer Test Data in the Pinal Model Area

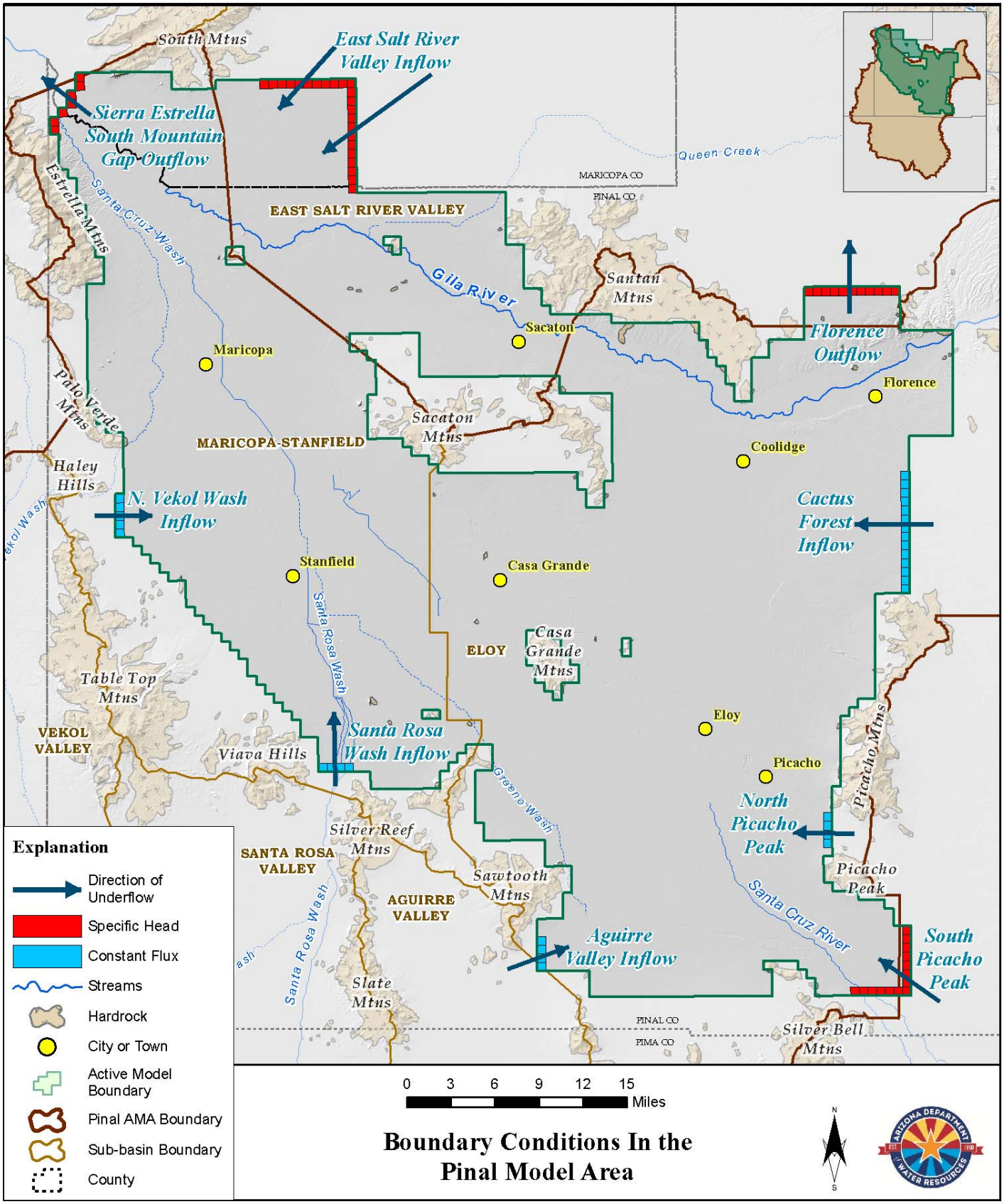

Figure 18 Boundary Conditions in the Pinal Model Area

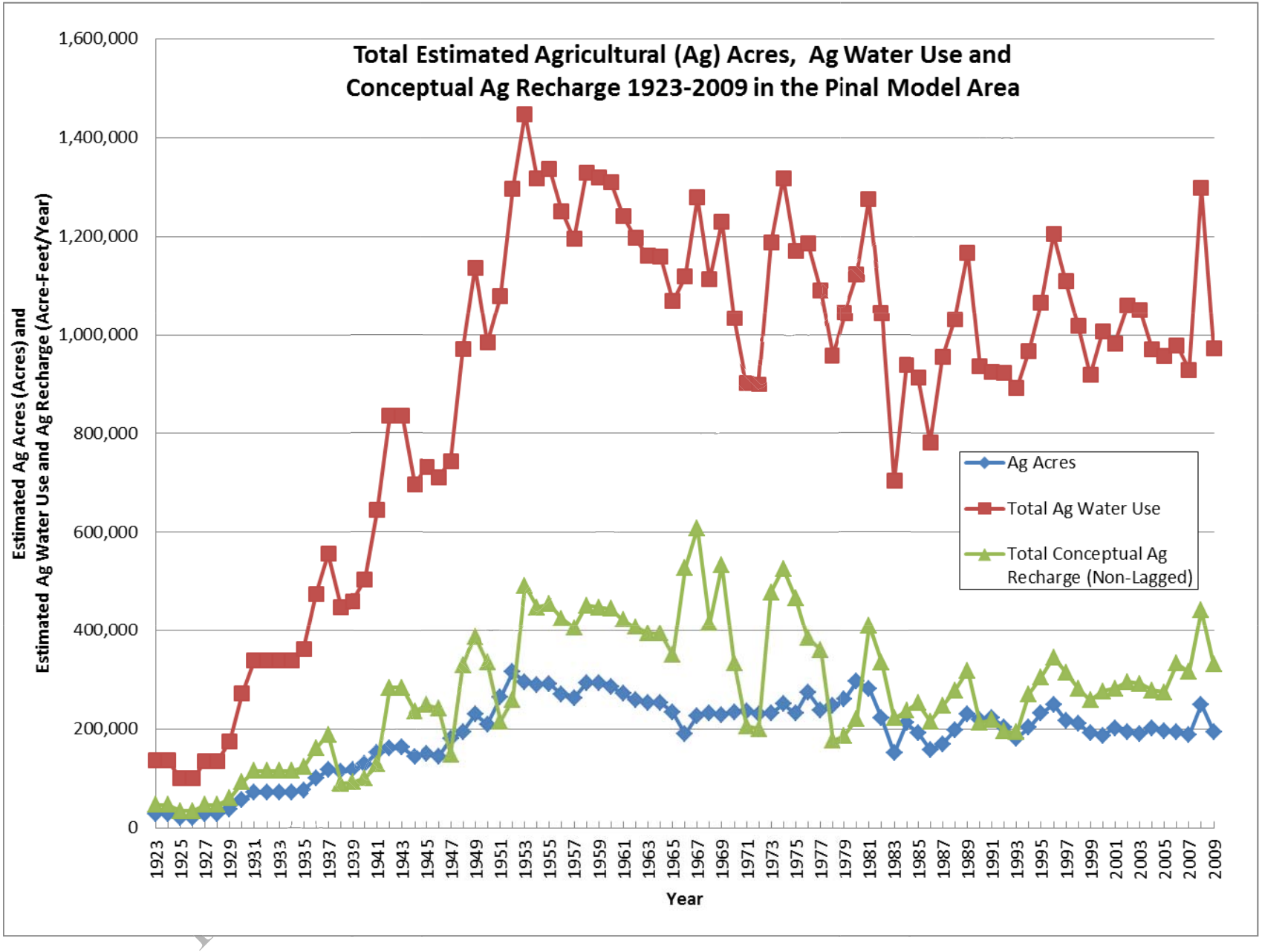

Figure 19 Total Estimated Agricultural Acres, Agricultural Water Use and Agricultural Recharge (1923 – 2009) in the Pinal Model Area

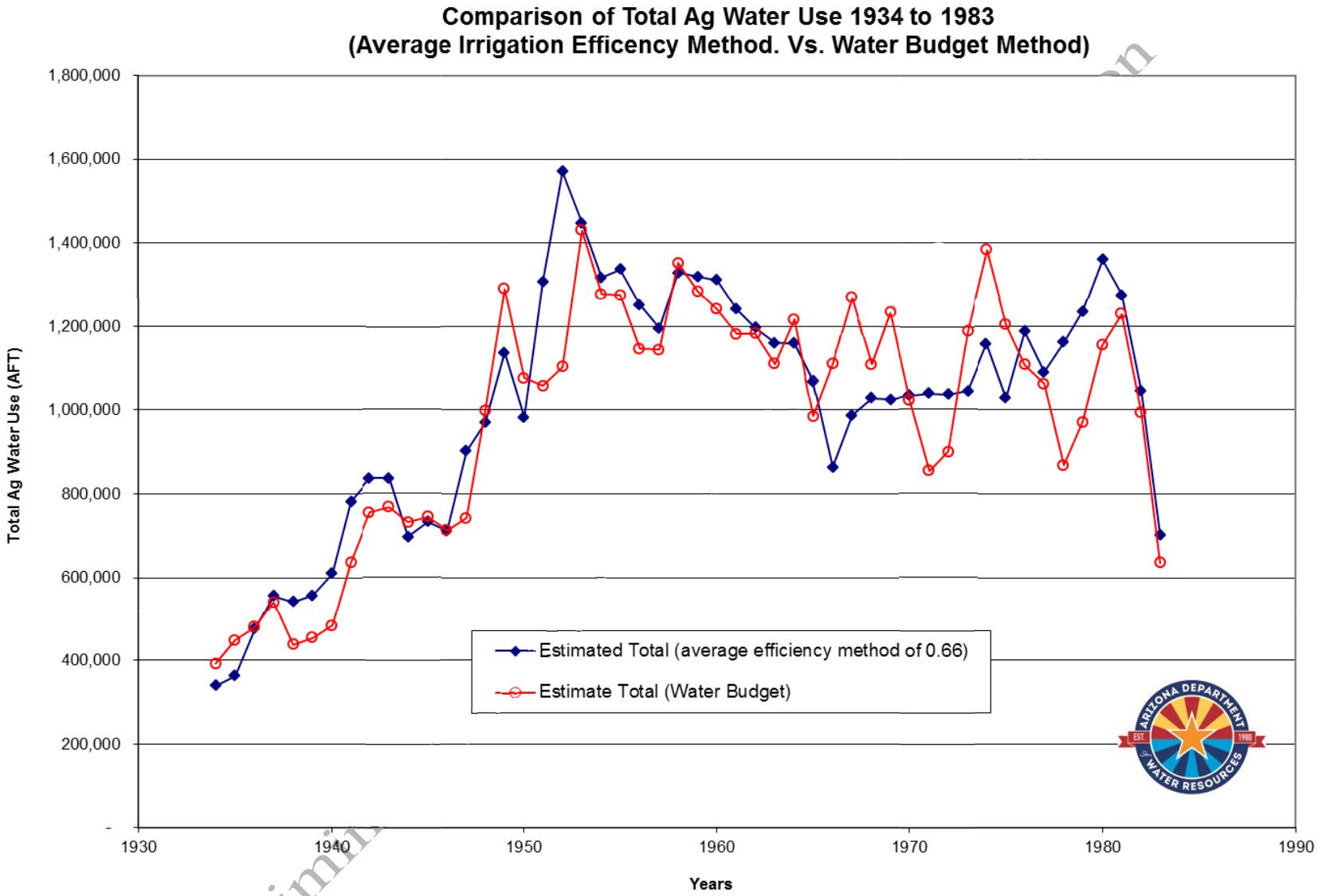

Figure 20 Comparison Of Total Agricultural Water Use Estimates in Pinal Model Area 1934 to 1983

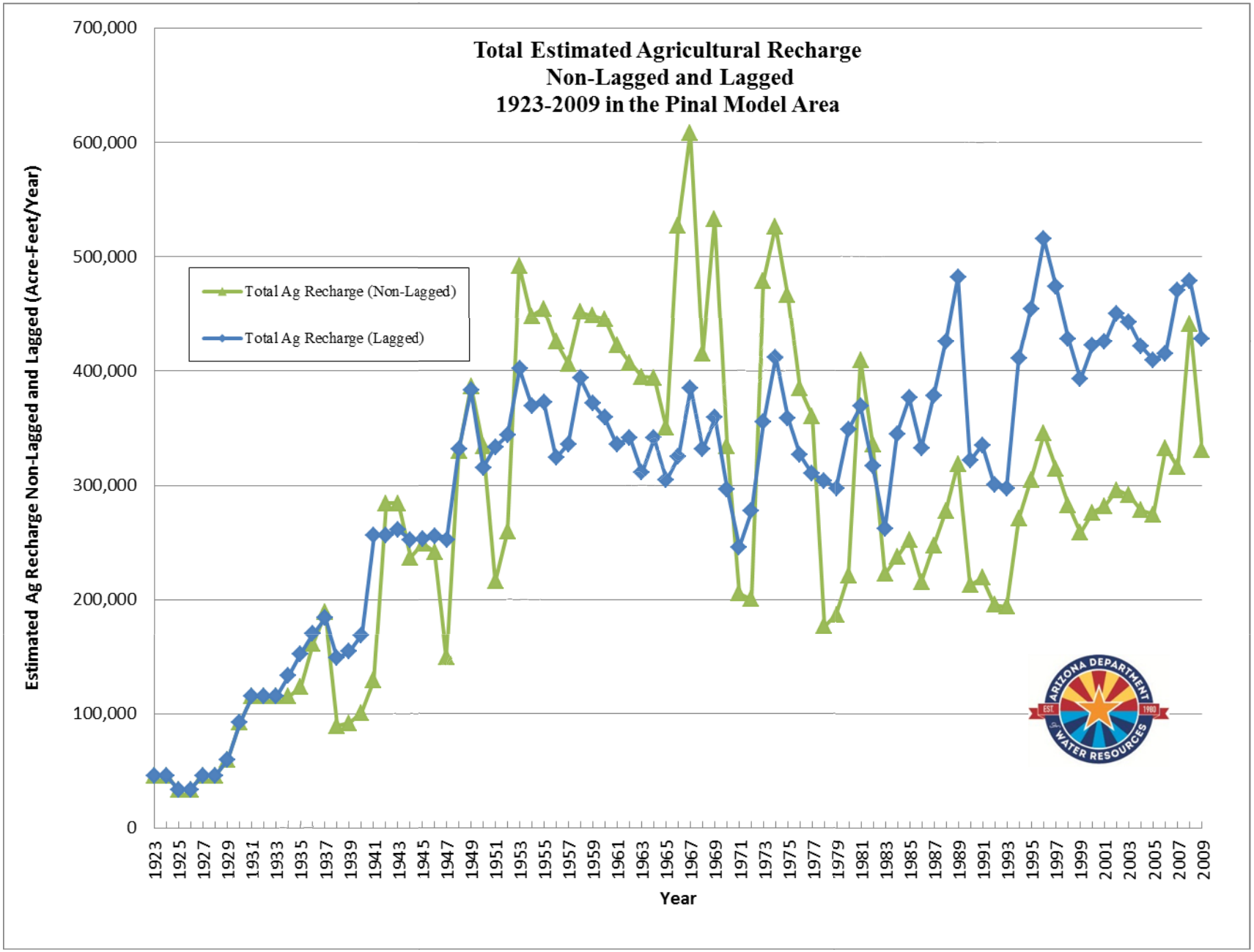

Figure 21 Total Estimated Agricultural Recharge in the Pinal Model Ares 1923-2009 (Lagged and Non-Lagged)

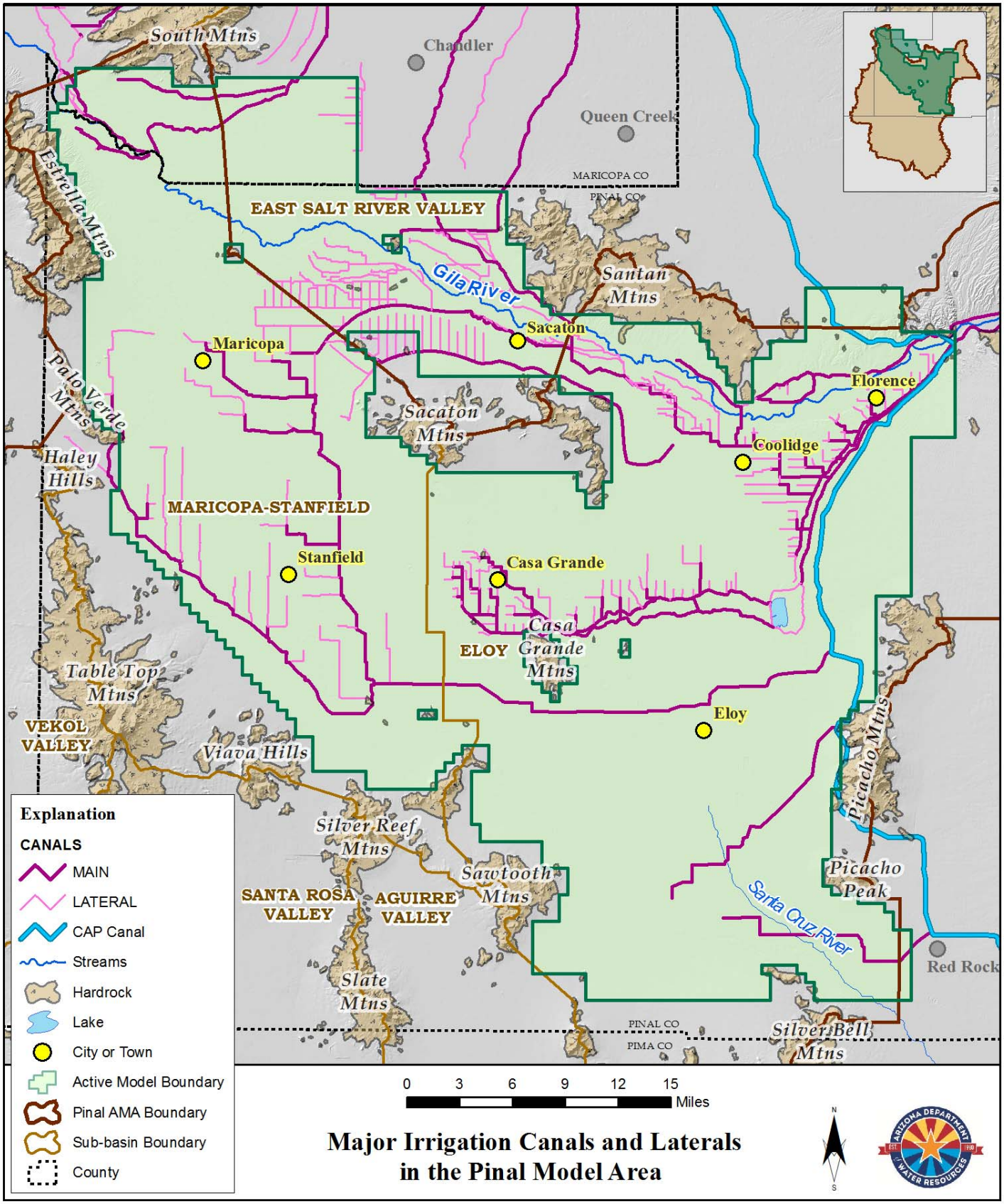

Major Irrigation Canals and Laterals in the Pinal Model Area

Figure 22 Major Irrigation Canals and Laterals in the Pinal Model Area

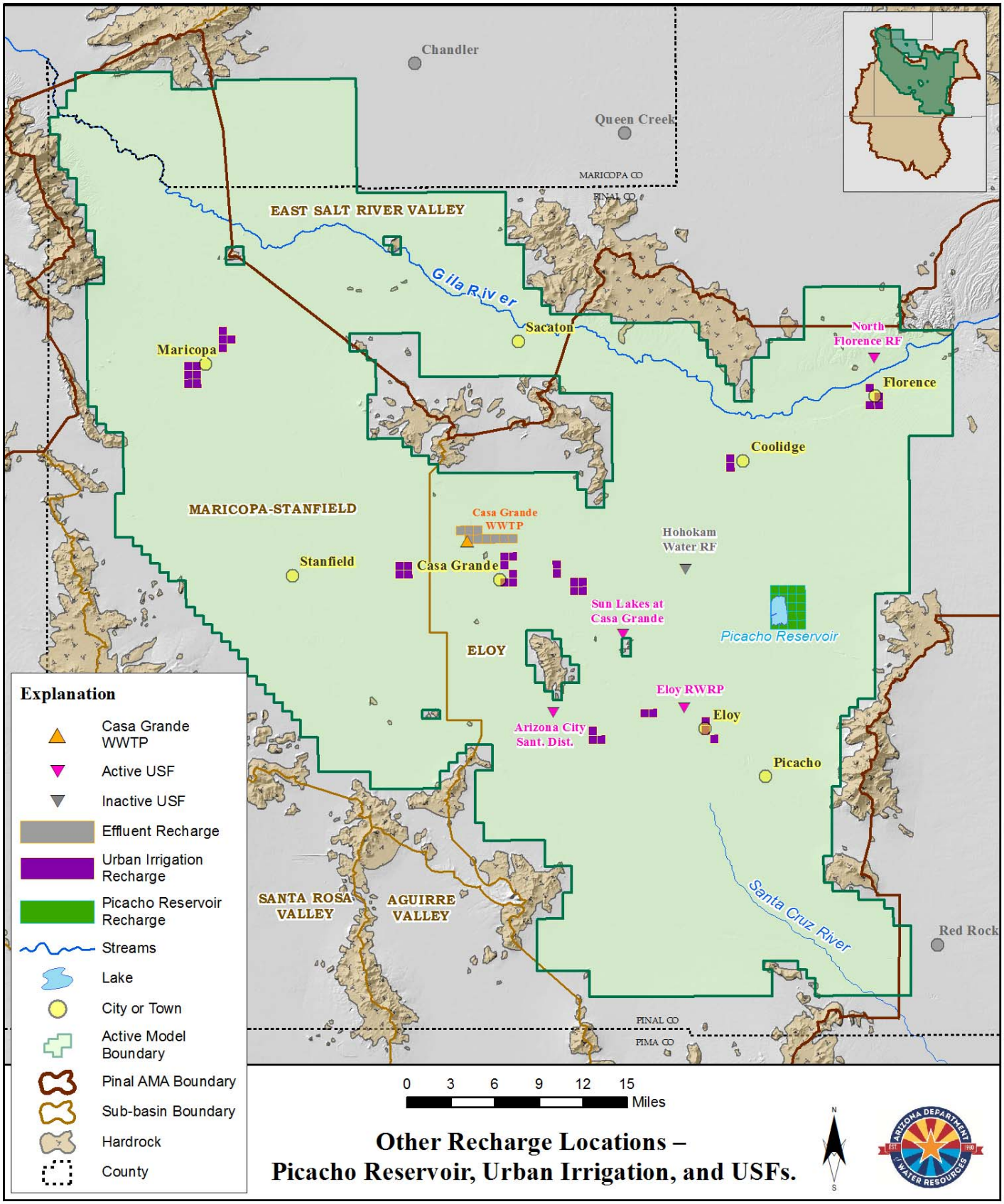

Figure 23 Other Recharge Locations – Picacho Reservoir, Urban Irrigation, and USFs.

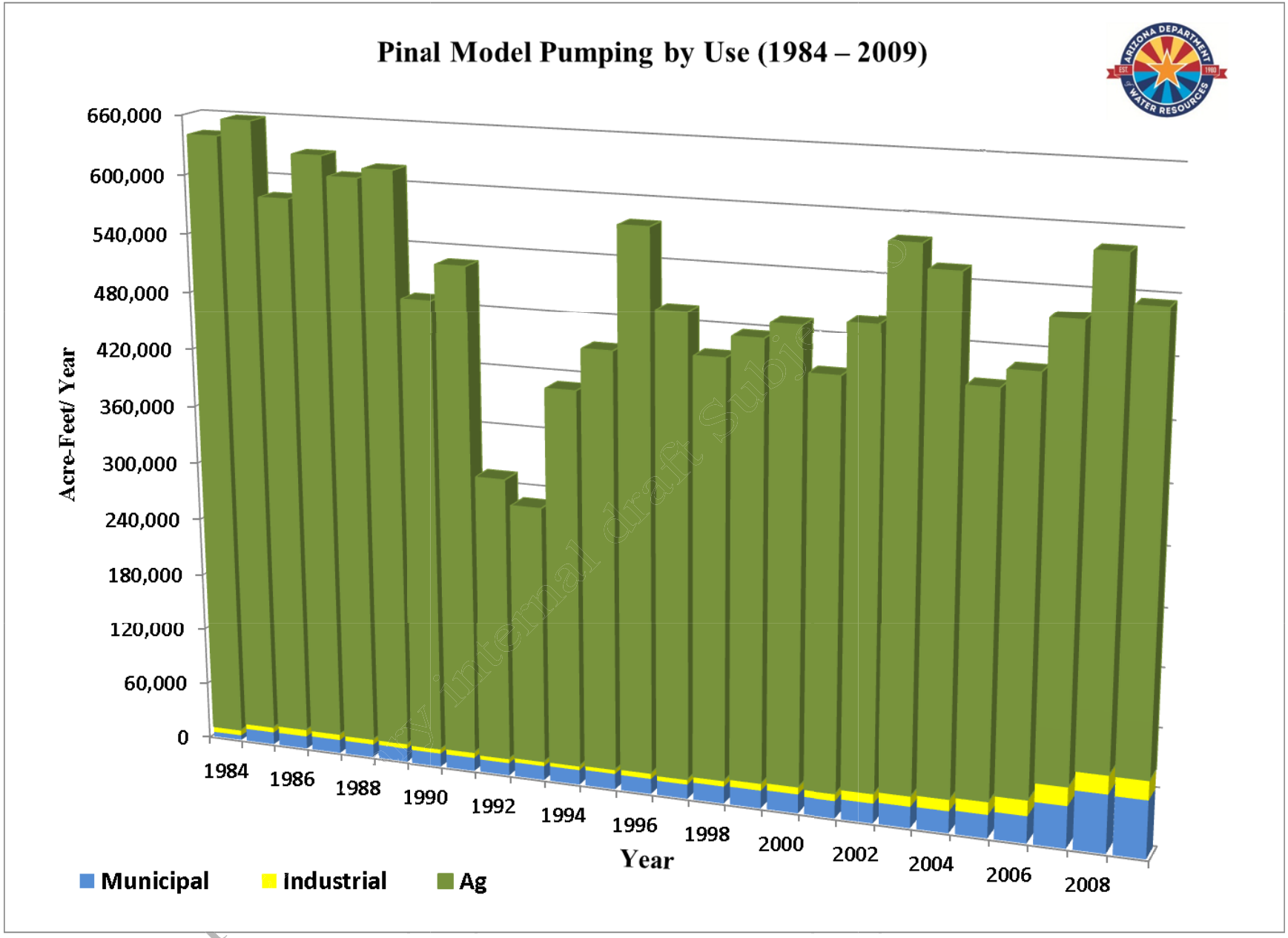

Figure 24 Pumping by Water Use for the Pinal Model Area from 1984 to 2009.

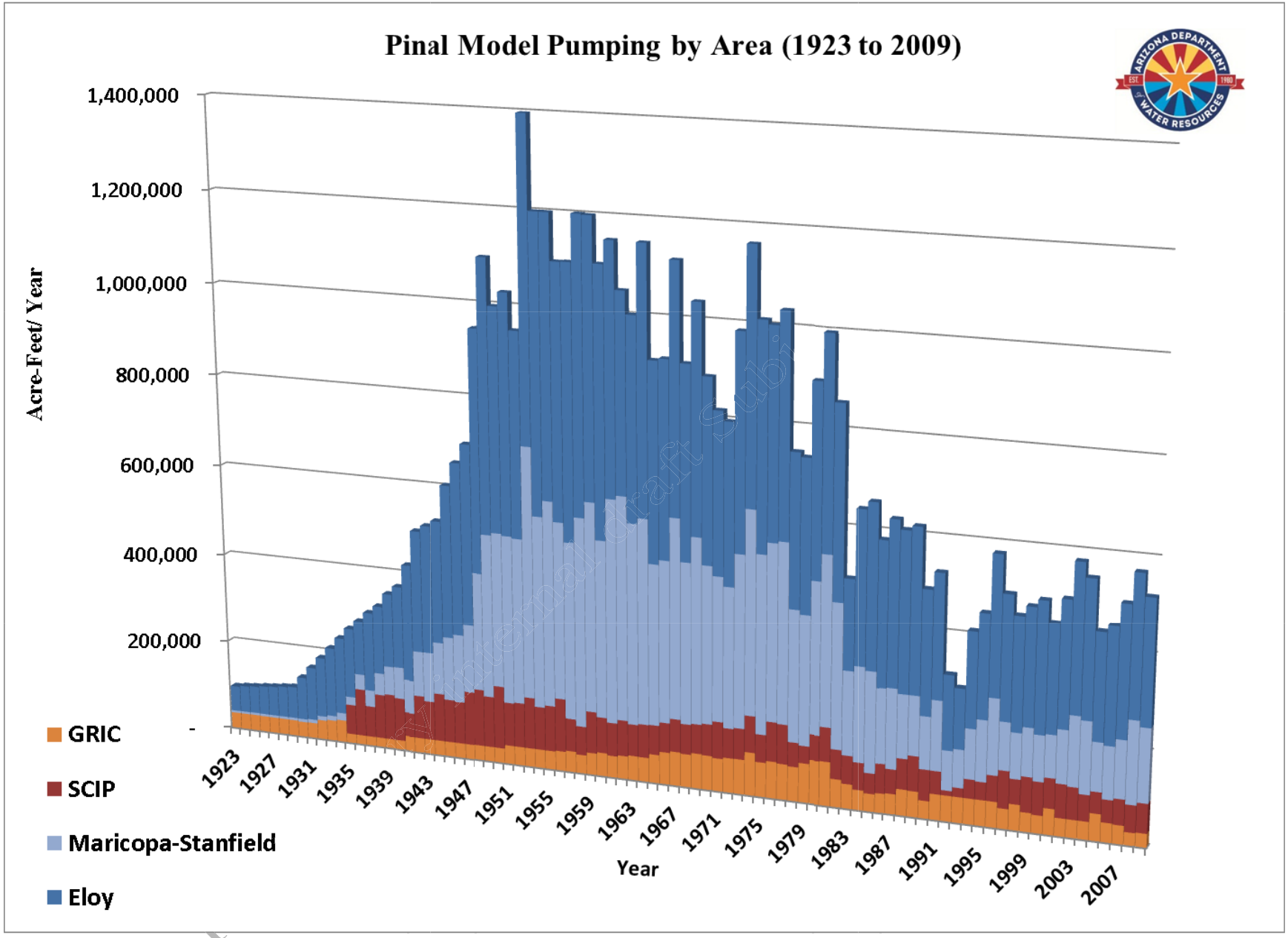

Figure 25 Pumping in the Pinal Model Area from 1923 to 2009

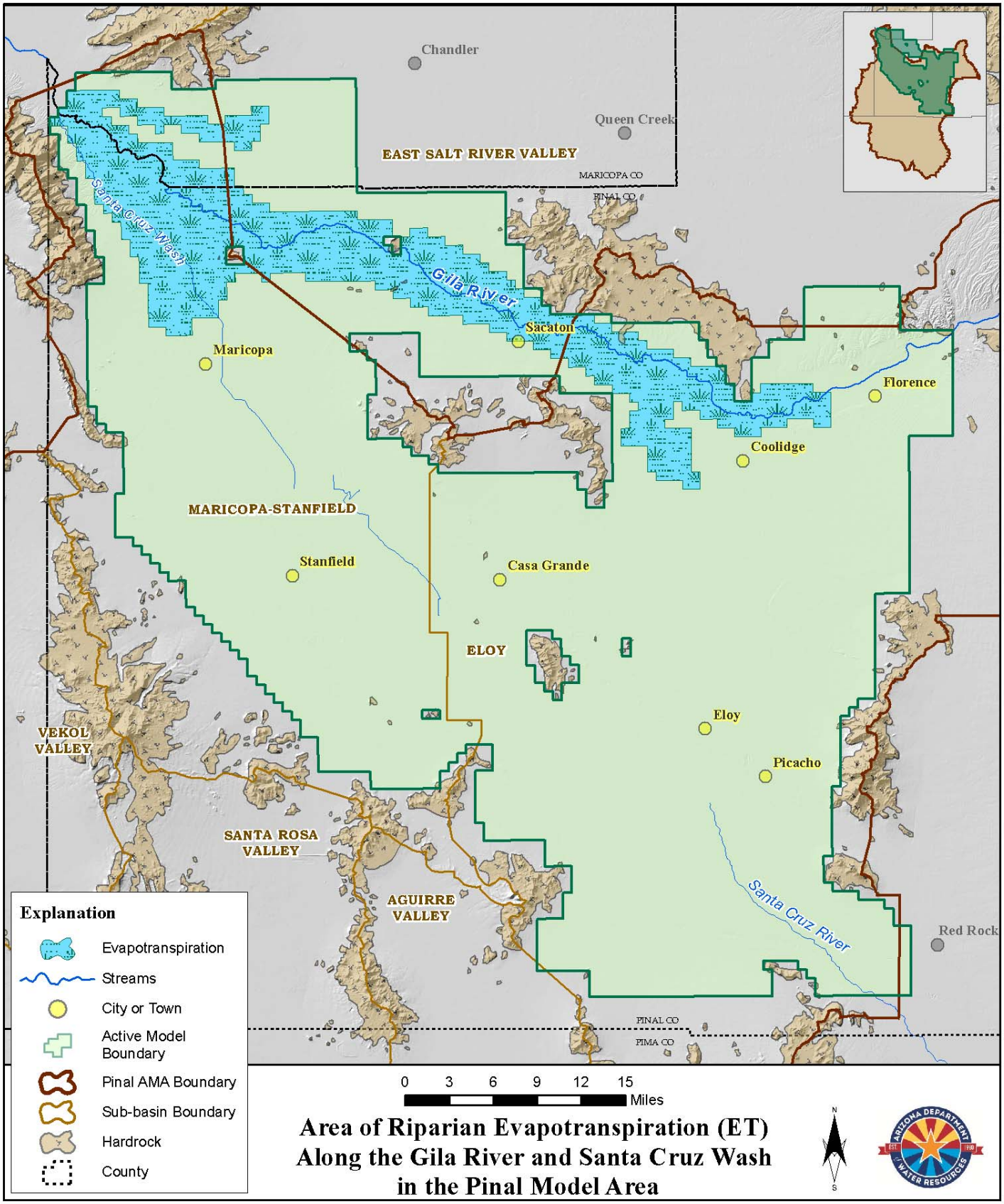

Figure 26 Area of Riparian Evapotranspiration (ET) Along the Gila River and Santa Cruz Wash in the Pinal Model Area

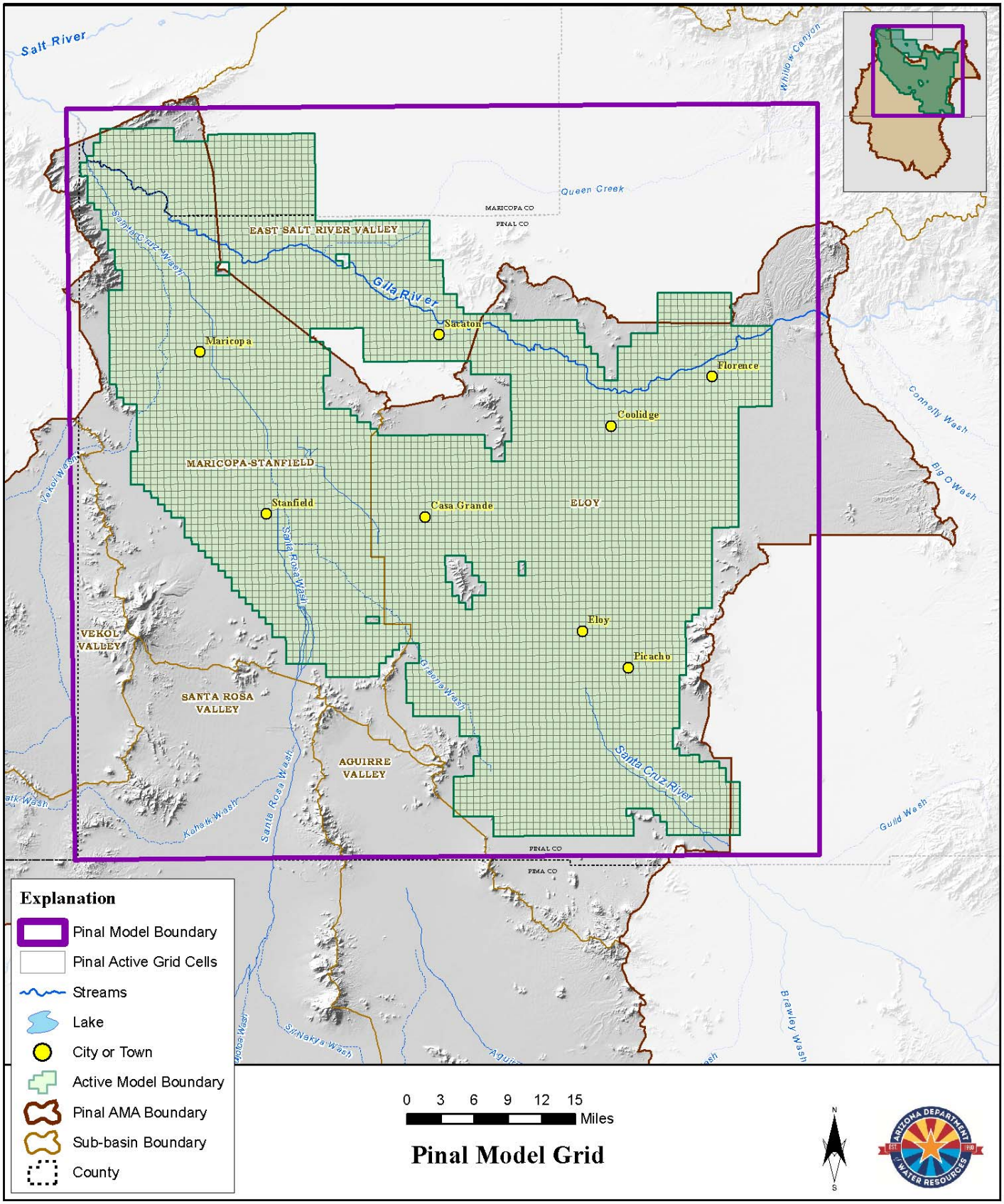

Figure 27 Pinal Model Grid

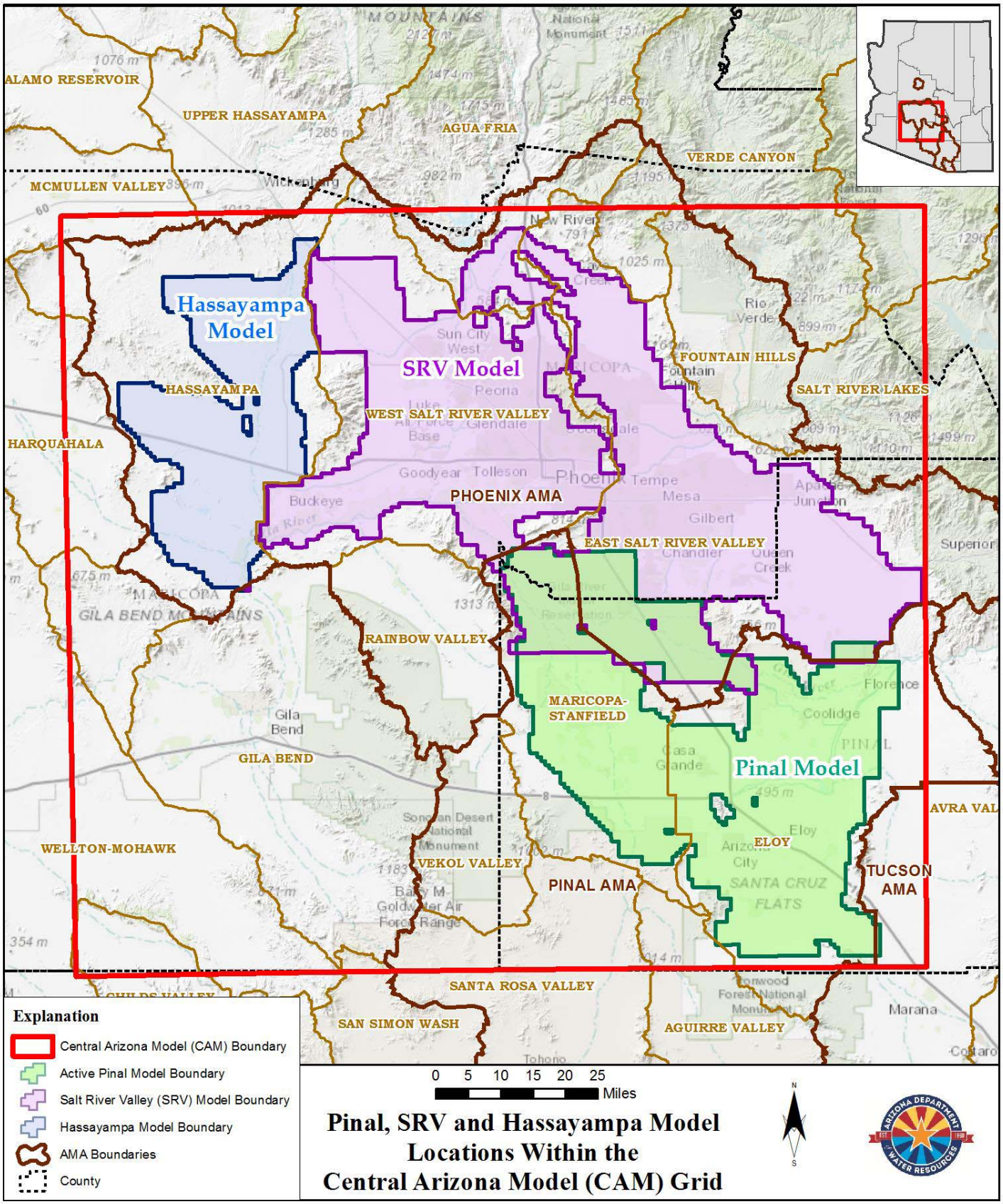

Figure 28 Pinal, SRV and Hassayampa Model Locations Within the Central Arizona Model (CAM) Grid

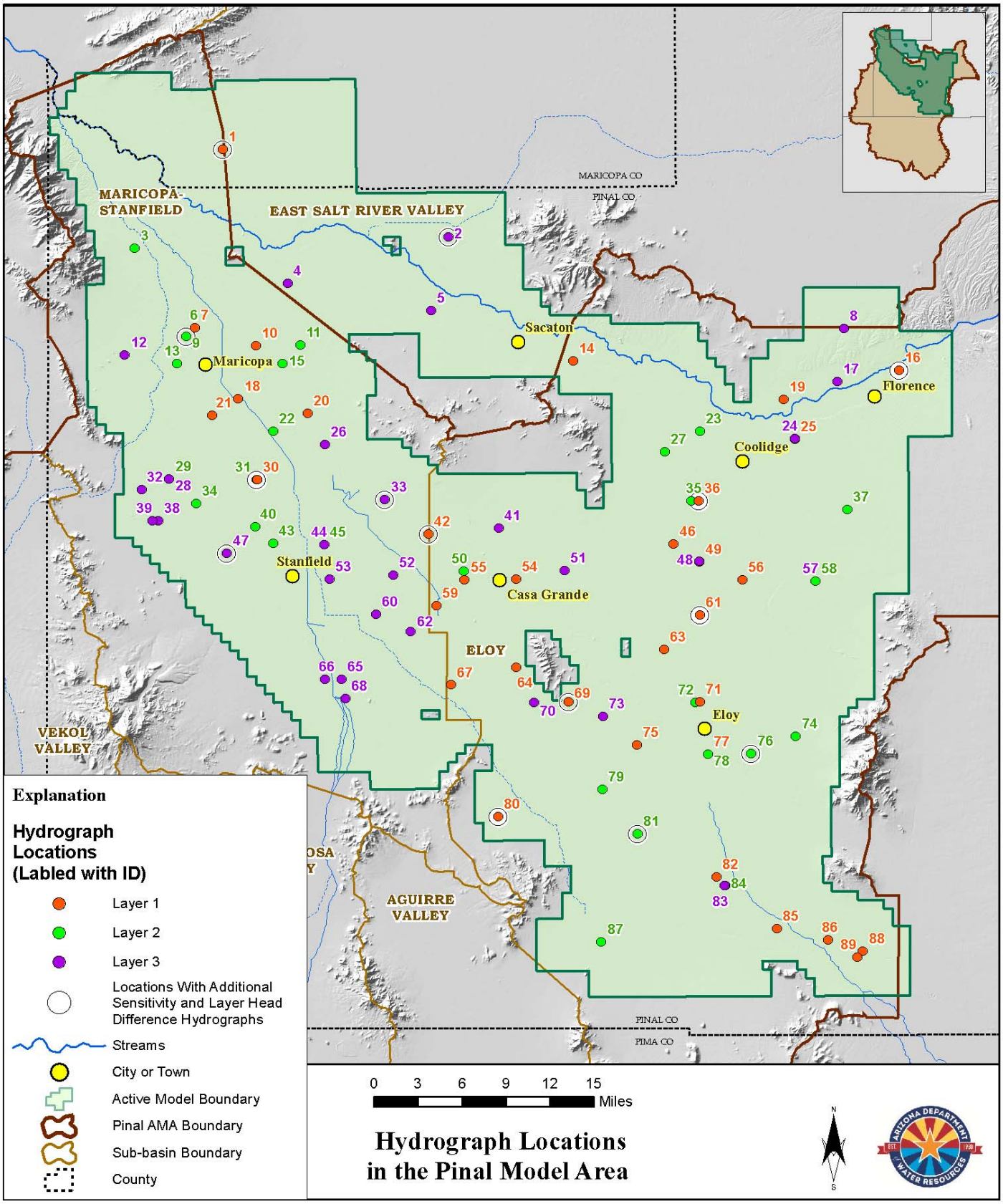

Figure 29 Hydrograph Locations in the Pinal Model Area

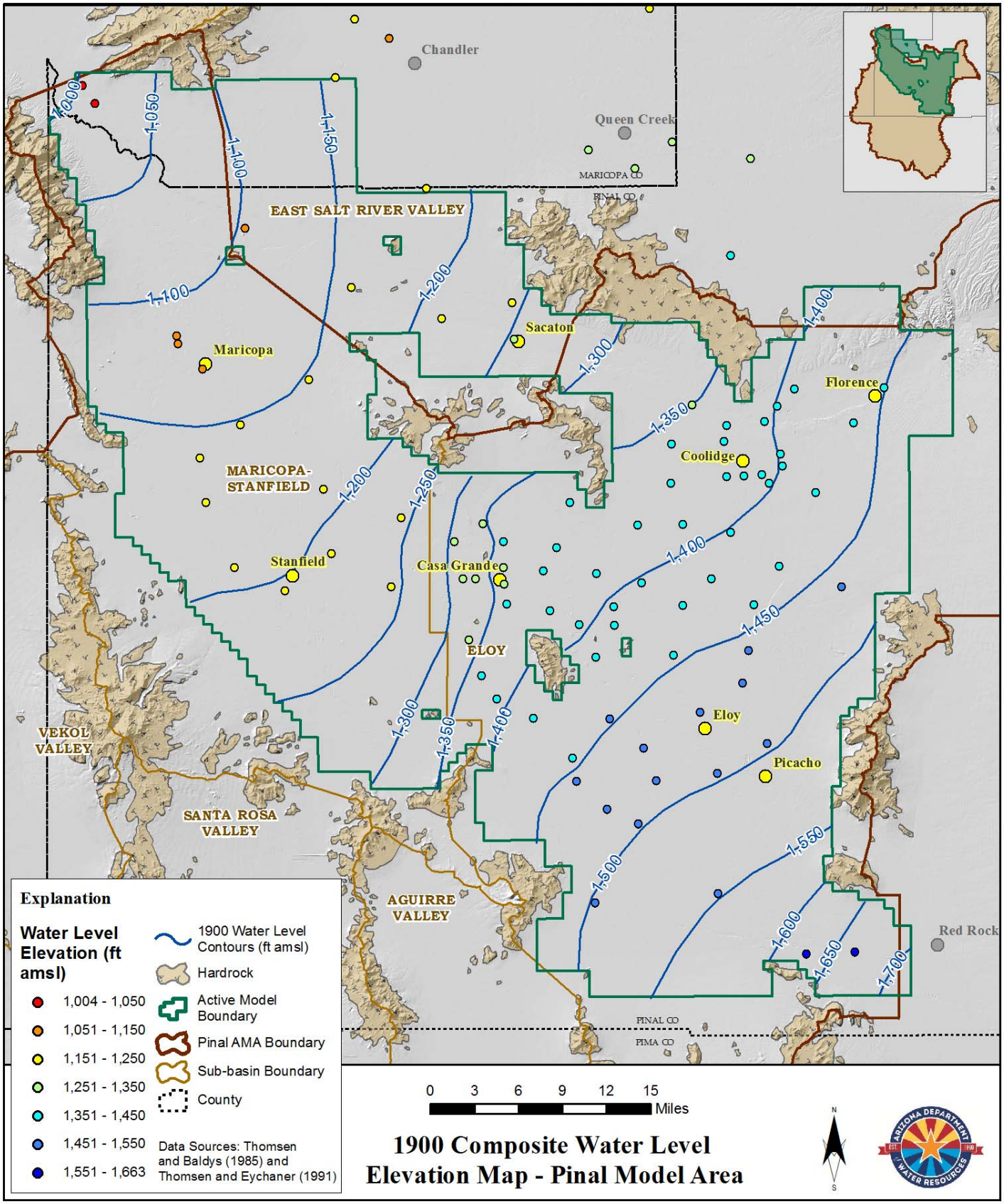

Figure 30 1900 Composite Water Level Elevation Map - Pinal Model Area

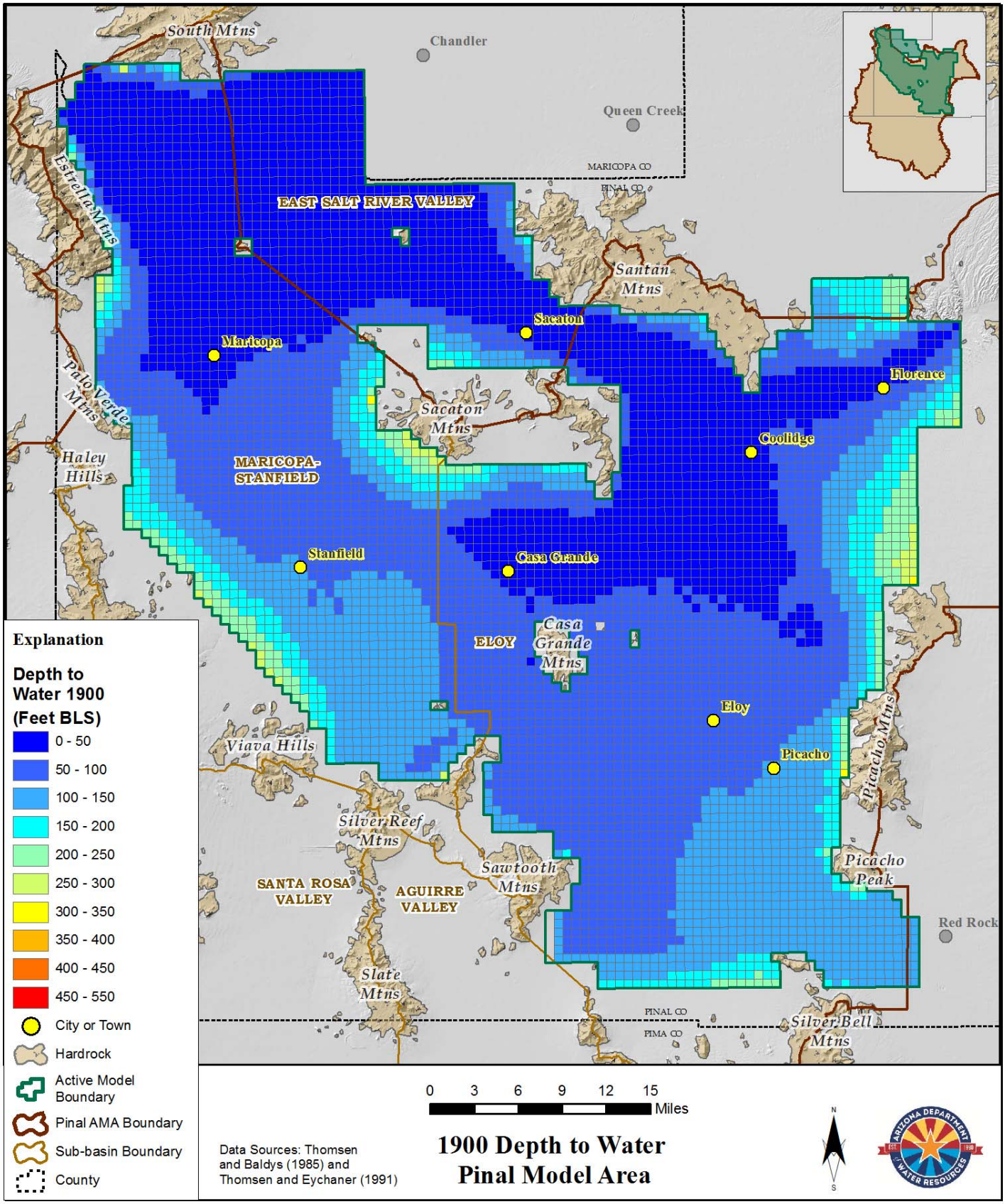

Figure 31 1900 Depth to Water - Pinal Model Area

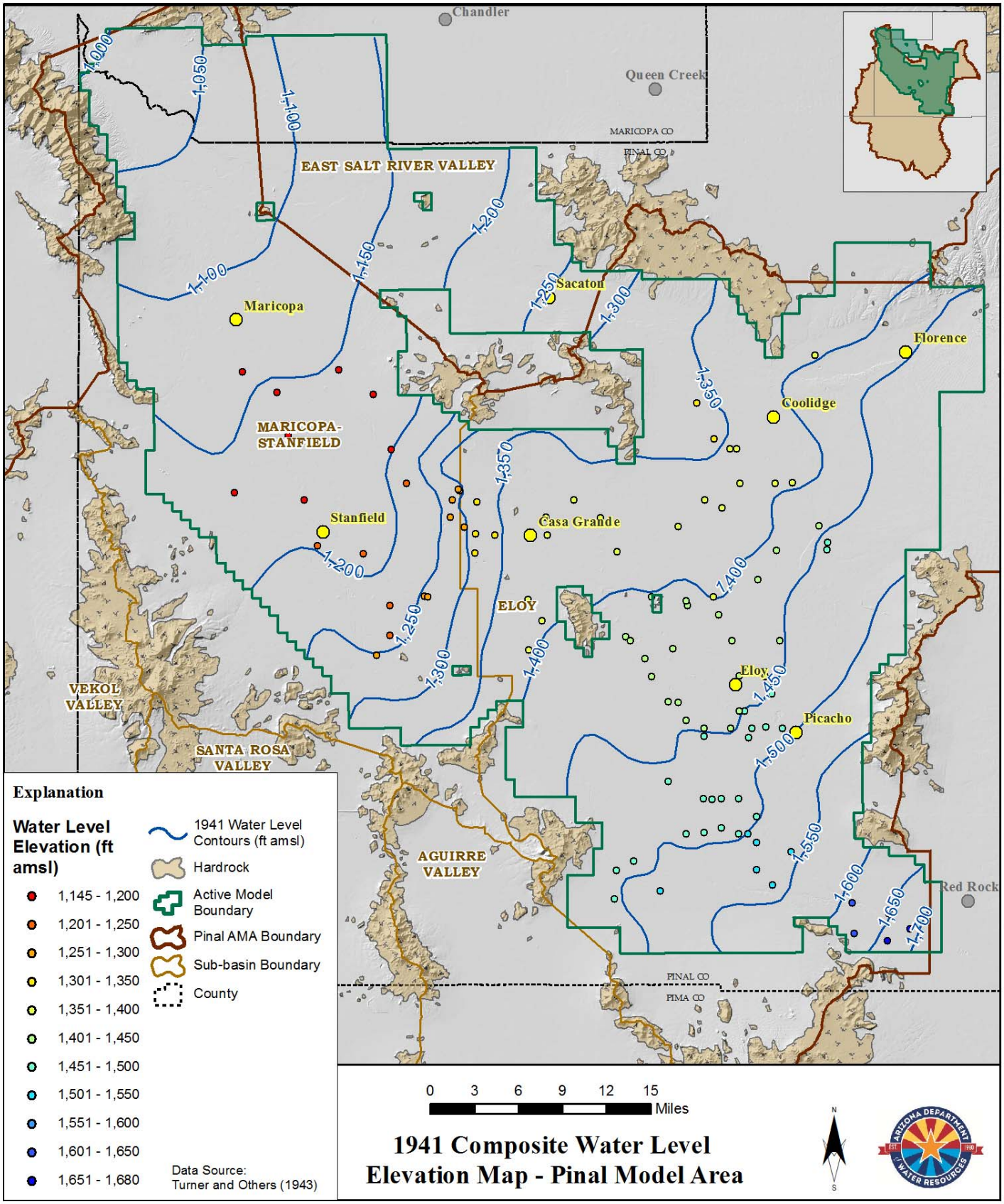

Figure 32 1941 Composite Water Level Elevation Map - Pinal Model Area

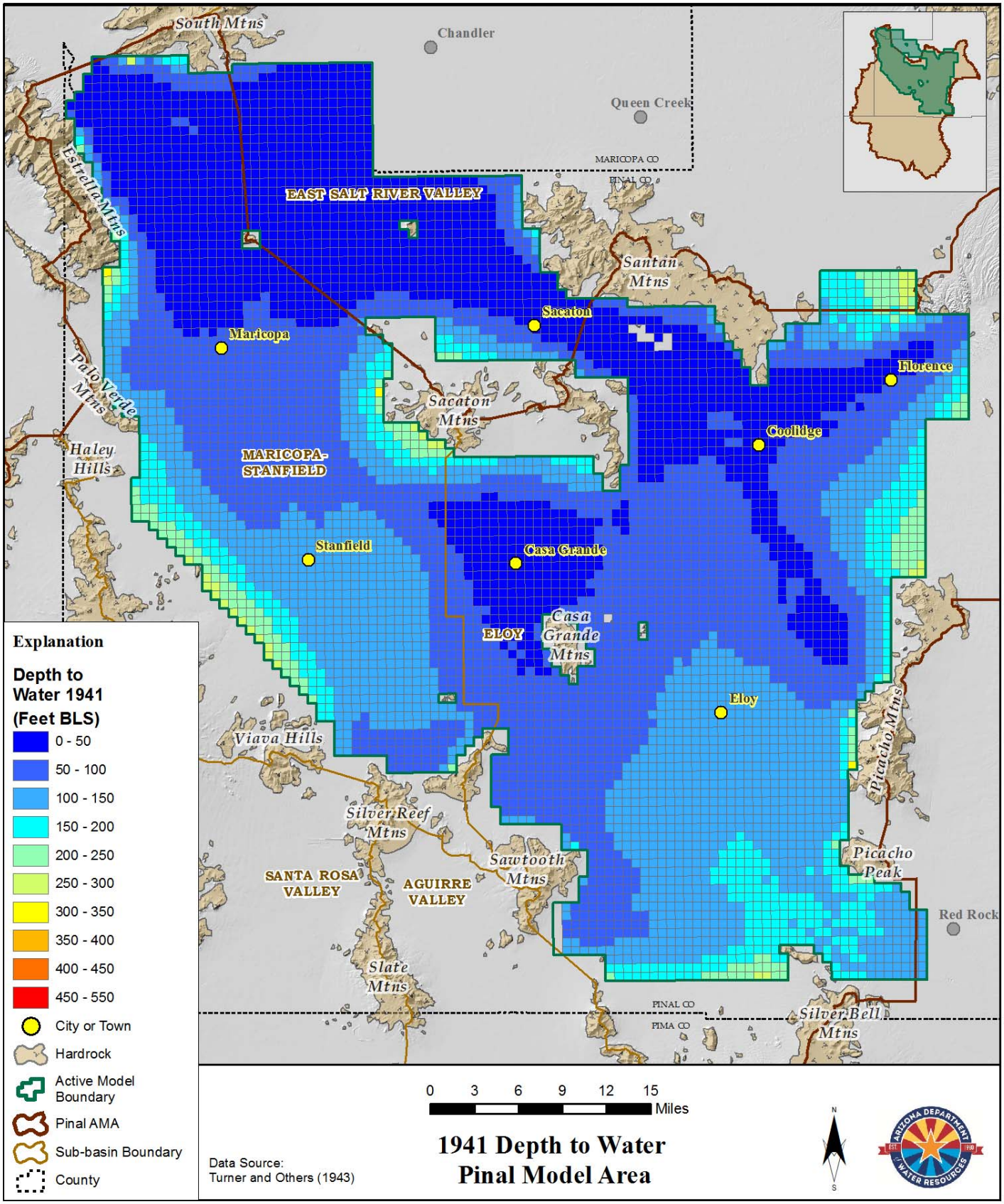

Figure 33 1941 Depth to Water Map - Pinal Model Area

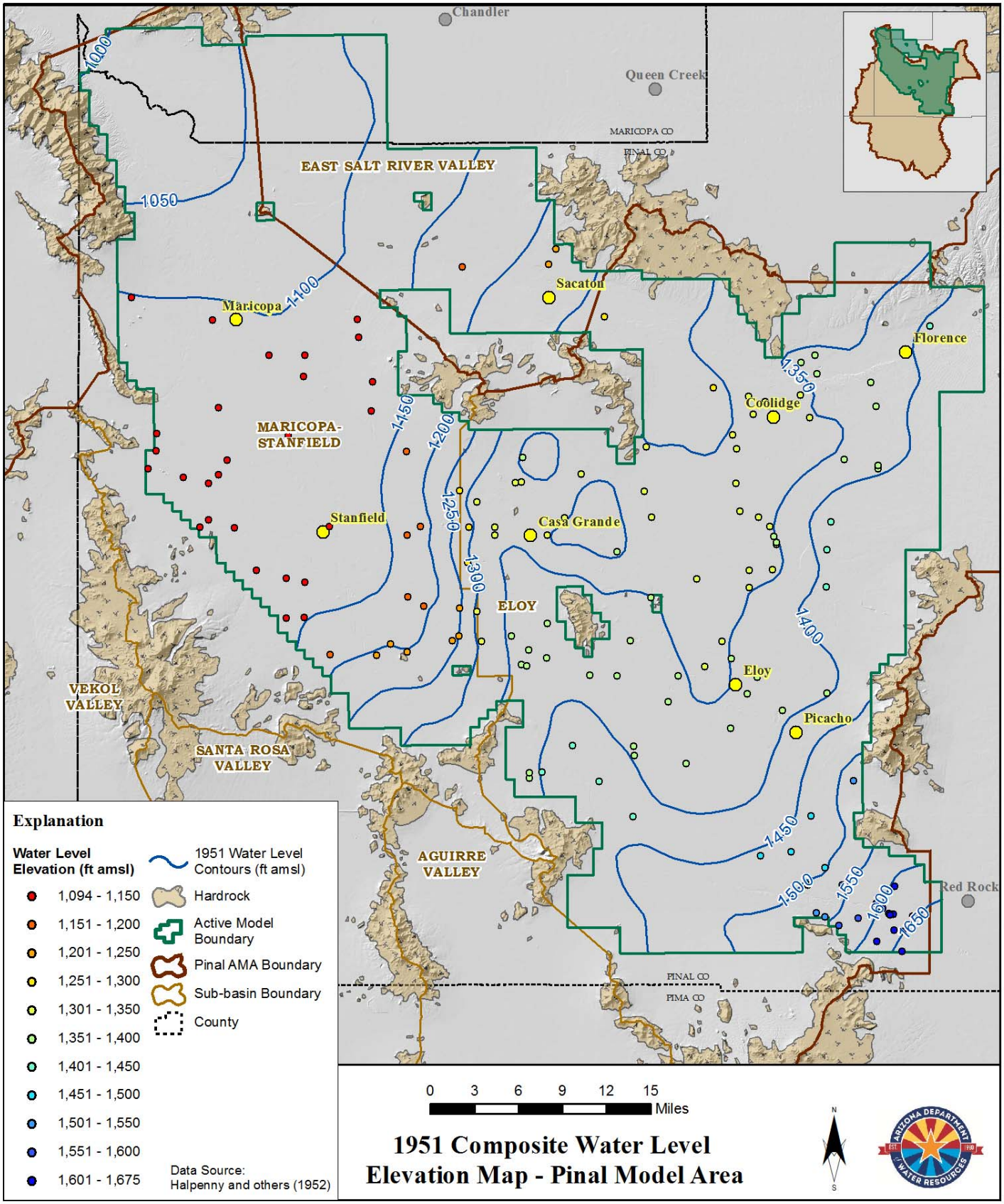

Figure 34 1951 Composite Water Level Elevation Map - Pinal Model Area

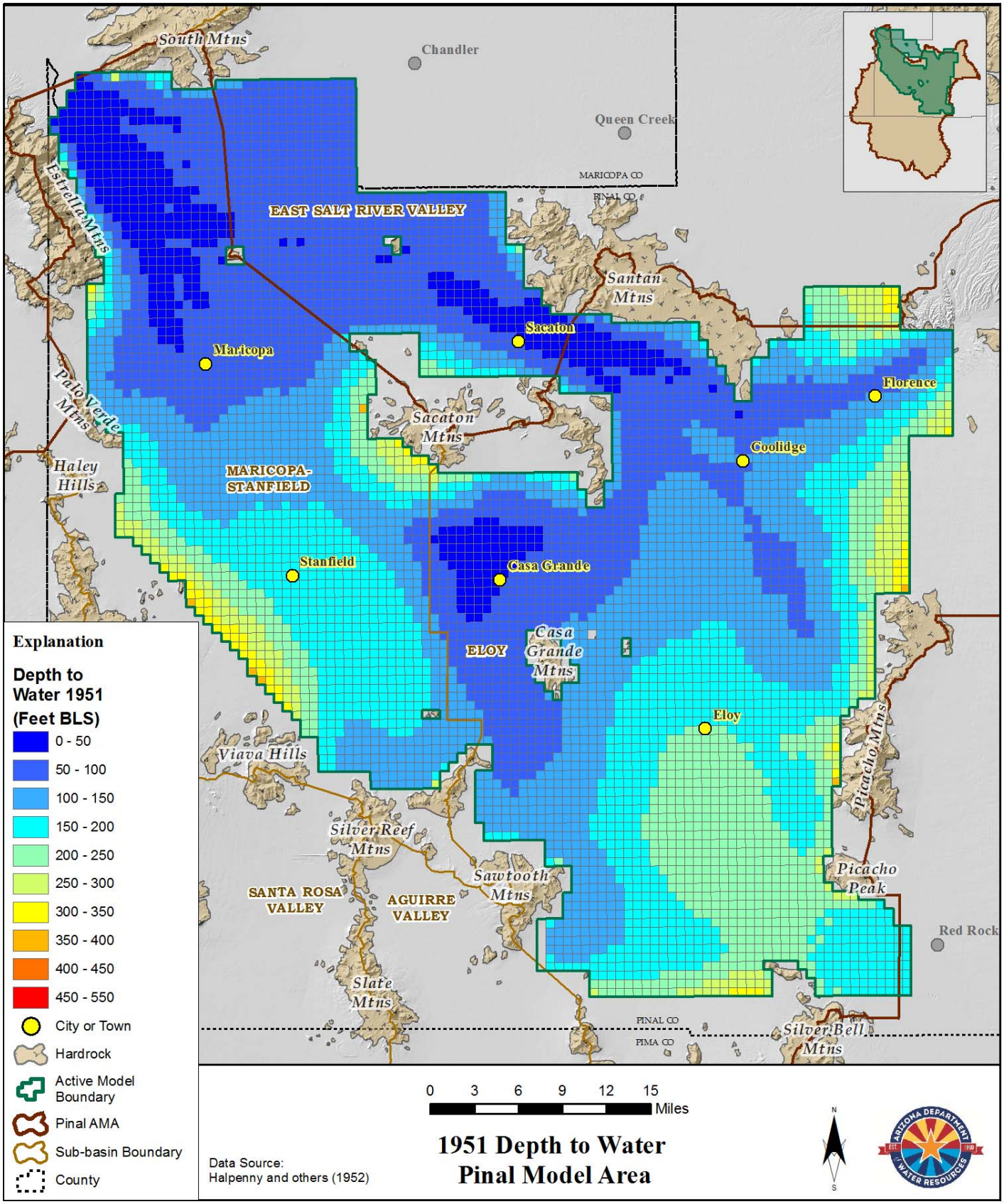

Figure 35 1951 Depth-to-Water Map - Pinal Model Area

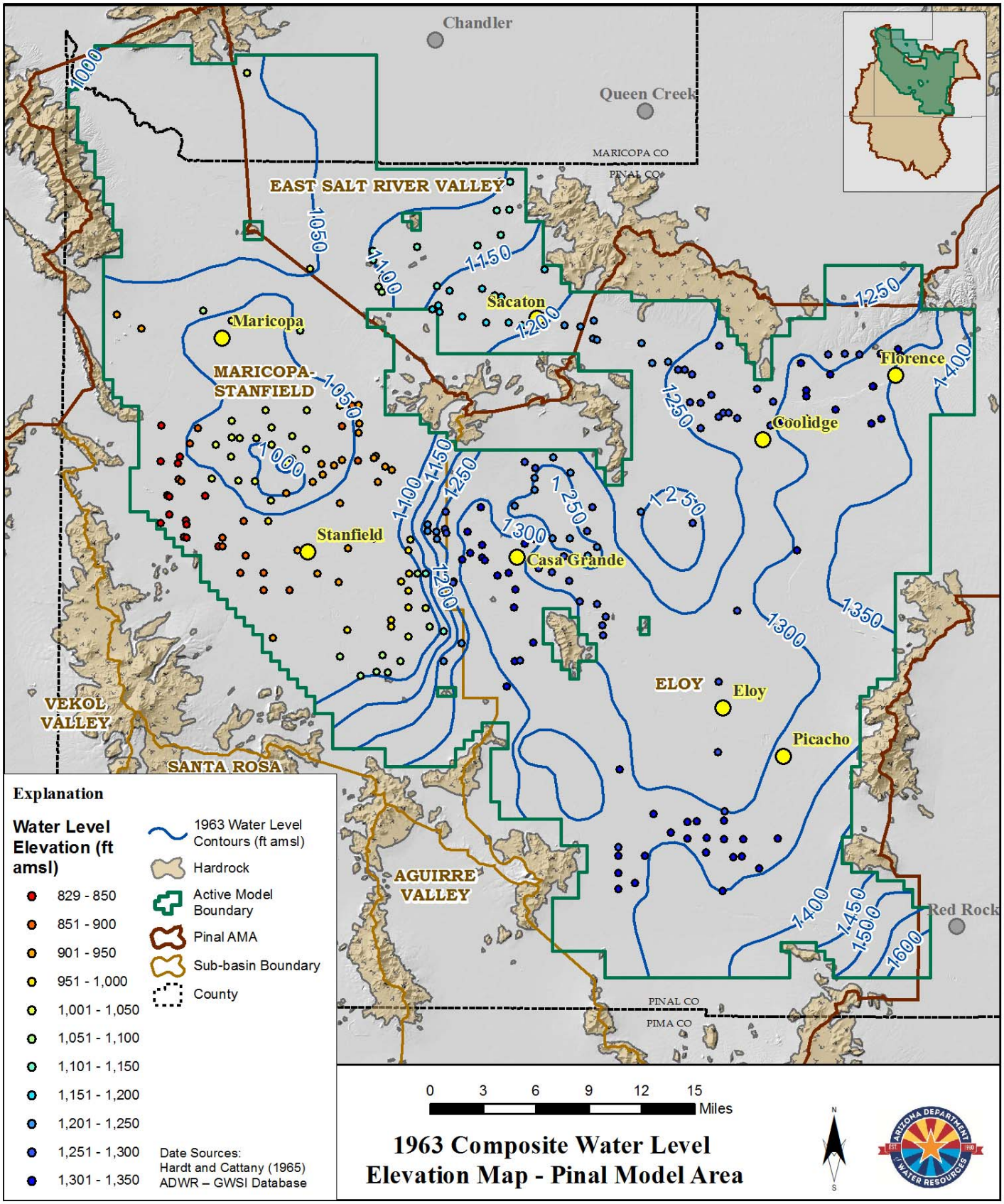

Figure 36. 1963 Composite Water Level Elevation Map - Pinal Model Area.

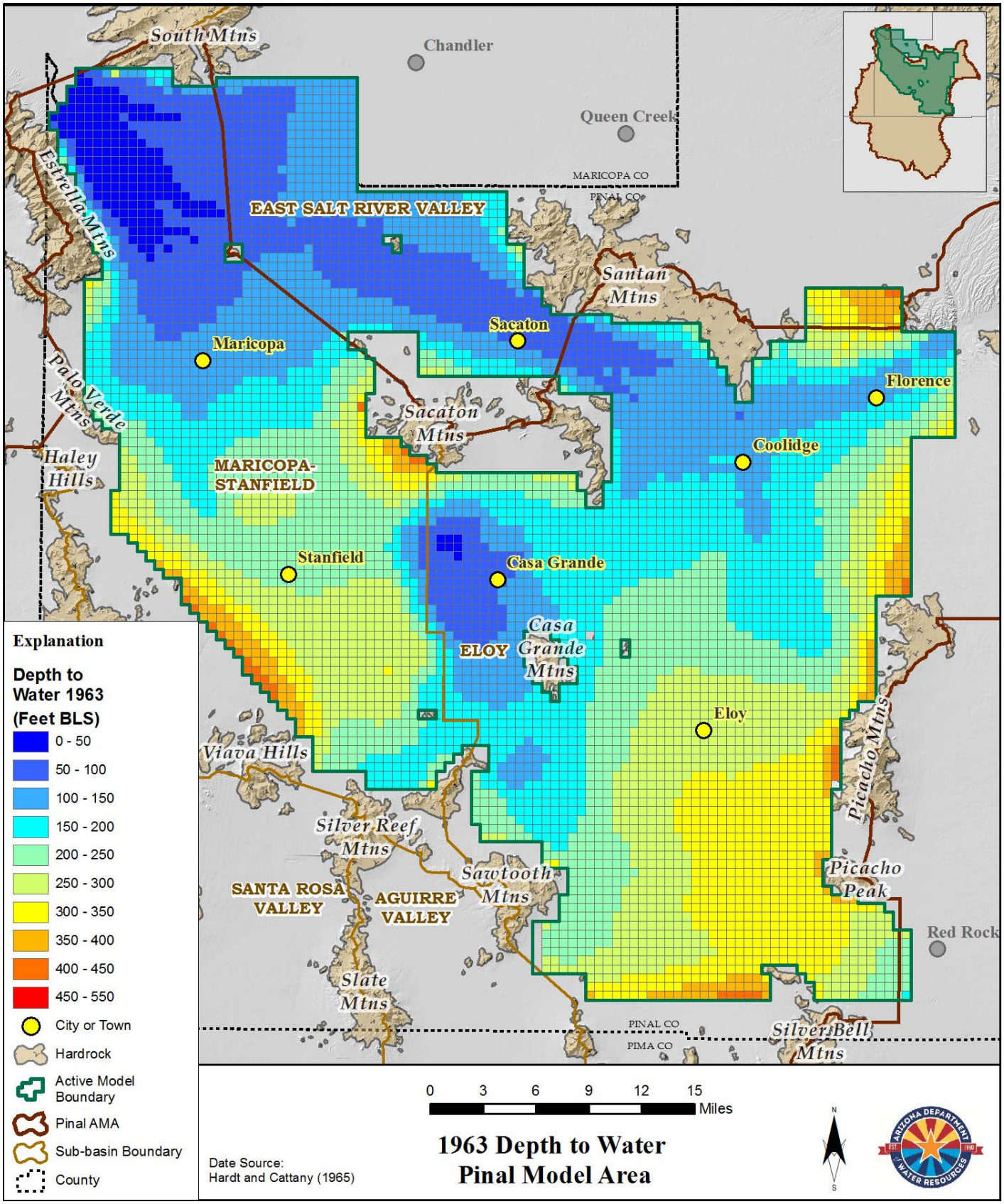

Figure 37 1963 Depth-to-Water Map - Pinal Model Area

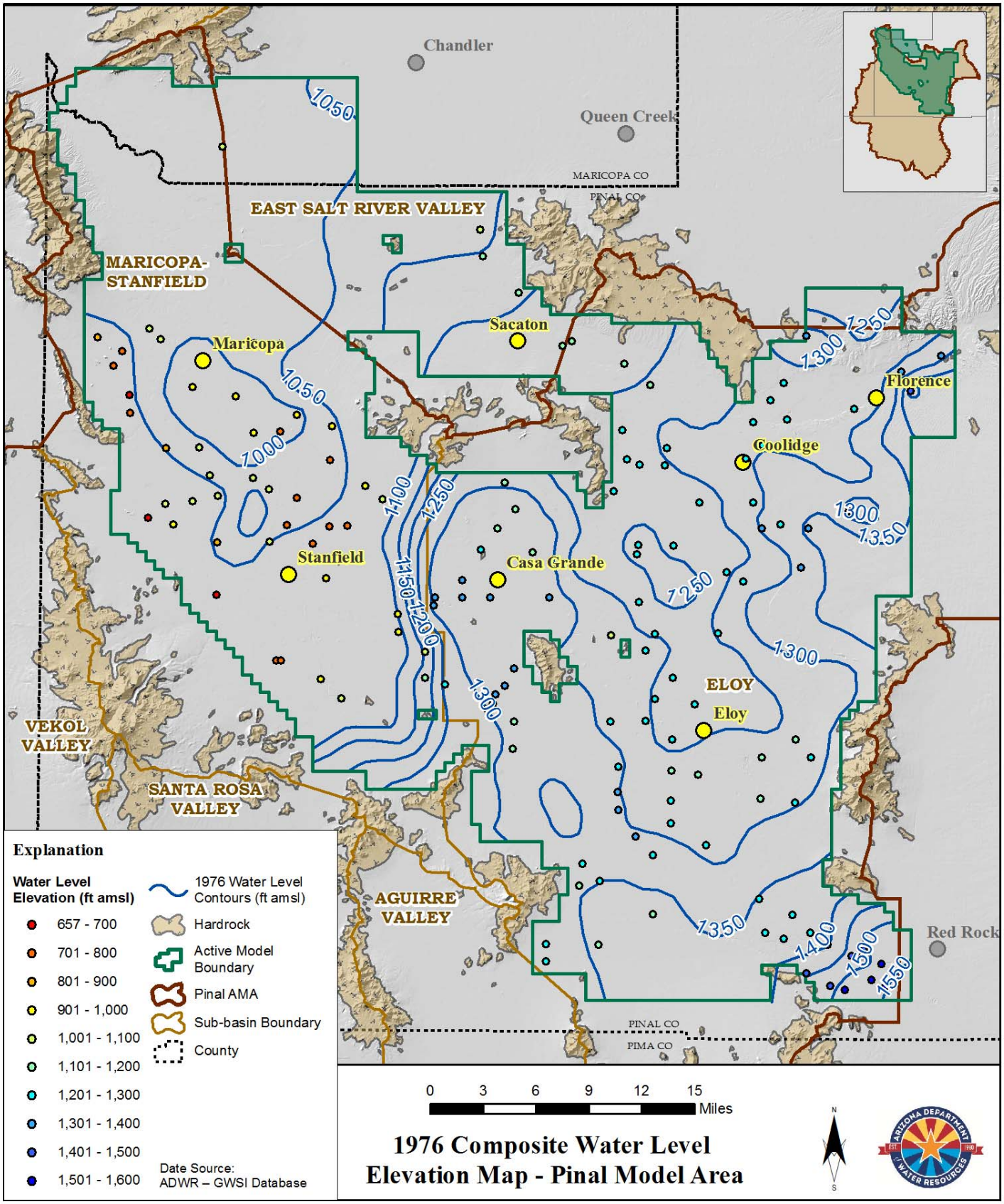

Figure 38 1976 Composite Water Level Elevation Map - Pinal Model Area

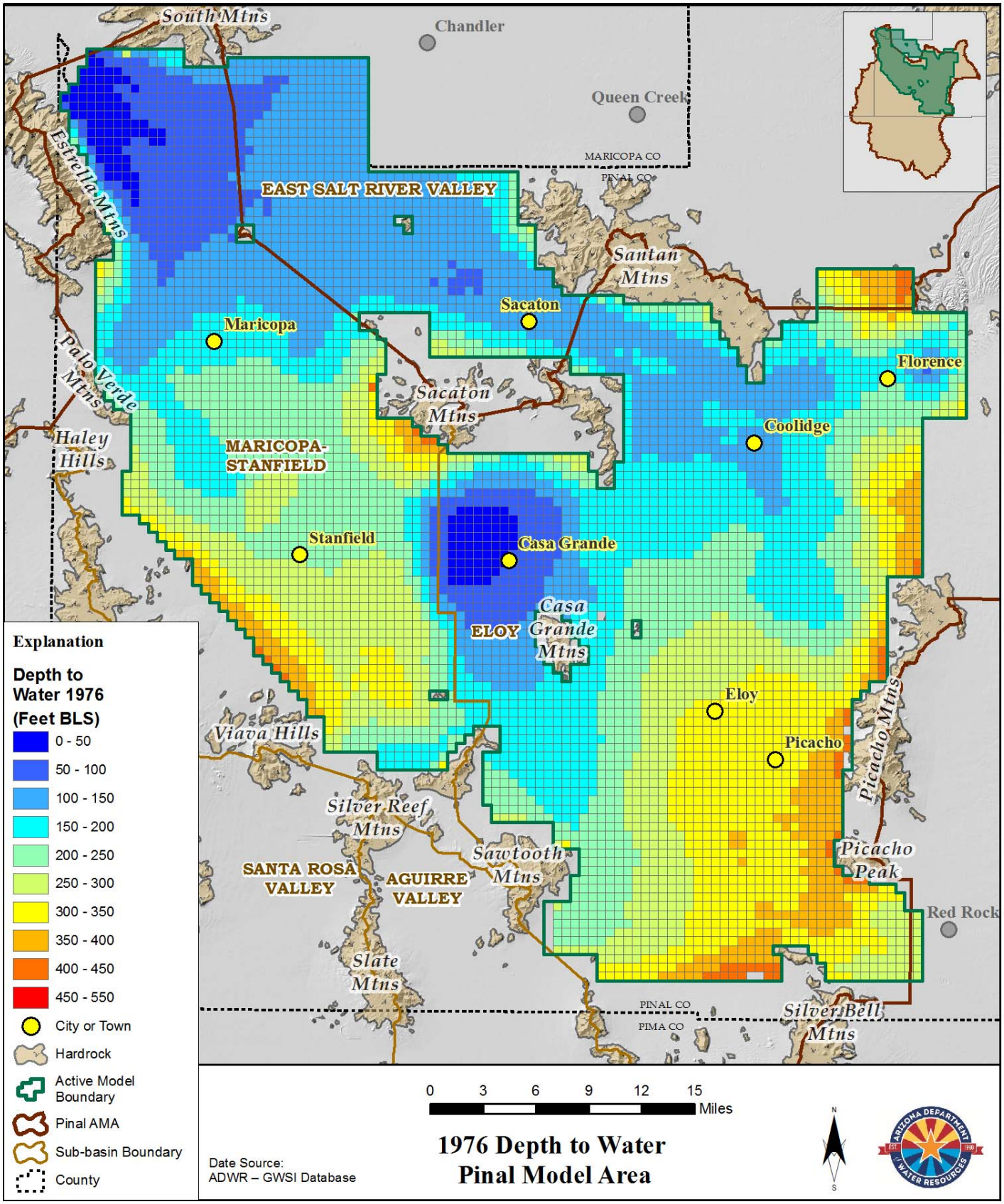

Figure 39 1976 Depth-to-Water Map - Pinal Model Area

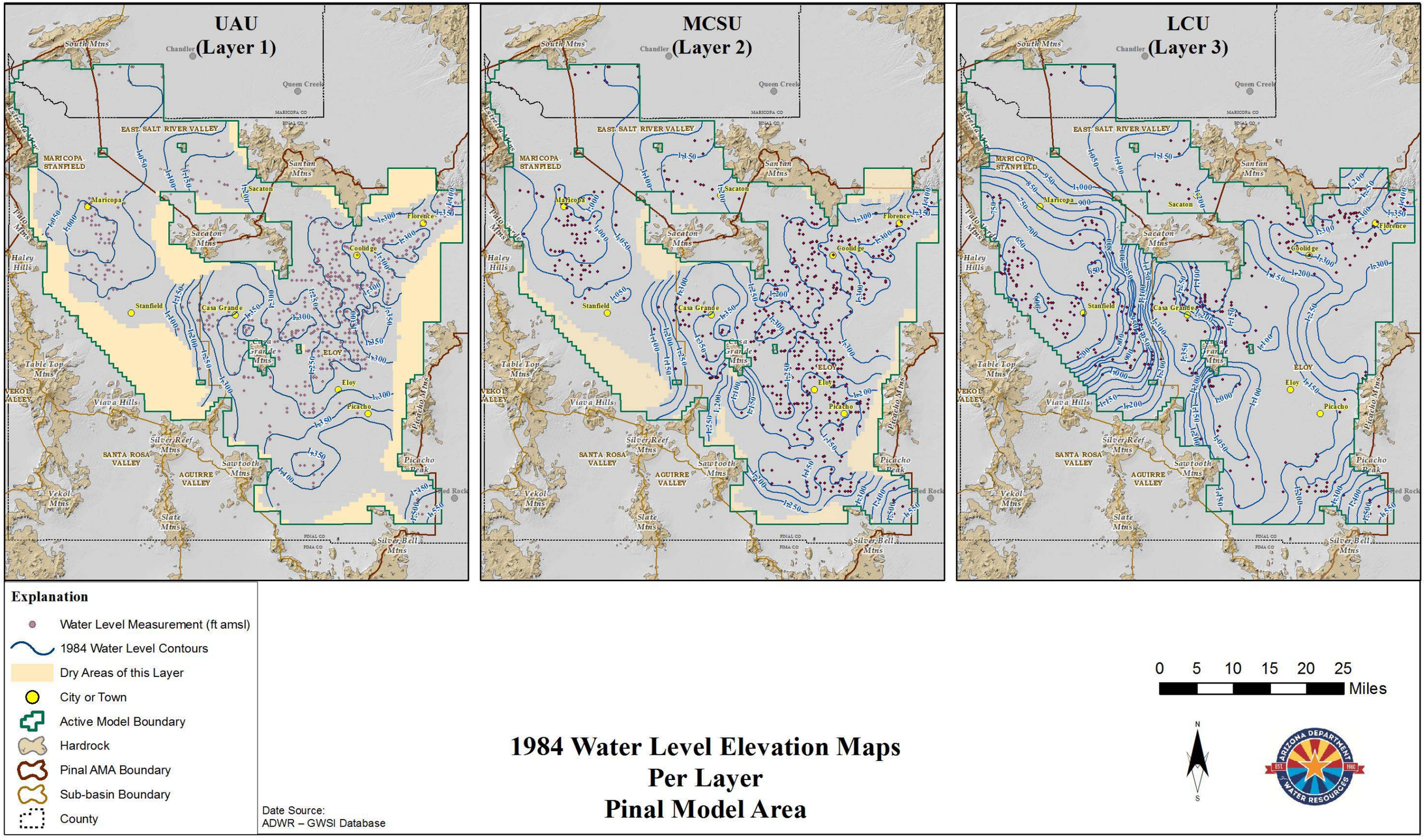

1984 Water Level Elevation Maps
Per Layer
Pinal Model Area

Figure 40 1984 Water Level Elevations Per Model Layer

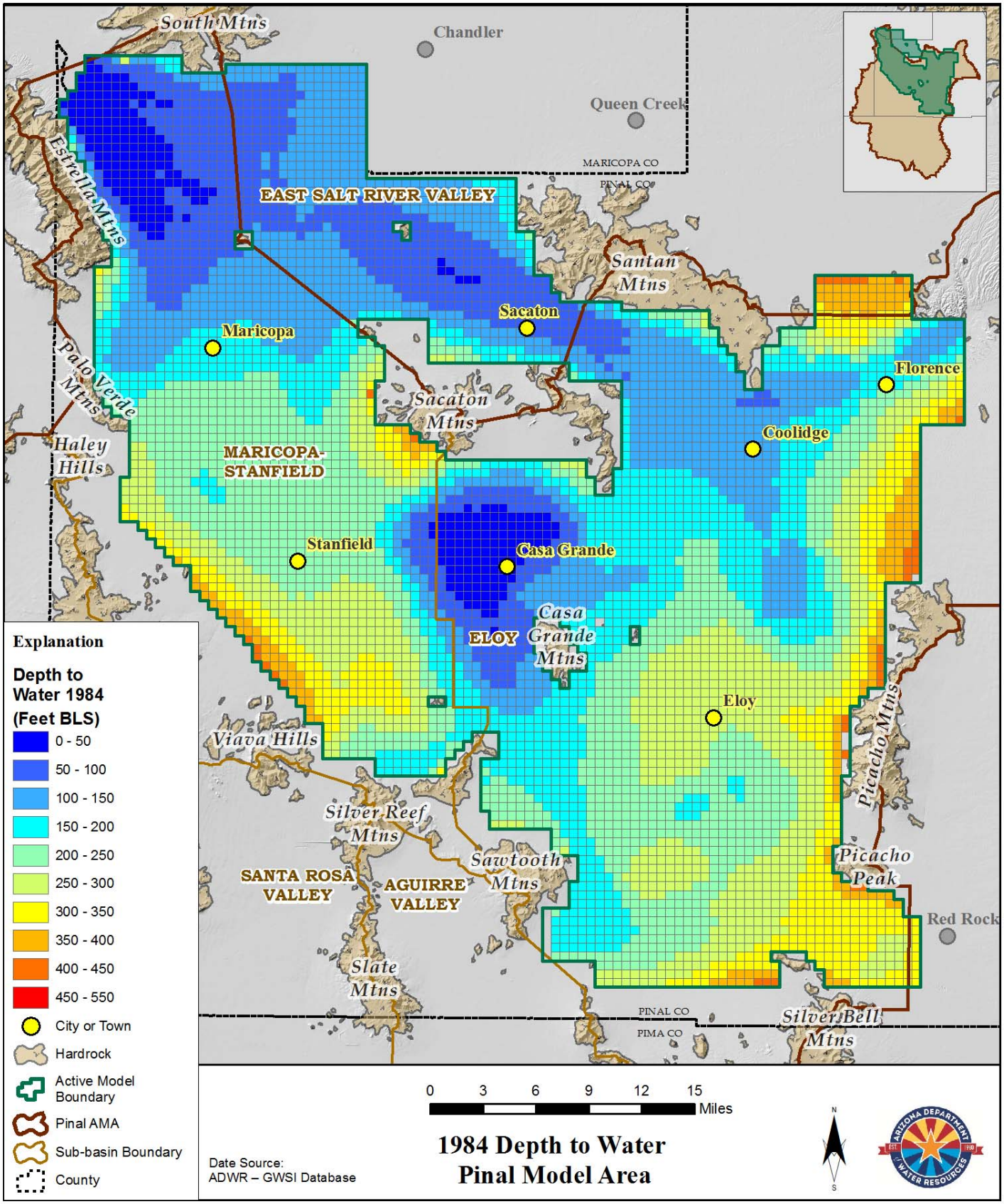

Figure 41 1984 Depth-to-Water Map - Pinal Model Area

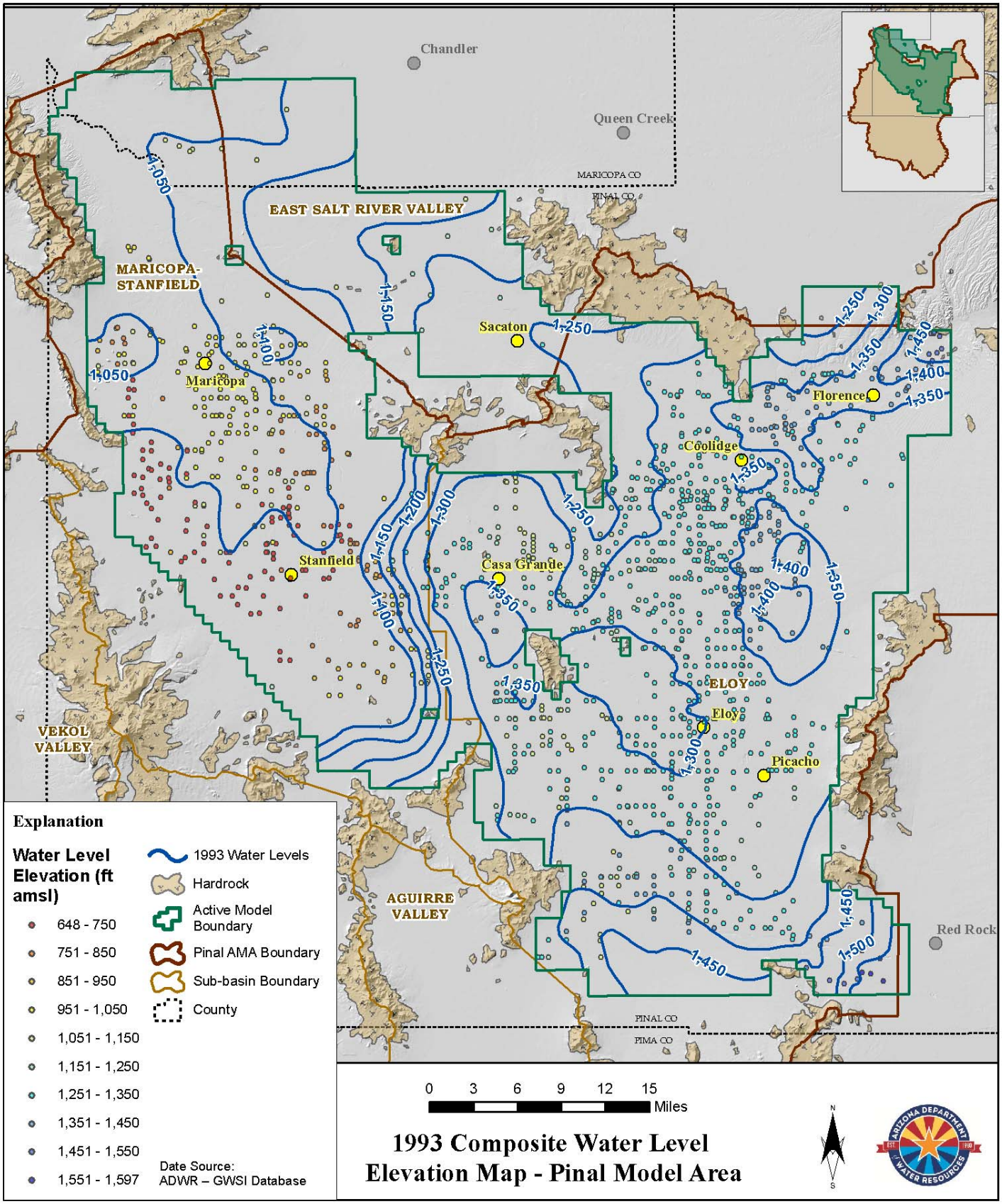

Figure 42 1993 Composite Water Level Elevation Map - Pinal Model Area

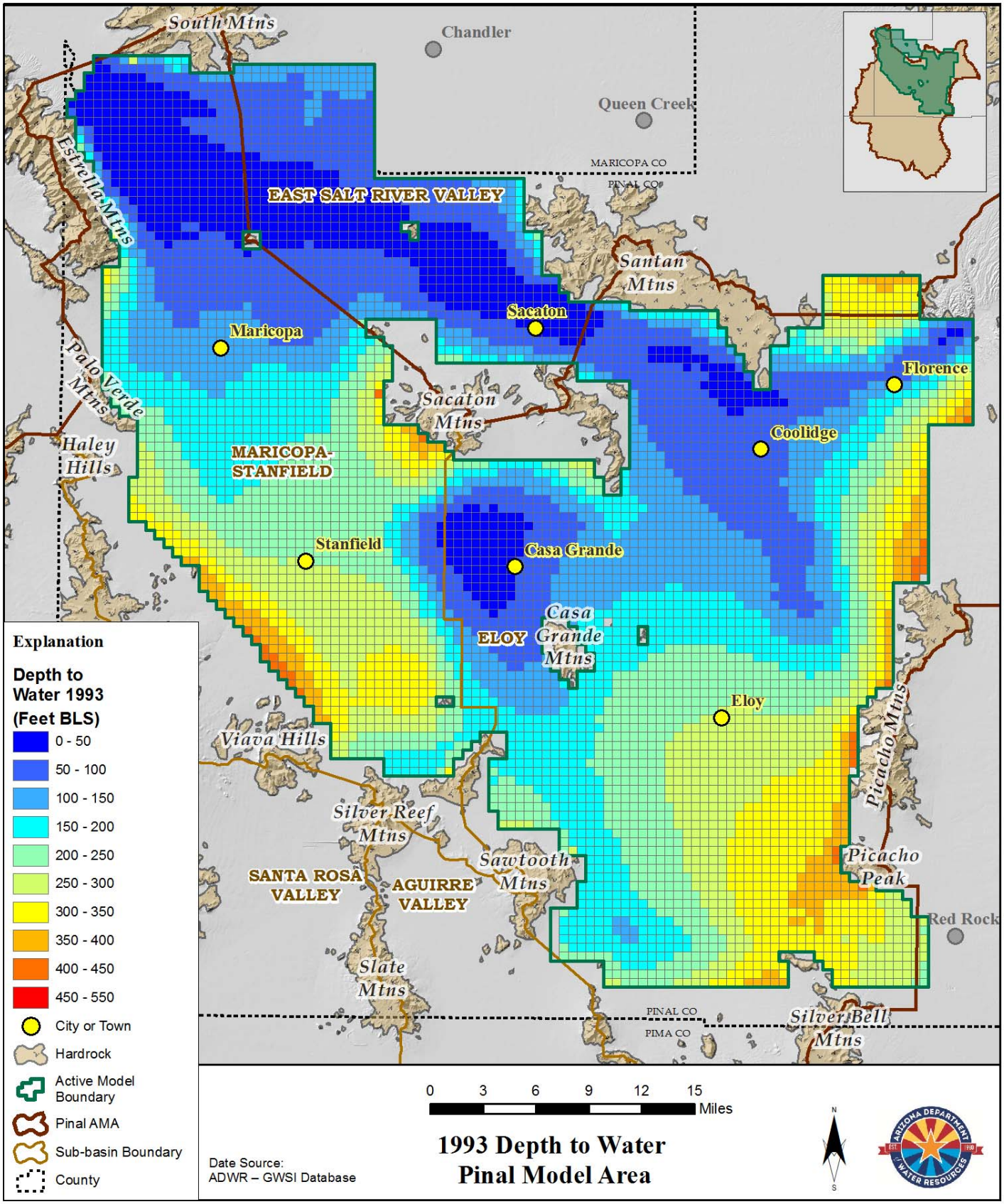

Figure 43 1993 Depth-to-Water Map - Pinal Model Area.

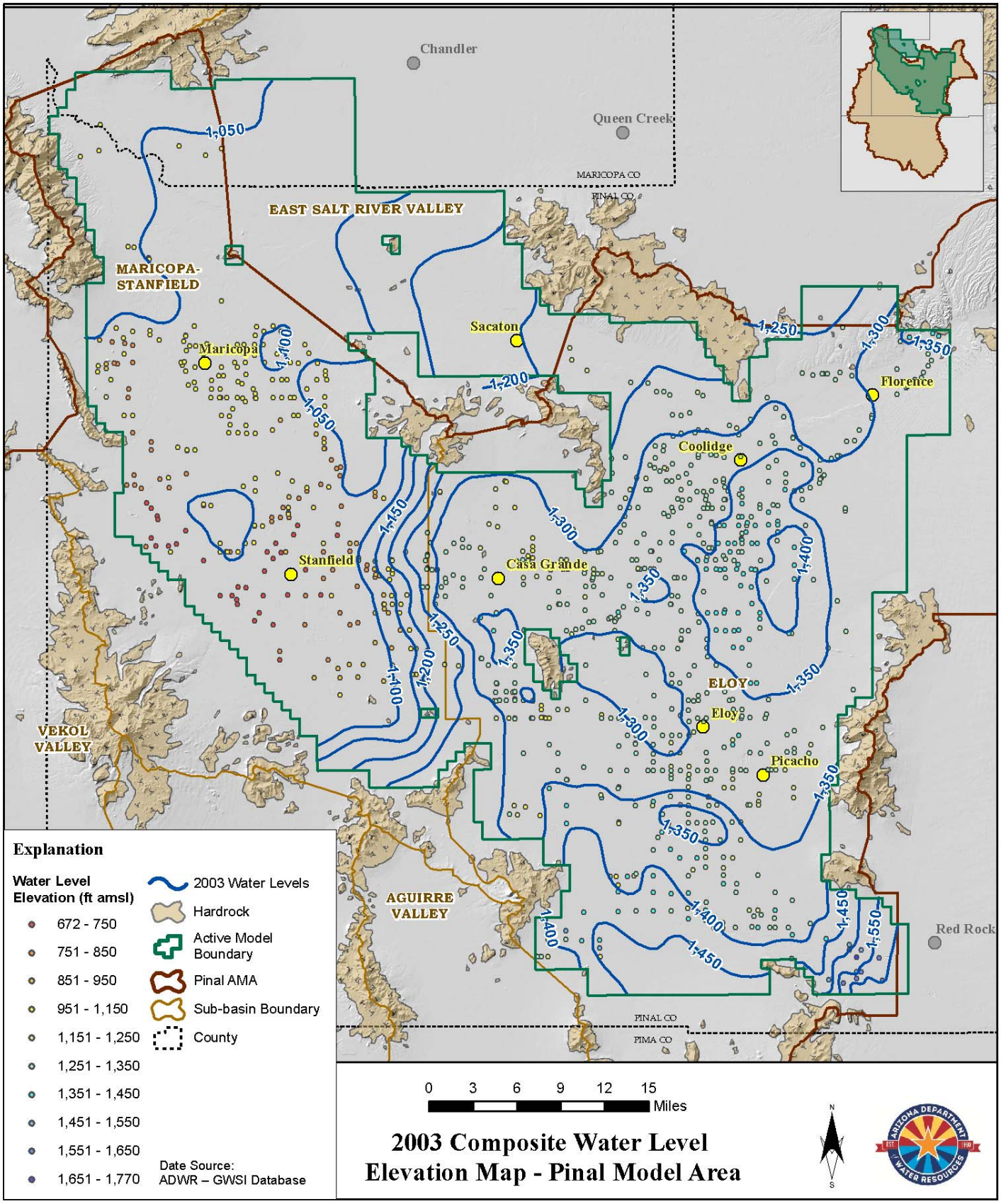

Figure 44 2003 Composite Water Level Elevation Map - Pinal Model Area

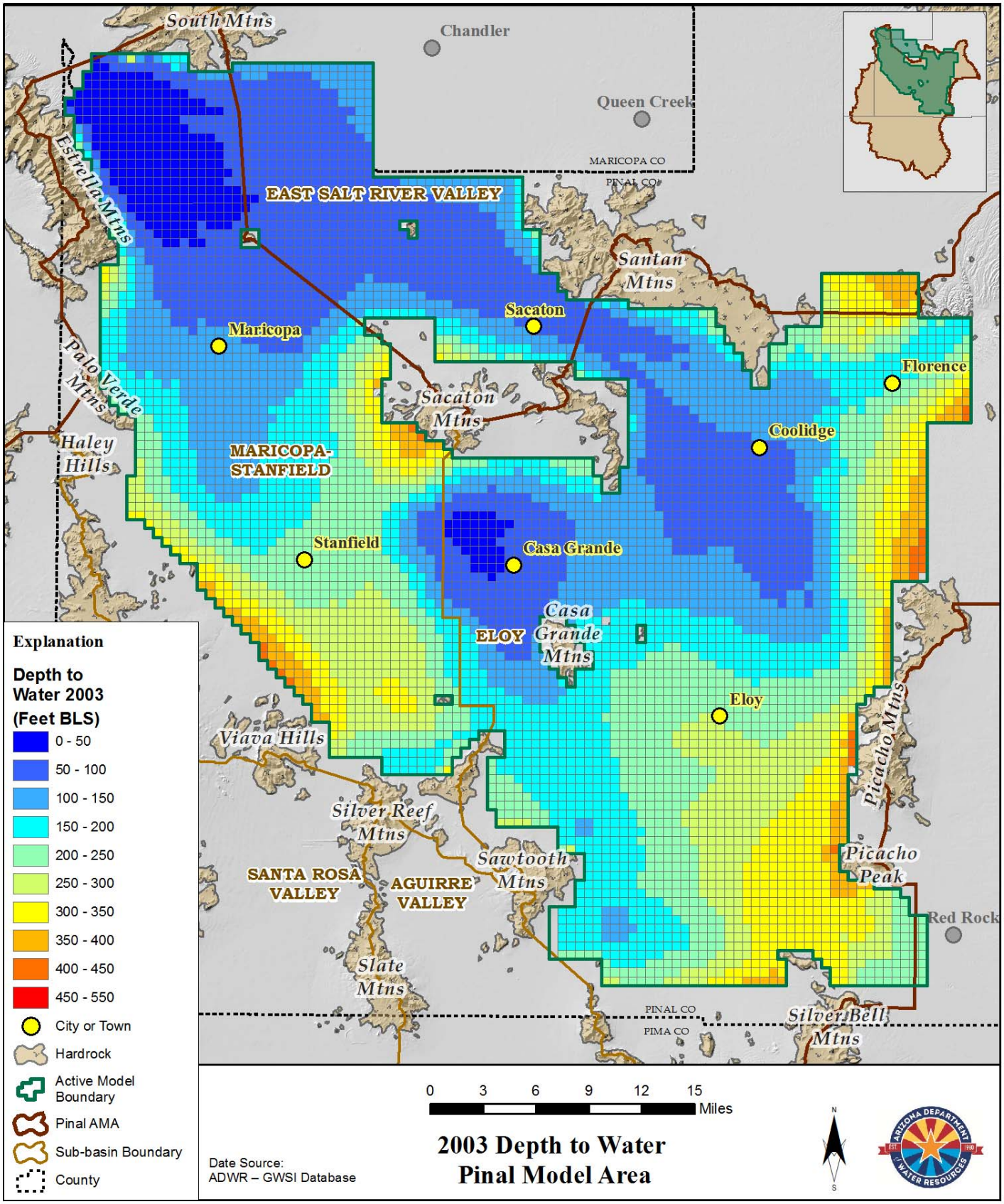

Figure 45 2003 Depth-to-Water Map - Pinal Model Area

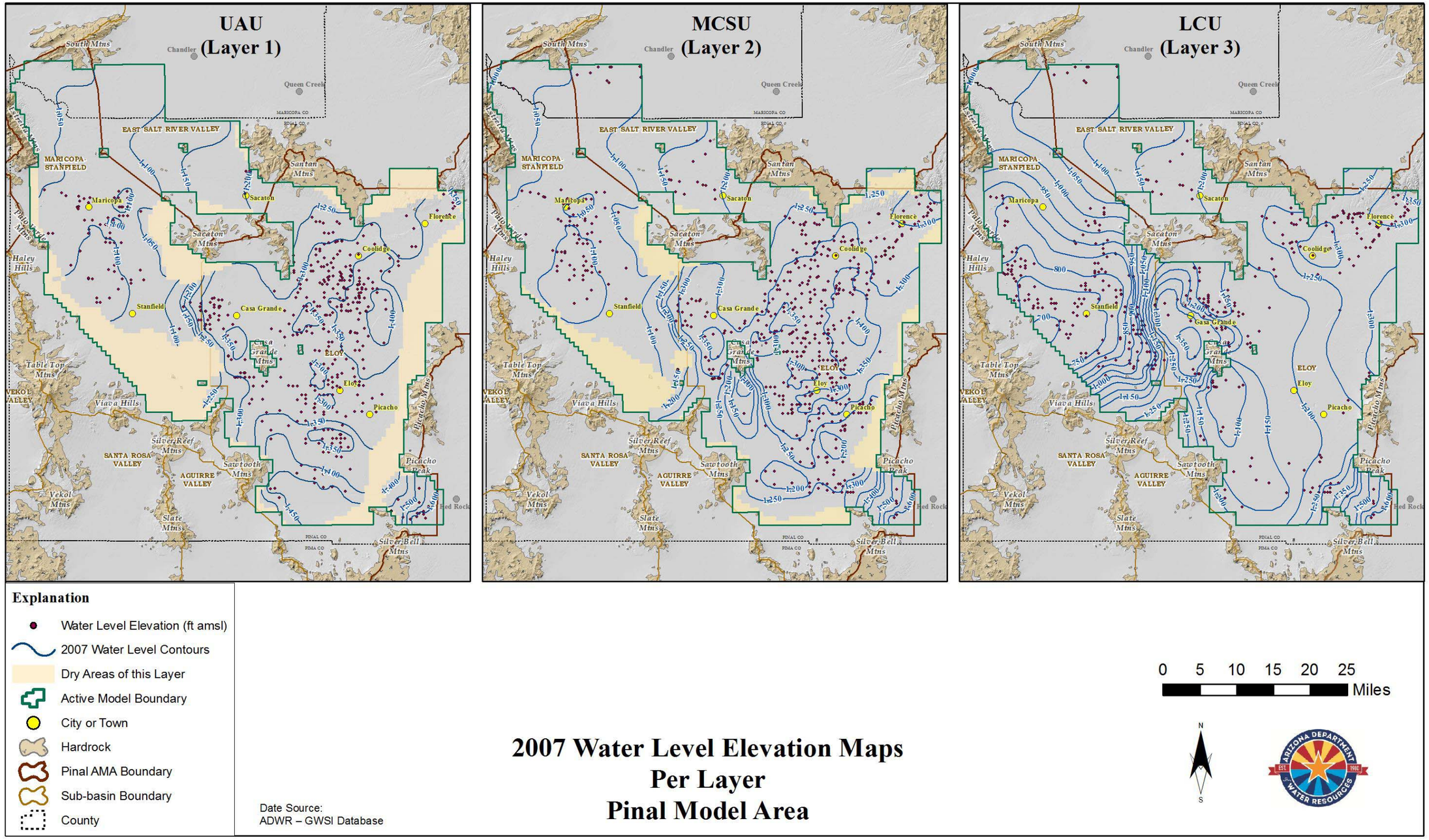

Figure 46 2007 Water Level Elevation Maps Per Layer Pinal Model Area

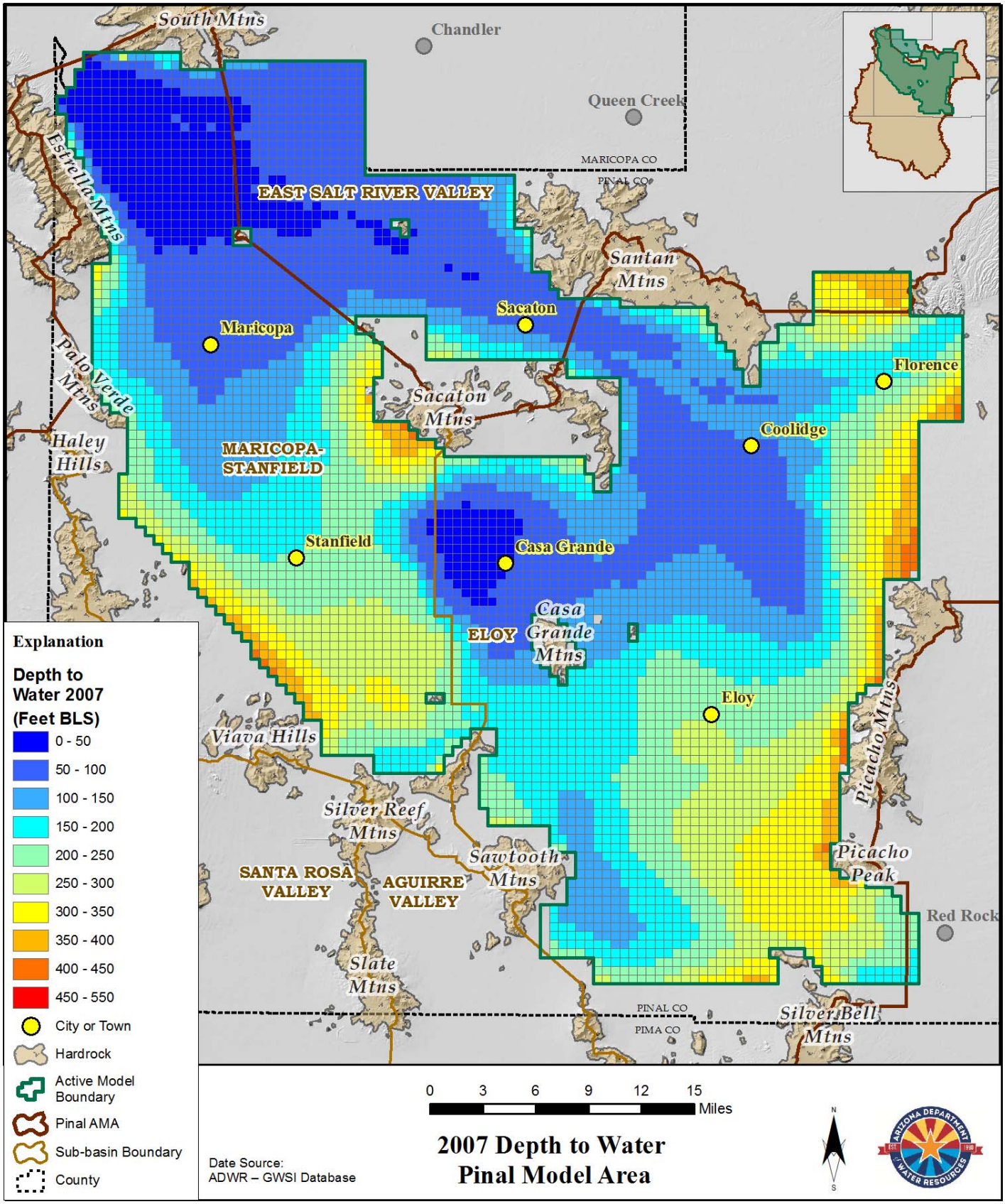

Figure 47 2007 Depth-to-Water Map - Pinal Model Area

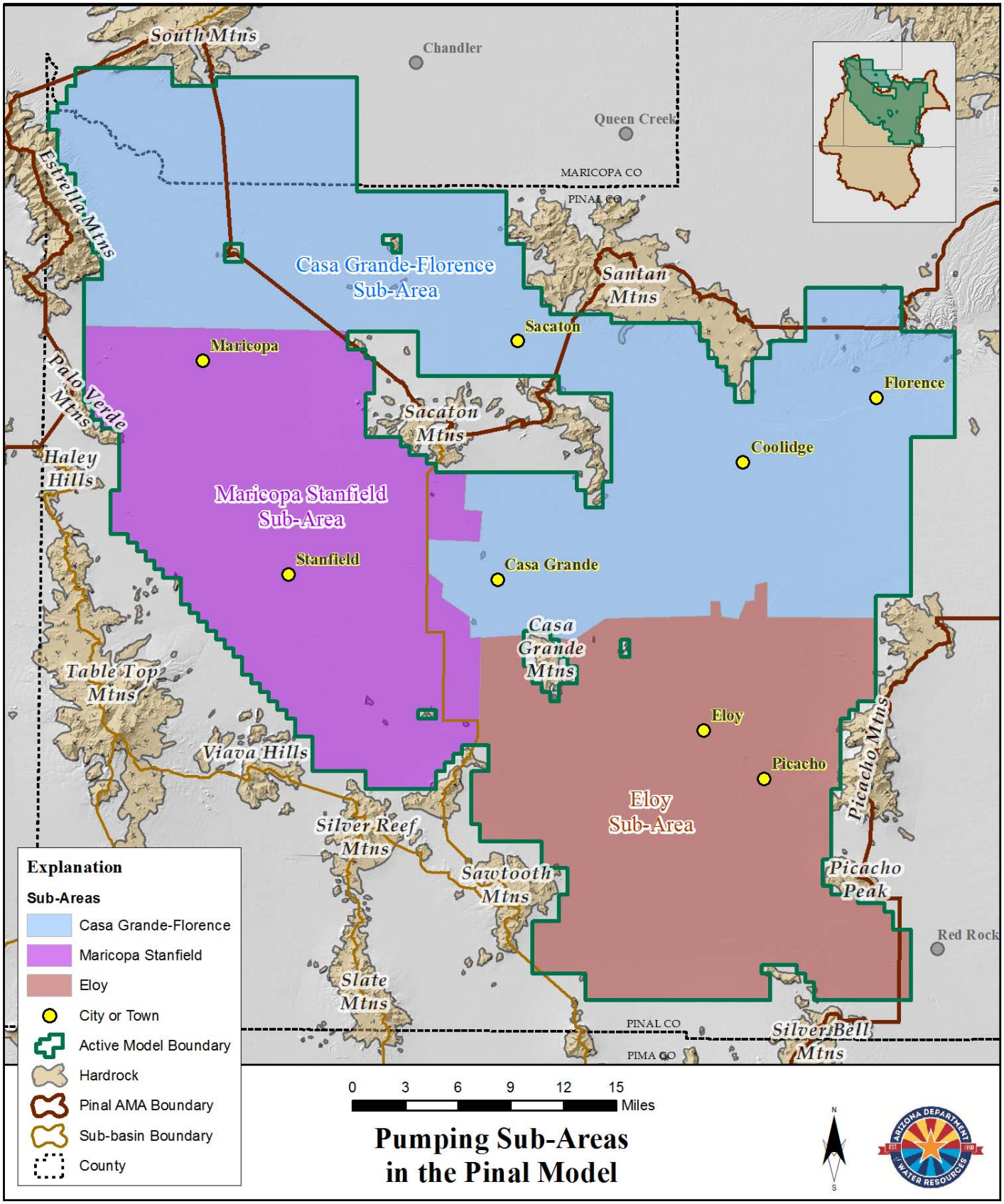

Figure 48 Pumping Sub-Areas in The Pinal Model

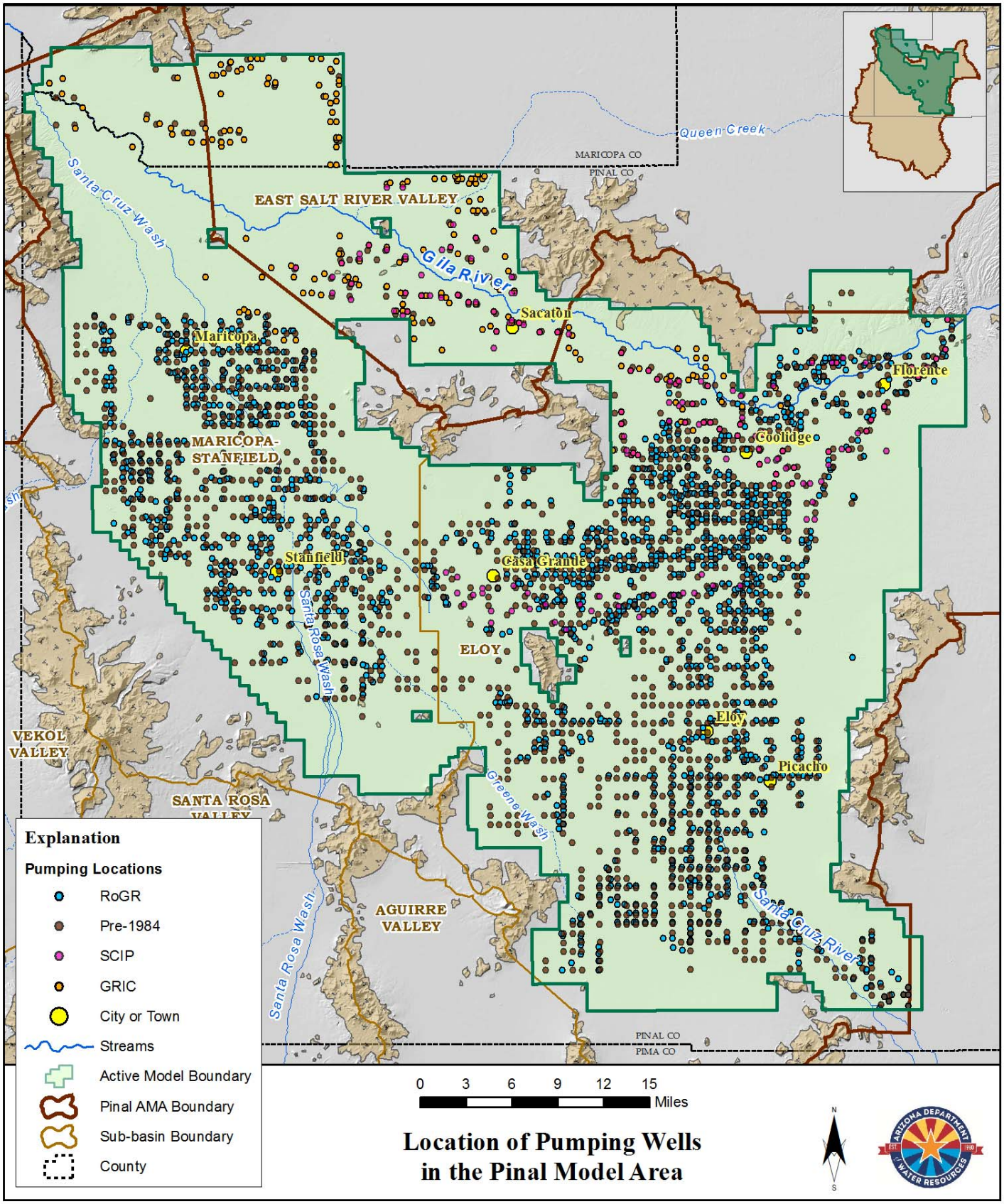

Figure 49 Location of Pumping Wells in the Pinal Model Area

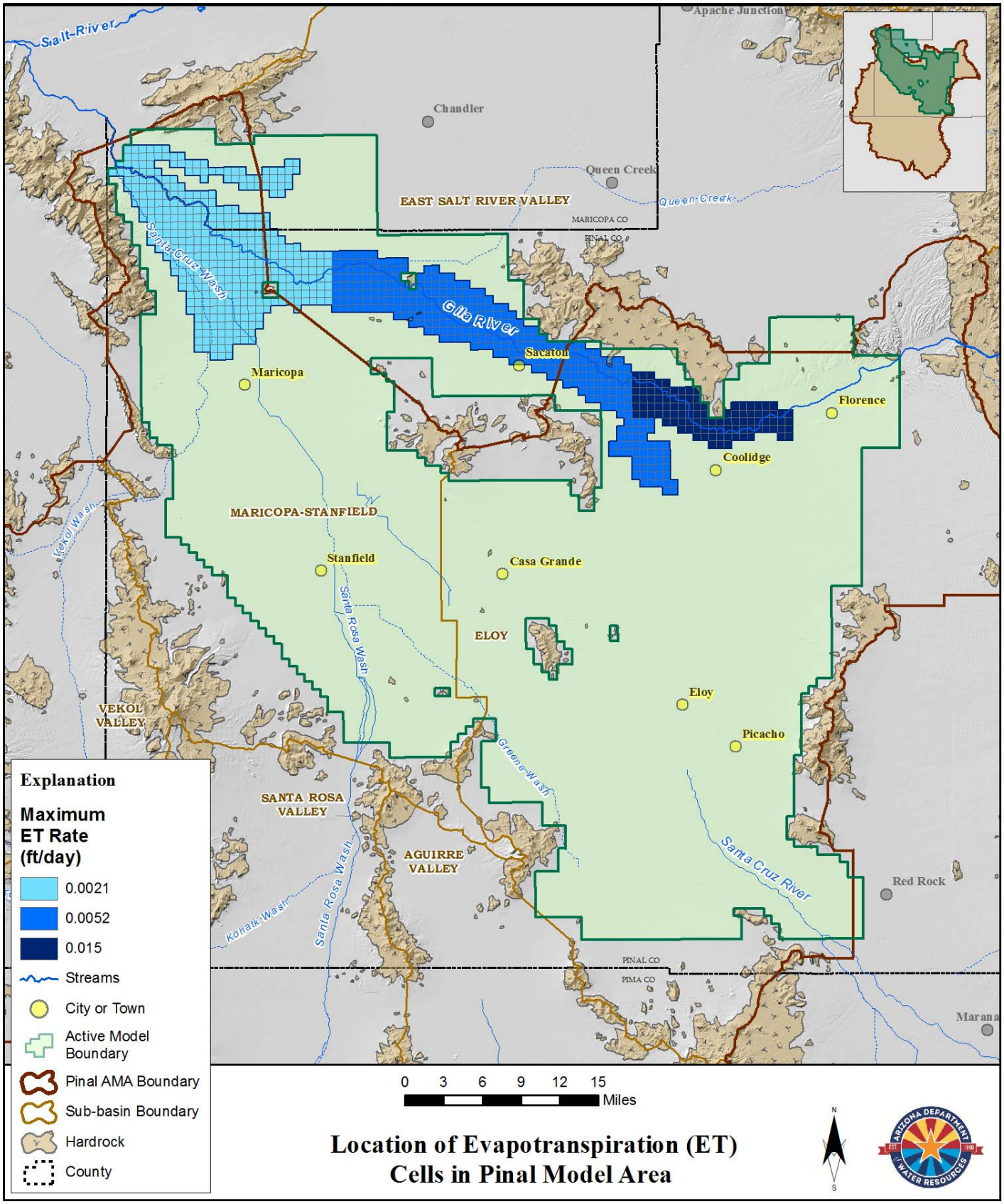

Figure 50 Location of Evapotranspiration (ET) Cells in Pinal Model Area

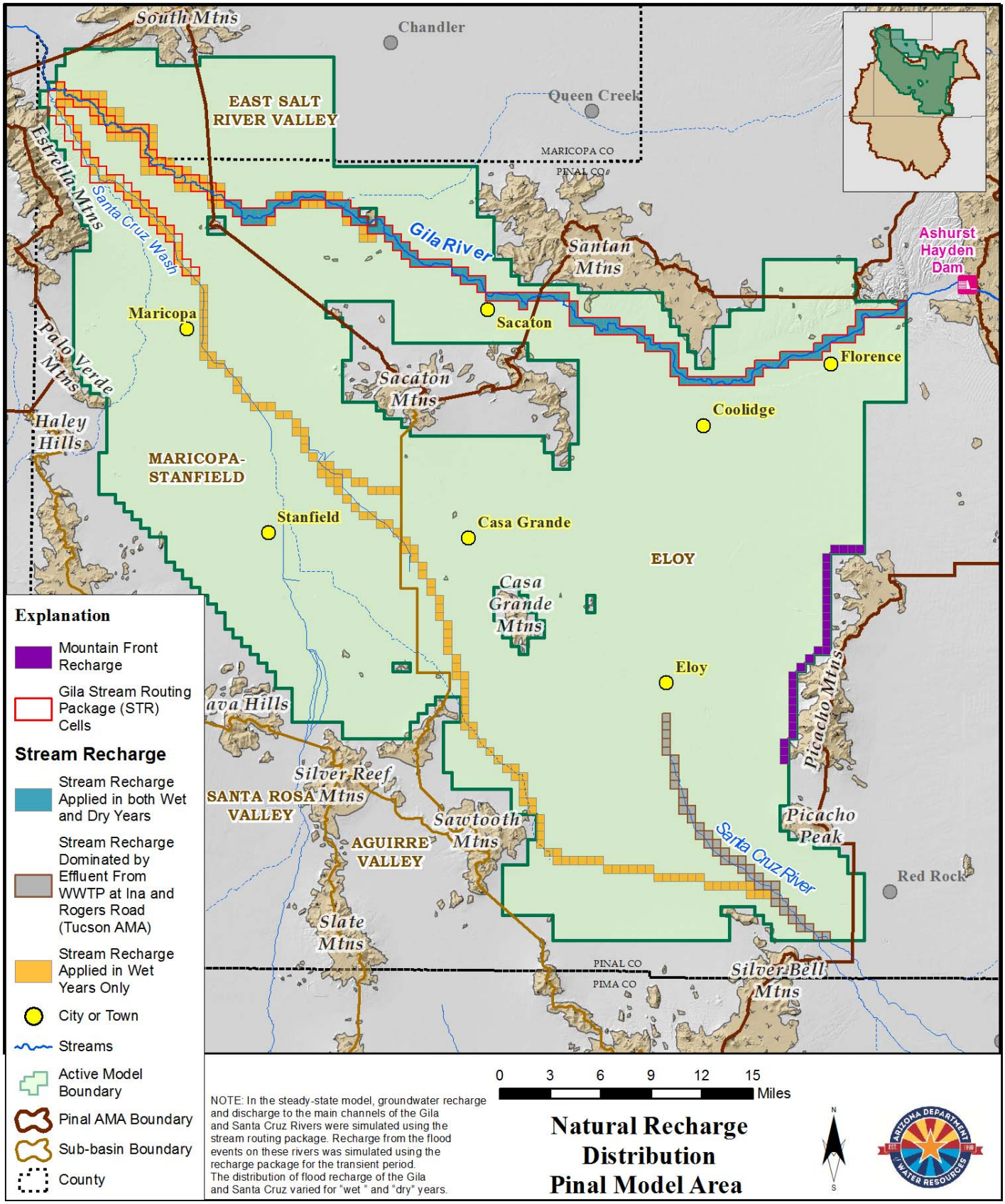

Figure 51 Natural Recharge Distribution - Pinal Model Area

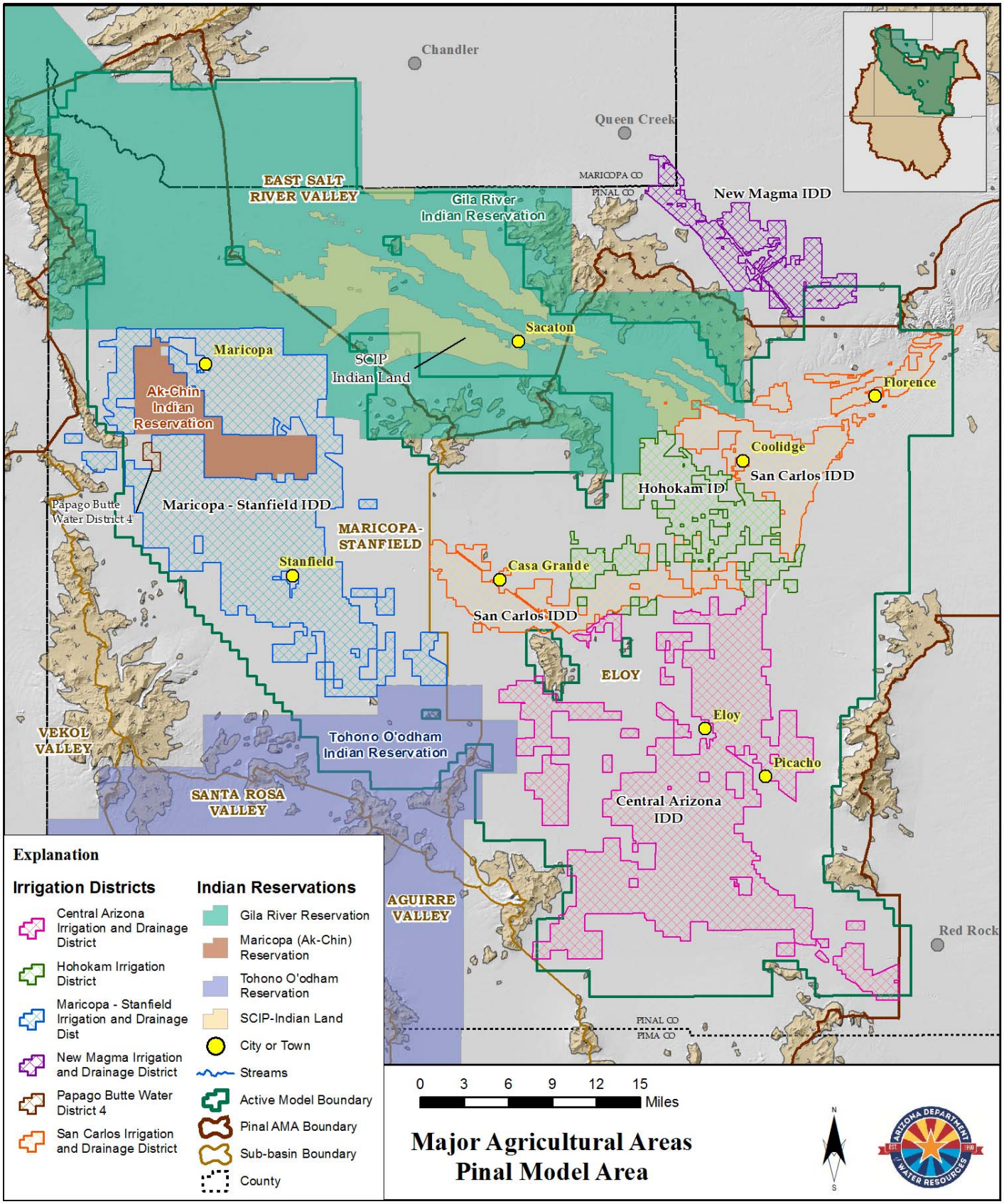

Figure 52 Major Agricultural Areas - Pinal Model Area

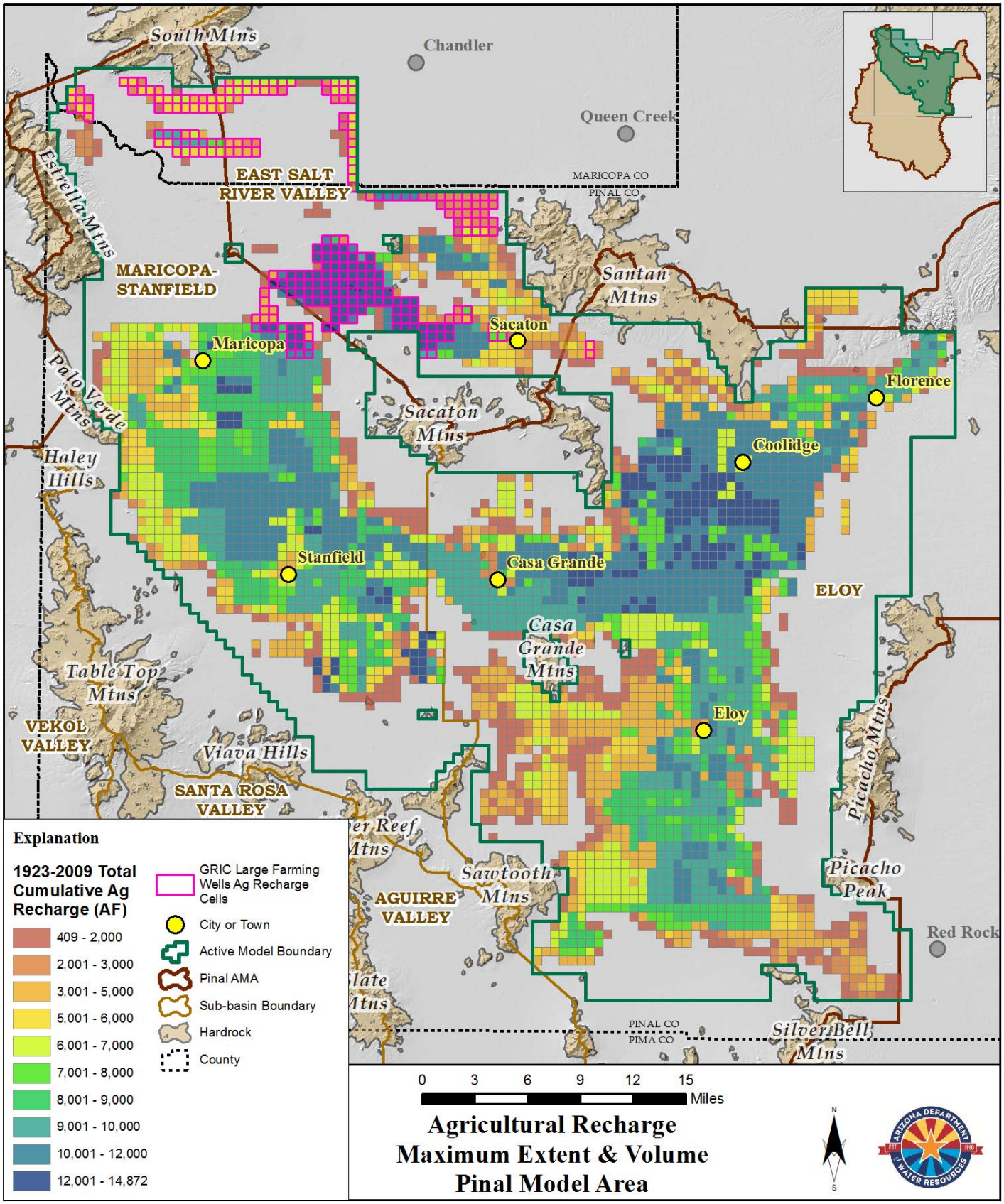

Figure 53 Agricultural Recharge Maximum Extent - Pinal Model Area

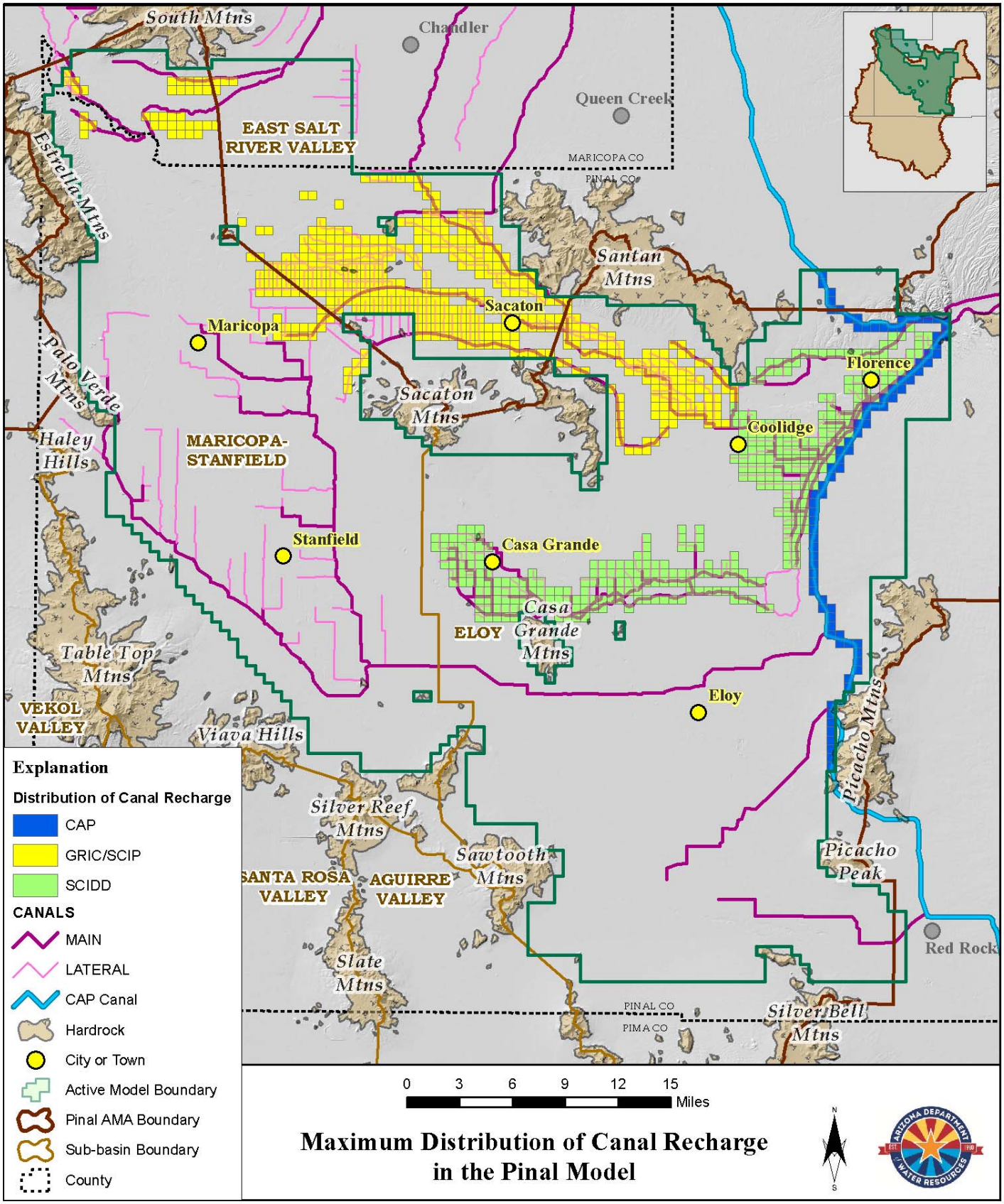

Figure 54 Maximum Distribution of Canal Recharge

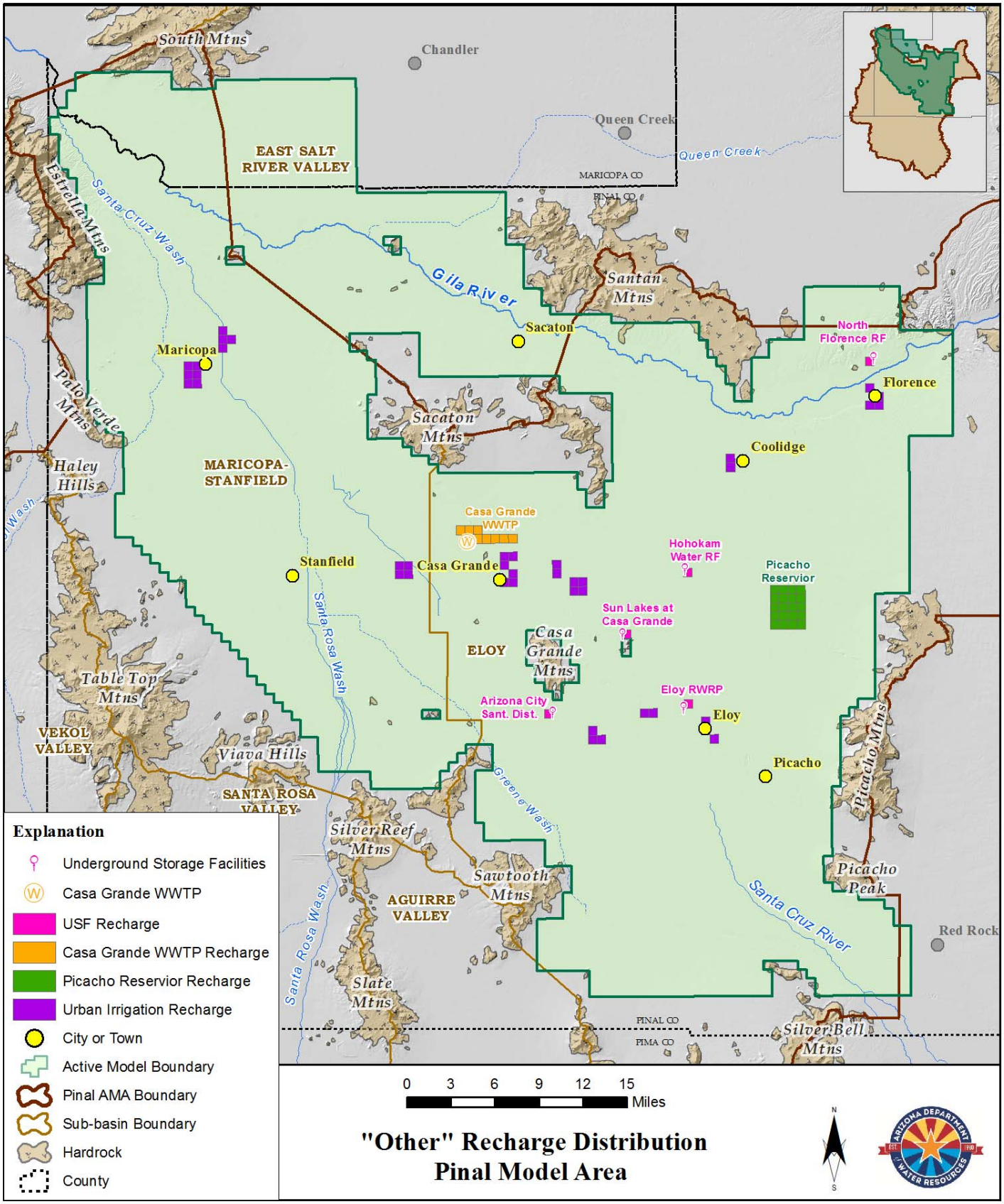

Figure 55 "Other" Recharge Distribution - Pinal Model Area

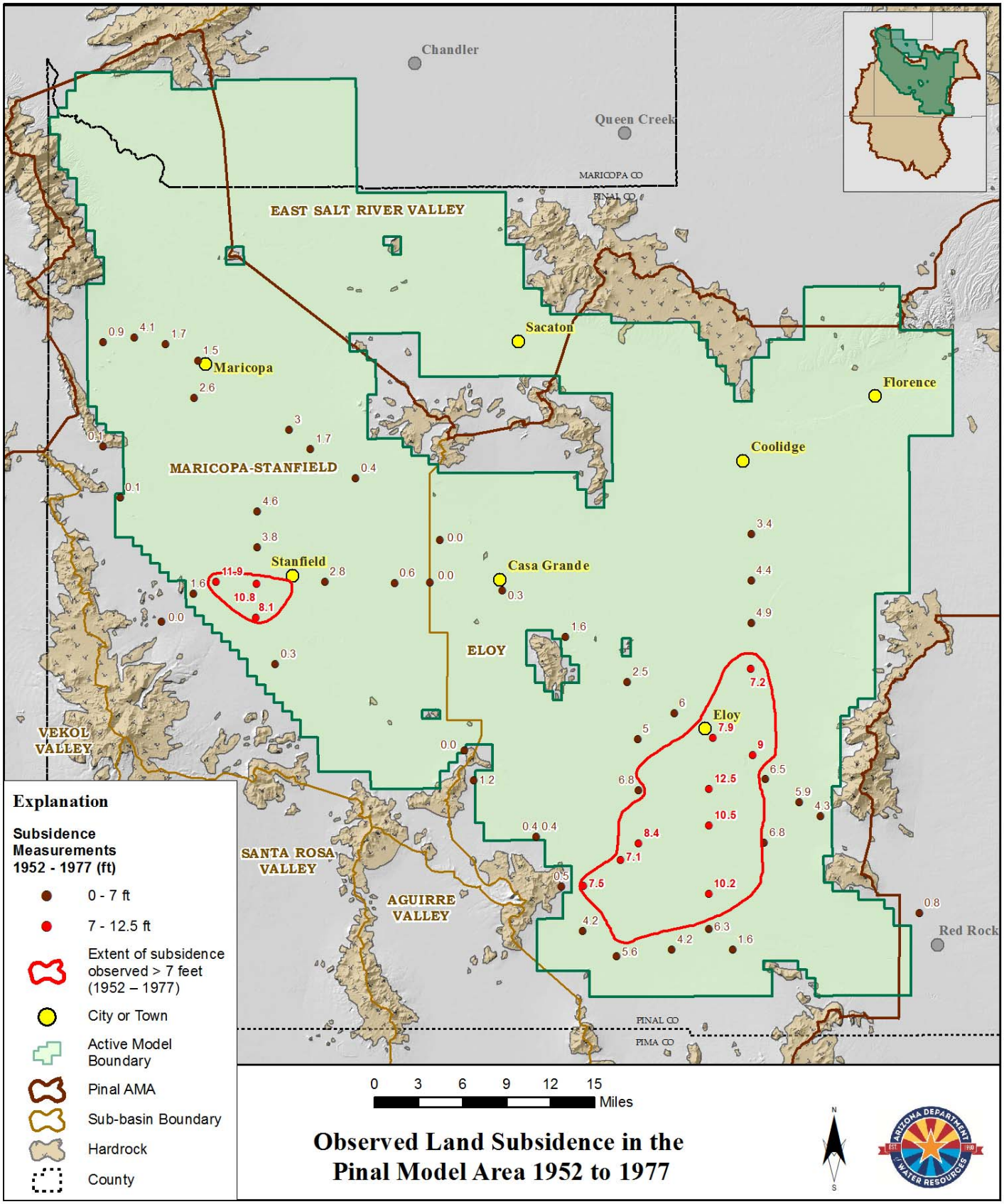

Figure 56 Observed Land Subsidence in the Pinal Model Area 1952 to 1977

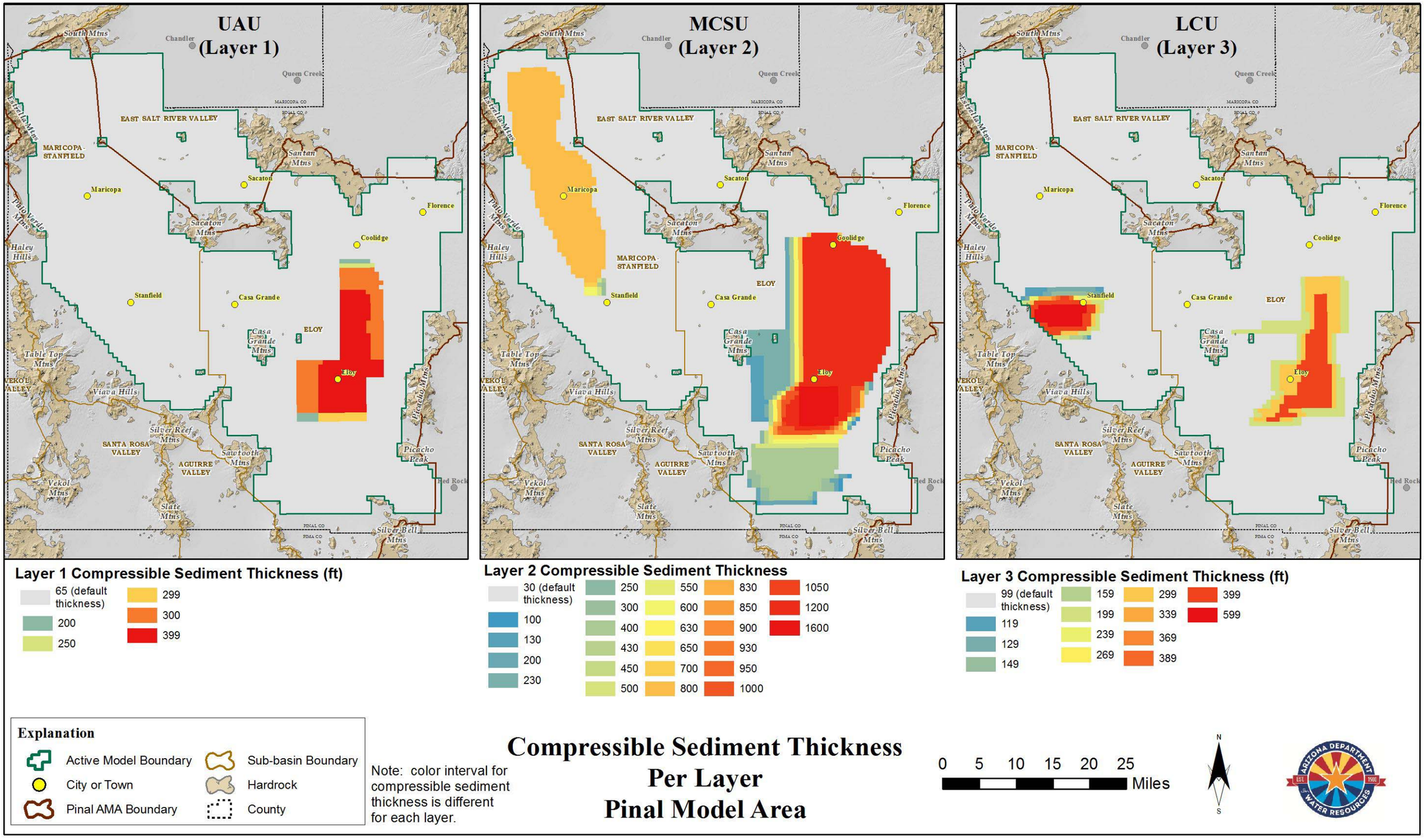

Figure 57 Compressible Sediment Thickness Per Layer – Pinal Model Area

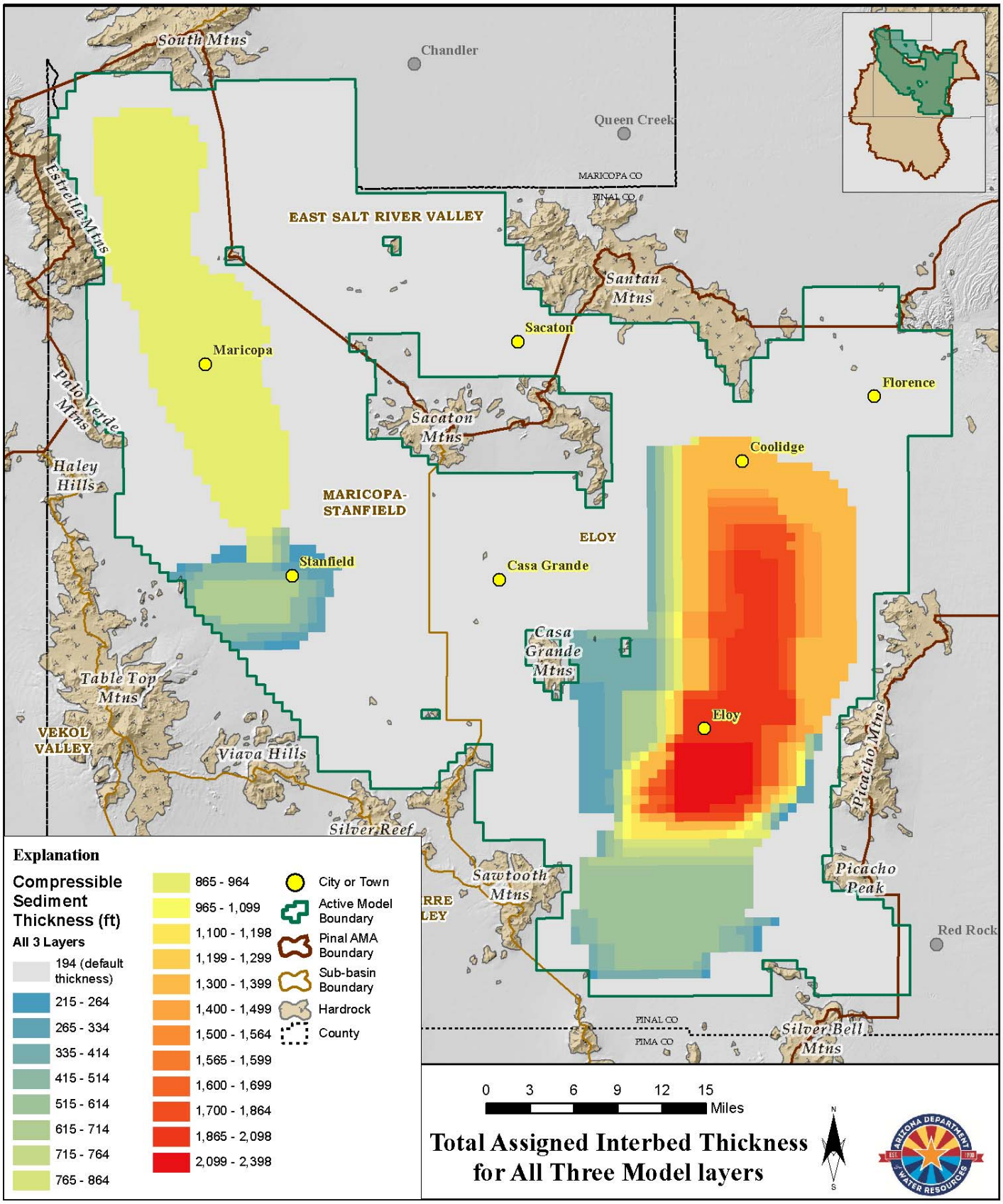

Figure 58 Total Assigned Interbed Thickness for All Three Model layers

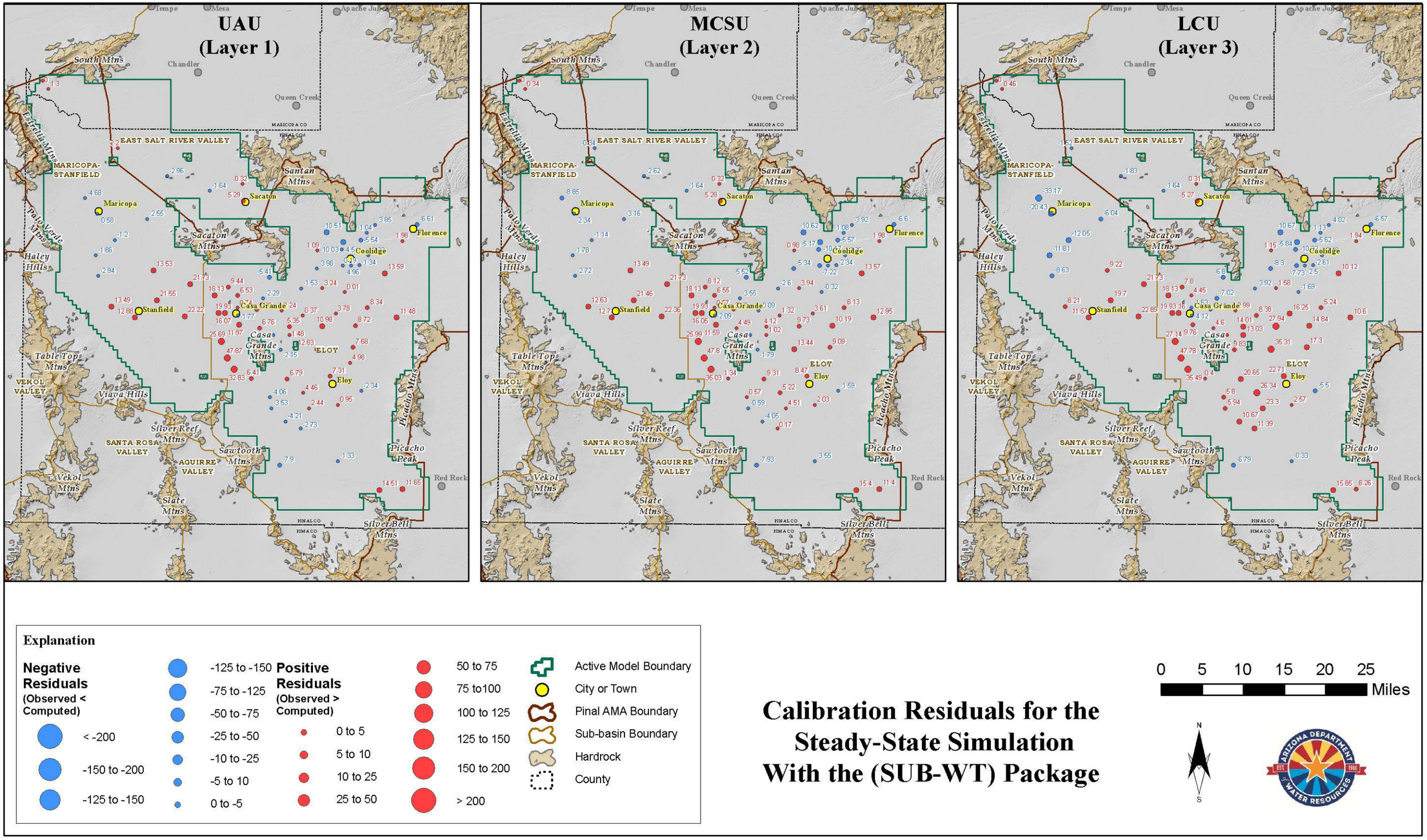

Figure 59 Calibration Residuals for the Steady-State Simulation With the (SUB-WT) Package

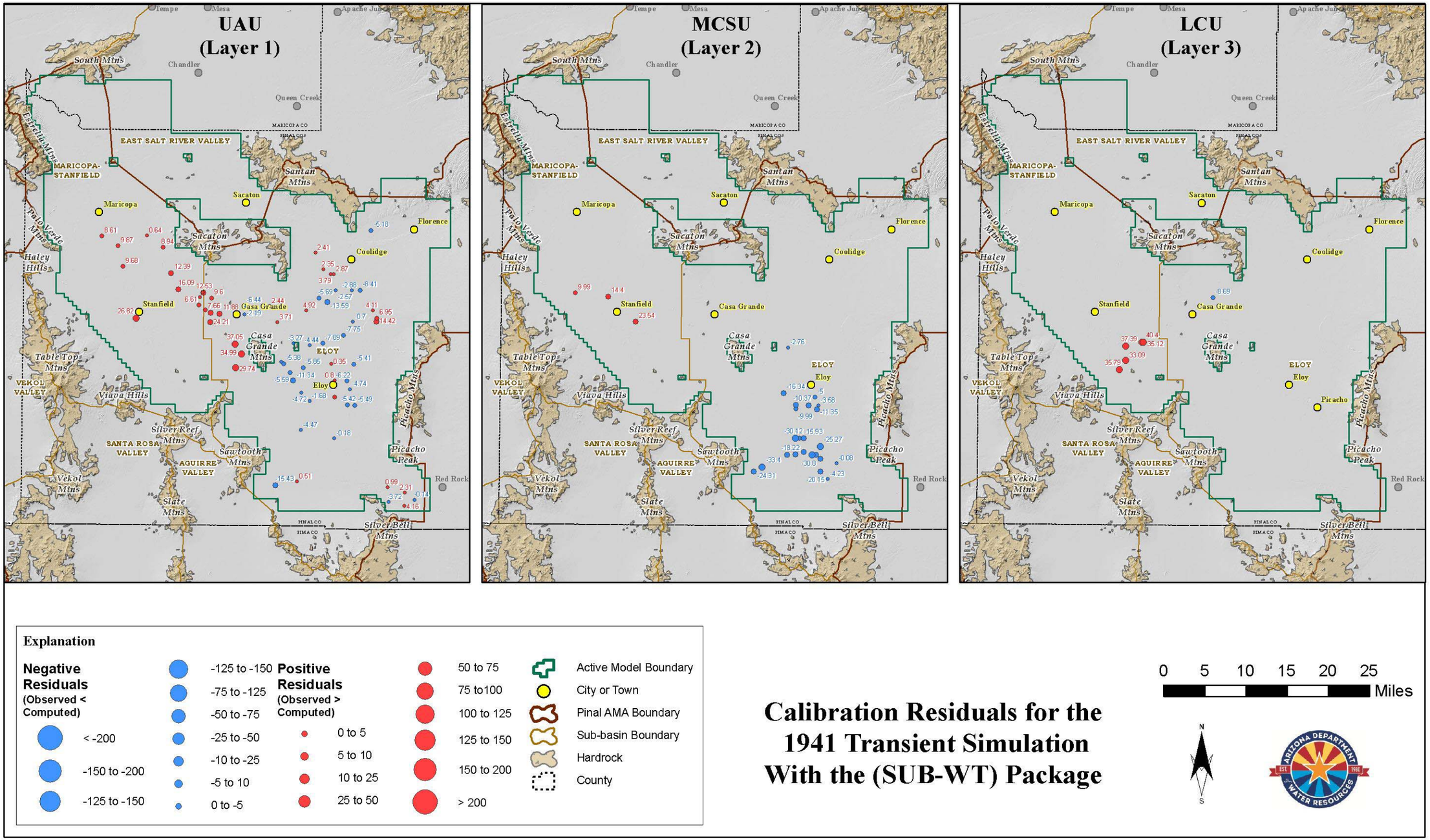

Calibration Residuals for the 1941 Transient Simulation With the (SUB-WT) Package

Figure 60 Calibration Residuals for 1941 Transient Simulation With the (SUB-WT) Package

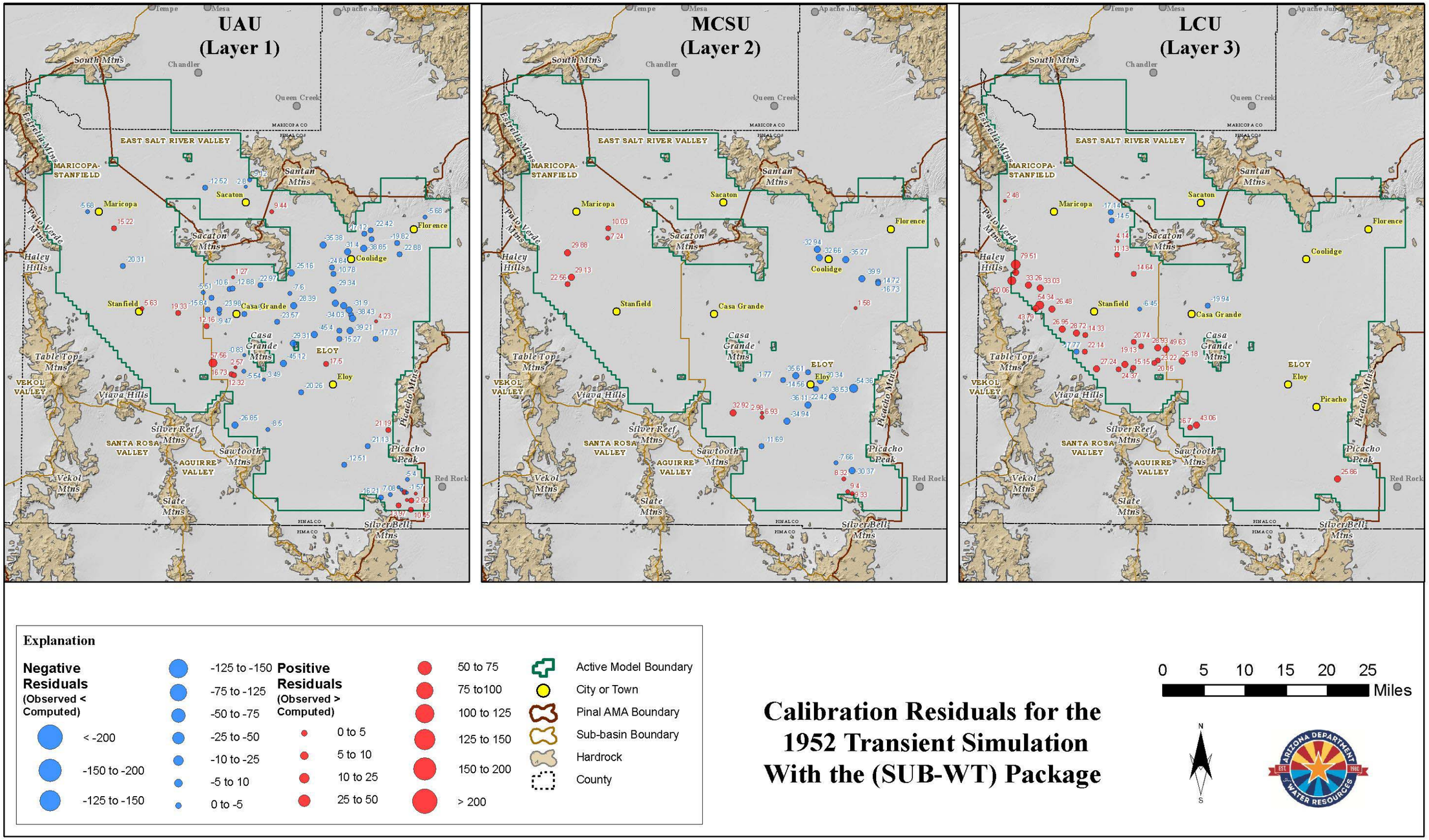

Calibration Residuals for the 1952 Transient Simulation With the (SUB-WT) Package

Figure 61 Calibration Residuals for 1952 Transient Simulation With the (SUB-WT) Package

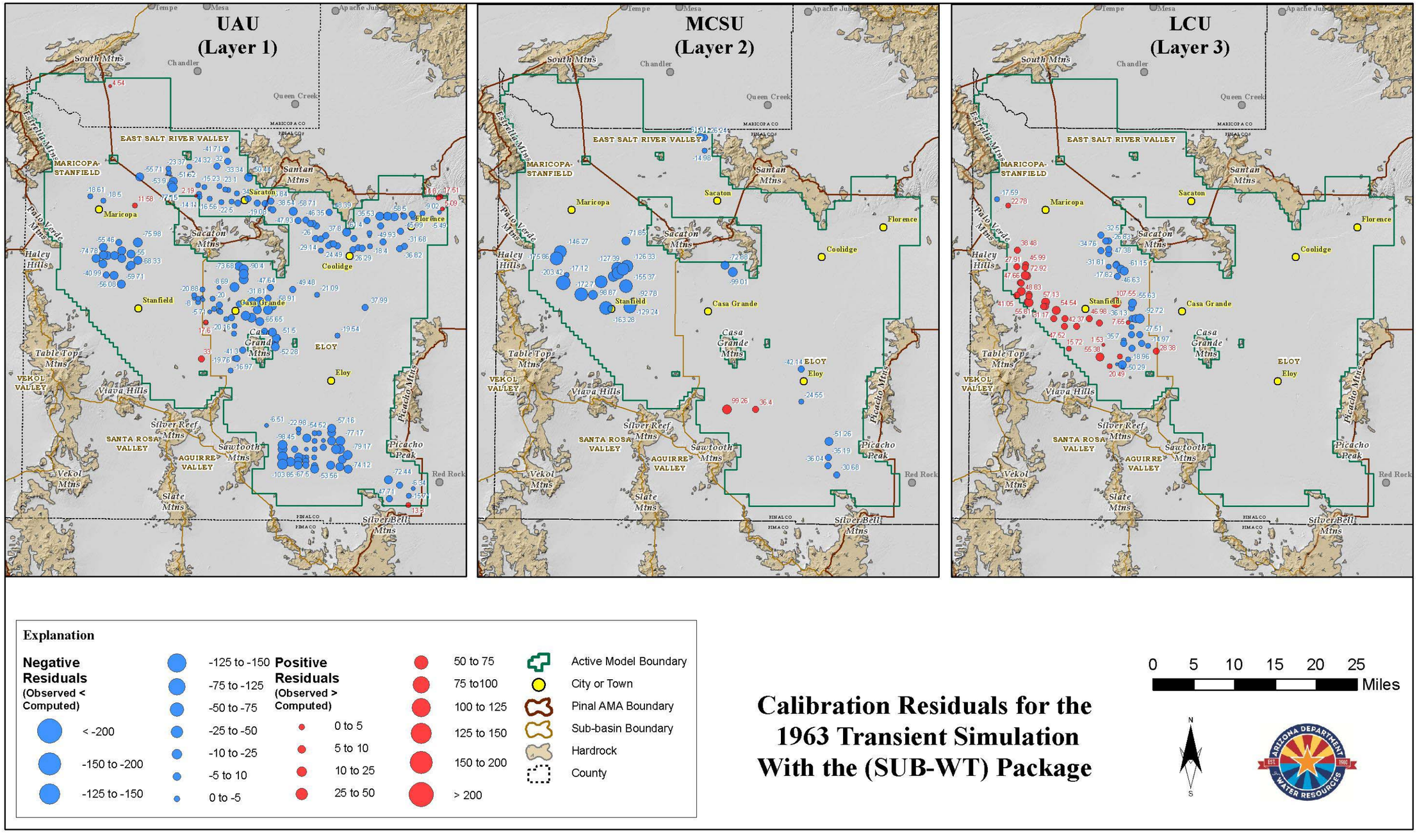

Calibration Residuals for the 1963 Transient Simulation With the (SUB-WT) Package

Figure 62 Calibration Residuals for 1963 Transient Simulation With the (SUB-WT) Package

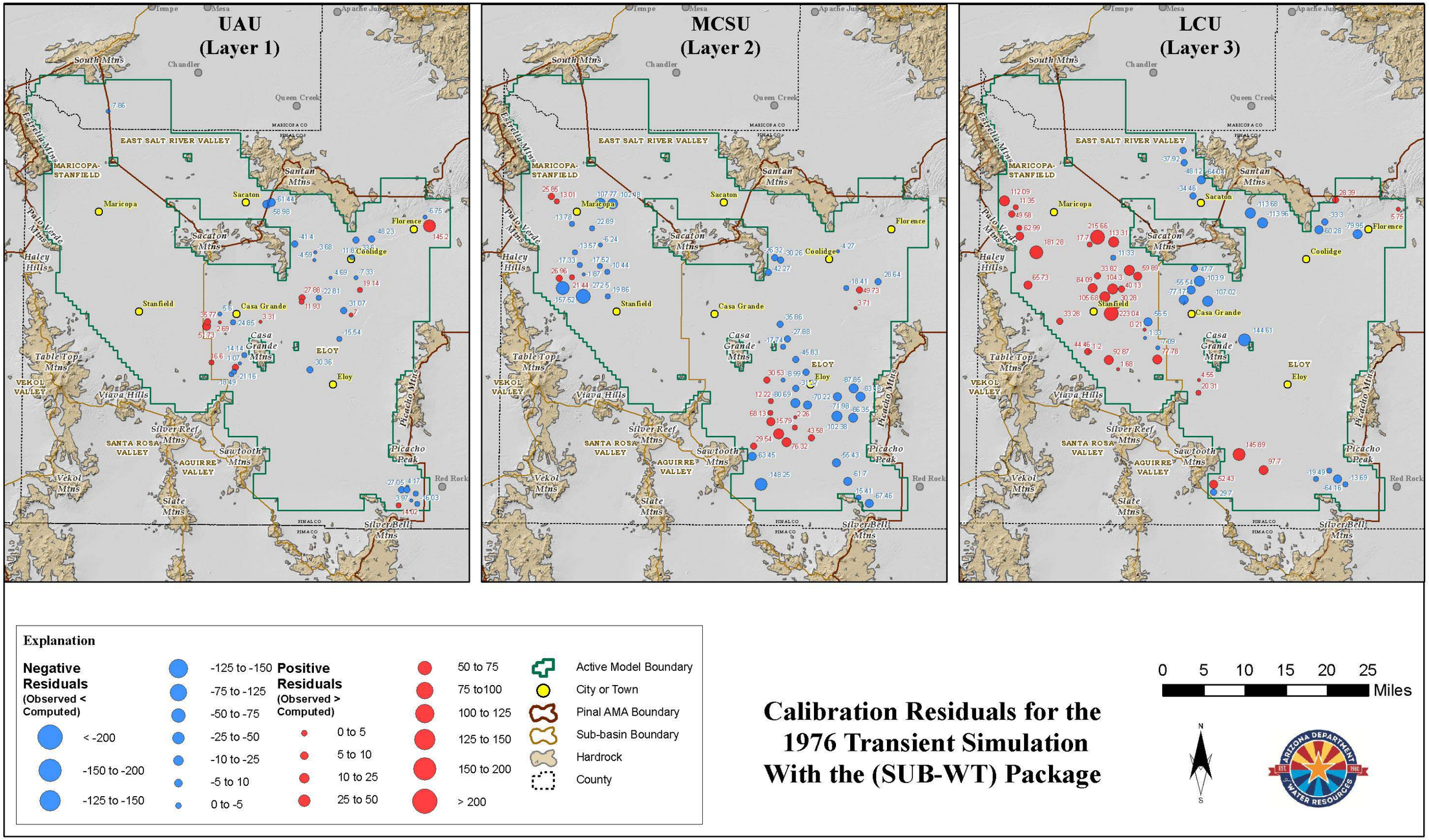

Calibration Residuals for the 1976 Transient Simulation With the (SUB-WT) Package

Figure 63 Calibration Residuals for 1976 Transient Simulation With the (SUB-WT) Package

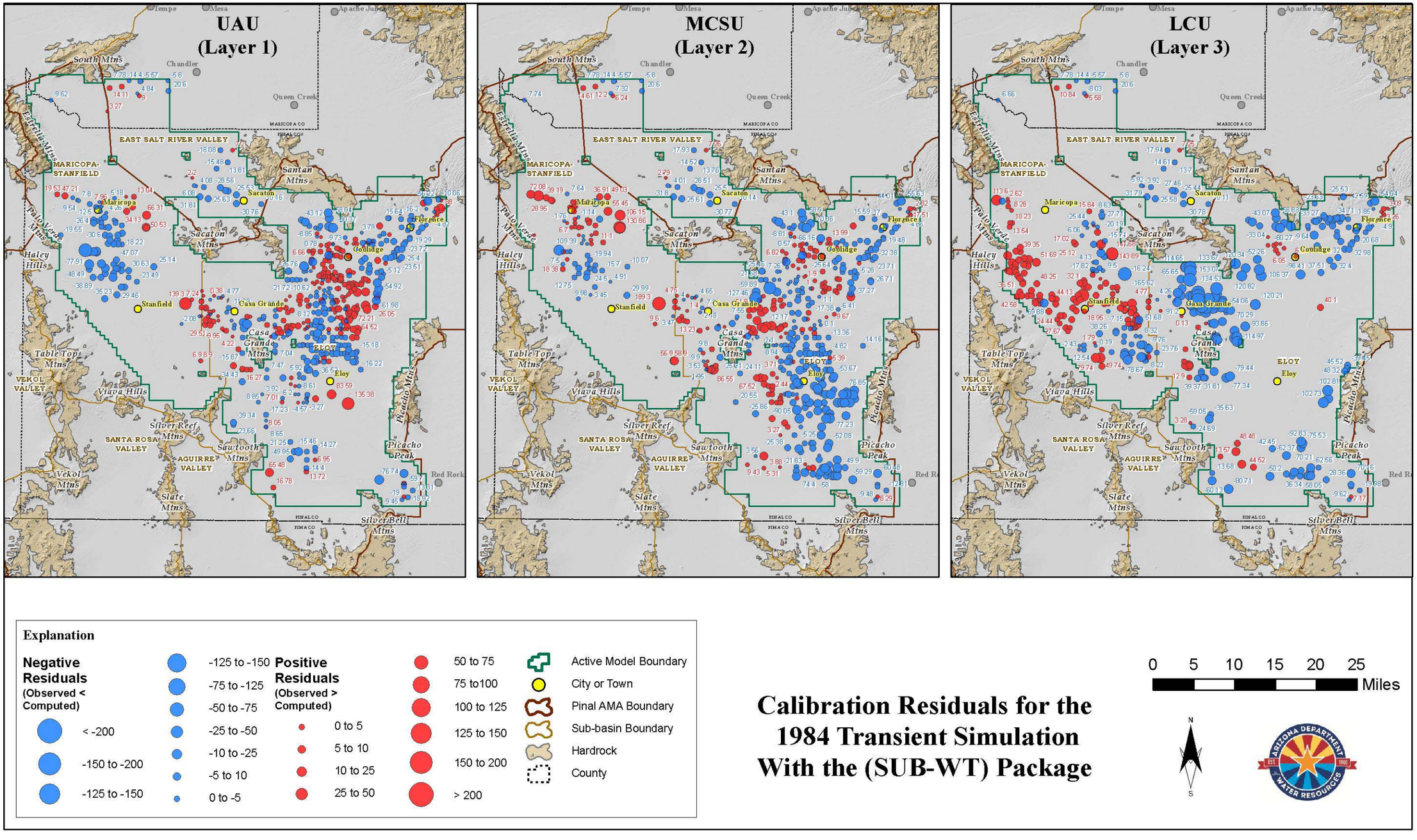

Figure 64 Calibration Residuals for 1984 Transient Simulation With the (SUB-WT) Package

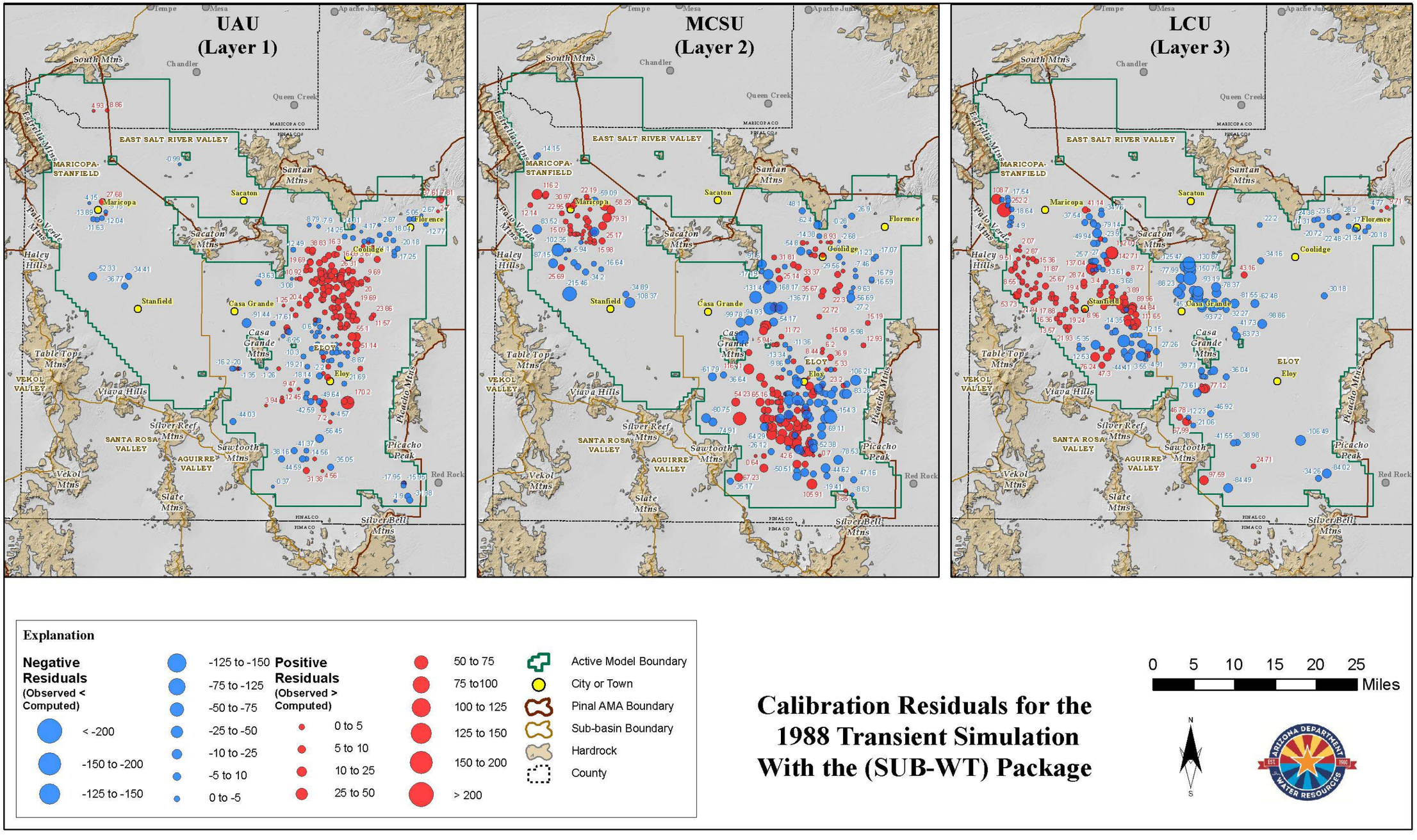

Figure 65 Calibration Residuals for 1988 Transient Simulation With the (SUB-WT) Package

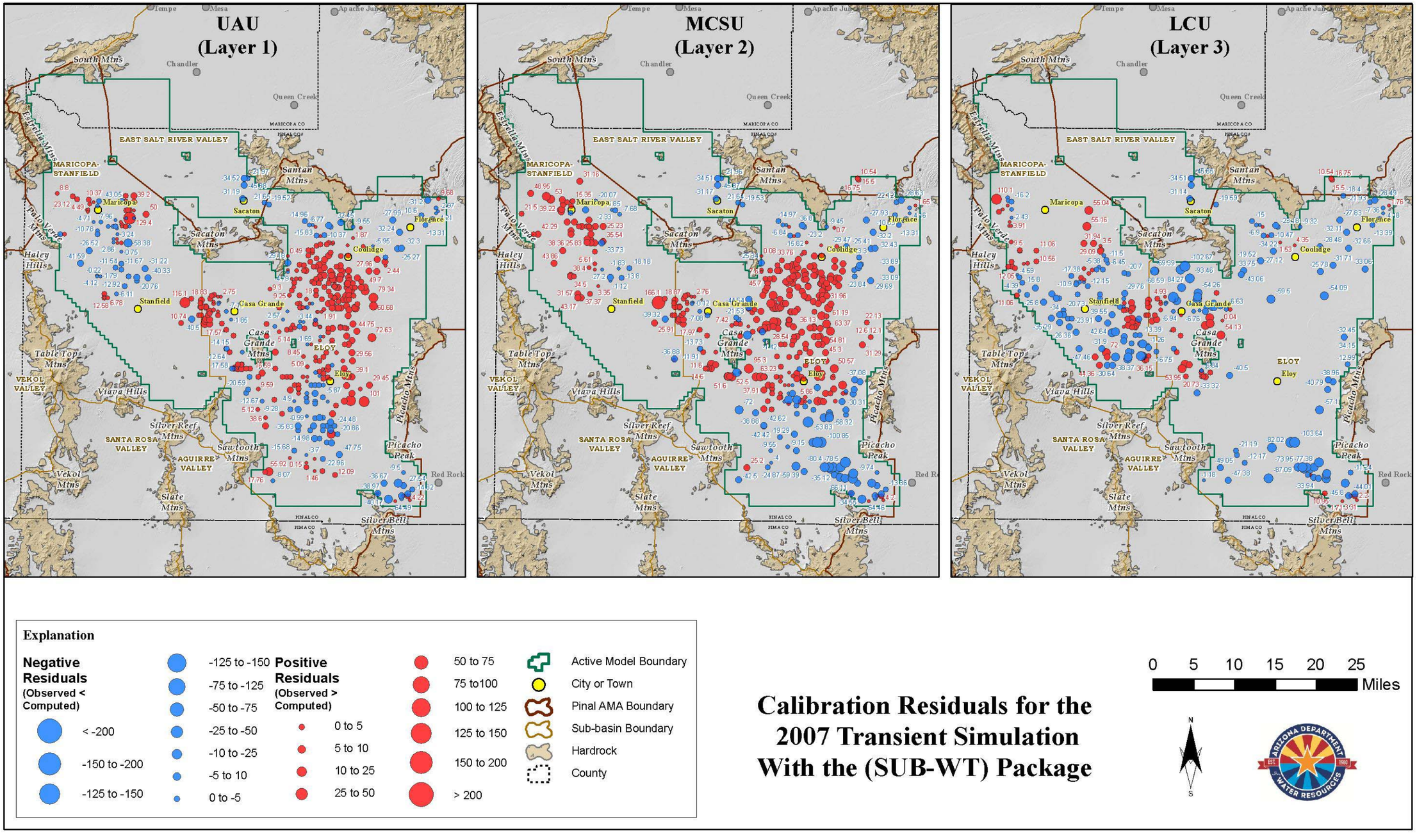

Calibration Residuals for the 2007 Transient Simulation With the (SUB-WT) Package

Figure 66 Calibration Residuals for 2007 Transient Simulation With the (SUB-WT) Package

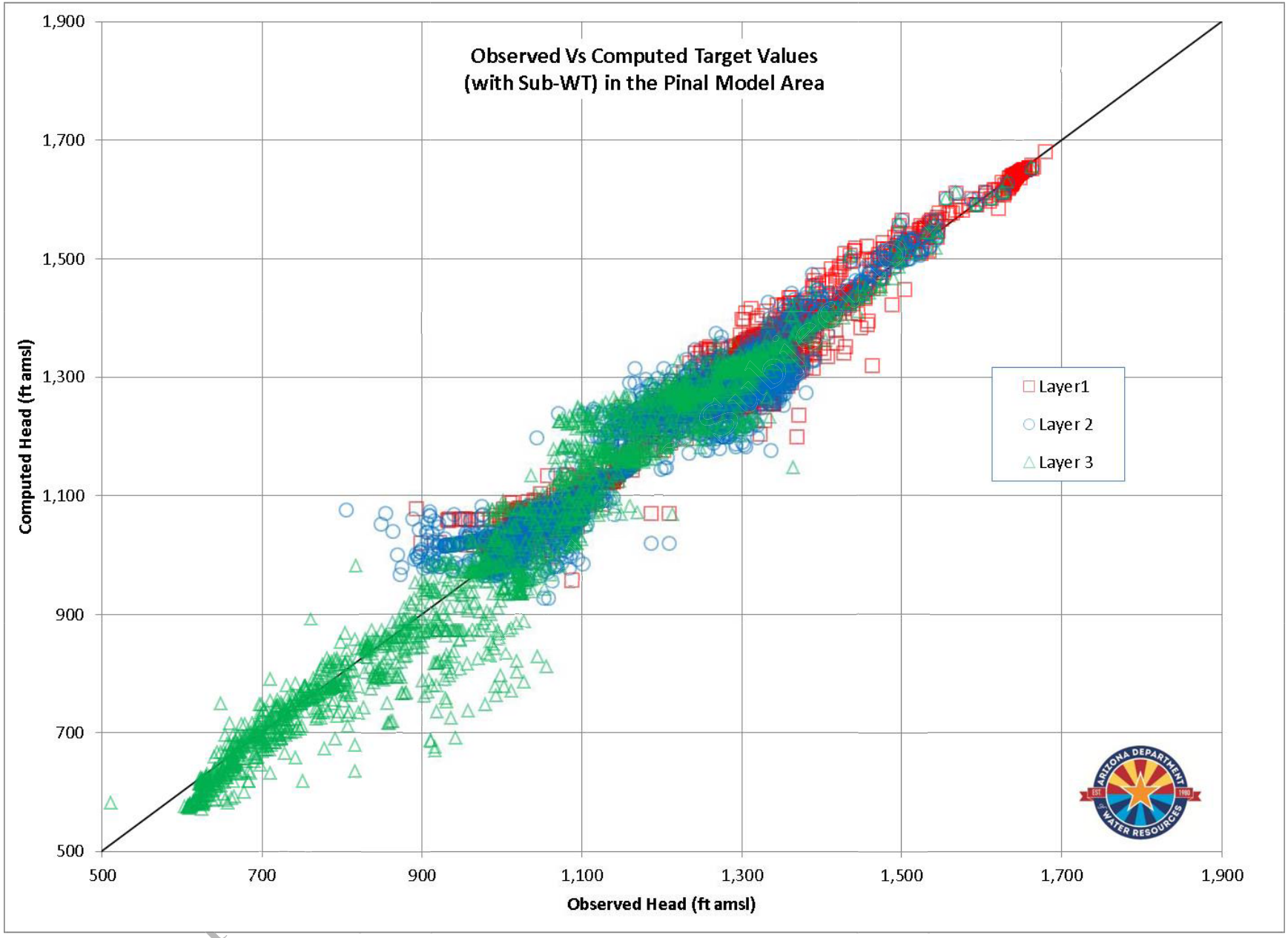

Figure 67 Plot of Observed Vs Computed Target Values (with SUB-WT) in the Pinal Model Area

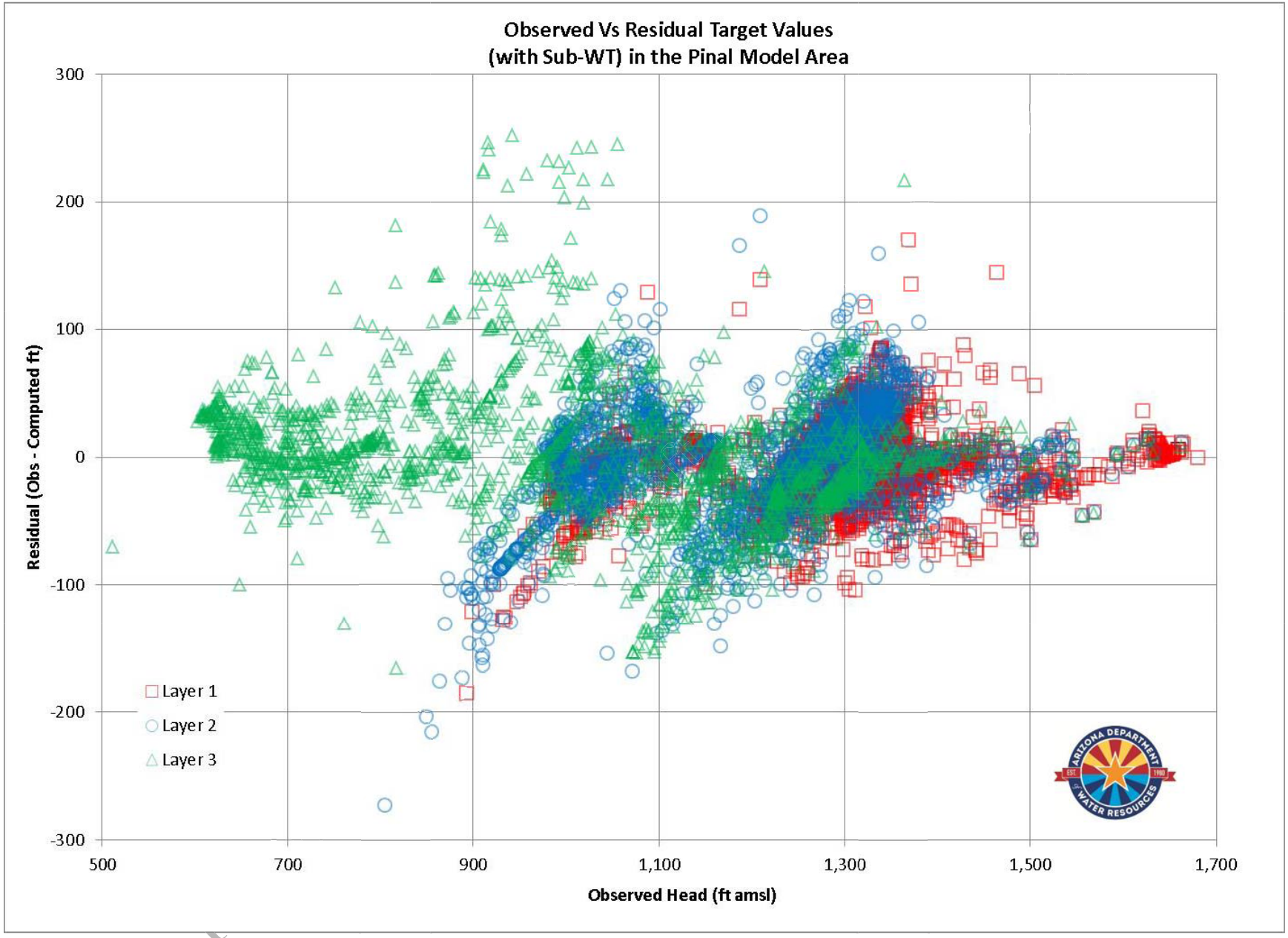

Figure 68 Plot of Observed Vs Residual Target Values (with SUB-WT) in the Pinal Model Area

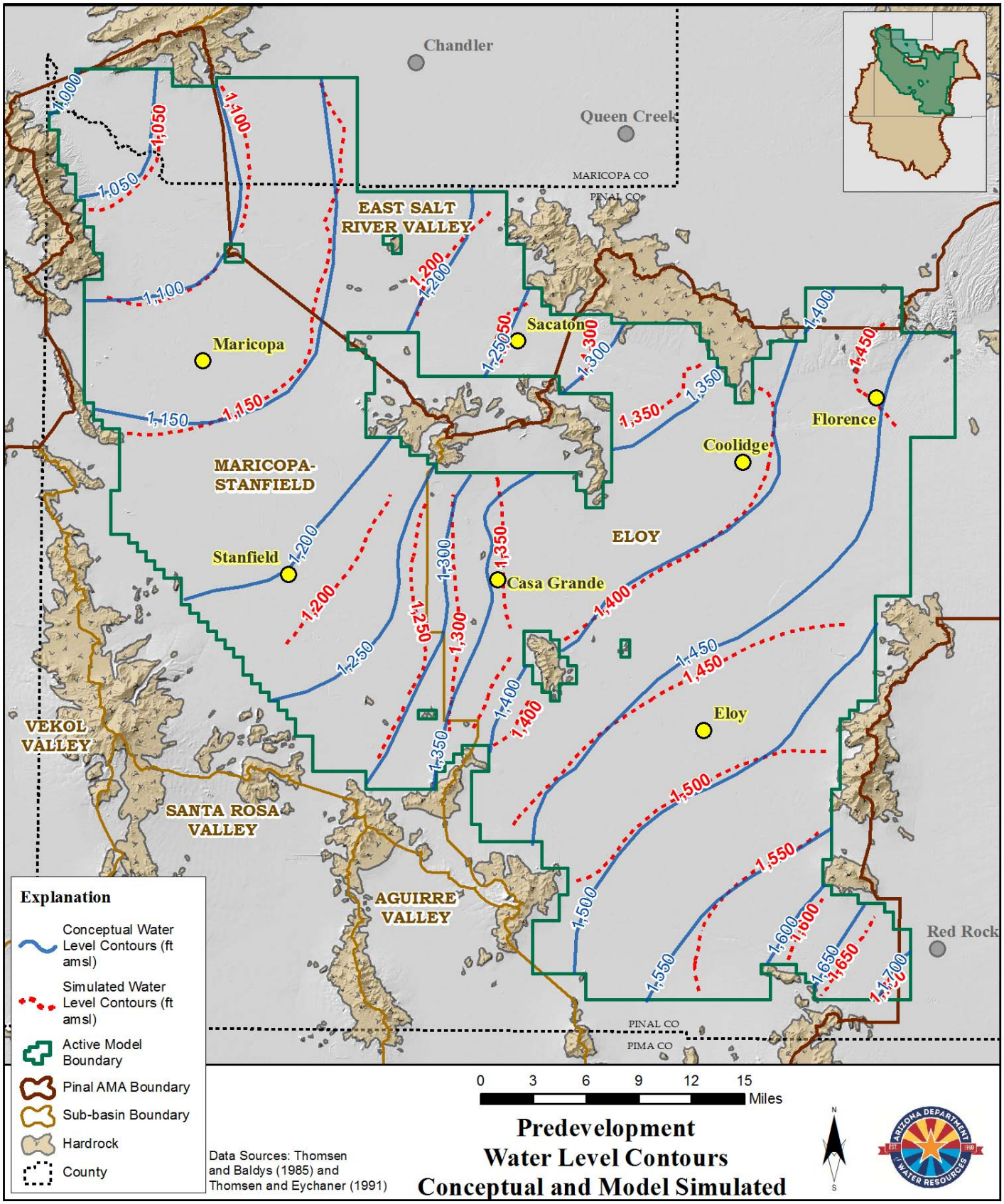

Figure 69 Predevelopment WL Contours - Conceptual and Model Simulated

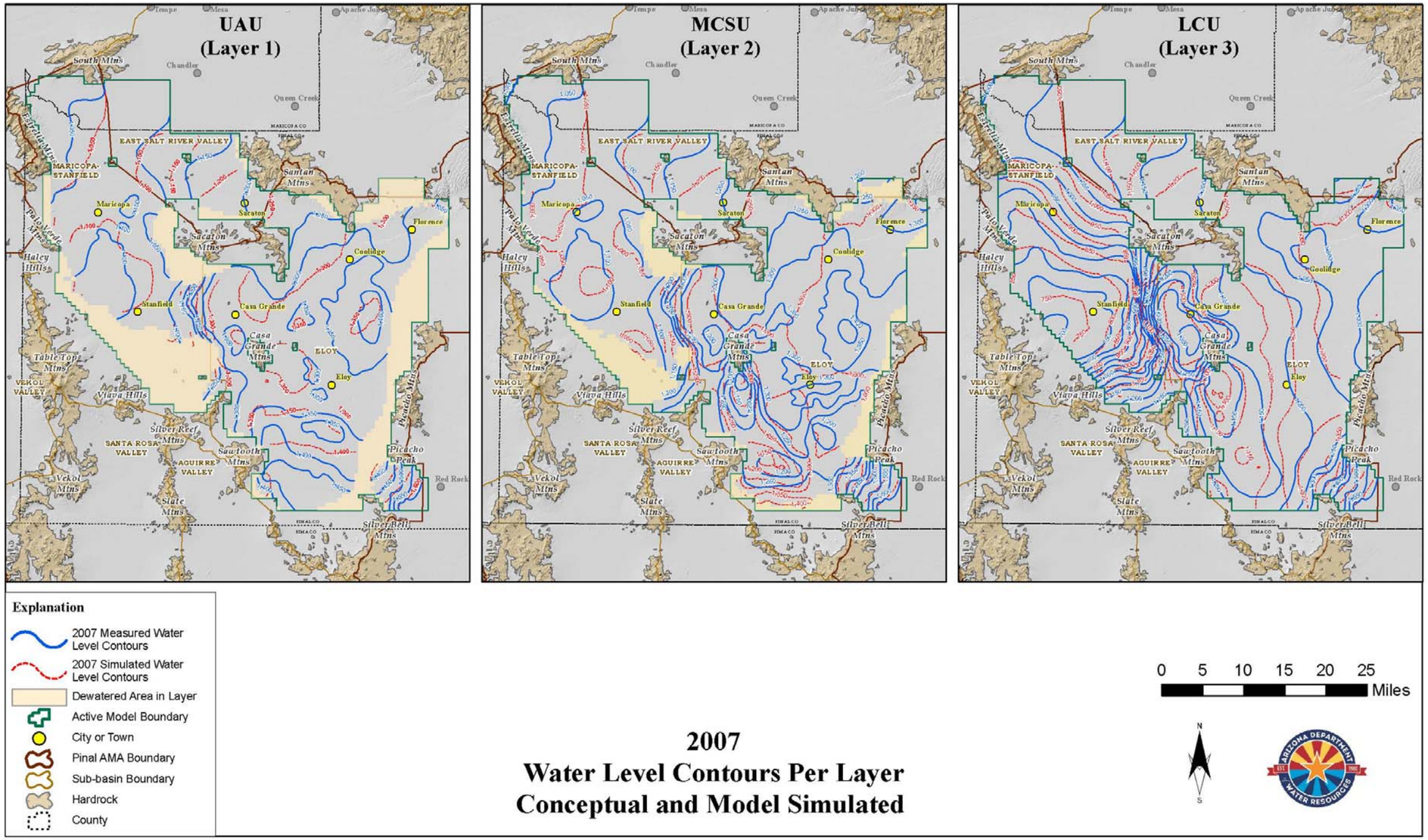

Figure 70 2007 Water Level Contours Per Layer Conceptual and Model Simulated

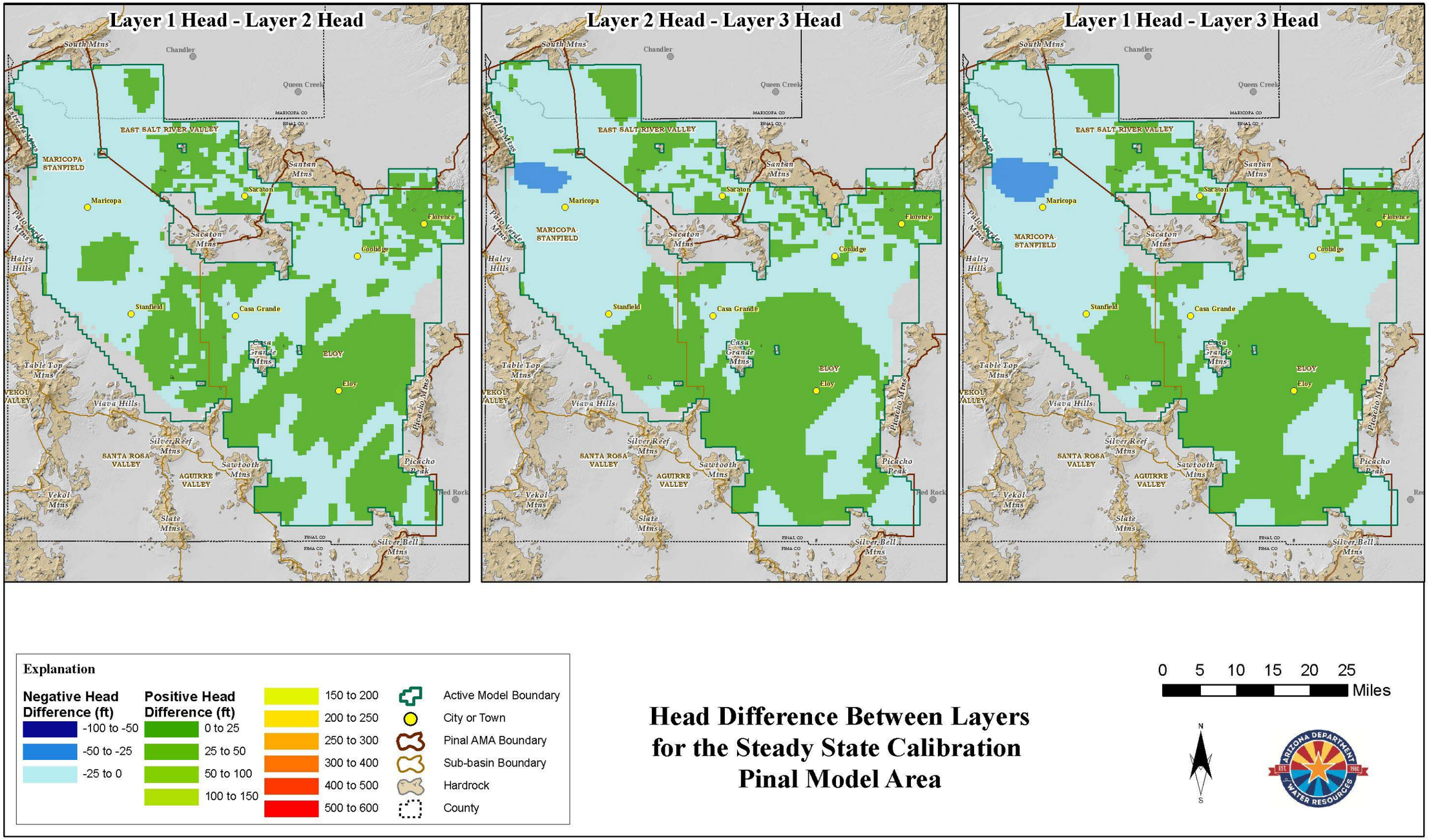

Figure 71 Head Difference Between Layers for the Steady State Calibration

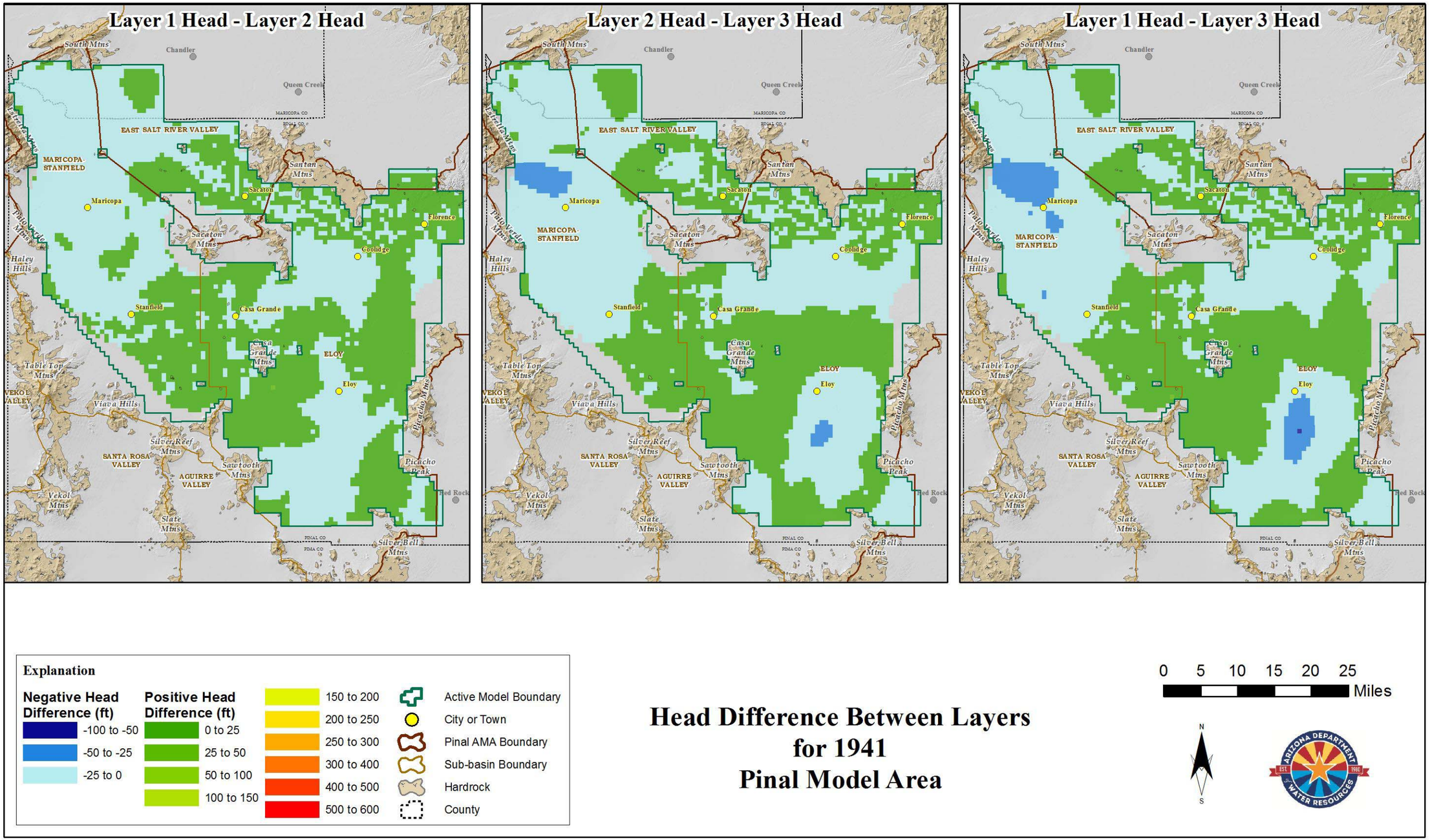

Figure 72 Head Difference Between Layers for 1941

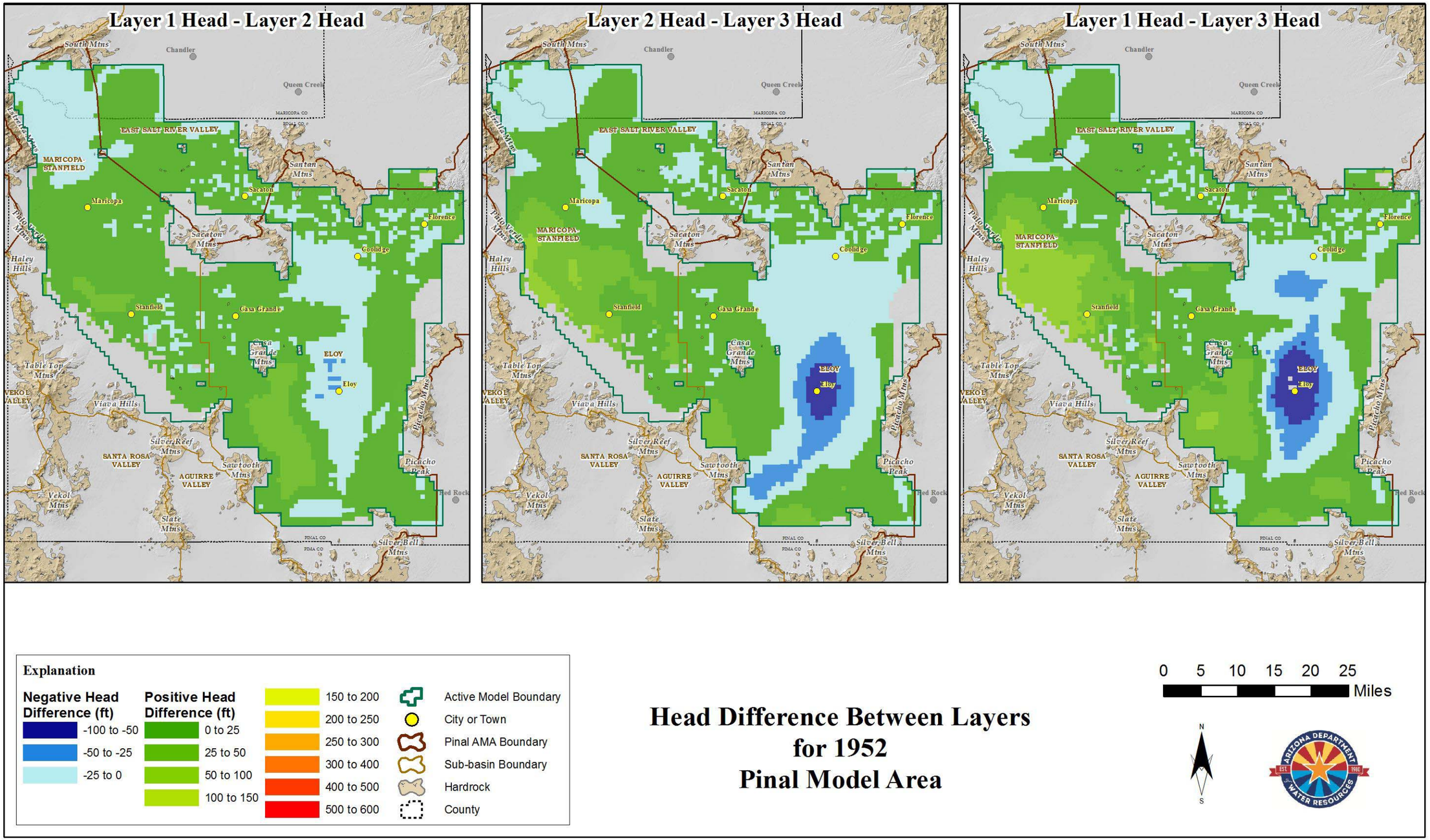

Figure 73 Head Difference Between Layers for 1952

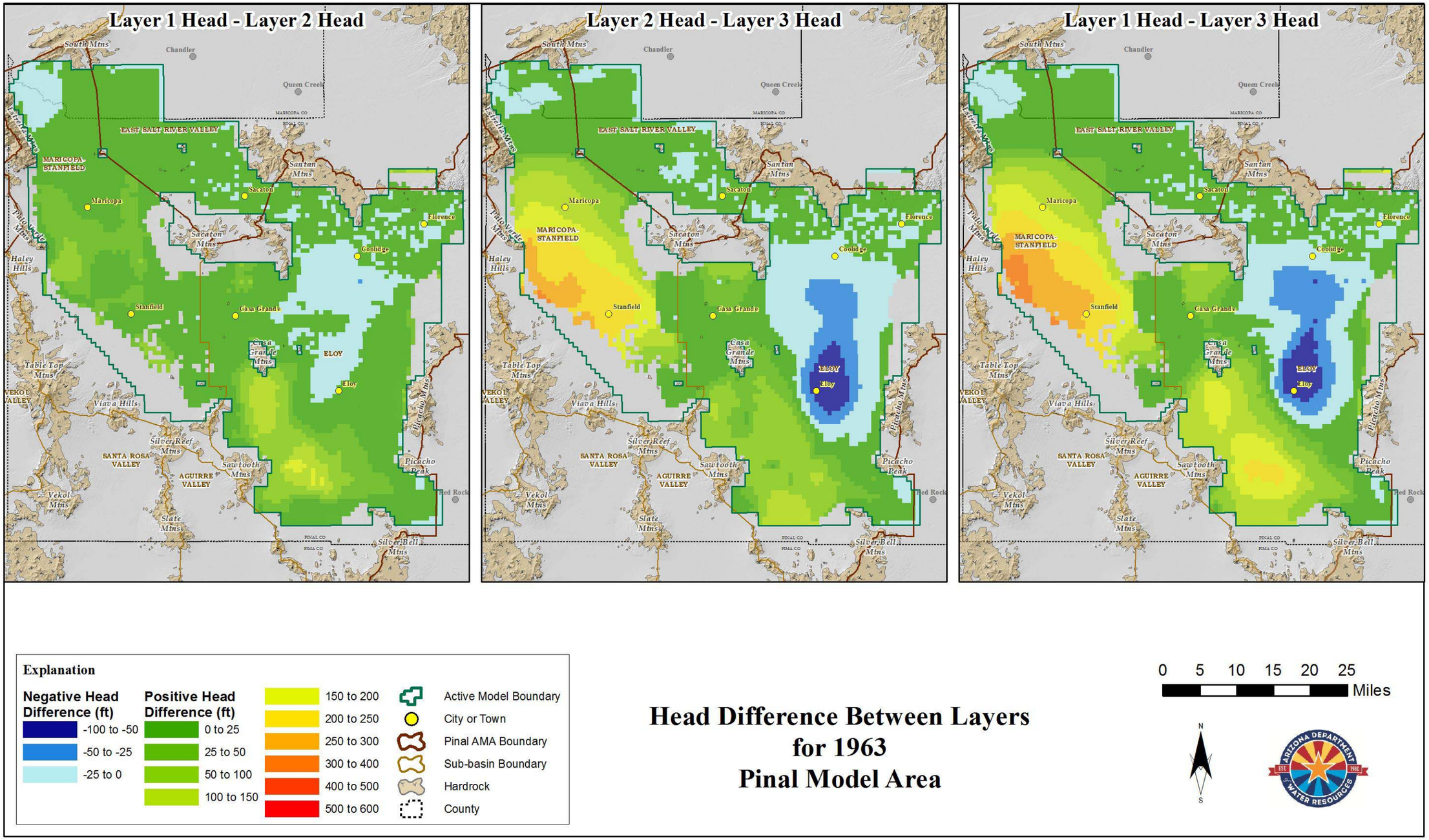

Figure 74 Head Difference Between Layers for 1963

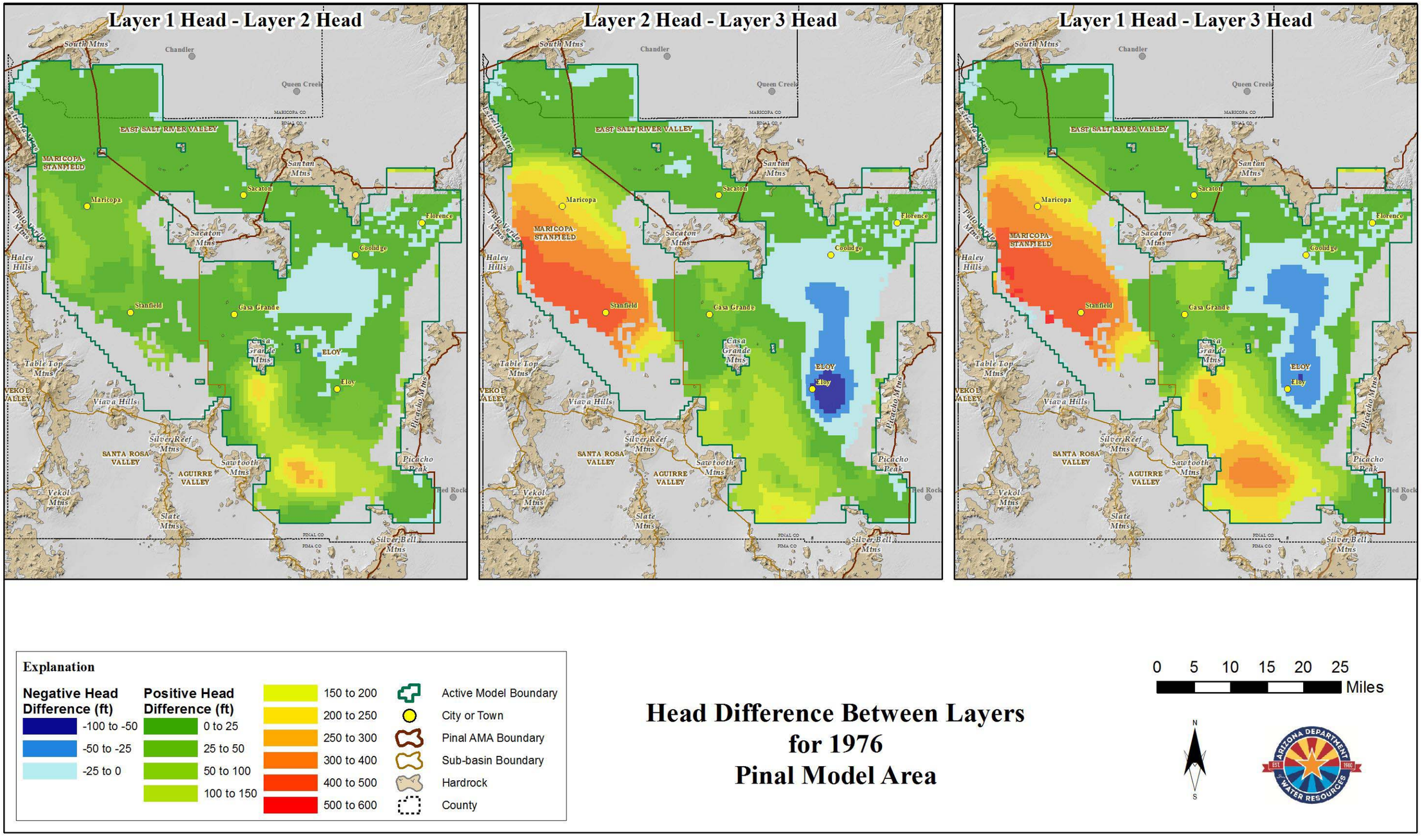

Figure 75 Head Difference Between Layers for 1976

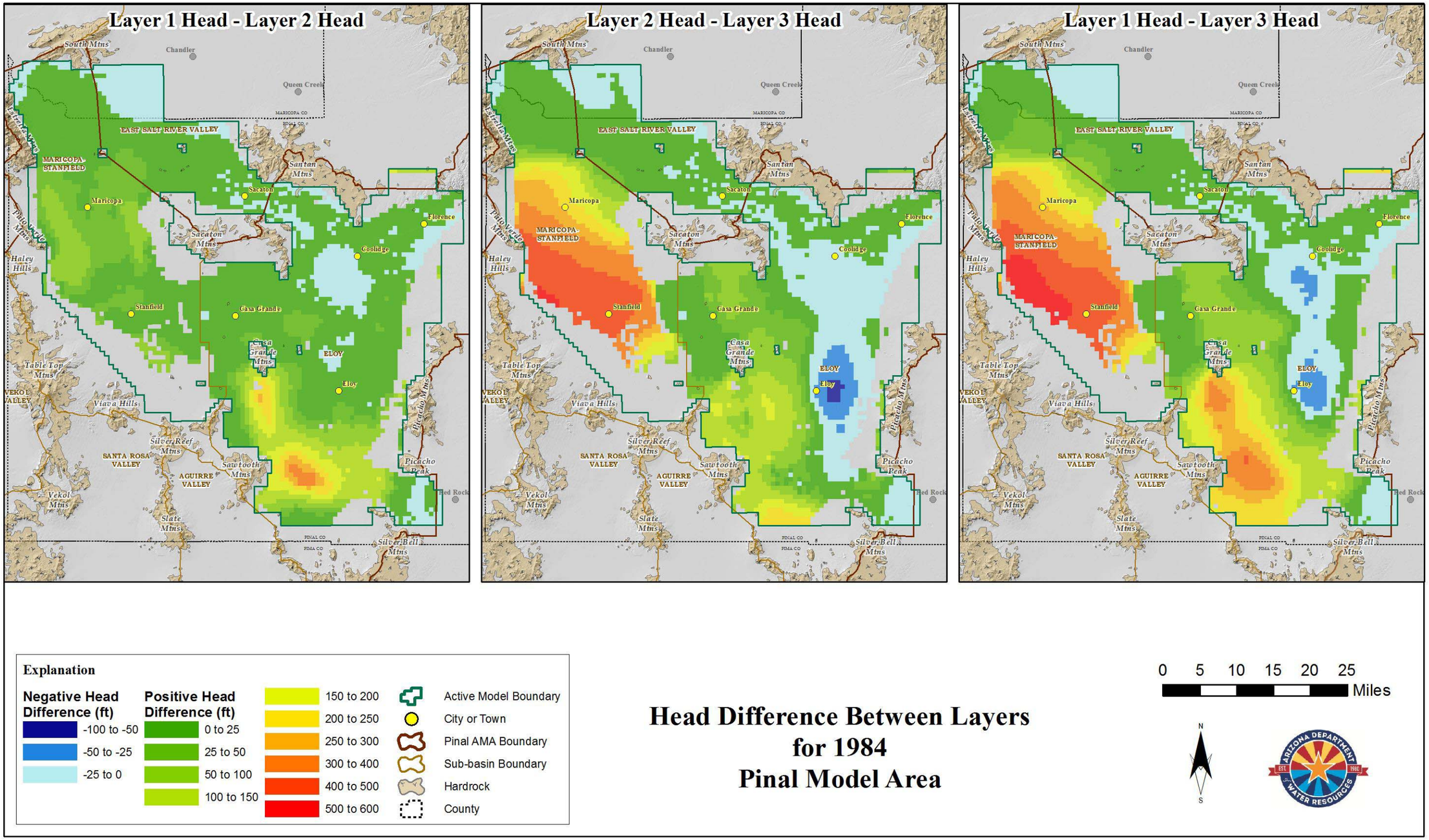

Figure 76 Head Difference Between Layers for 1984

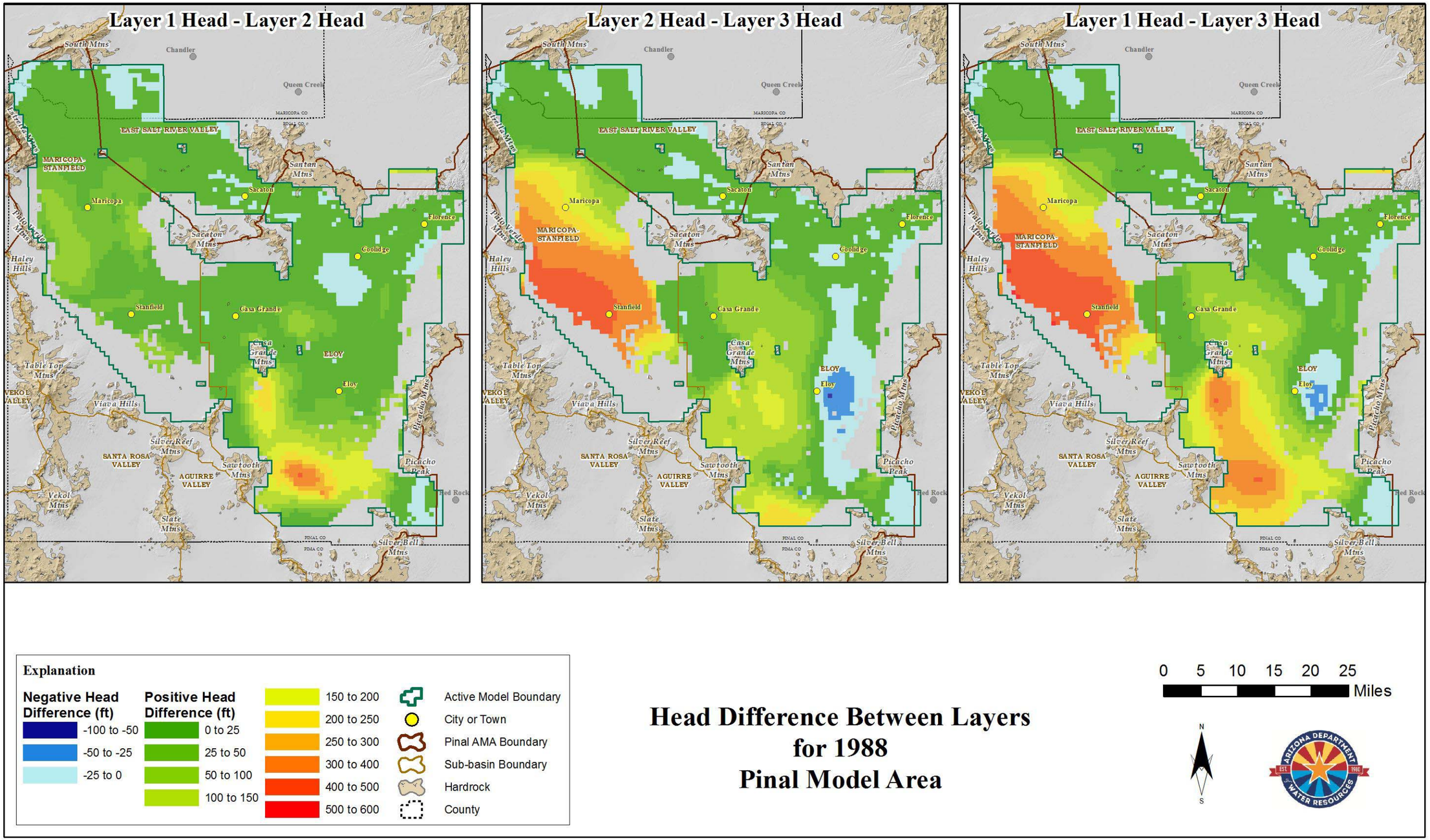

Figure 77 Head Difference Between Layers for 1988

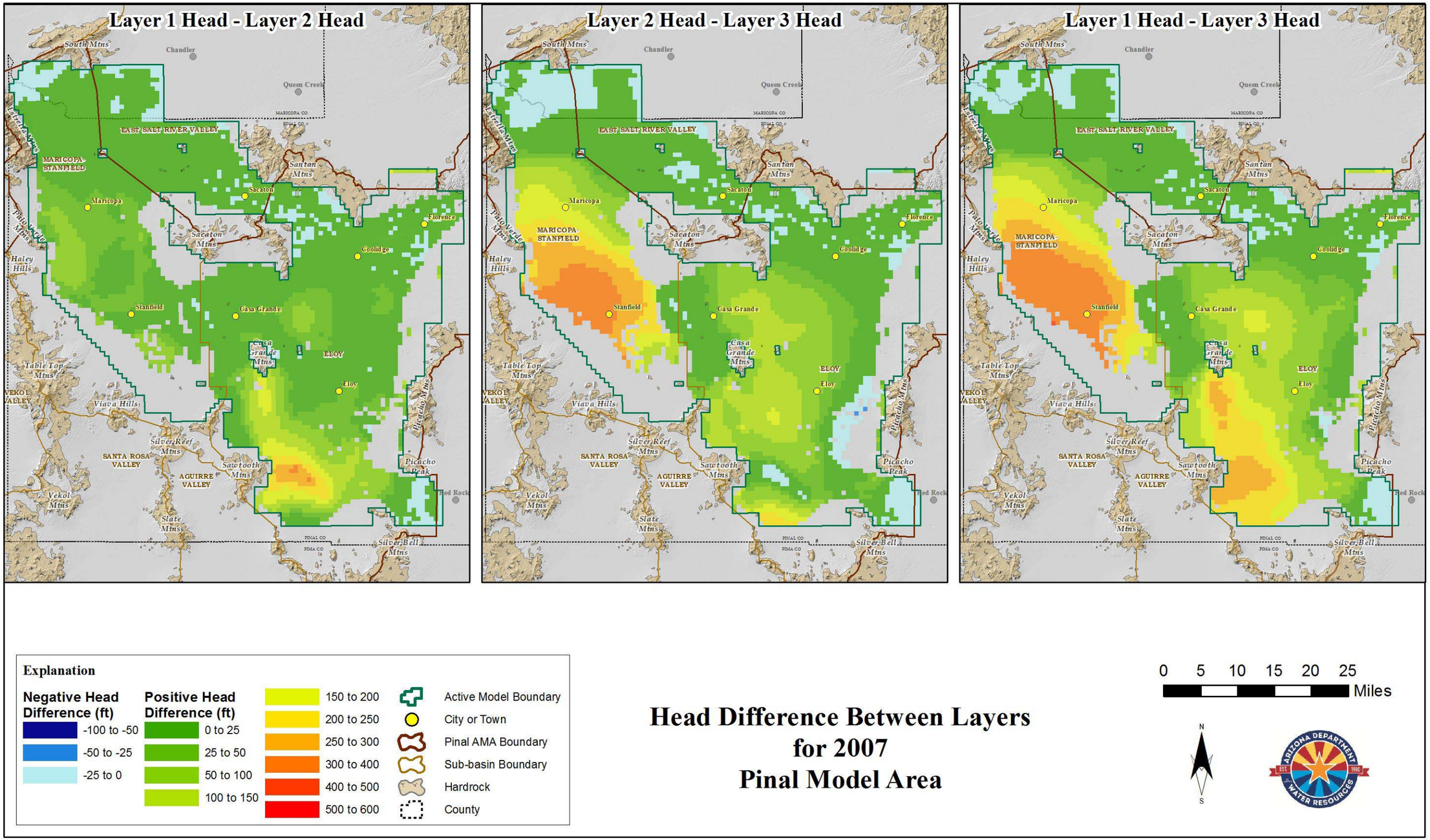

Figure 78 Head Difference Between Layers for 2007

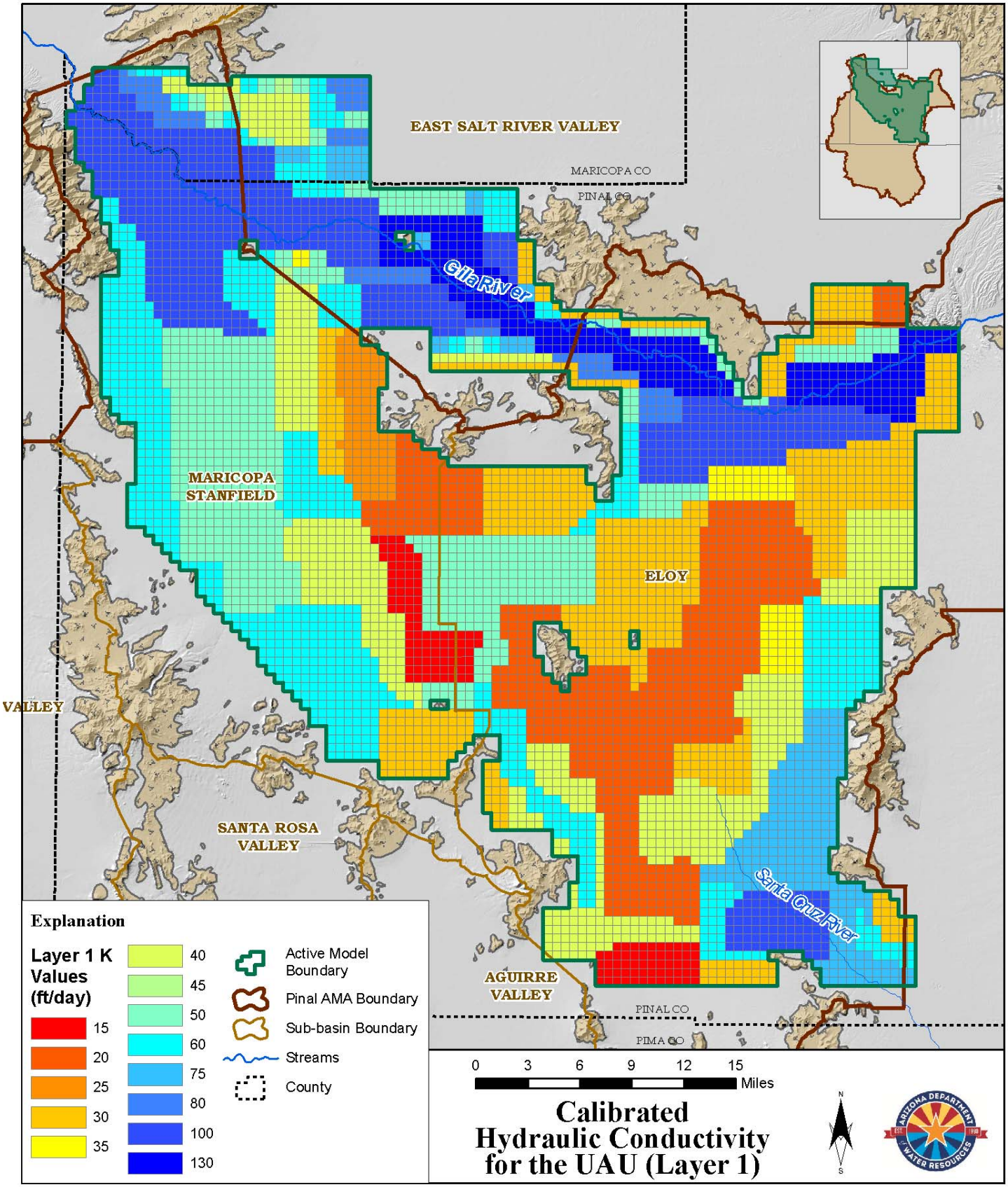

Figure 79 Calibrated Hydraulic Conductivity for the UAU (Layer 1)

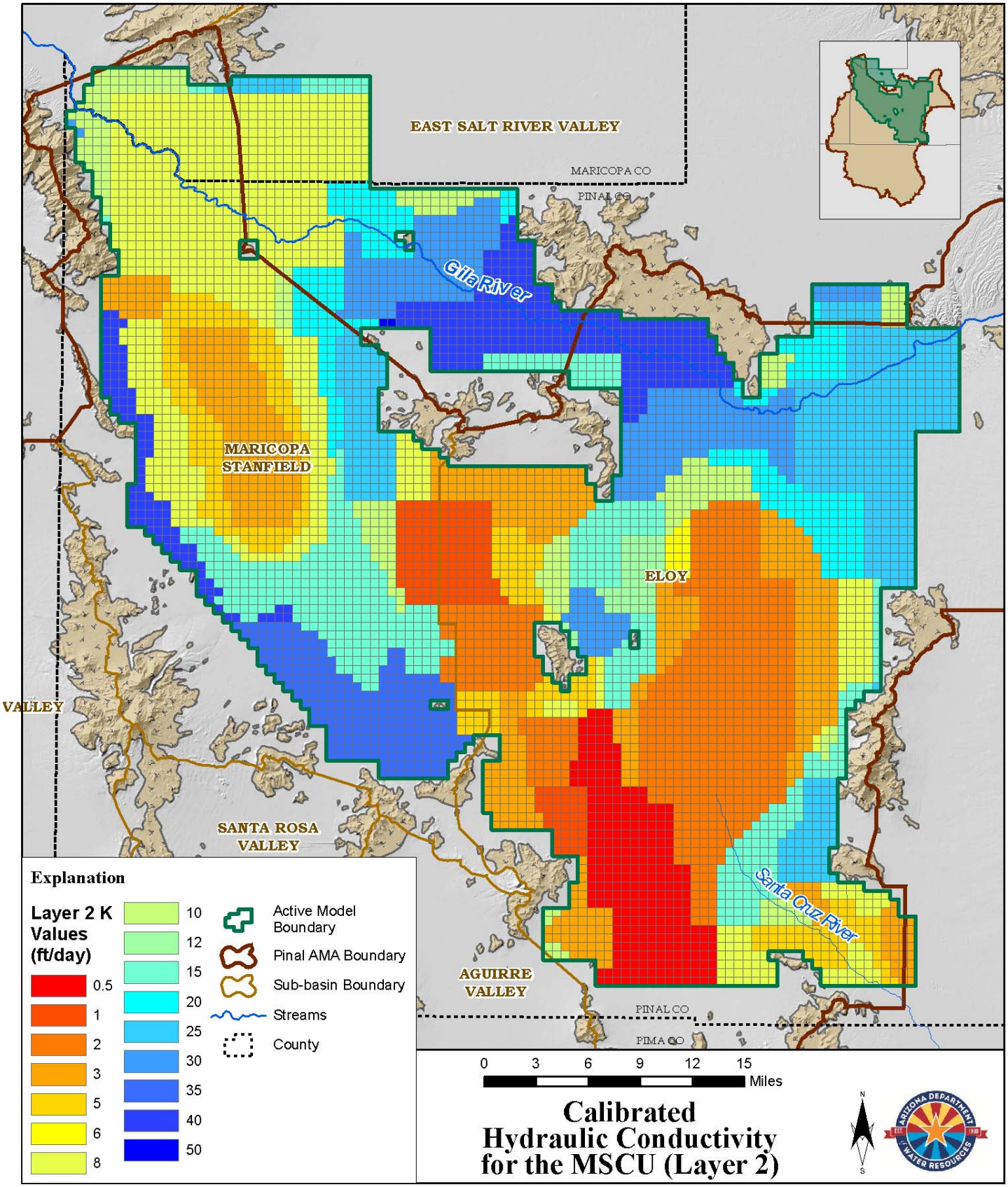

Figure 80 Calibrated Hydraulic Conductivity for the MSCU (Layer 2)

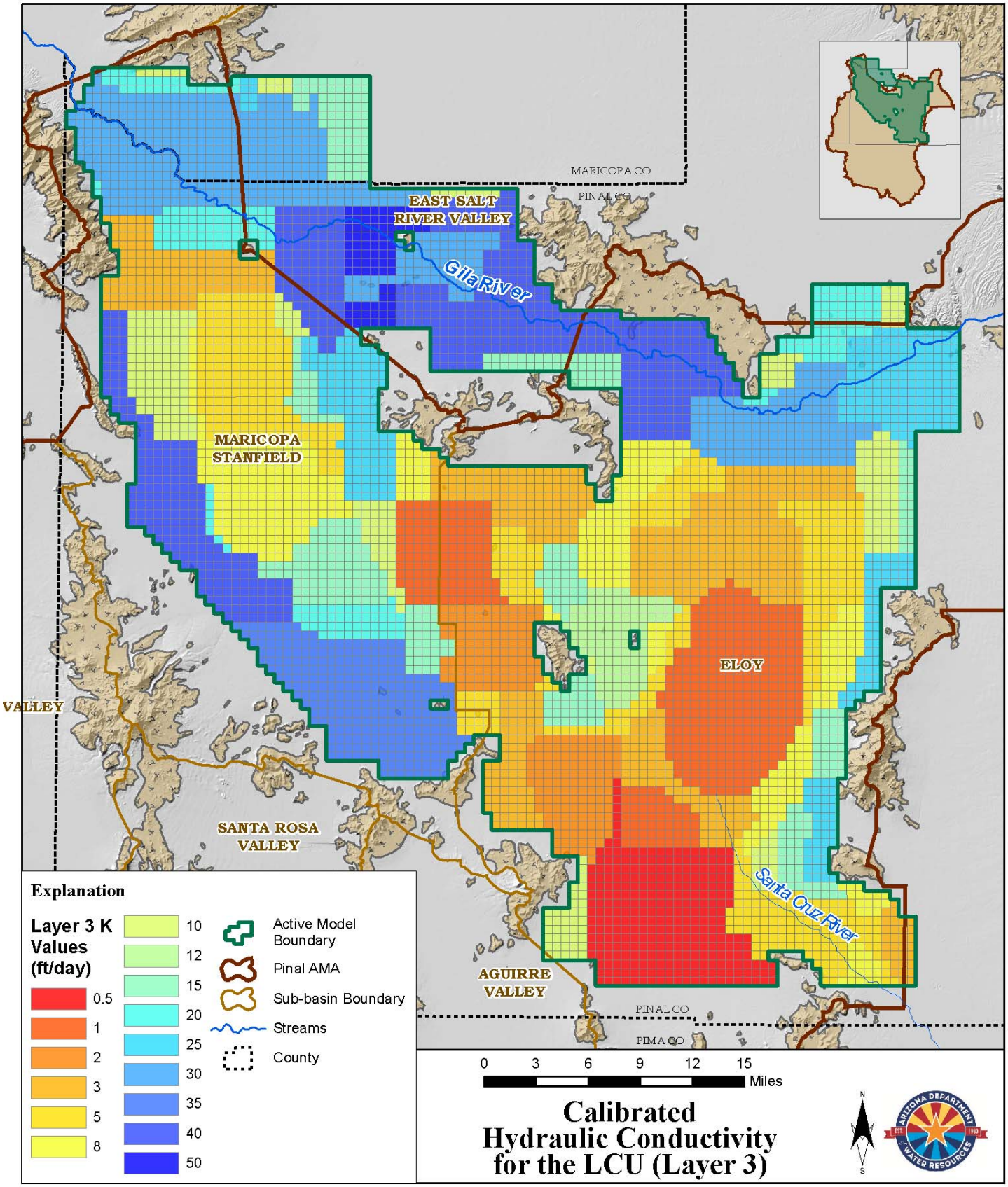

Figure 81 Calibrated Hydraulic Conductivity for the LCU (Layer 3)

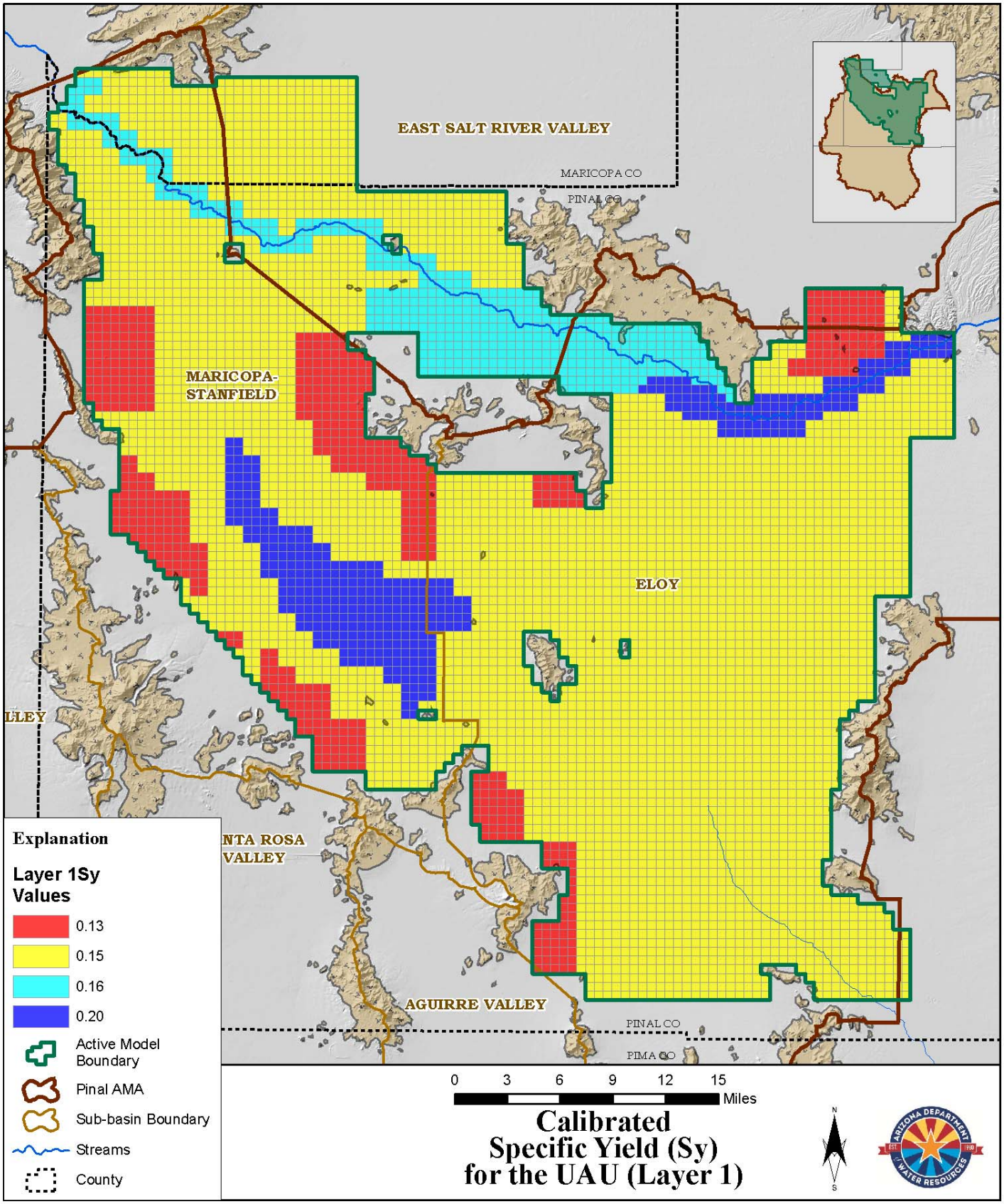

Figure 82 Calibrated Specific Yield for the UAU (Layer 1)

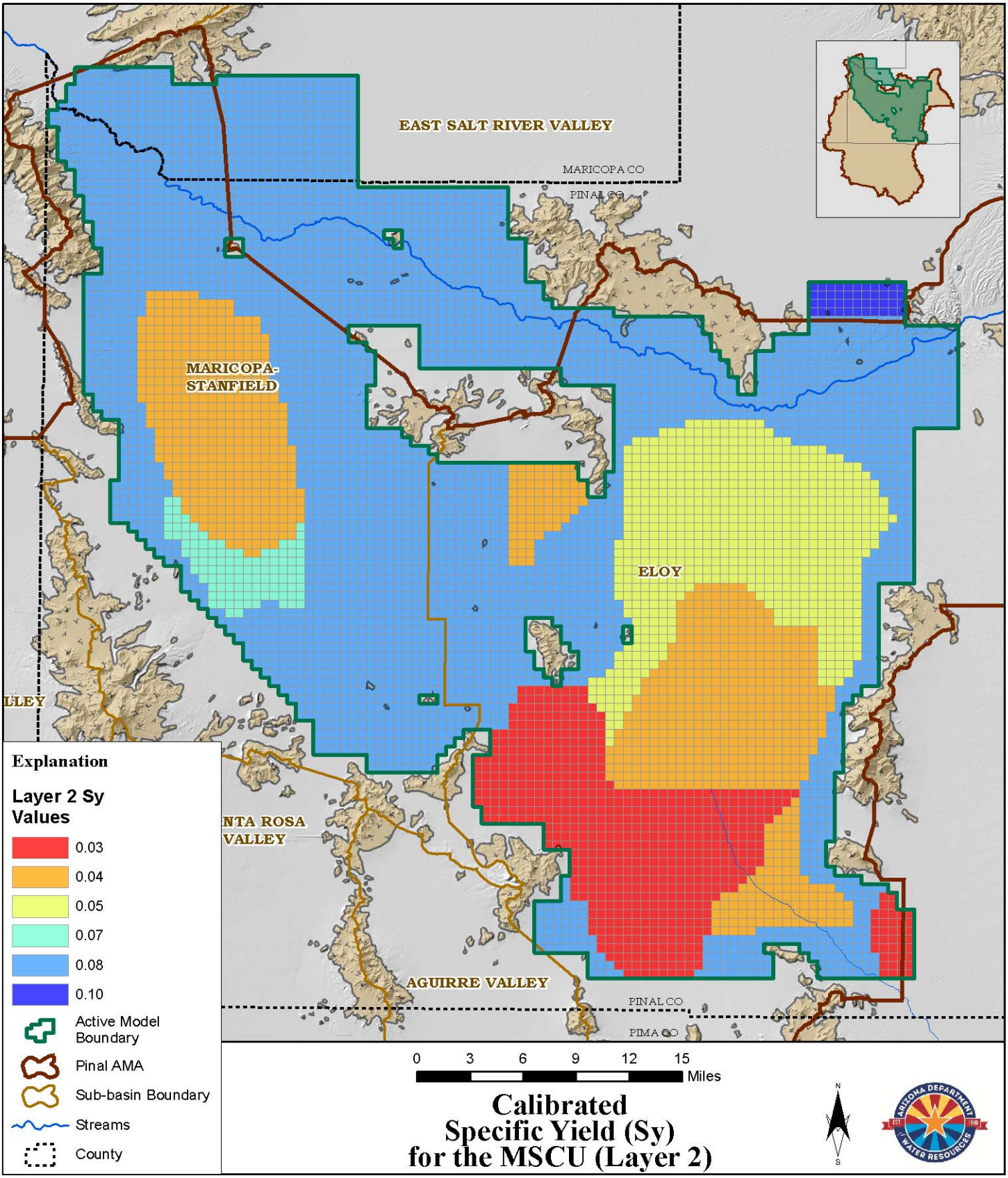

Figure 83 Calibrated Specific Yield for the MSCU (Layer 2)

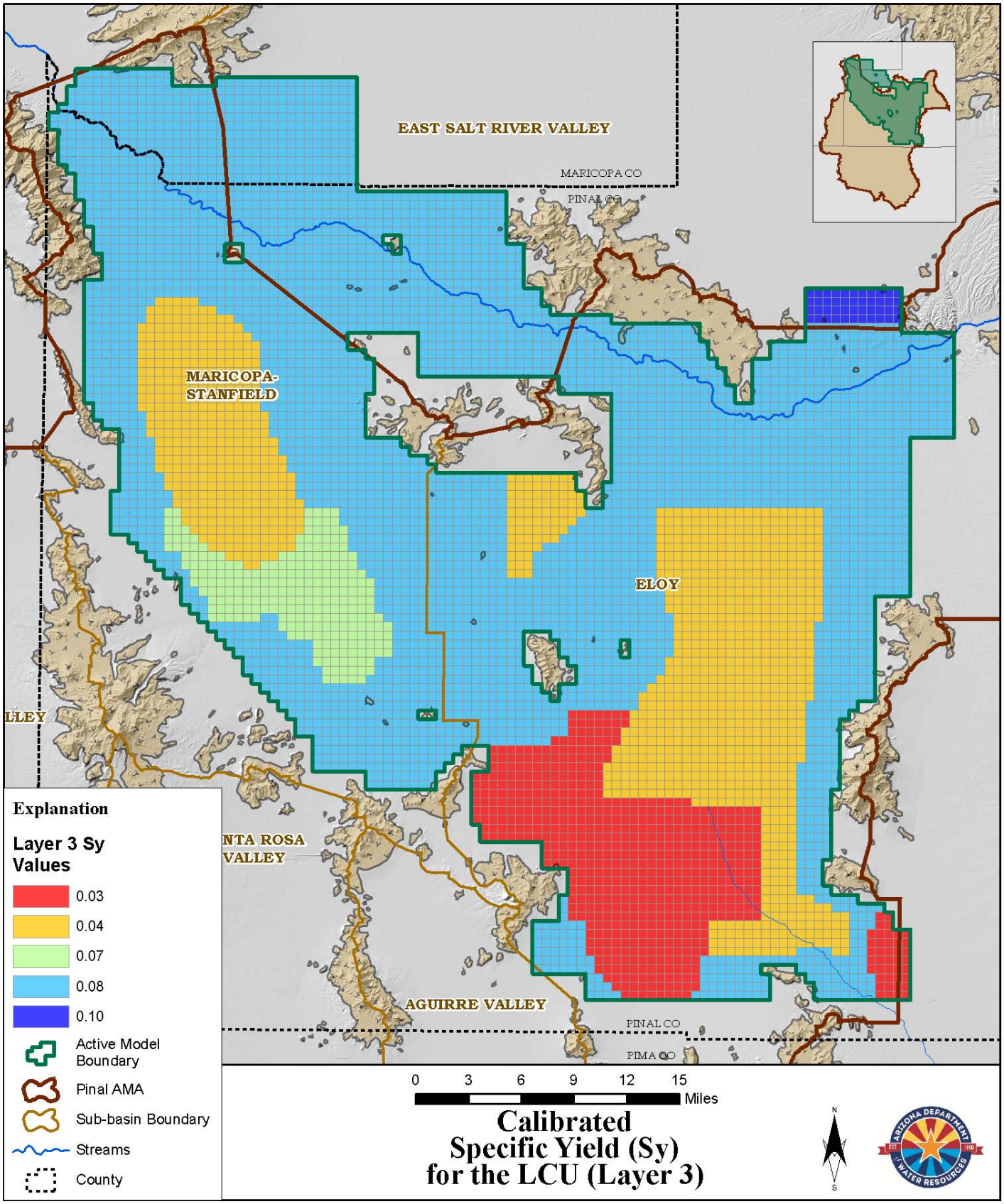

Figure 84 Calibrated Specific Yield for the LCU (Layer 3)

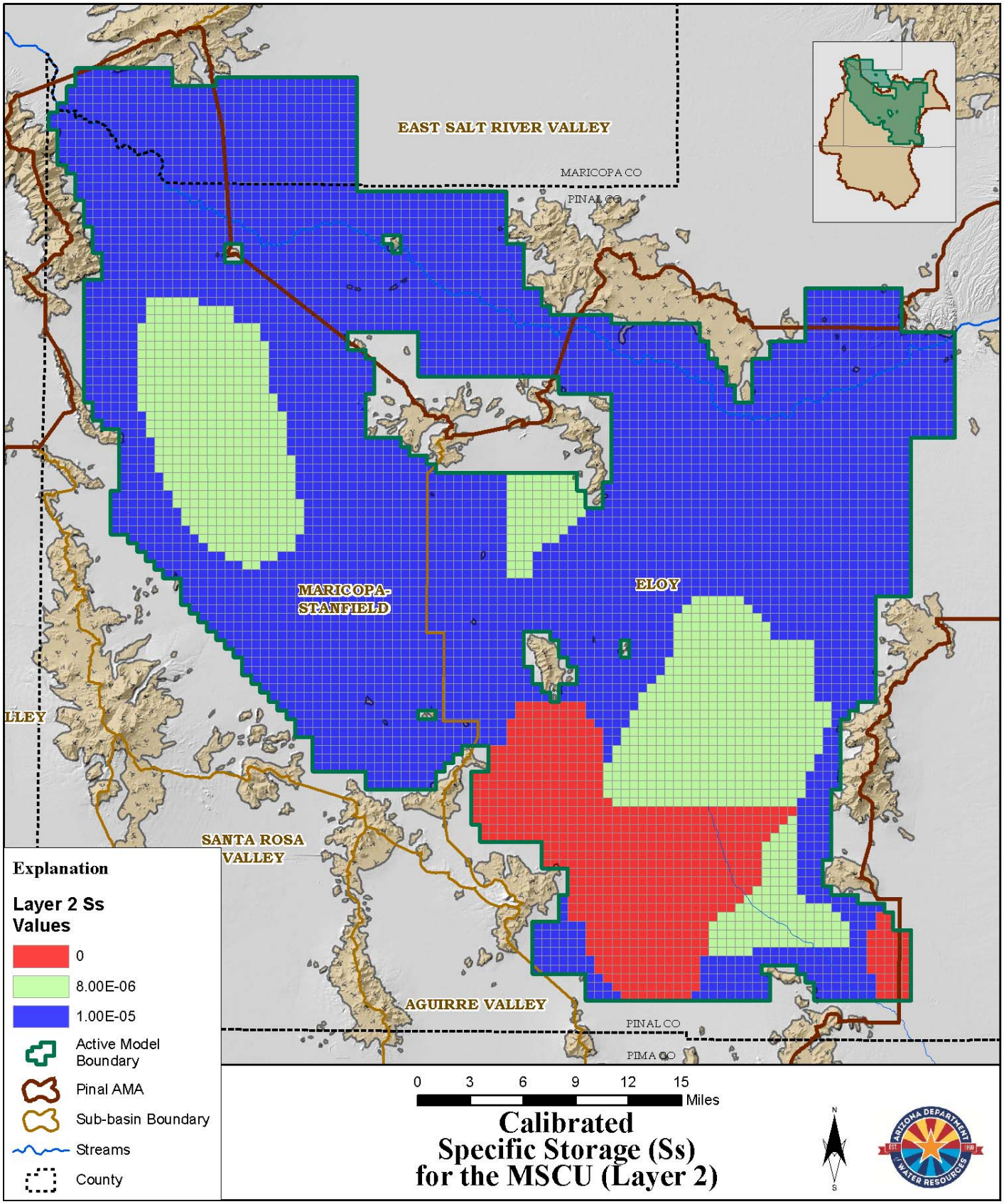

Figure 85 Calibrated Specific Storage for the MSCU (Layer 2)

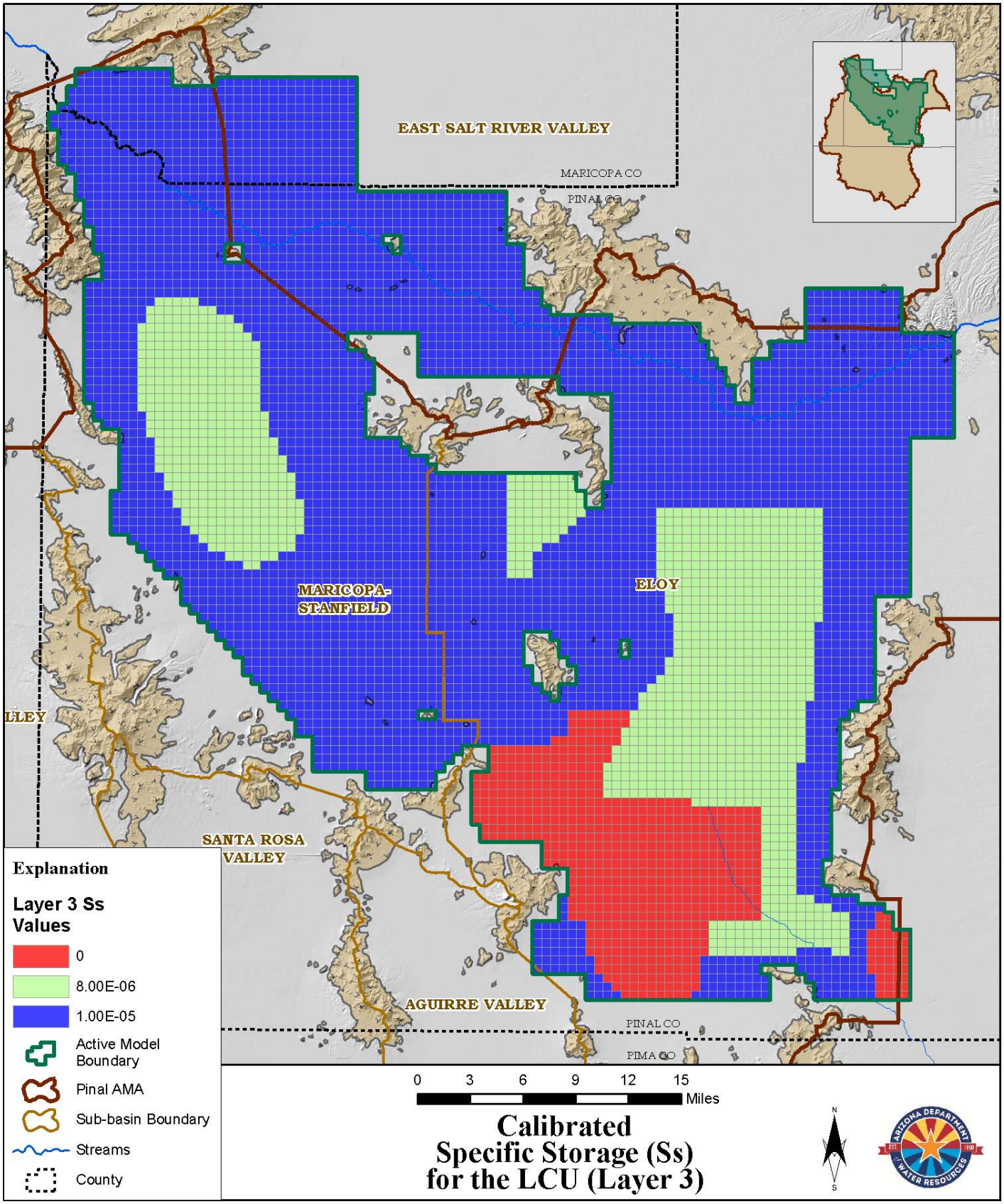

Figure 86 Calibrated Specific Storage for the LCU (Layer 3)

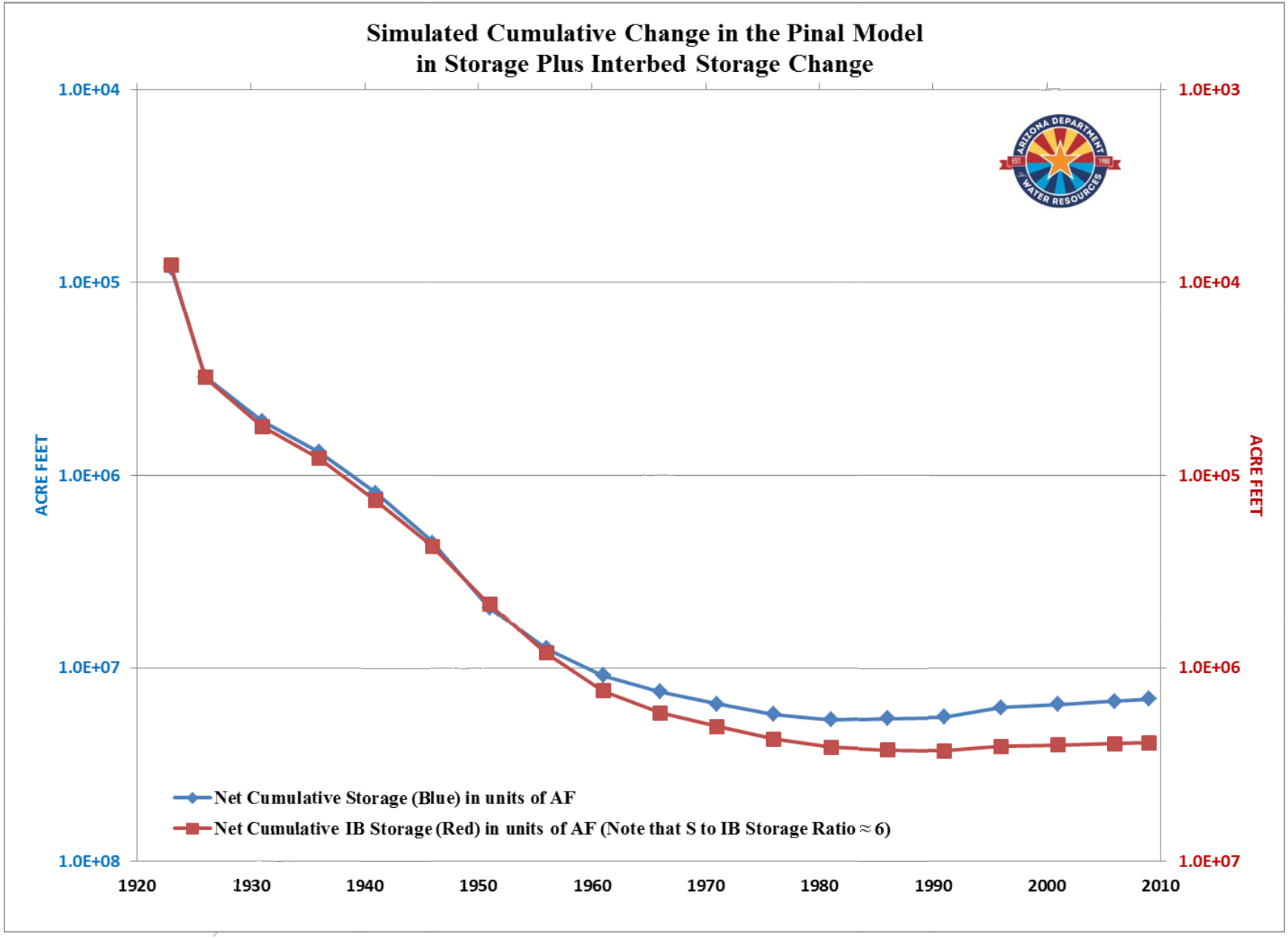

Figure 87 Simulated Pinal Model Cumulative Change in Storage Plus Interbed Storage Change

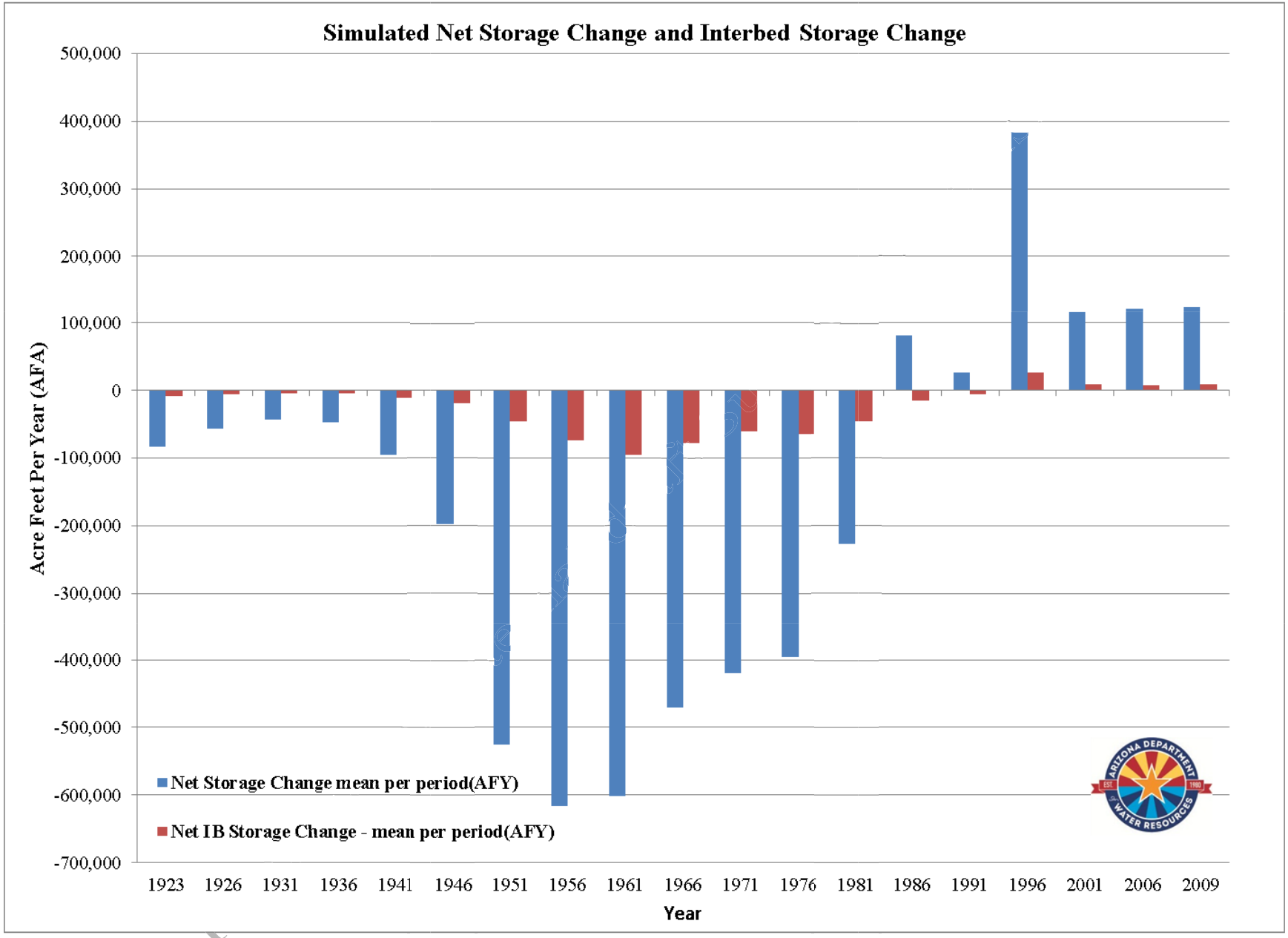

Figure 88 Simulated Net Storage Change and Interbed Storage Change

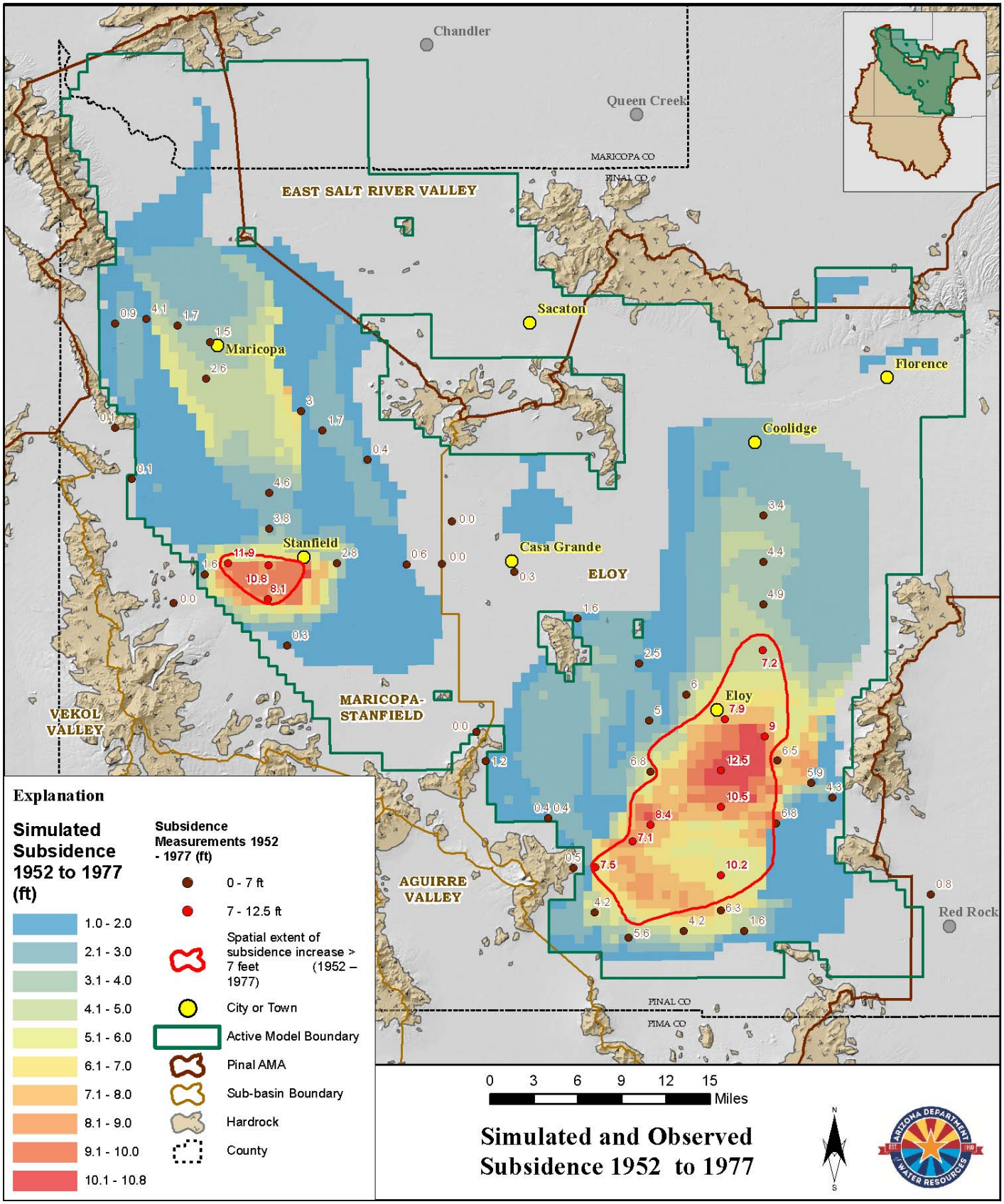

Figure 89 Simulated and Observed Subsidence 1952 to 1977

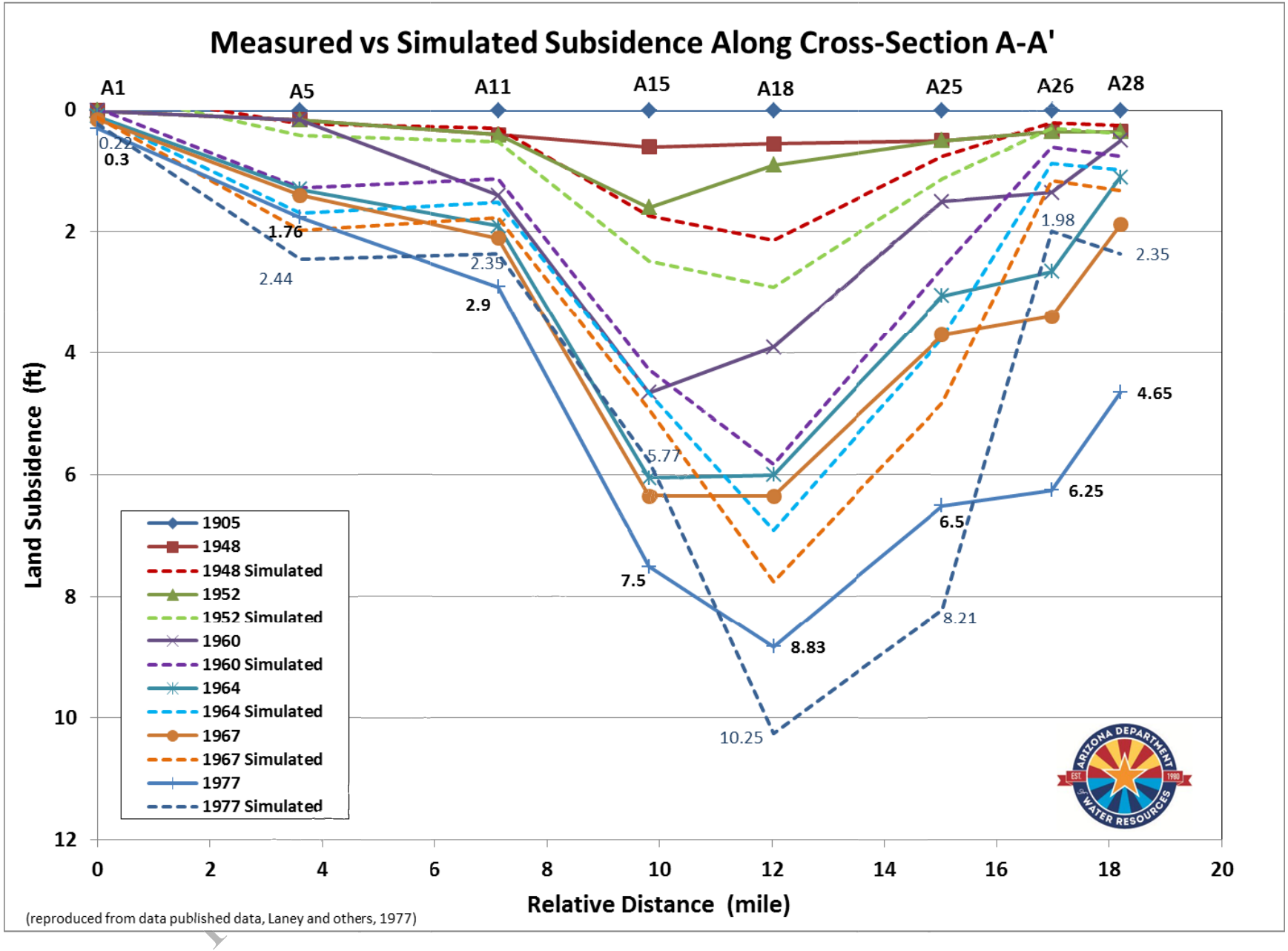

Figure 90 Measured vs Simulated Subsidence Along Cross-Section A – A'

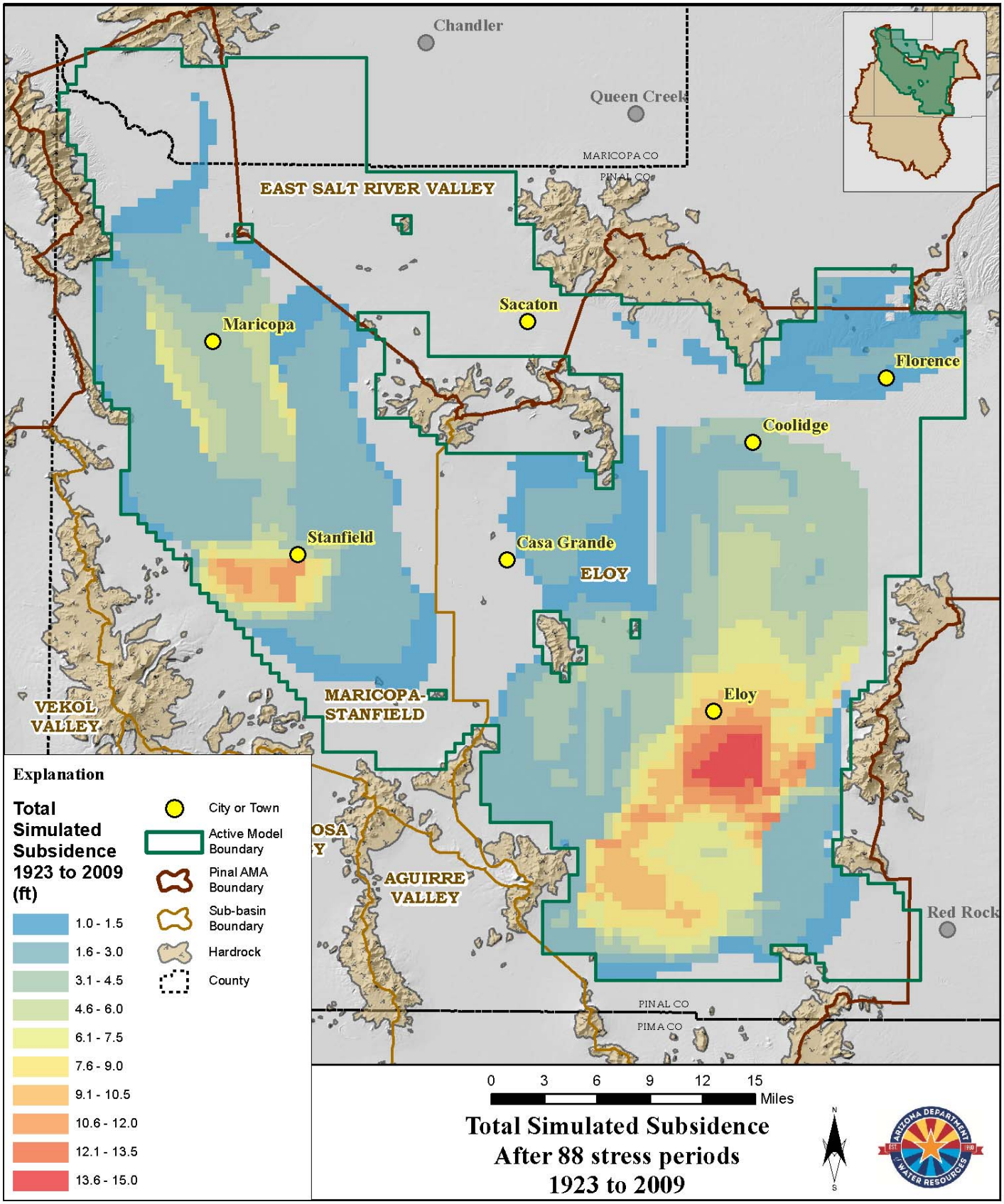

Figure 91 Total Simulated Subsidence after 88 stress periods, from 1923 to 2009

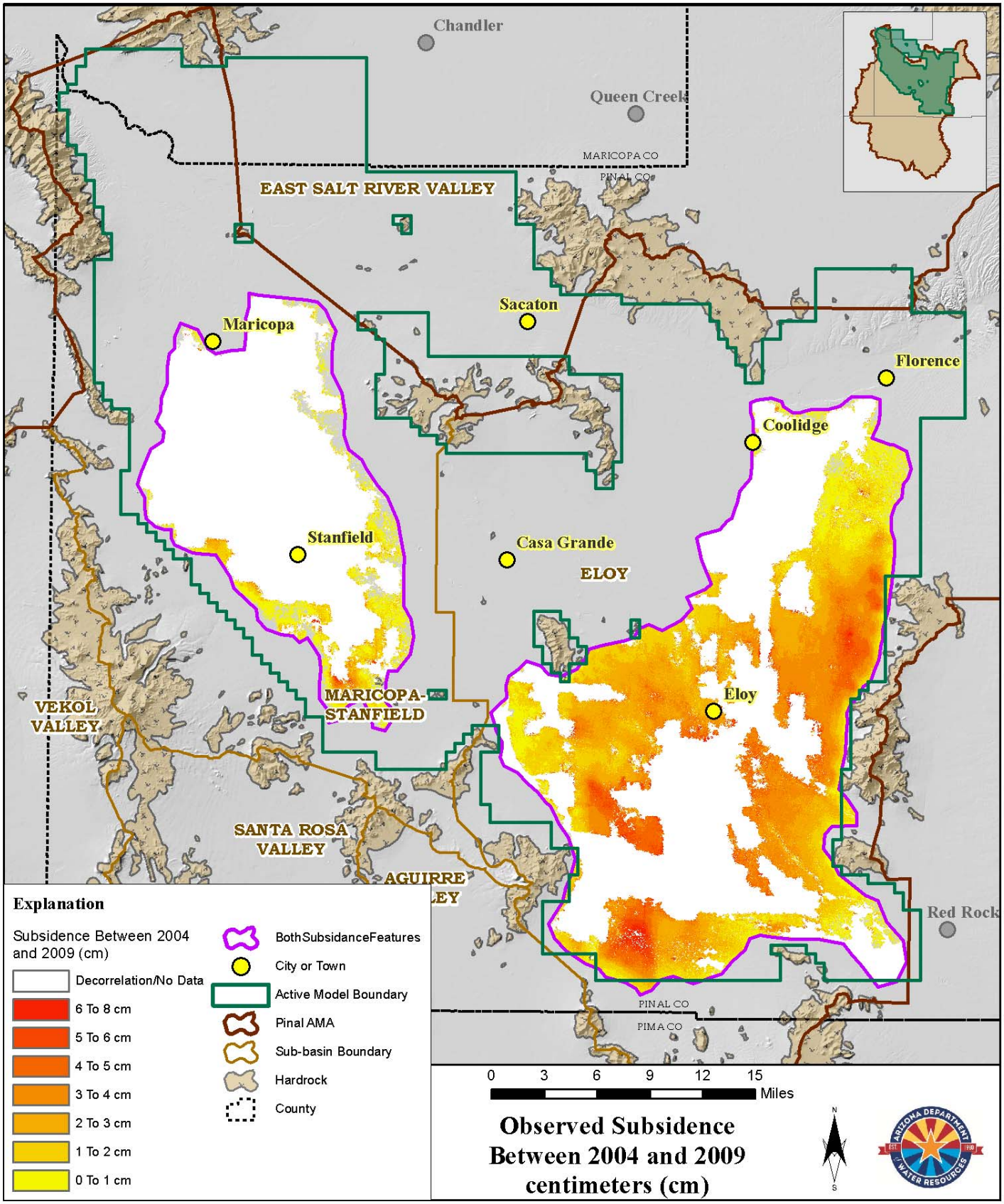

Figure 92 Observed Subsidence Between 2004 and 2009

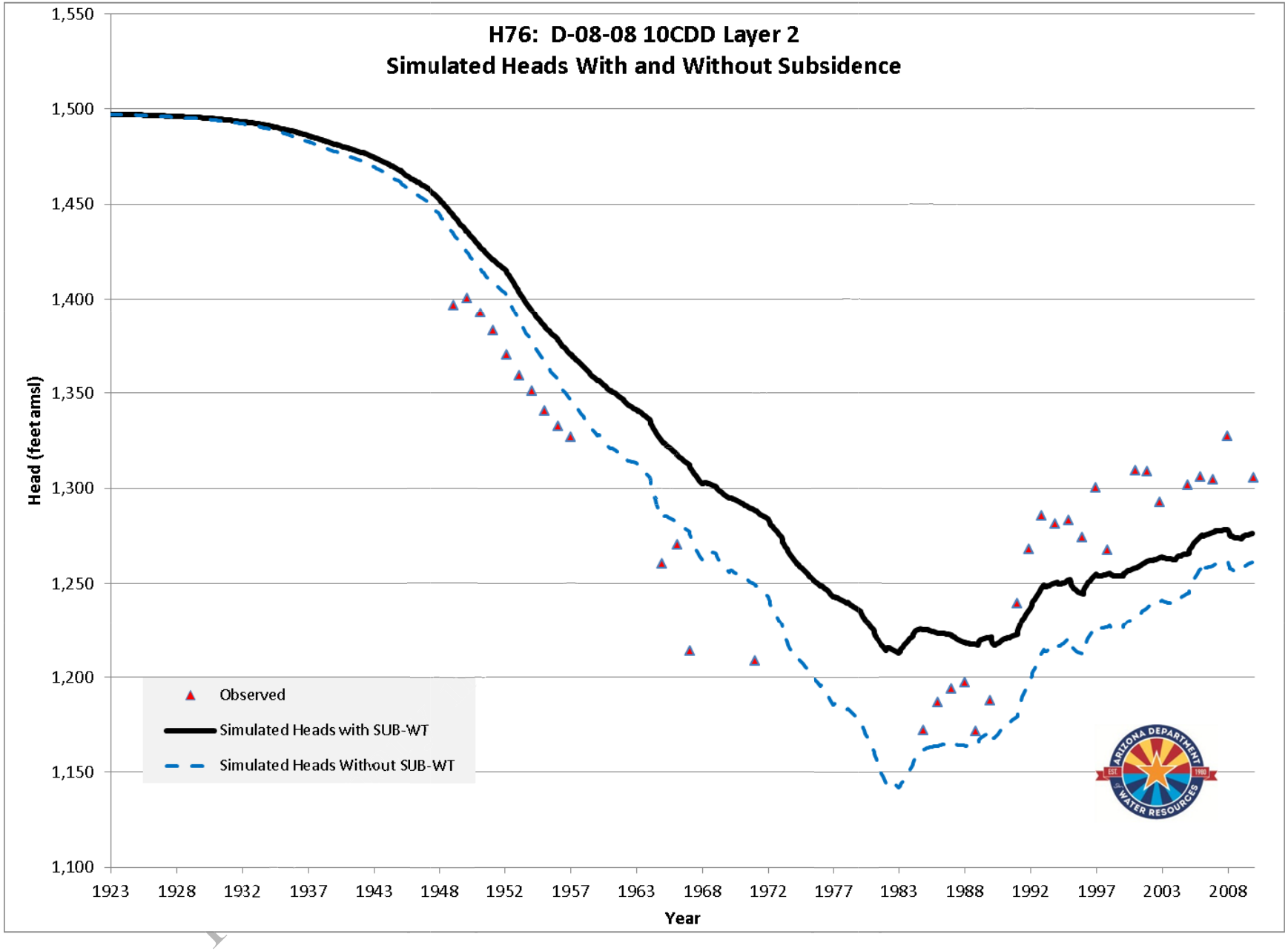

Figure 93 Hydrograph at location H76 Layer 2 Simulated Heads With and Without Subsidence

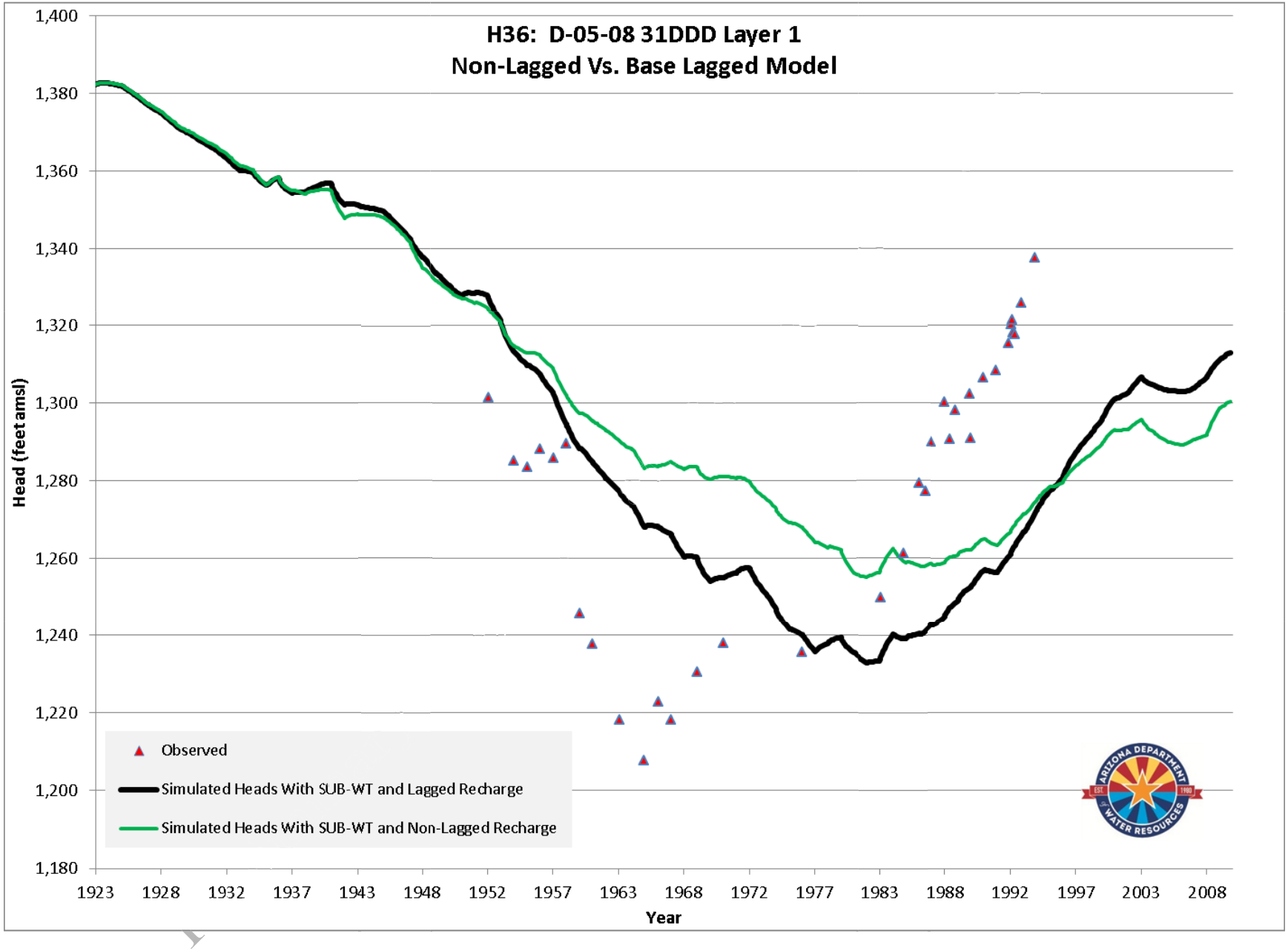

Figure 94 Hydrograph at location H36 Layer 1 Simulated Heads Lagged and Non-Lagged Recharge

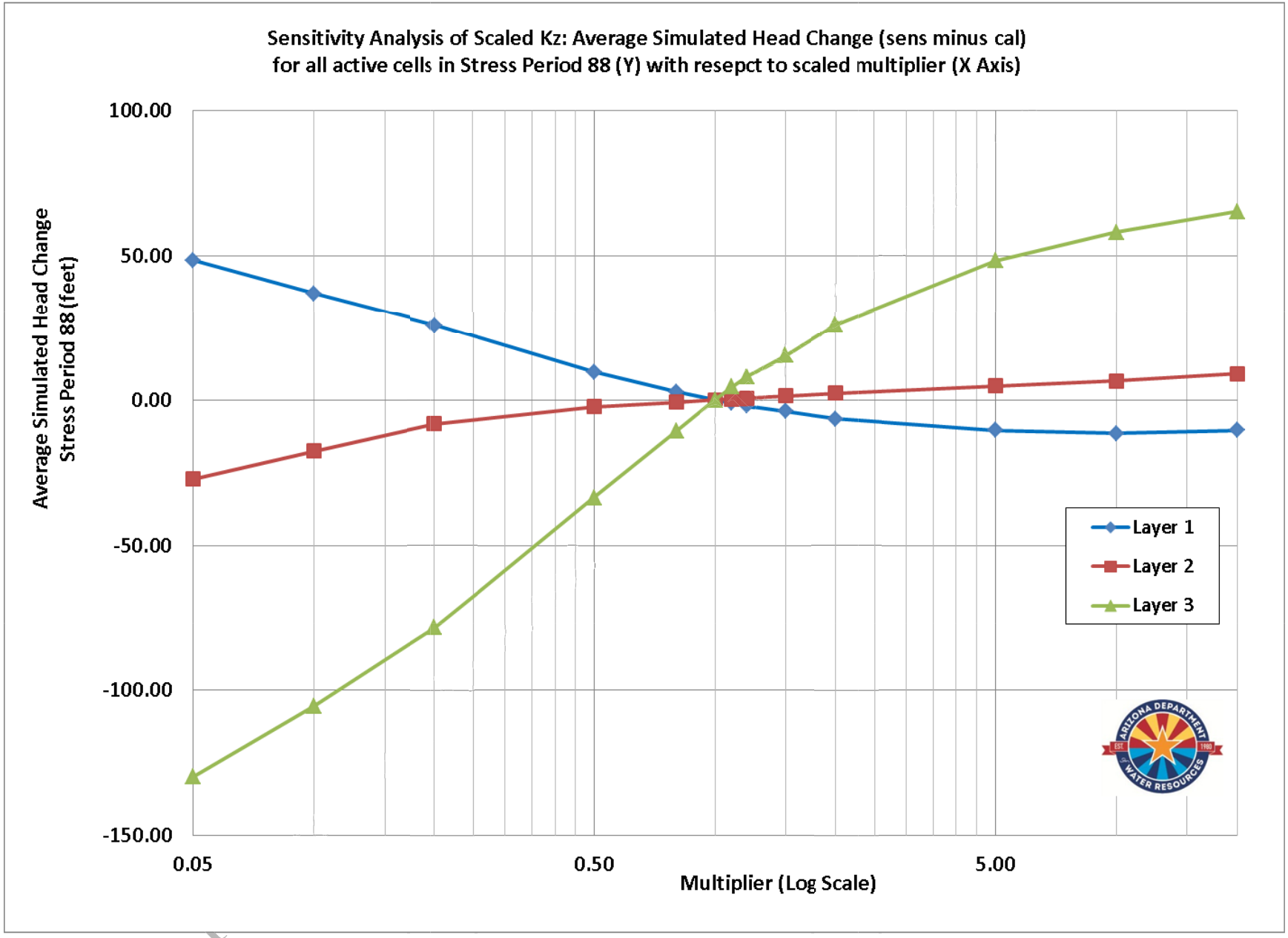

Figure 95 Average head change (At SP 88) scaled multiplier of Kz per model layer

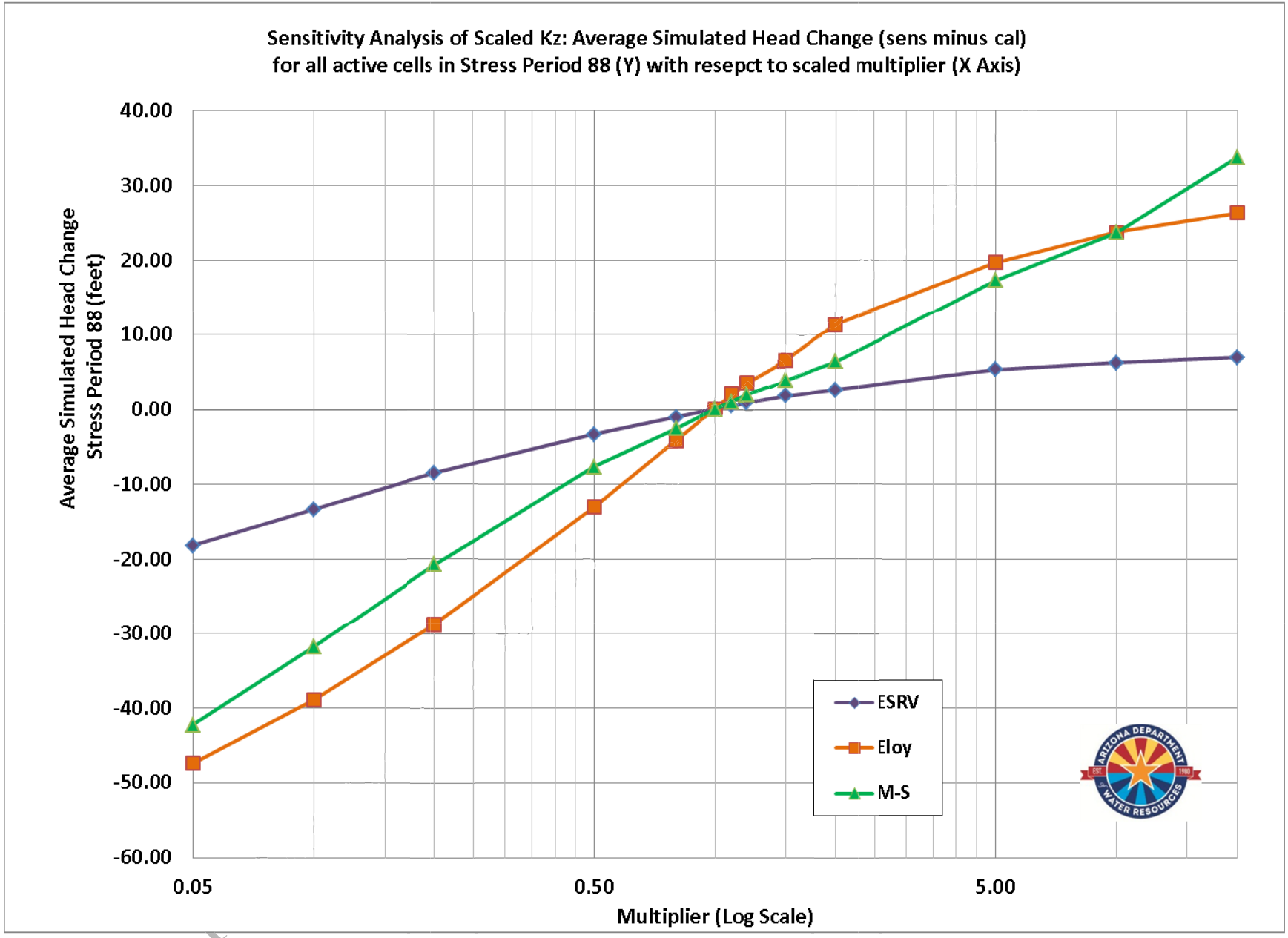

Figure 96 Average head change (At SP88) with respect to scaled multiplier of Kz per model sub-basin

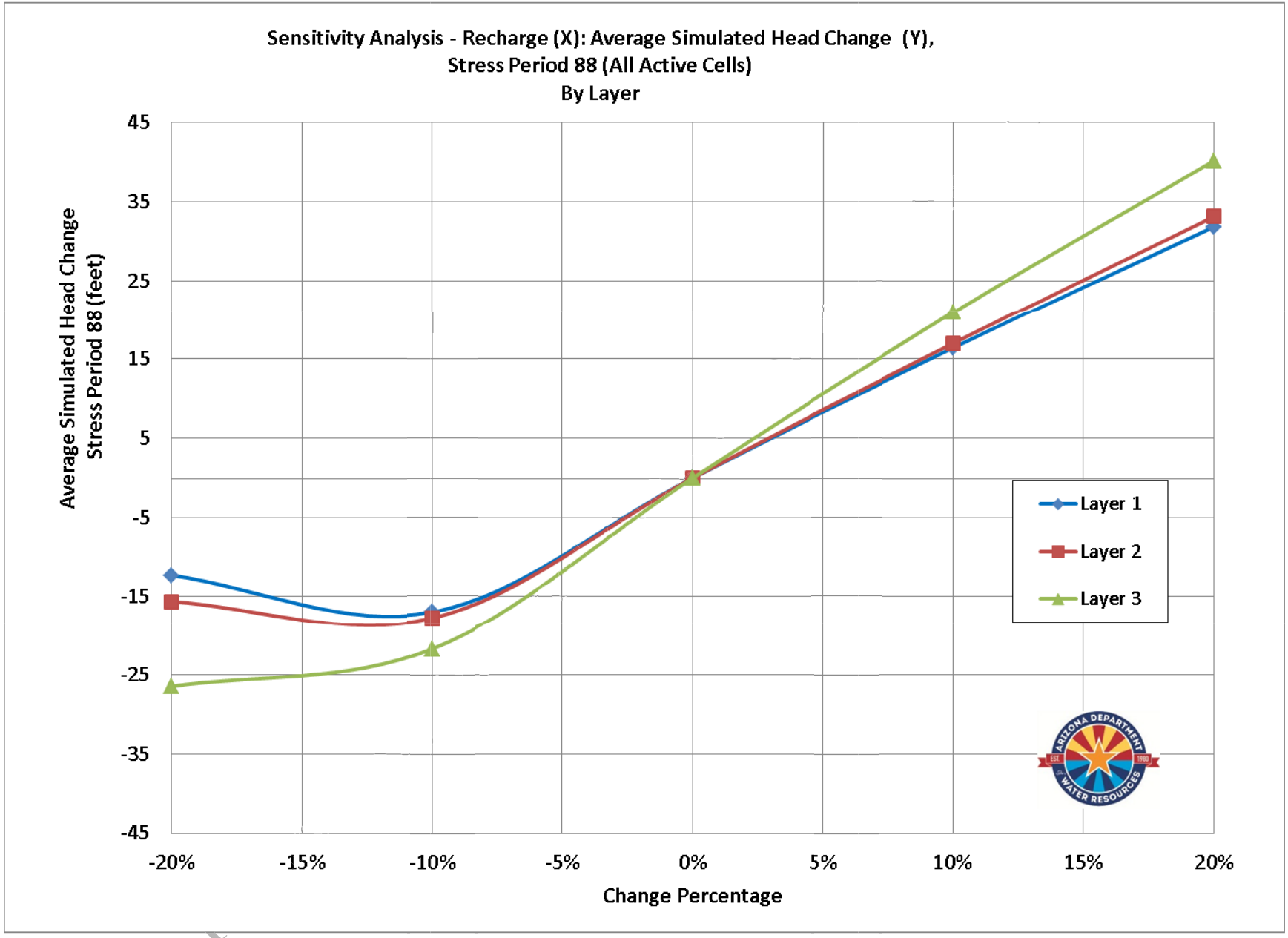

Figure 97 Average head change (At SP 88) Percentage Change in Recharge By Model Layer

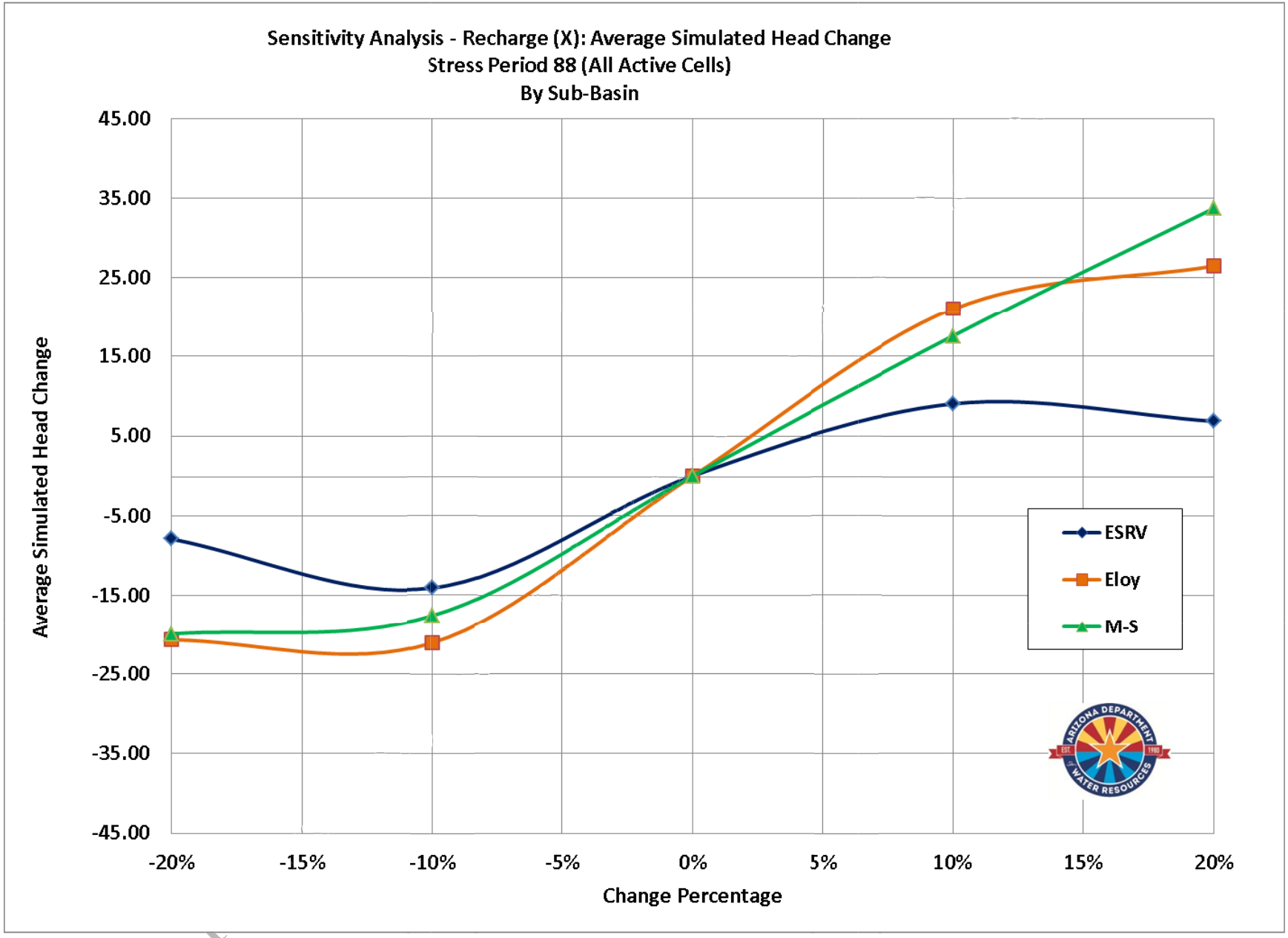

Figure 98 Average head change (At SP 88) Percentage Change in Recharge By Sub-Basin

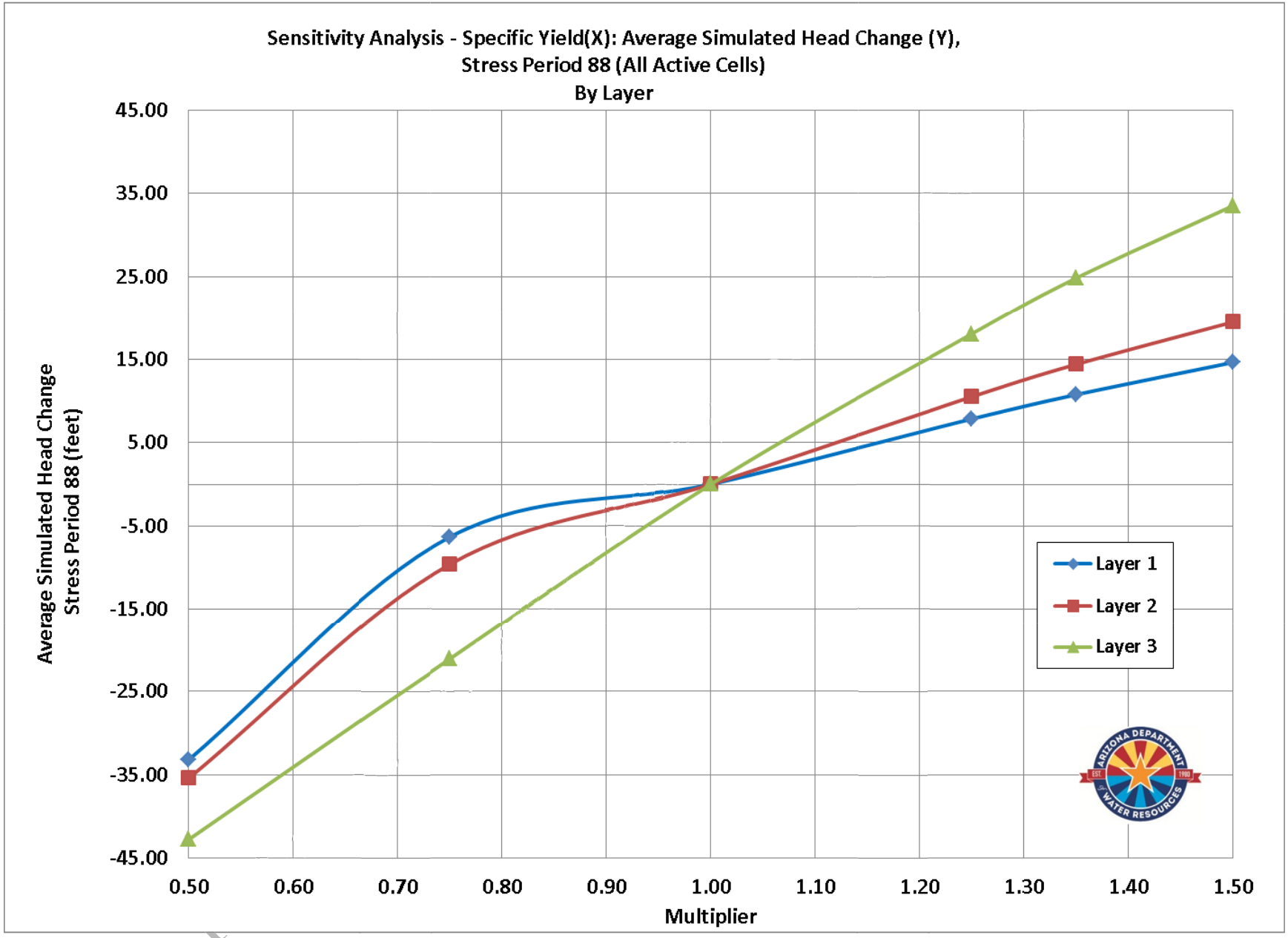

Figure 99 Average head change (At SP 88) Sy Multiplier By Model Layer

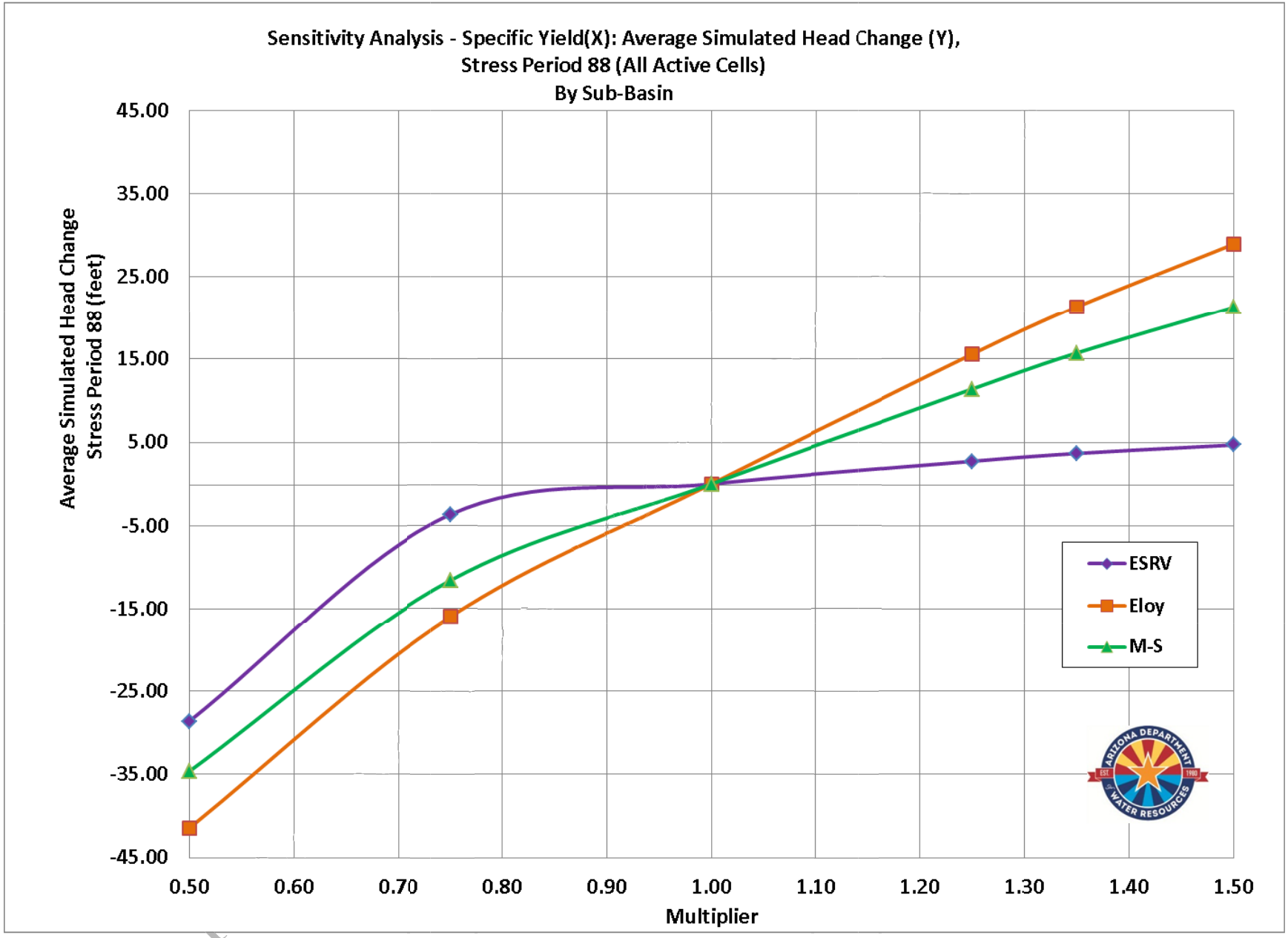

Figure 100 Average head change (At SP 88) Sy Multiplier By Sub-Basin

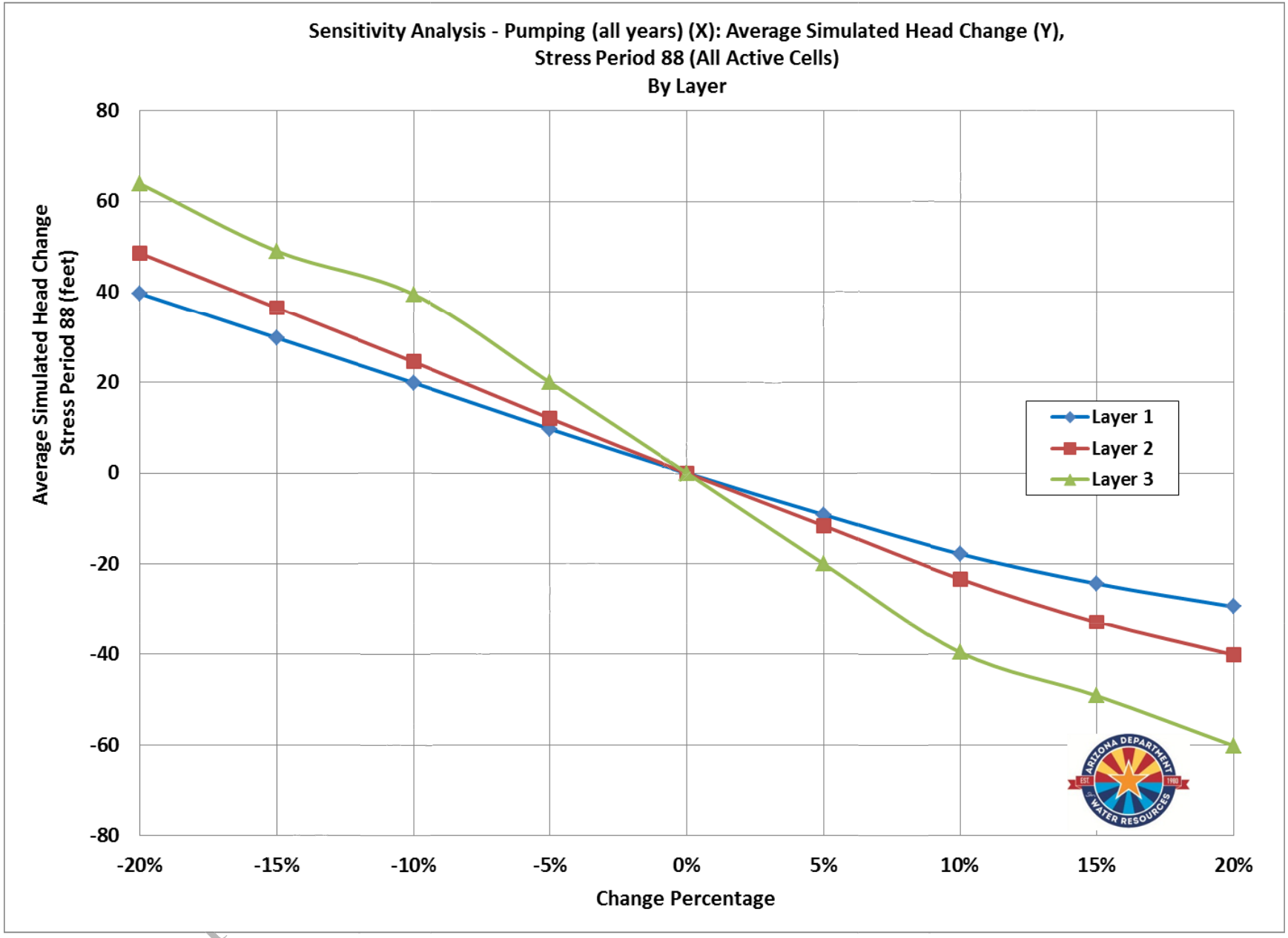

Figure 101 Average head change (At SP 88) Pumping Multiplier By Model Layer

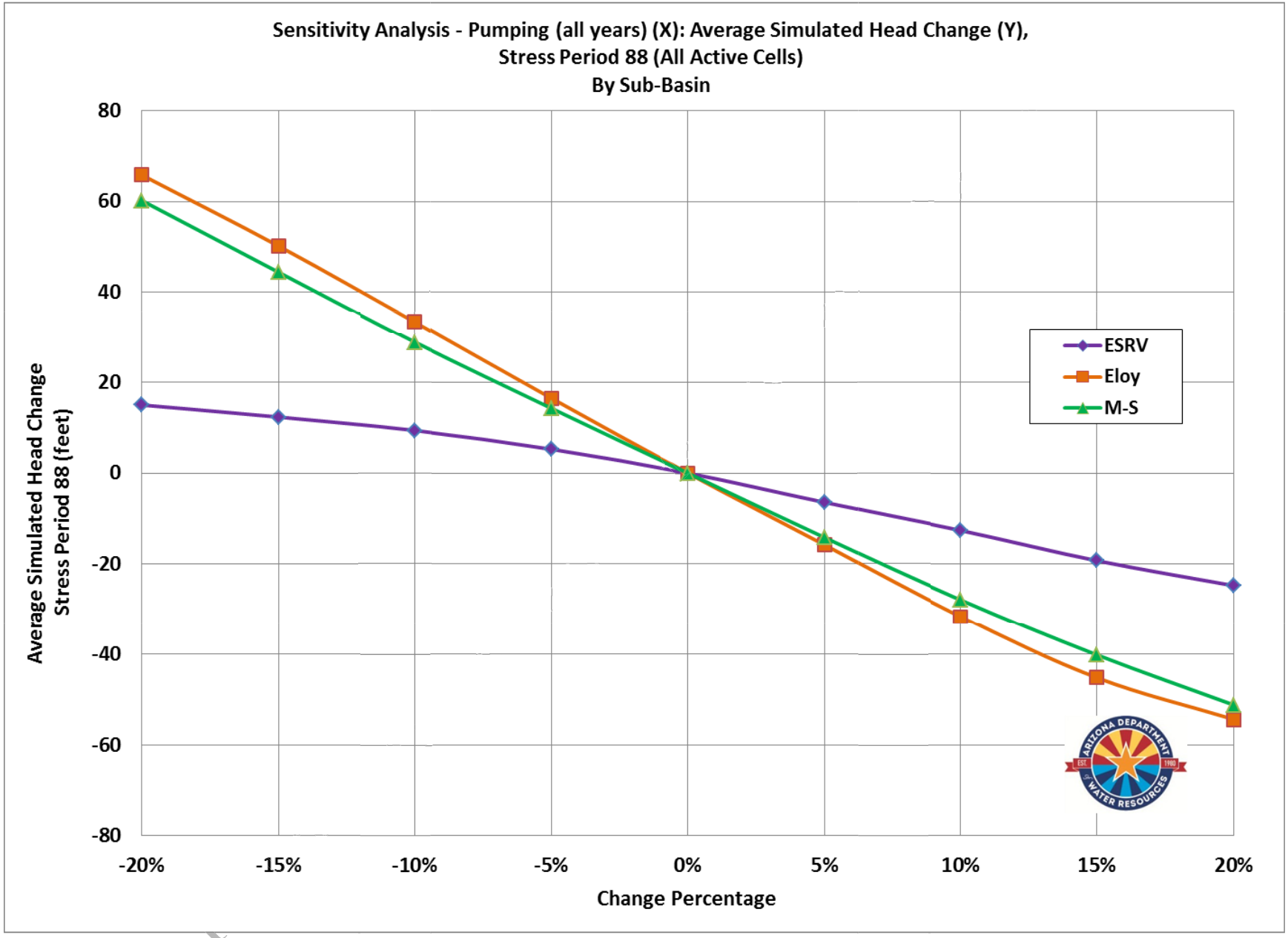

Figure 102 Average head change (At SP 88) Pumping Multiplier By Sub-Basin

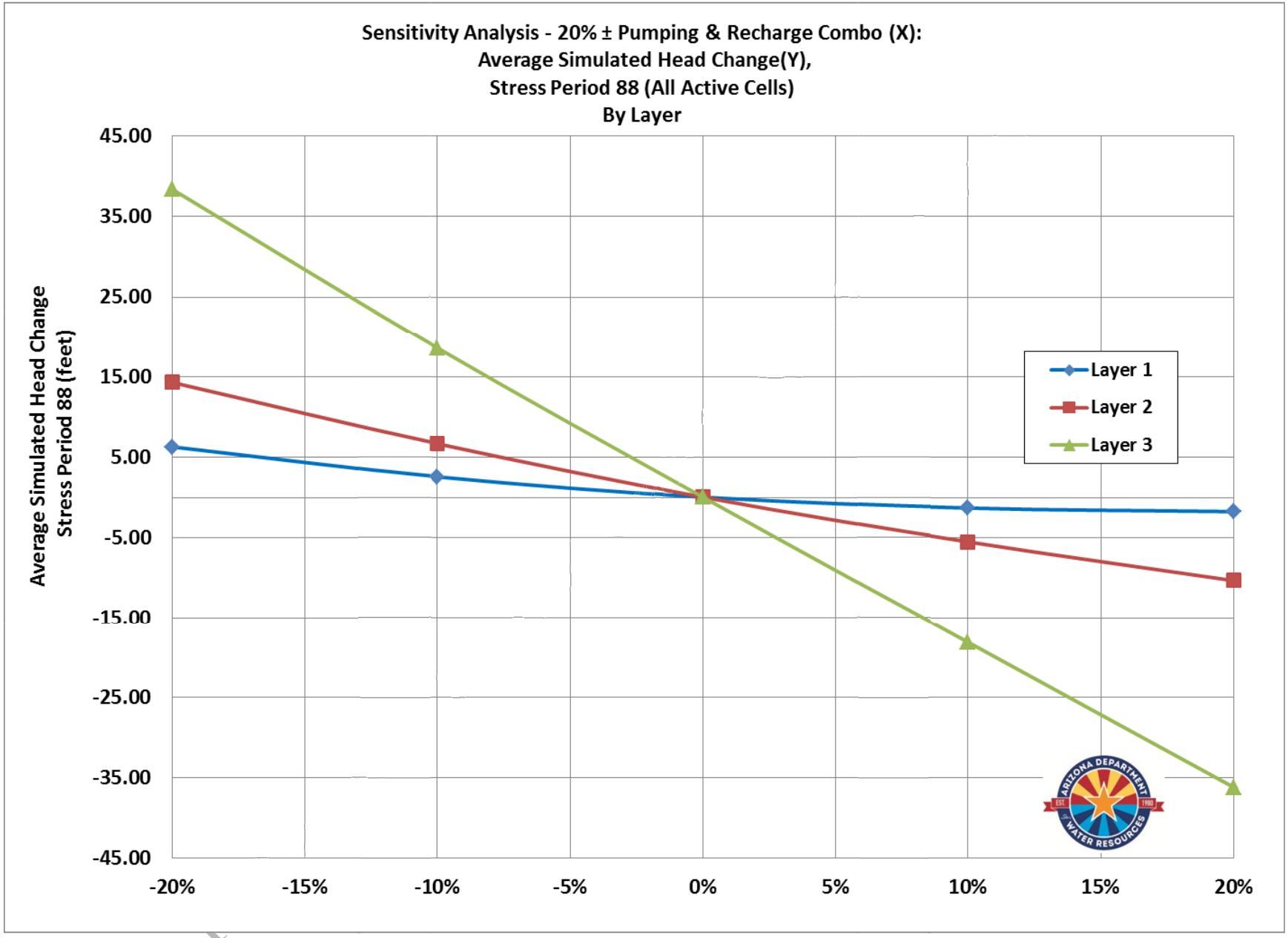

Figure 103 Average Head Change (At SP 88) Combined Pumping and Recharge Change By Model Layer

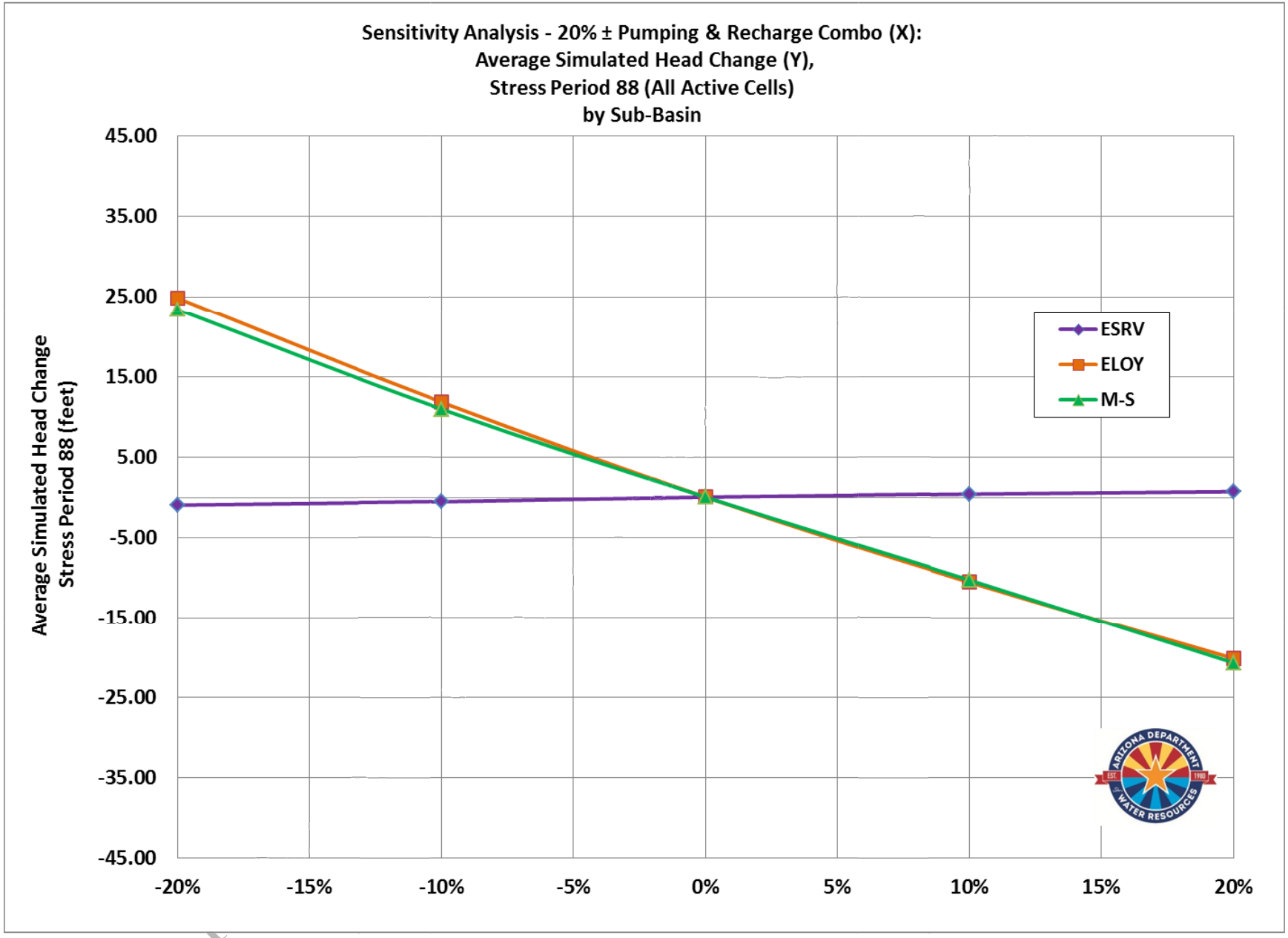

Figure 104 Average Head Change (At SP 88) Combined Pumping and Recharge By Sub-Basin

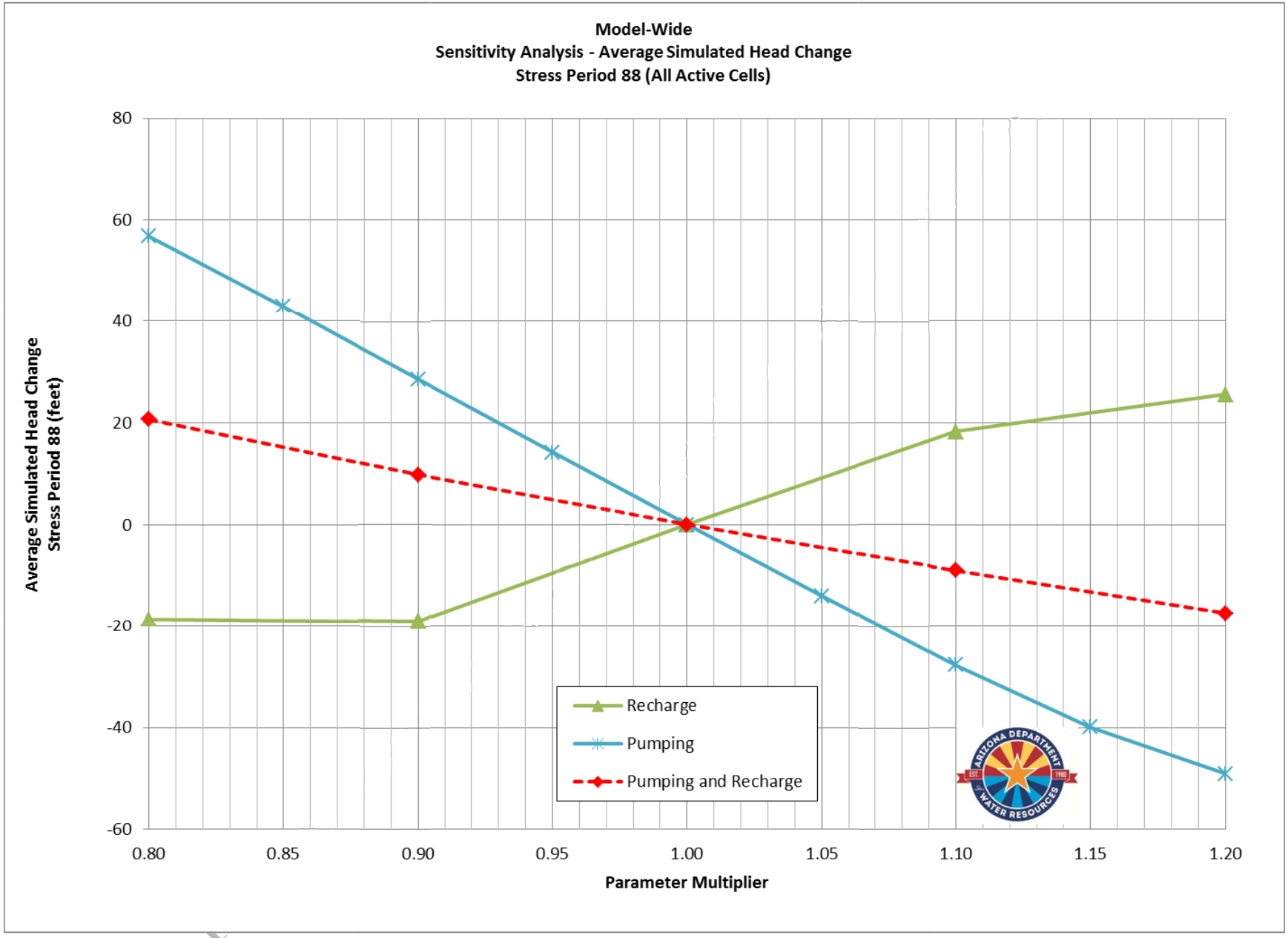

Figure 105 Model-Wide Average change in Head (At SP 88) of the Individual vs. Combined Pumping and Recharge.

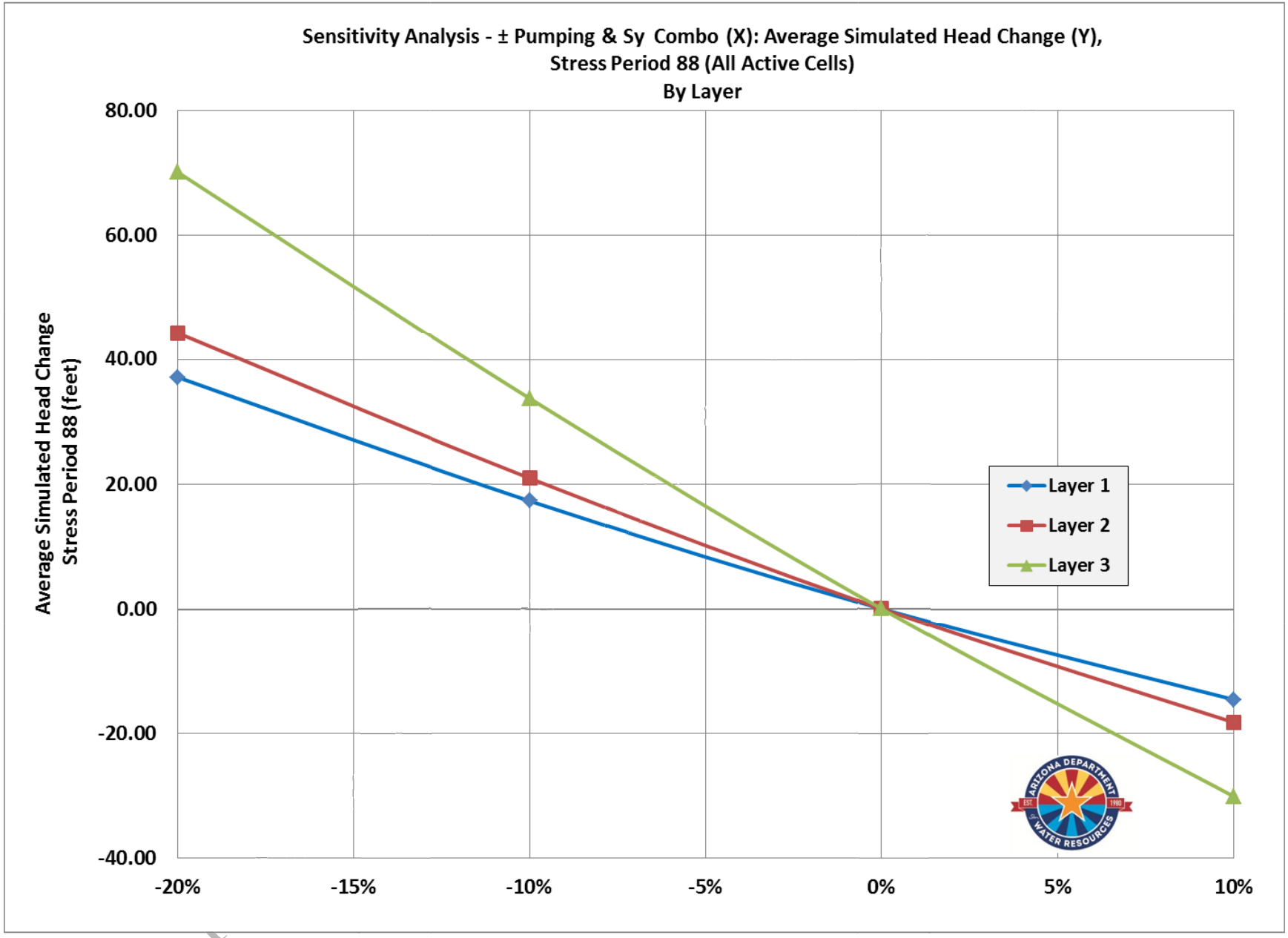

Figure 106 Average head change (At SP 88) the Combined Pumping and Specific Yield Change By Model Layer

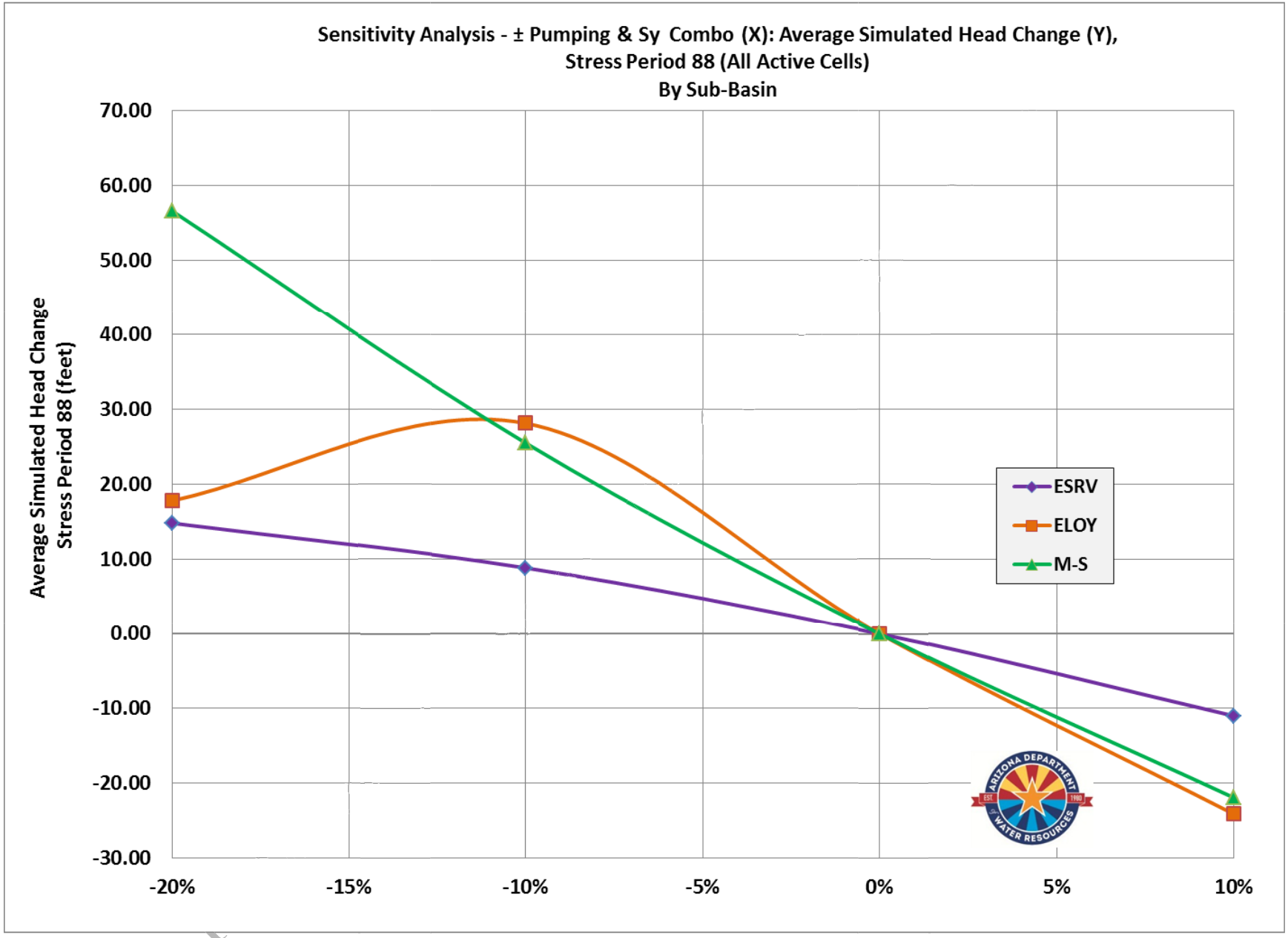

Figure 107 Average head change (At SP 88) the Combined Pumping and Specific Yield Change By Sub-Basin

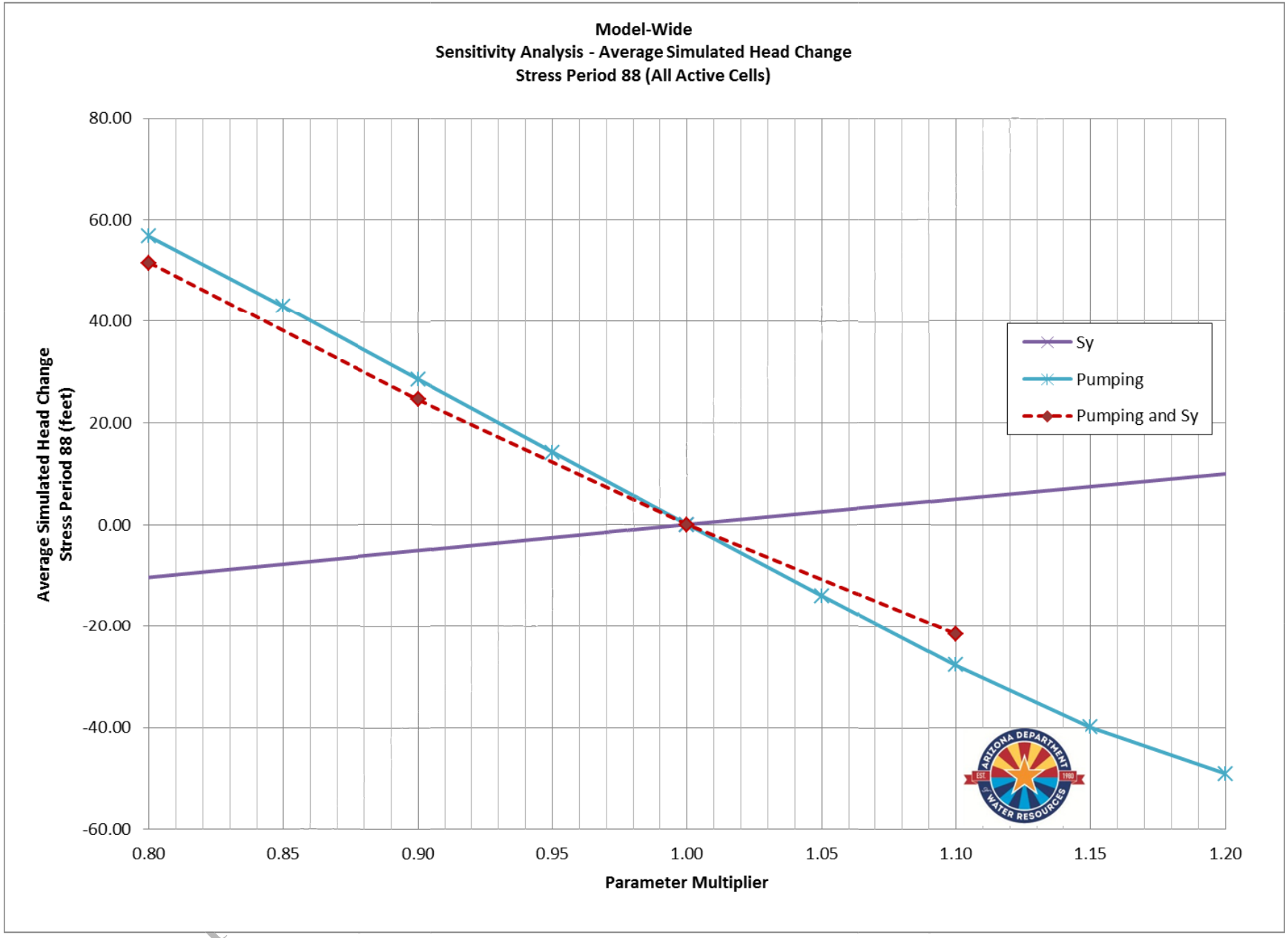

Figure 108 Model-Wide Average Change in Head (At SP 88) of the Individual vs. Combined Pumping and Specific Yield (Sy)

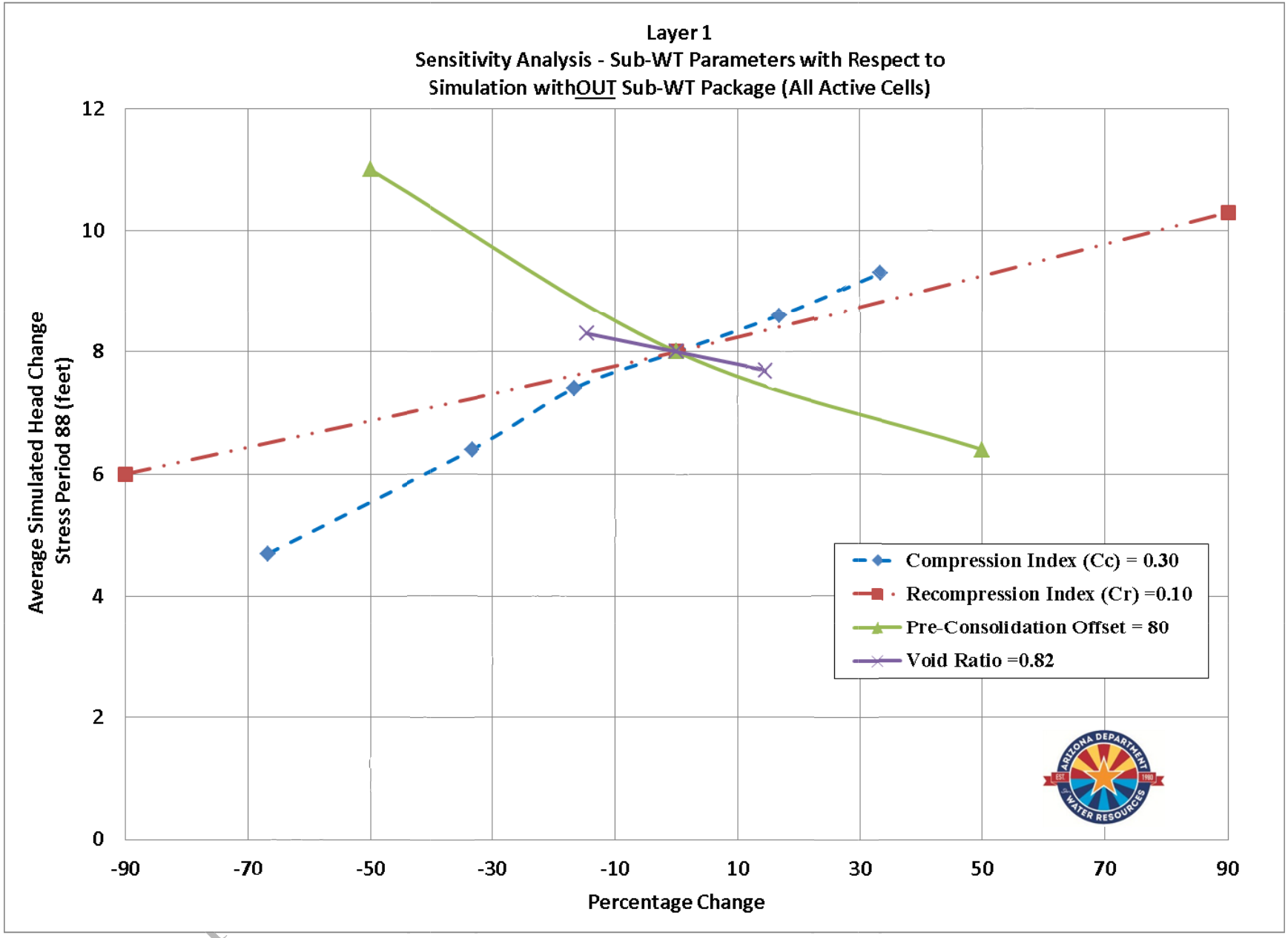

Figure 109 Sensitivity of SUB-WT Parameters (Cc, Cr, Precon, Void Ratio) – Layer 1

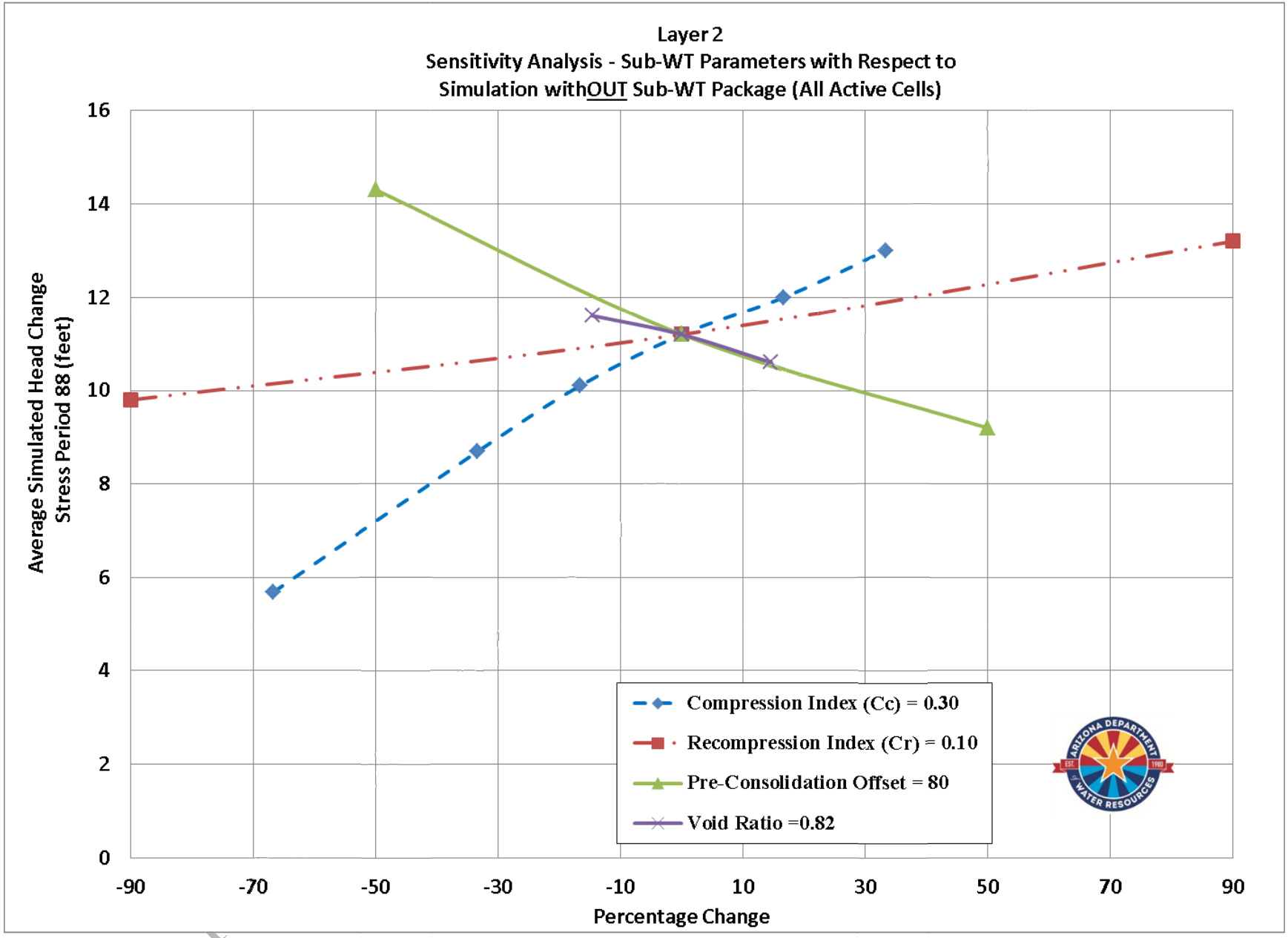

Figure 110 Sensitivity of SUB-WT Parameters (Cc, Cr, Precon, Void Ratio) – Layer 2

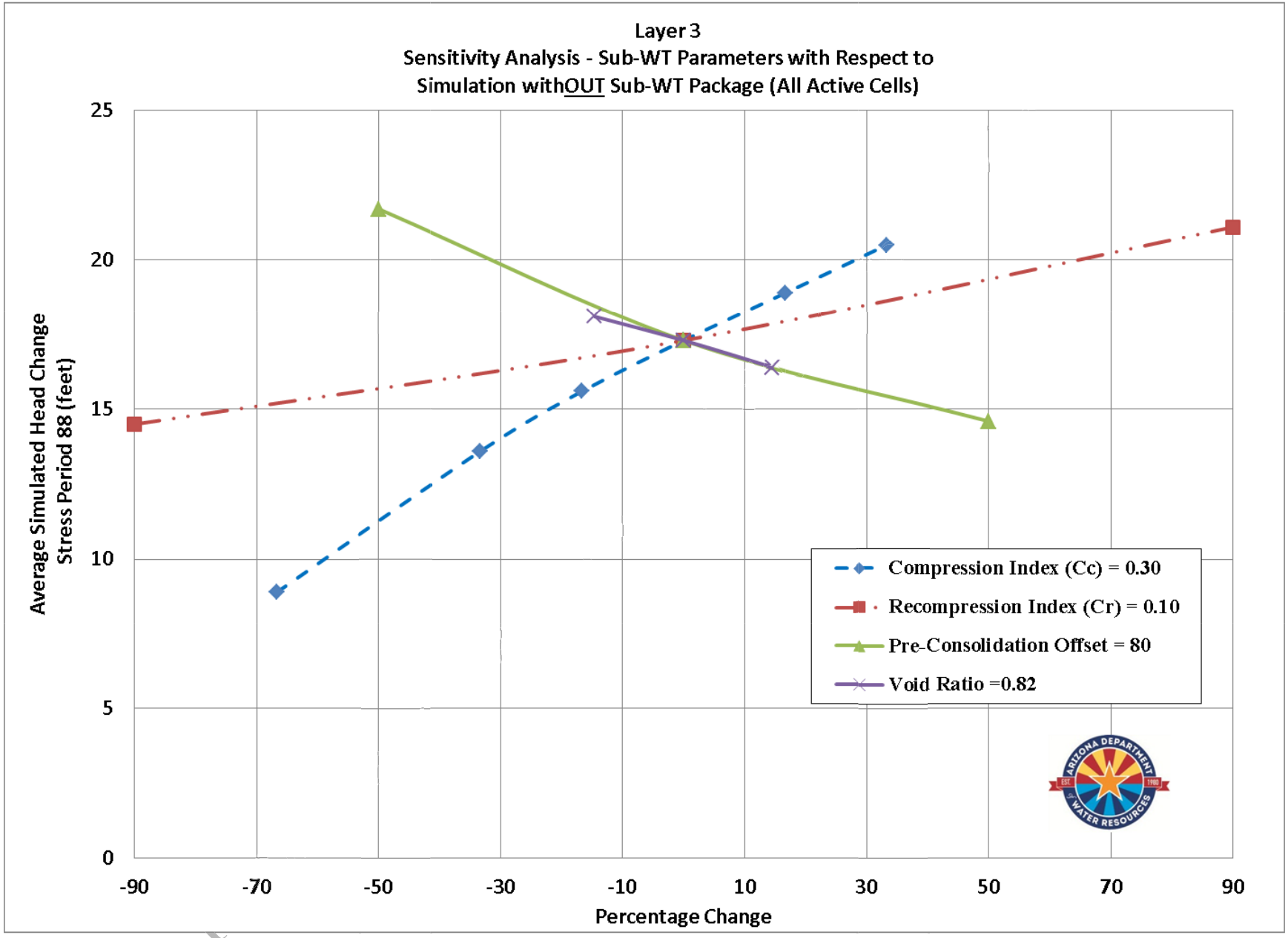

Figure 111 Sensitivity of SUB_SWT Parameters (Cc, Cr, Precon, Void Ratio) – Layer 3

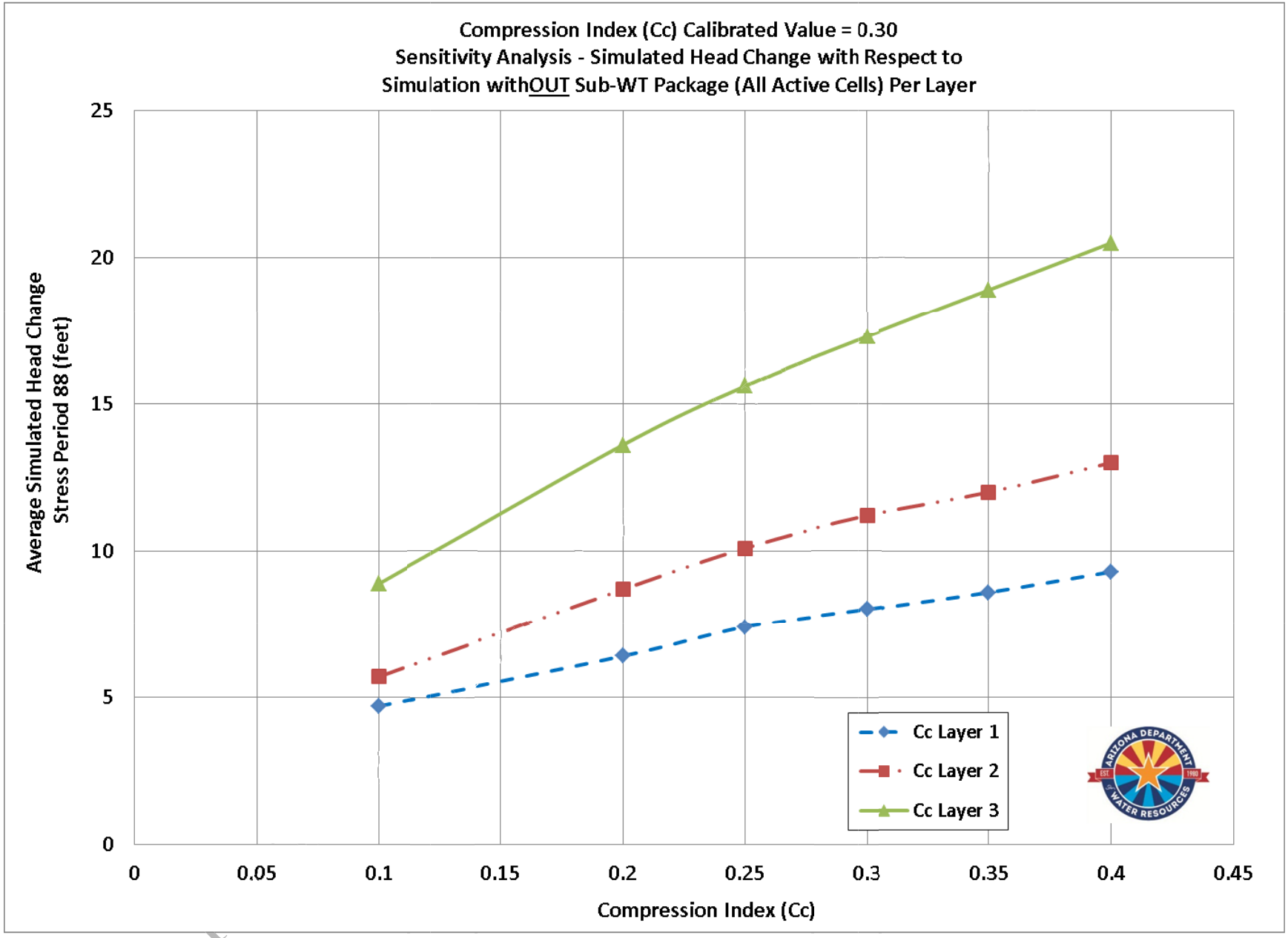

Figure 112 Sensitivity of SUB_SWT Parameter (Cc) – All Layers

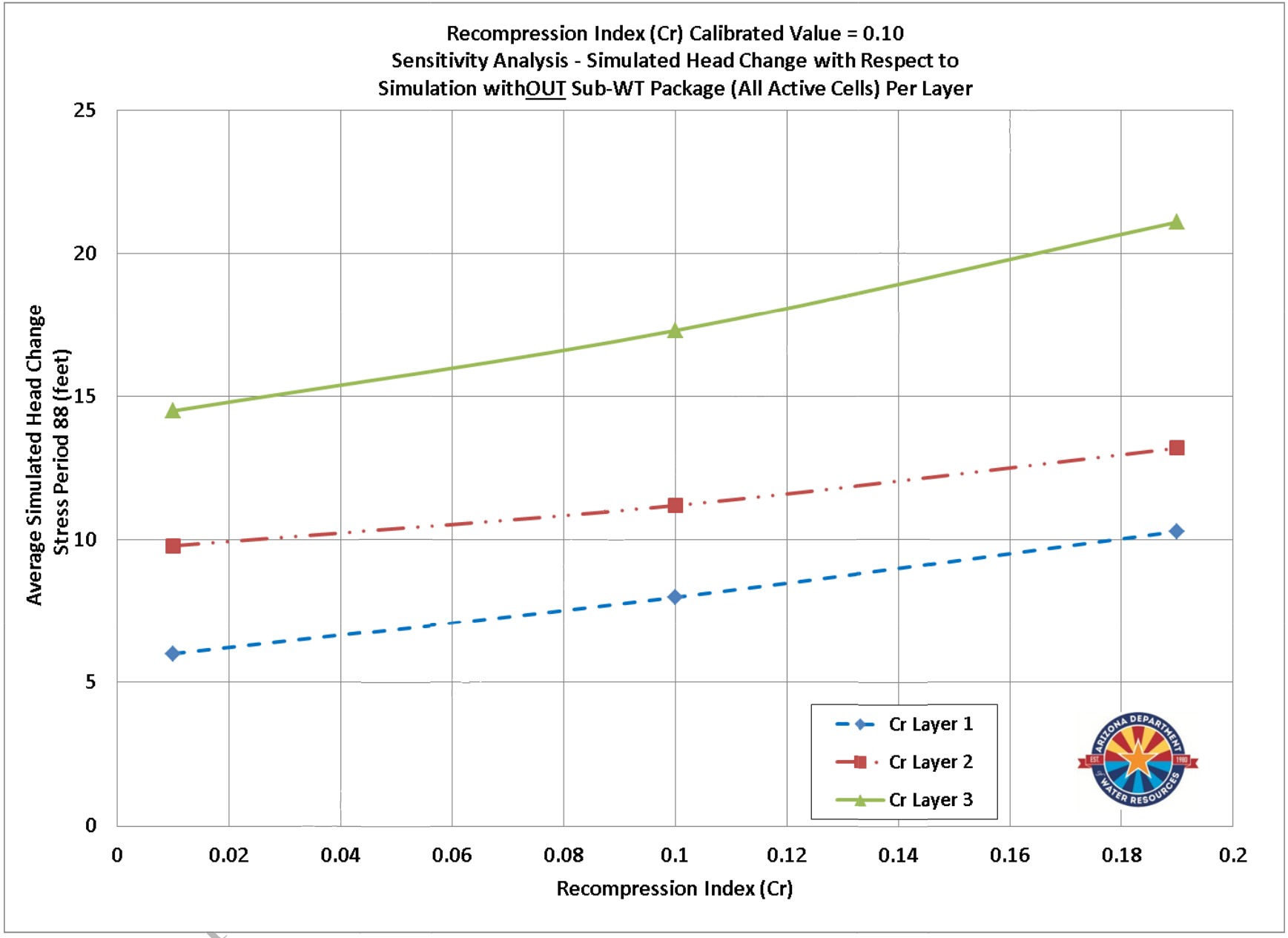

Figure 113 Sensitivity of SUB-WT Parameter (Cr) – All Layers

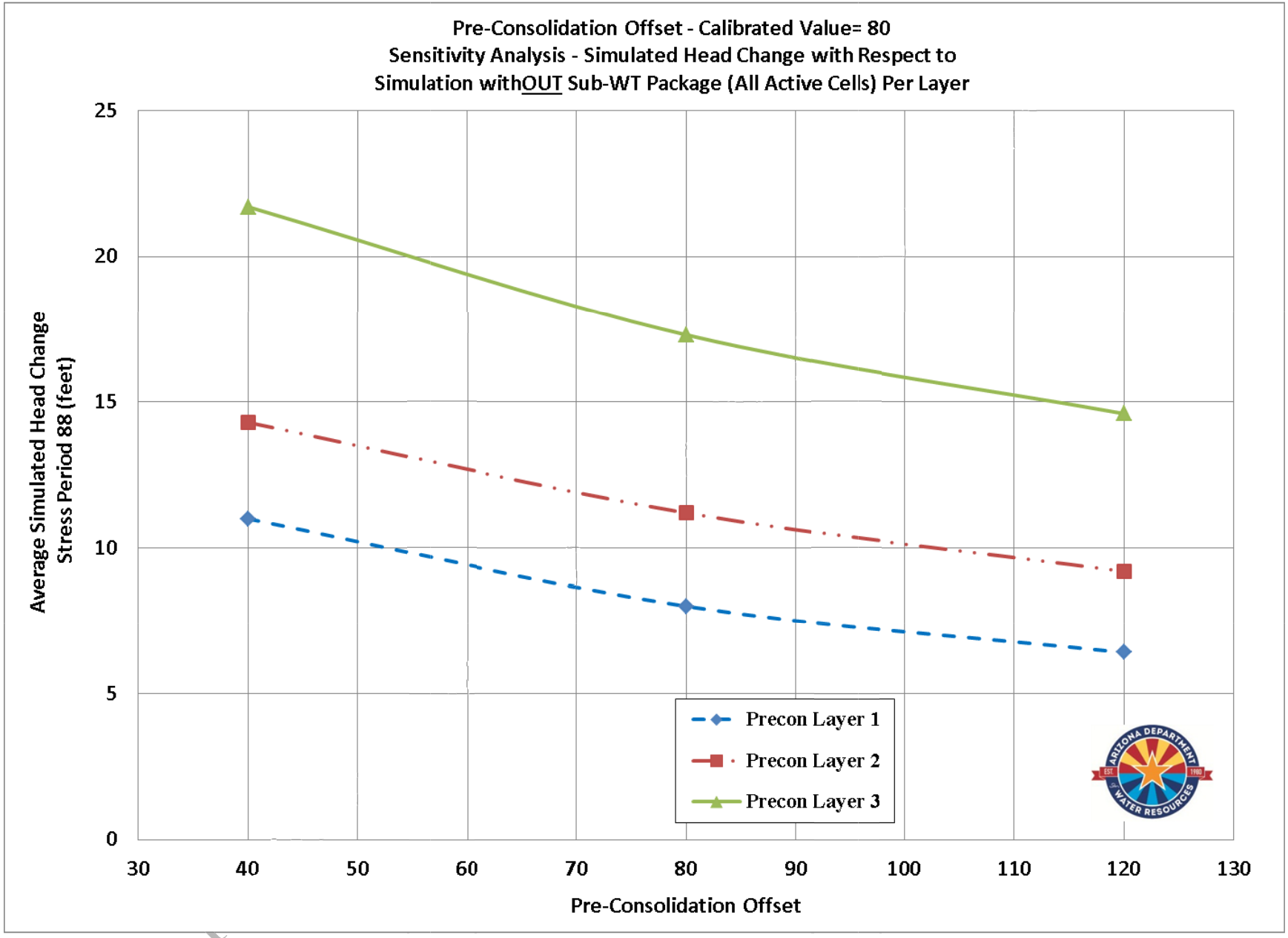

Figure 114 Sensitivity of SUB-WT Parameter (Precon) – All Layers

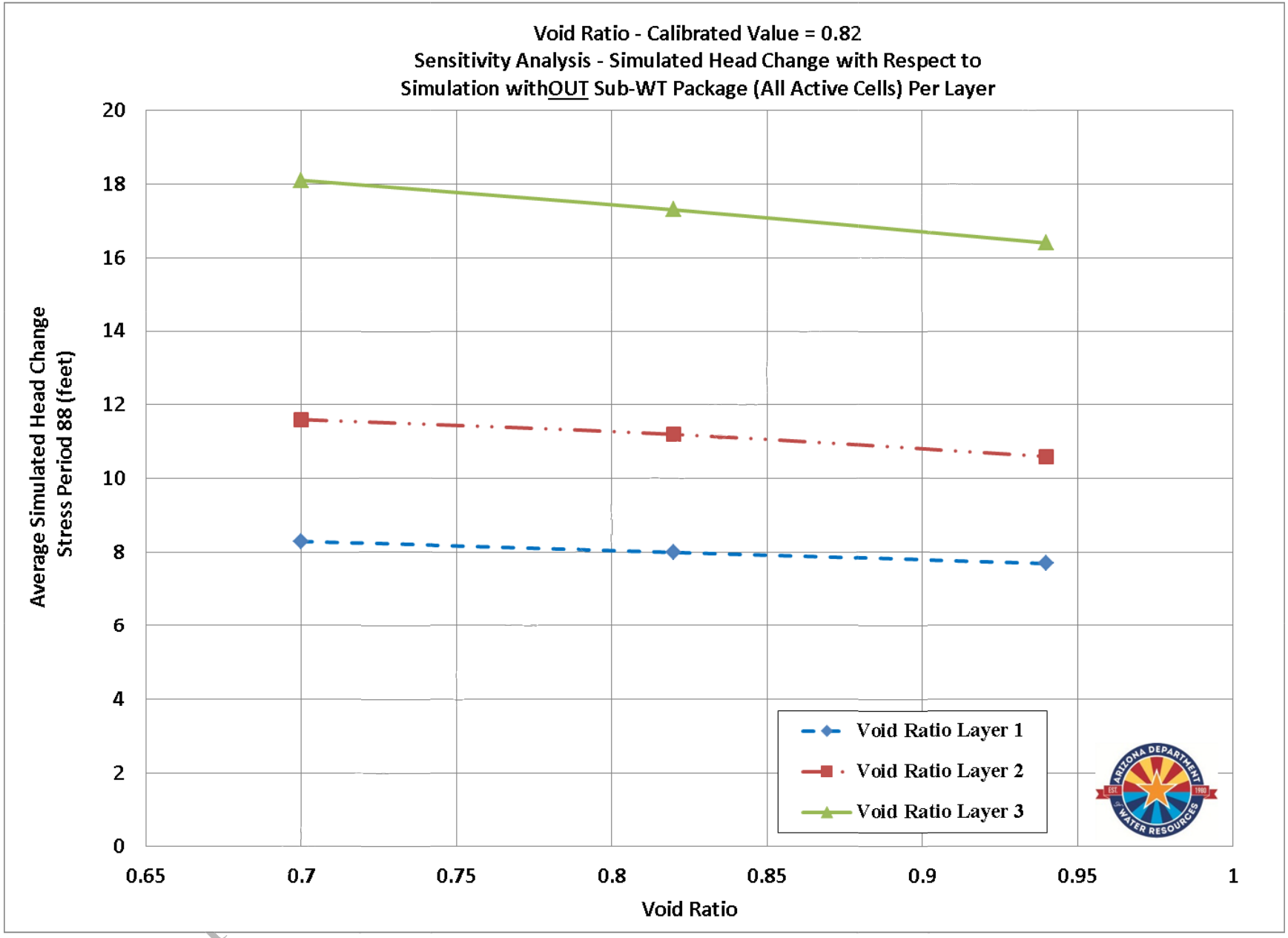

Figure 115 Sensitivity of SUB-WT Parameter (Void Ratio) – All Layers

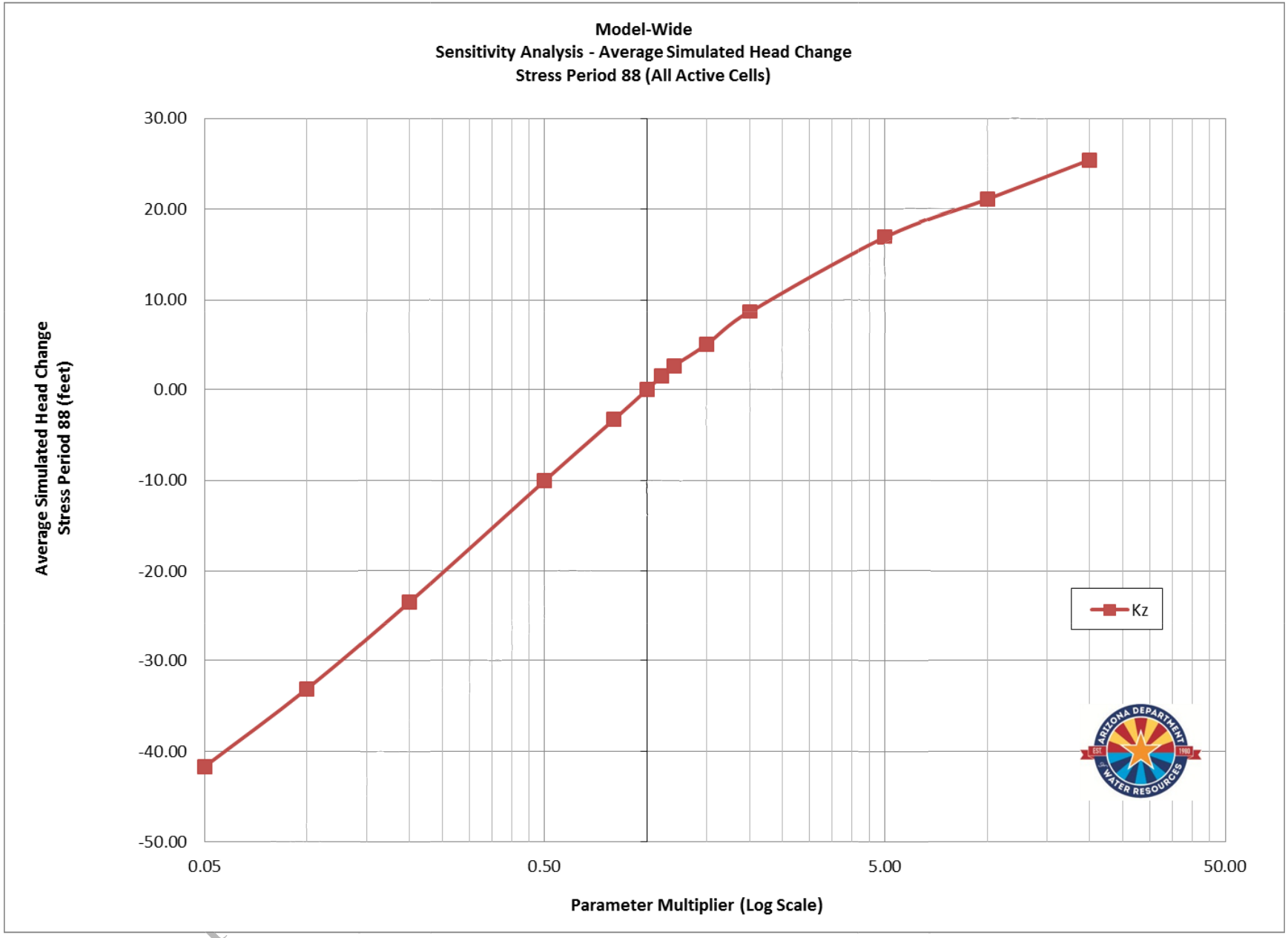

Figure 116 Model-Wide Average Change in Head (At SP 88) Vertical Hydraulic Conductivity (Kz)

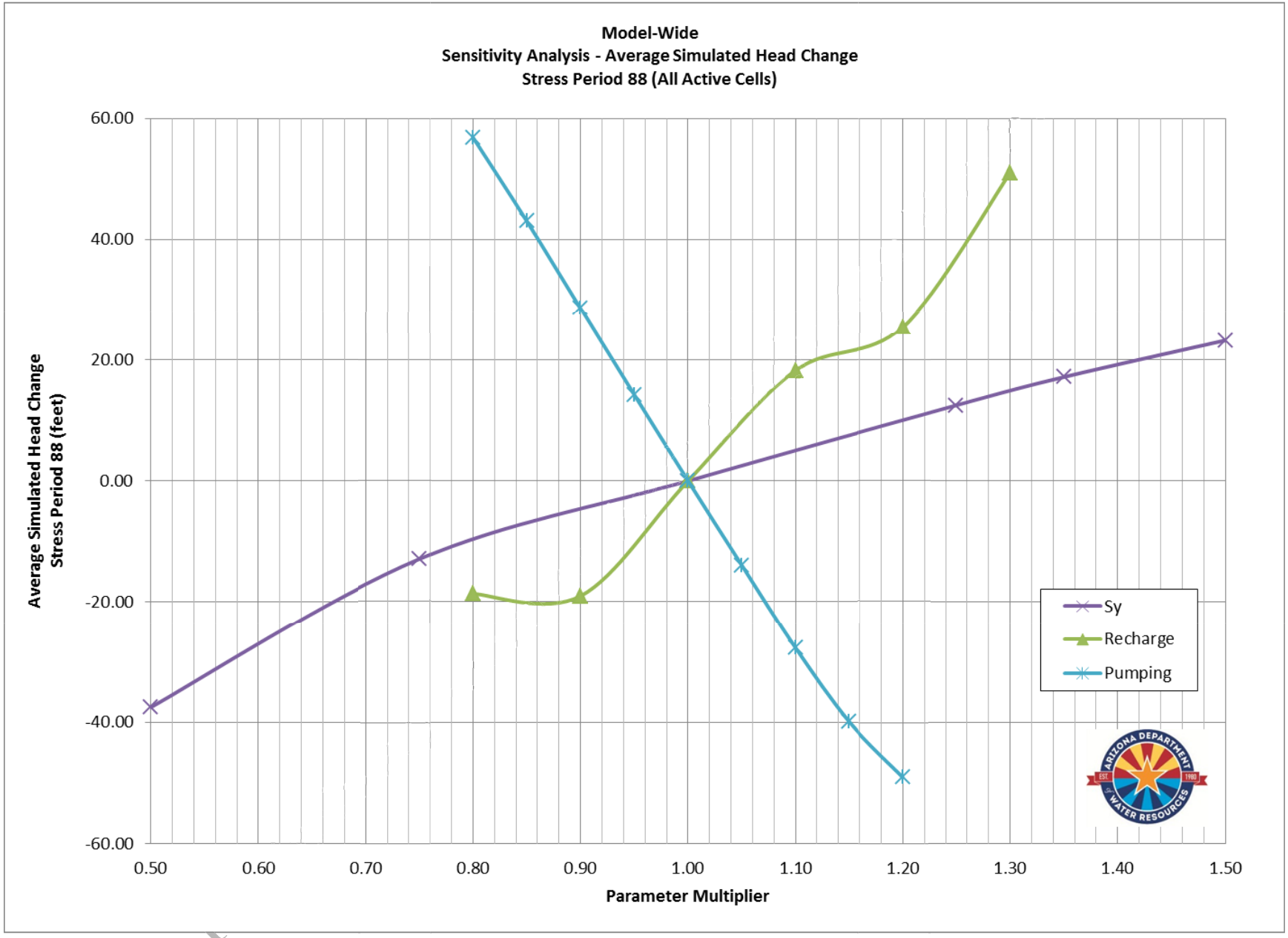

Figure 117 Comparison of the Model-Wide Average Changes in Head (At SP 88) Between Pumping, Recharge and Specific Yield (Sy)

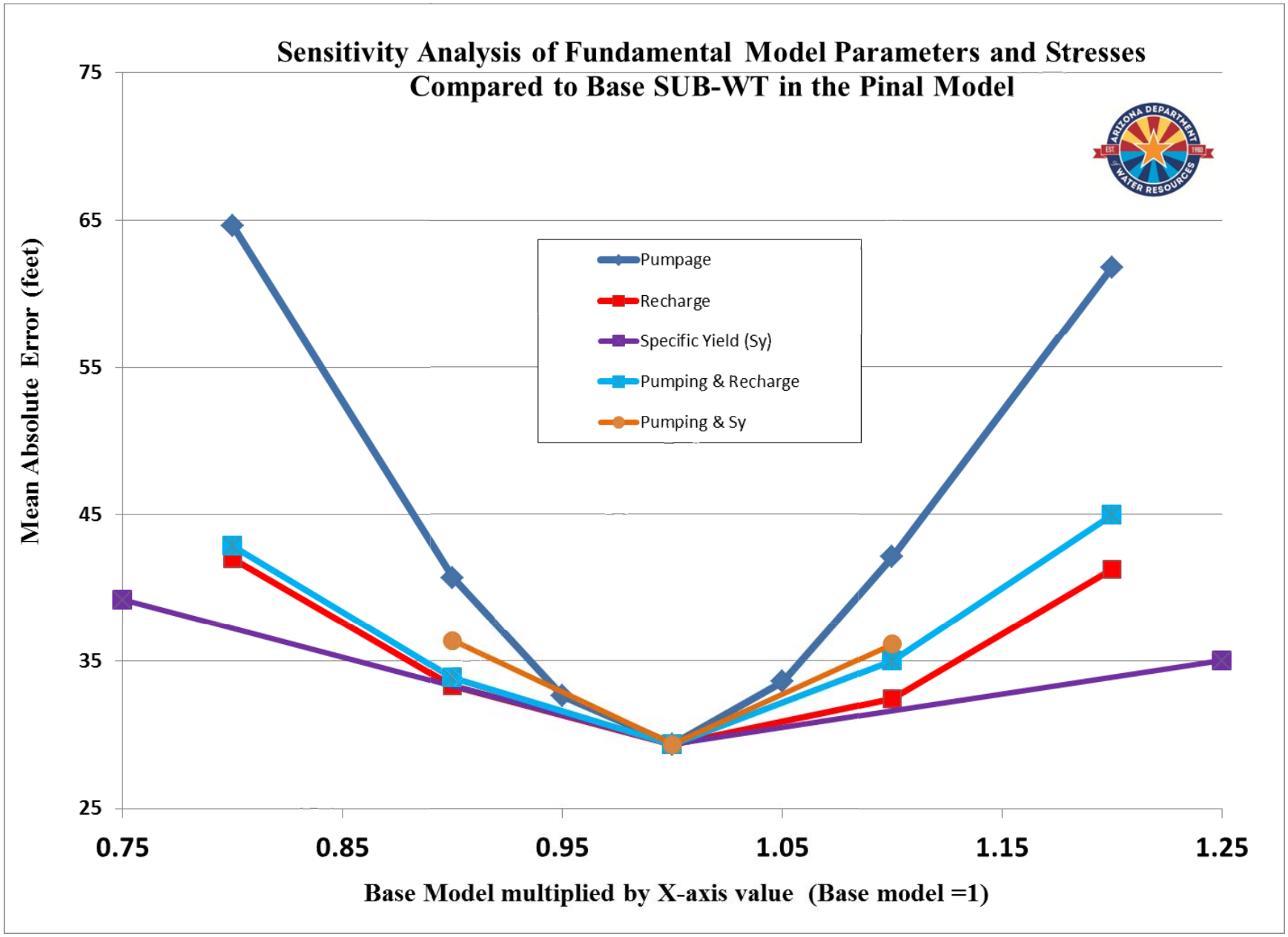

Figure 118 Sensitivity Analysis of Fundamental Model Parameters and Stresses Compared to Base SUB-WT in the Pinal Model

Preliminary internal draft Subject to Revision